REPORT UAG-8
PART II

WORLD DATA CENTER A

Upper Atmosphere Geophysics

DATA ON SOLAR-GEOPHYSICAL ACTIVITY
OCTOBER 24 - NOVEMBER 6, 1968

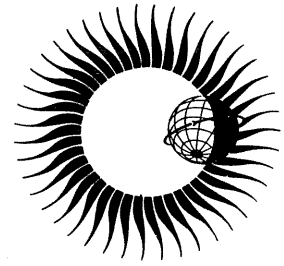

March 1970

WORLD DATA CENTER A

National Academy of Sciences

2101 Constitution Avenue, N. W. Washington, D. C. U.S.A., 20418

World Data Center A consists of the Coordination Office

and eight subcenters:

World Data Center A
Coordination Office
National Academy of Sciences
2101 Constitution Avenue, N.W.
Washington, D.C., U.S.A. 20418
Telephone (202) 961-1404

Solar and Interplanetary Phenomena, Ionospheric Phenomena, Flare-Associated Events, Aurora, Cosmic Rays, Airglow:
World Data Center A:
Upper Atmosphere Geophysics
Environmental Science Services Administration
Boulder, Colorado, U.S.A. 80302
Telephone (303) 447-1000 Ext. 3381

Geomagnetism, Seismology, Gravity and Tsunami:
World Data Center A:
Geomagnetism, Seismology, Gravity & Tsunami
Environmental Data Service, ESSA
Rockville, Maryland, U.S.A. 20852
Telephone (301) 496-8160

Glaciology:
World Data Center A:
Glaciology
American Geographical Society
Broadway at 156th Syreet
New York, New York, U.S.A. 10032
Telephone (212) 234-8100

Longitude and Latitude:
World Data Center A:
Longitude & Latitude
U.S. Naval Observatory
Washington, D.C., U.S.A. 20390
Telephone (202) 698-8422

Meteorology (and Nuclear Radiation):
World Data Center A:
Meteorology
National Weather Records Center
Asheville, North Carolina, U.S.A. 28801
Telephone (704) 253-0481

Oceanography:
World Data Center A:
Oceanography
Building 160
Second and N Streets, S.E.
Washington, D.C., U.S.A. 20390
Telephone (202) 698-3753

Rockets and Satellites:
World Data Center A::
Rockets and Satellites
National Academy of Sciences
2101 Constitution Avenue, N.W.
Washington, D.C., U.S.A. 20418
Telephone (202) 961-1404

Upper Mantle Project:
World Data Center A:
Upper Mantle Project
Lamont Geological Observatory
Palisades, New York, U.S.A. 10964
Telephone (914) 359-2900 Ext. 209

Notes:

(1) World Data Centers conduct international exchange of geophysical observations in accordance with the principles set forth by the International Council of Scientific Unions. WDC-A is established in the United States under the auspices of the National Academy of Sciences.

(2) Communications regarding data interchange matters in general and World Data Center A as a whole should be addressed to: World Data Center A, Coordination Office (see address above).

(3) Inquiries and communications concerning data in specific disciplines should be addressed to the appropriate subcenter listed above.

WORLD DATA CENTER A

Upper Atmosphere Geophysics

REPORT UAG-8 PART II

DATA ON SOLAR-GEOPHYSICAL ACTIVITY

OCTOBER 24 - NOVEMBER 6, 1968

compiled by

J. Virginia Lincoln

WDC-A, Upper Atmosphere Geophysics

Boulder, Colorado

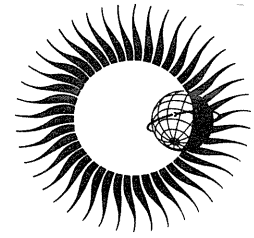

Prepared by Research Laboratories, ESSA, Boulder, Colorado
and published by

U.S. DEPARTMENT OF COMMERCE
ENVIRONMENTAL SCIENCE SERVICES ADMINISTRATION
ENVIRONMENTAL DATA SERVICE
ASHEVILLE, NORTH CAROLINA, USA 28801

March 1970

SUBSCRIPTION PRICE: $9.00 a year; $2.50 additional for foreign mailing; single copy price varies.* Checks and money orders should be made payable to the Superintendent of Documents. Remittance and correspondence regarding subscriptions should be sent to the Superintendent of Documents, Government Printing Office, Washington, D.C. 20402.

*Price of this issue $1.75

TABLE OF CONTENTS

PART II

TABLE OF CONTENTS

PART II (Continued)

6. SOLAR X-RAYS

"Solar X-ray Emission October 26, 1968-November 4, 1968"

by

D. M. Horan, R. G. Taylor, and R. W. Kreplin
E. O. Hulburt Center for Space Research
Naval Research Laboratory
Washington, D. C. 20390

During the period October 26 through November 4, 1968, the Naval Research Laboratory's SOLRAD 9 Satellite (Explorer 37, 1968-17A) provided solar x-ray data which are sufficiently continuous to say that no major solar x-ray event escaped detection unless it occurred between 1900 and 2242 UT on November 3. The data for this 222 minute period were lost during transmission from the satellite. No other gaps in the data last more than 35 minutes and it is unlikely that a significant solar event could completely run its course in so short a time. The satellite's memory is able to store up to 14.25 hours of data for the 0.5 to 3A, 1 to 8A, and 8 to 20A bands with a time resolution of one minute.

Figures 1 through 10 are plots of the solar x-ray flux vs. time during the period of interest. In each of the plots the top curve represents the solar x-ray emission in the 8 to 20A band, and the next lower curve represents solar x-ray emission in the 1 to 8A band. In both cases a gray body solar emission spectrum [Kreplin, 1961] with a 2×10^6 K color temperature was assumed in converting from detector current output to energy flux units. The third curve from the top represents emission in the 0.5 to 3A band assuming a gray body spectrum with a 10×10^6 K color temperature for the emitting region on the sun. Since the 0.5 to 3A band solar emission is generally below the threshold level of the detector, the curve representing these data will be quite intermittent.

The x-ray emission is plotted in units of ergs/cm /sec on a logarithmic scale. The abscissa is linear with the integers denoting hours in Universal Time (UT). Charged-particle interference with x-ray detectors, which can cause the plotted flux levels to be higher or lower than the actual flux, is indicated by the lowest data curve. The ionization chamber current caused by the charged-particle background is digitized and recorded as a "count". The number of "counts" is linearly related to the current generated in the 0.5 to 3A ionization chamber by penetrating charged particles when the detector is facing away from the sun. Counts of 10 to 15 indicate no particle interference with the detectors. Counts of 20 to the maximum value of 127 indicate increasing amounts of particle interference. However, the data processing computer program does not plot data obviously contaminated by particle interference, and this feature causes randomly spaced data gaps of 30 minutes duration or less.

The SOLRAD 9 detectors measure the x-ray emission from the entire visible disk with no spatial resolution whatsoever. The solar x-ray emission from even a small flare can easily be ten times more intense than the background x-ray emission from the nonflaring sun. Large solar flares can emit hundreds or even thousands of times more x-ray energy per second than the normal solar background emission. Therefore, when a solar flare occurs, the solar x-ray emission from the entire disk is effectively the flare emission. When the lifetimes of several solar flares overlap, only the emission from the predominant x-ray event will be recognizable in the SOLRAD 9 data plots and it is always possible that smaller events are occurring simultaneously.

Figure 1 shows that the solar x-ray emission on October 26, 1968 was dominated by two small events: a Class 1N [ESSA 1969a] flare whose x-ray emission reached a peak at 0130 UT and a normal subflare whose peak x-ray emission occurred at 1652 UT. Both events occurred in McMath Plage Region 9740. The solar background emission rose from moderately high values around 0900 to high values by 1200 and the high values persisted for the remainder of the day. Many very small x-ray events are visible on the plot.

The record of x-ray emission for October 27, Figure 2, shows three instances where two or more distinct x-ray events occurred with very slight time separation between them. In the first instance the x-ray emission rose sharply to double peaks at 0011 and 0020 UT. The decay from the second peak was quite rapid and at 0055 UT it merged with the slow rise of a subsequent event which peaked at 0130 UT. The 0011 and 0130 UT peaks are reported as Class 1B flares from Region 9740 but the second peak at 0020 UT was apparently not noted optically. The 0130 UT event had decayed to moderately high background values by 0900 UT with evidence of several very small x-ray events between 0700 UT and 0830 UT. At 1111 UT an x-ray peak corresponding to a reported normal subflare marked the first of another series of x-ray events. A smaller peak at 1134 UT, which does not correspond to any reported optical event, was followed by a peak at 1148 UT which corresponds to a Class 1N flare observed in Region 9740. A smaller peak at 1207, which corresponds to a faint subflare reported by the Crimean Observatory, terminated this series of events. Two very large x-ray events corresponding to two optical events which had several maximum phases then occurred in Region 9740. The first x-ray peak occurred at 1238 and corresponds to the Class 1B principal maximum of the first optical event at approximately 1237. The x-ray emissions from secondary maxima at 1253 and 1307 UT

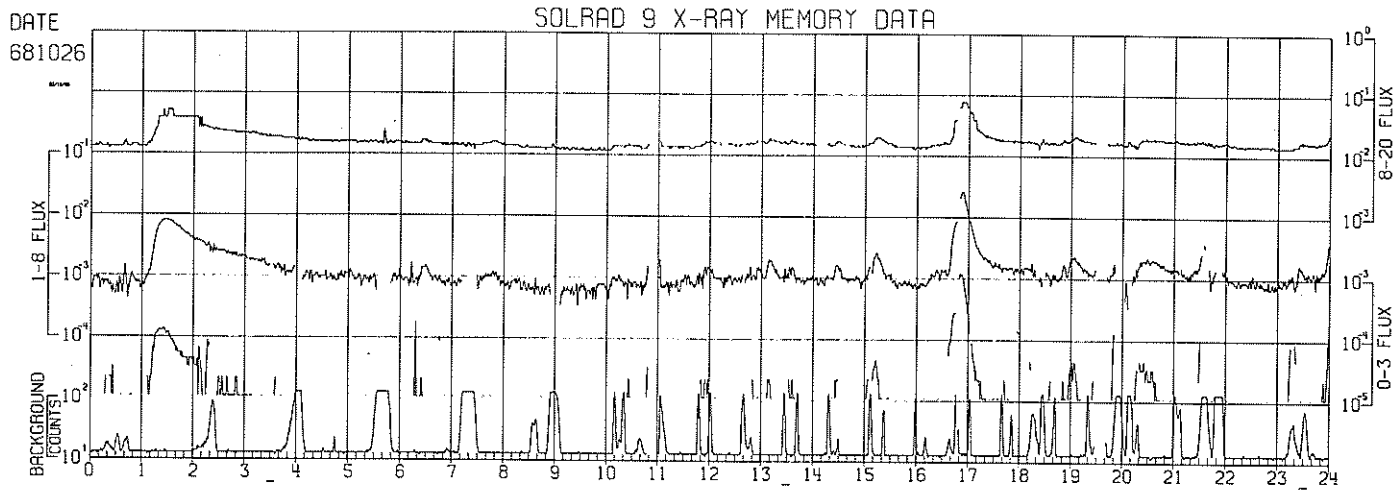

Fig. 1. Solar x-ray flux for October 26, 1968.

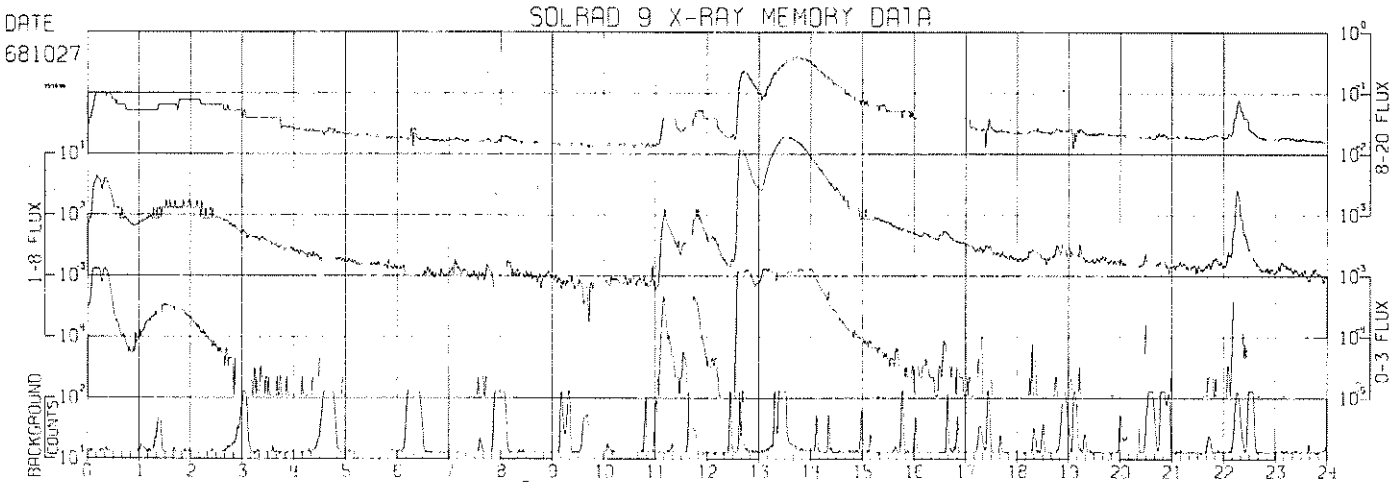

Fig. 2. Solar x-ray flux for October 27, 1968.

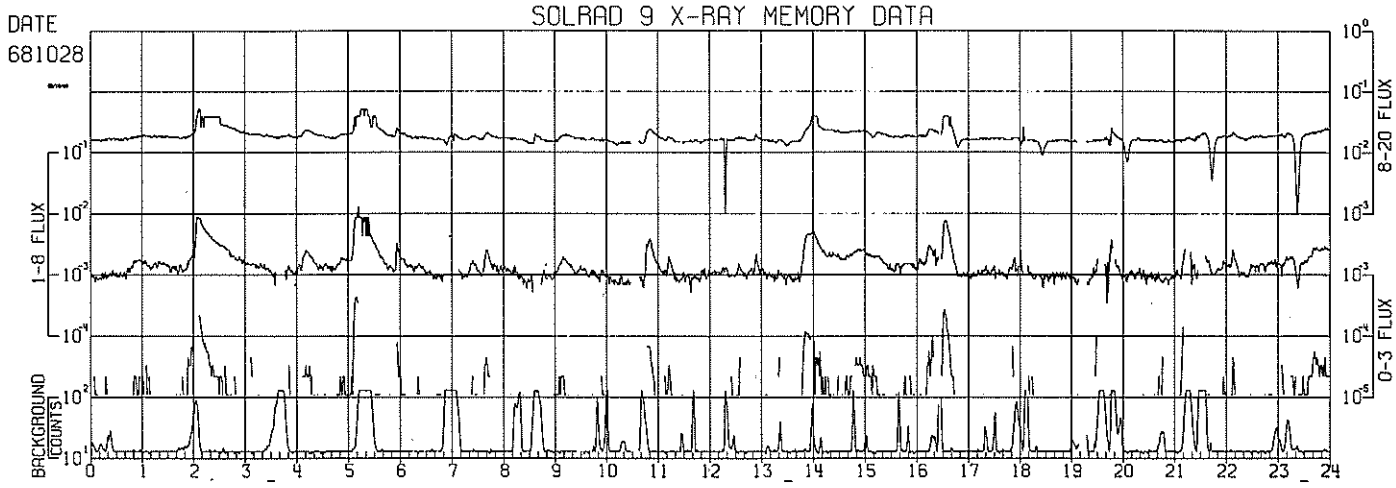

Fig. 3. Solar x-ray flux for October 28, 1968.

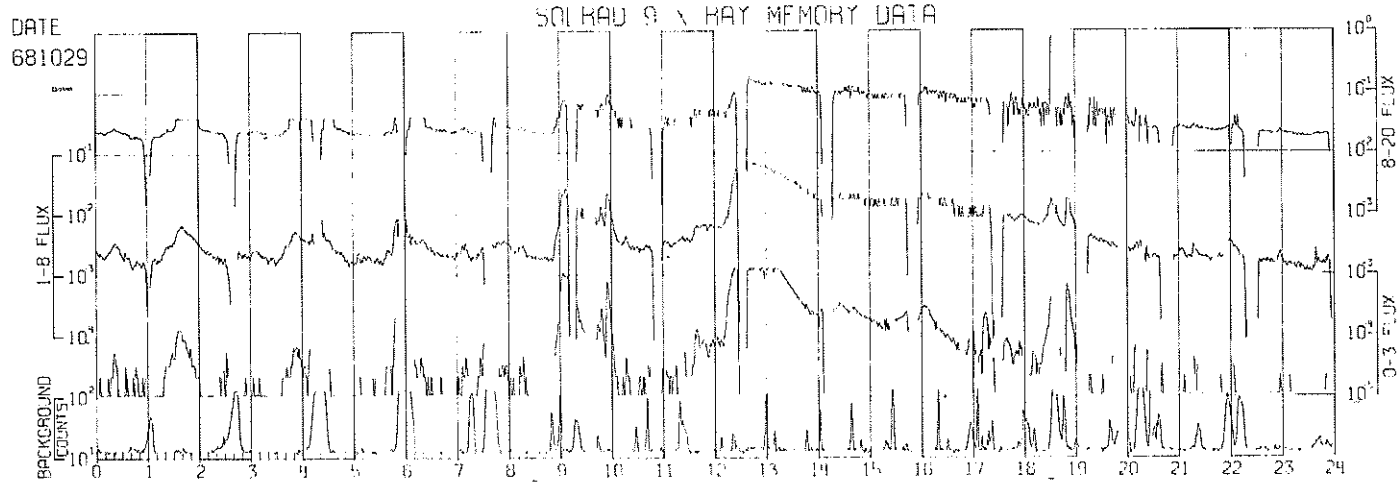

Fig. 4. Solar x-ray flux for October 29, 1968.

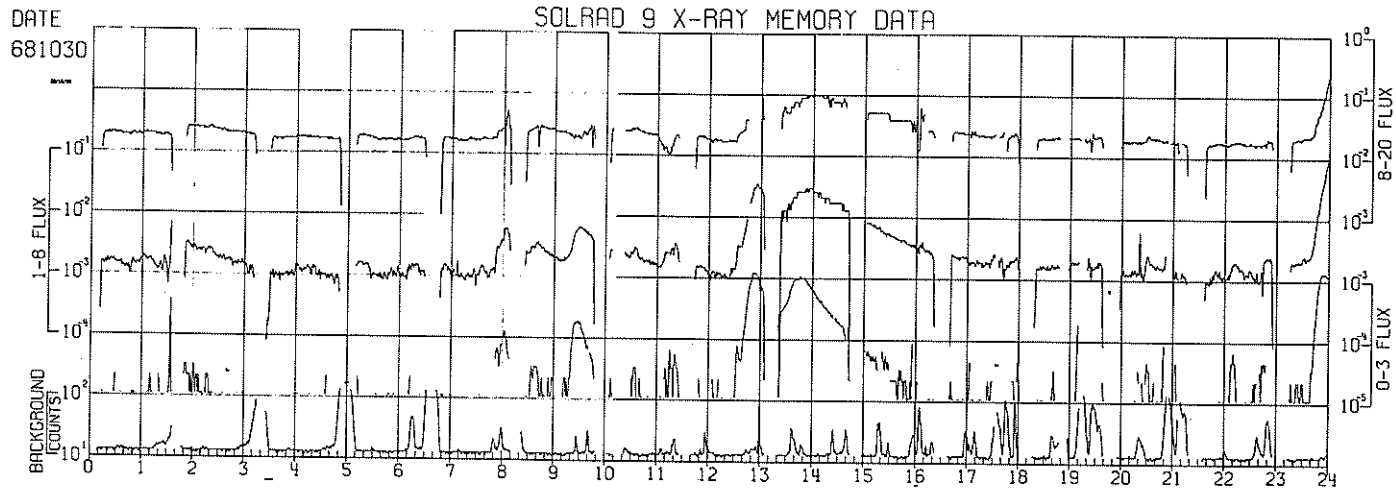

Fig. 5. Solar x-ray flux for October 30, 1968.

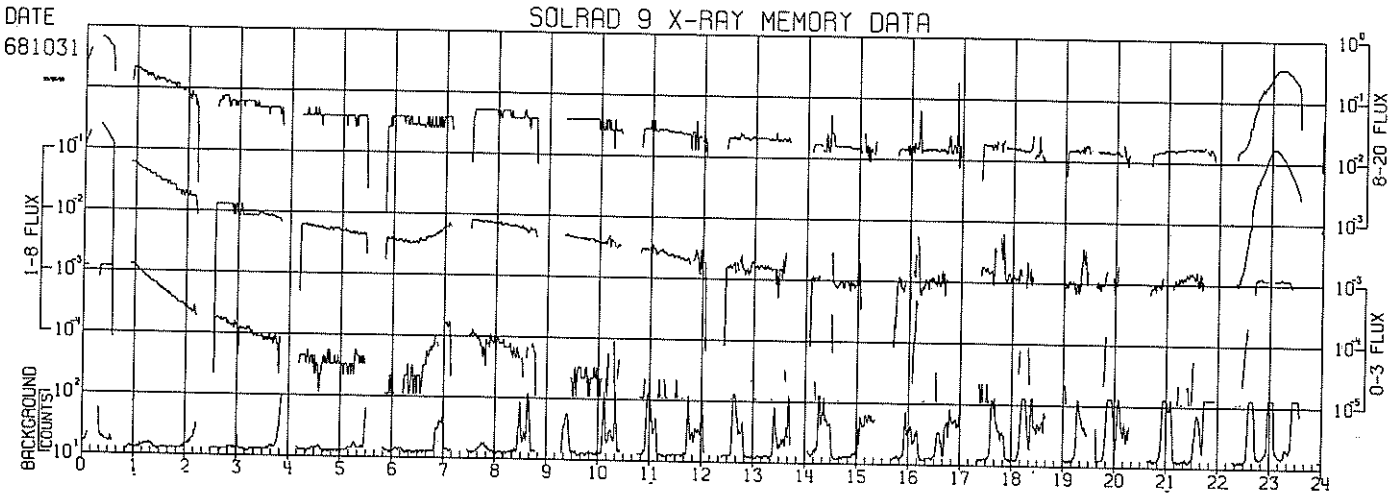

Fig. 6. Solar x-ray flux for October 31, 1968.

are not discernible on the plot but are probably hidden by the decaying emission from the 1238 event and the emission slowly rising toward a peak at 1334. The very large x-ray event at 1334 corresponds to an optical event which had four maximum phases; a Class 2N principal maximum at 1324, and secondary maxima at 1350, 1413, and 1450 rated as 2B, 1N, and a faint subflare,respectively. Between 1600 and 2200 the decaying emission from this event was interrupted by several very small x-ray events. A final small event peaked at 2216, and quickly decayed to the high background levels which persisted for the remainder of the day.

Figure 3 shows that no x-ray events comparable to the 1238 and 1334 events of the previous day occurred on October 28. The x-ray emission for that day can be described as a series of small x-ray events superimposed on high background levels. Attenuation of solar x-ray emission by passage through the earth's atmosphere causes the periodic dip in flux levels appearing first in the 8 to 20A data curve at 1508 and in the 1 to 8A data curve at 2323.

The x-ray record for October 29, Figure 4, displays so many x-ray events that at no time is the background level recognizable. A series of small events, quite closely spaced in time, preceded the predominant x-ray event of the day. This event, whose x-ray peak occurred between 1227 and 1240 when the satellite was in the earth's shadow, corresponds to a multiple maxima optical event whose principal maximum occurred at 1234 and was classified as a 2B flare. The long decay of the x-ray emission from this event was interrupted several times by smaller events. The regularly spaced gaps in all three bands starting at 0100 are caused by the passage of SOLRAD 9 through the earth's shadow.

Figure 5 shows high background x-ray levels throughout October 30 interrupted by many small events and one medium-sized, double-peaked event. The first of the twin peaks occurred at 1255 UT and corresponds to the Class 2B principal maximum phase at 1253 of a triple maxima optical event in Region 9740. The second x-ray peak occurred at approximately 1352 and corresponds to the Class 2N secondary maximum at 1348. The Class 1B secondary maximum at approximately 1413 is not obvious on the x-ray plot. By 1800, the x-ray emission had decayed to high background levels which continued, with occasional small x-ray flare activity, until 2344 UT when an extremely rapid rise marked the beginning of a very large x-ray flare.

October 31, Figure 6, commenced with the largest x-ray flare since July 1968 already in progress. The peak x-ray emission occurred between 0006 and 0019 UT but the peak data are missing because of particle interference during the satellite's passage through the South Atlantic Anomaly. The maximum phase of this 3B flare in Region 9740 was observed at 0013. The decaying x-ray emission from this event dominated the three monitored bands until 0630 when the emission from a small but relatively long-lived x-ray event became discernible. Subflare activity was observed to have maximum phases at 0652 and 0714. The enhancement over the decaying x-ray emission from the 3B flare was unusually large and long-lived for subflare activity. By 1500 the x-ray emission had decayed to high background levels which continued until 2228 when a sharp increase marked the beginning of a large x-ray event which corresponds to an optical event in Region 9740 which had three distinct Class 2 maximum phases. The peak x-ray emission from this event came at 2301 and the optical maximum phases occurred at 2245, 2303, and 0041 on November 1. A change in slope is visible at 2245 on the x-ray plot and this may correspond to the principal maximum phase at 2245.

Figure 7 shows that the x-ray emission decayed without interruption until 0500 on November 1. Two small x-ray events preceded a fairly large event which peaked at 0907 UT. Three optical maximum phases were observed [ESSA, 1969b] during the x-ray event; two of which, at 0844 and 0905, were rated as Class 1 and the third, at approximately 0928, was rated as Class 2F. Between 1200 and 2000 UT the x-ray emission was primarily background emission with sporadic, minor flare activity. At 2000 the x-ray levels commenced a very steep rise to a peak at 2007. The peak values obtained were large but the x-ray levels dropped almost as sharply as they had risen. By 2038 the x-ray emission from this event, which corresponds to a Class 1B flare in Region 9740, was indistinguishable from the background and minor flare emission which continued until 0926 on November 2, Figure 8. The peak emission from a reported subflare occurred at 0933. This event was immediately followed by a predominant x-ray event of the day, whose peak emission occurred at 1000. This large event corresponds to an optical event in Region 9740 which was observed to have two Class 2B and one Class 1N maximum phases. A small x-ray event, which corresponds to a Class 1N flare reported by the McMath-Hulbert Observatory, peaked at 1534. This event terminated significant x-ray flare activity for November 2.

Several small, short-lived x-ray events are clearly recognizable above the background levels on Figure 9, November 3, 1968. There were no large events unless one occurred between 1900 and 2242 UT. However, only one Class 1 flare and several subflares were observed during this period for which the satellite data were lost.

November 4, Figure 10, commenced with high background levels which were overshadowed between 0200 and 0447 UT by the emission from several small flares. When the data continued at 0519 after a gap caused by satellite night, the x-ray emission from a very large flare was already beyond the highest on-scale readings obtainable with SOLRAD 9's 0.5 to 3A and 1 to 8A experiments. At 0525 the 8 to 20A experiment also became saturated and continued in that state until 0533. The 1 to 8A

experiment recovered from saturation at 0536. The decaying emission from this event dominated the solar x-ray emission for several hours. This event corresponds to a Class 1B flare observed in Region 9740. The peak x-ray emission occurred between 0447 and 0533 and that agrees with the observation of maximum phase at 0529 by Carnarvon.

This event is a good example of a solar flare whose x-ray emission is disproportionate to its reported optical class, 1B. Its peak emission levels in the 1 to 8A and 8 to 20A bands were considerably higher than those of any Class 2 or Class 3 event occurring between October 26 and November 3, 1968, and its x-ray emission remained at enhanced levels longer than most of the Class 2 events.

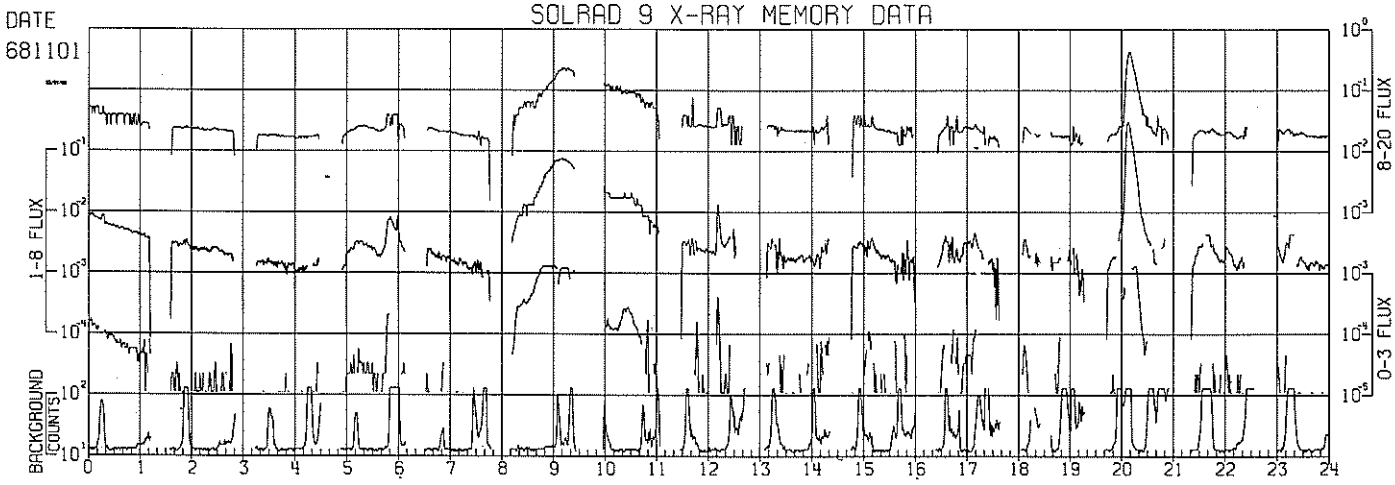

Fig. 7. Solar x-ray flux for November 1, 1968.

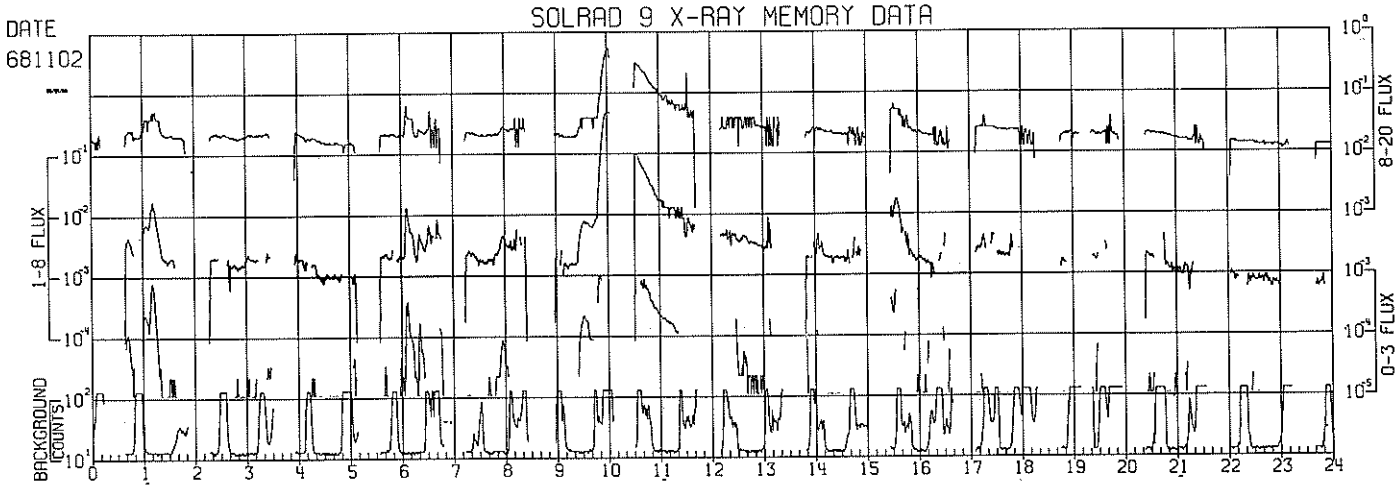

Fig. 8. Solar x-ray flux for November 2, 1968.

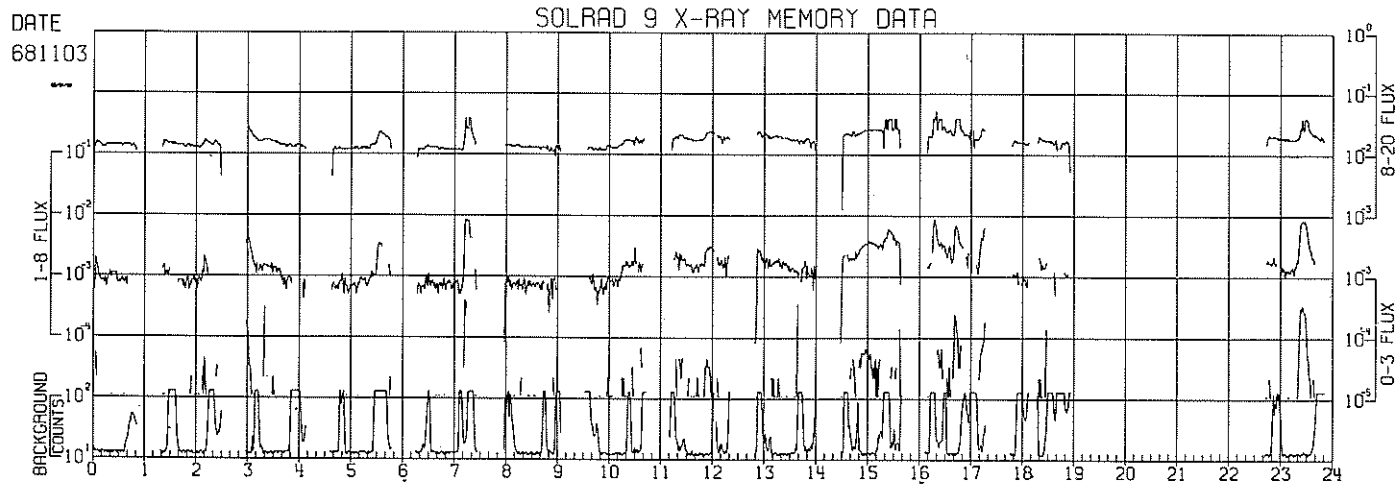

Fig. 9. Solar x-ray flux for November 3, 1968.

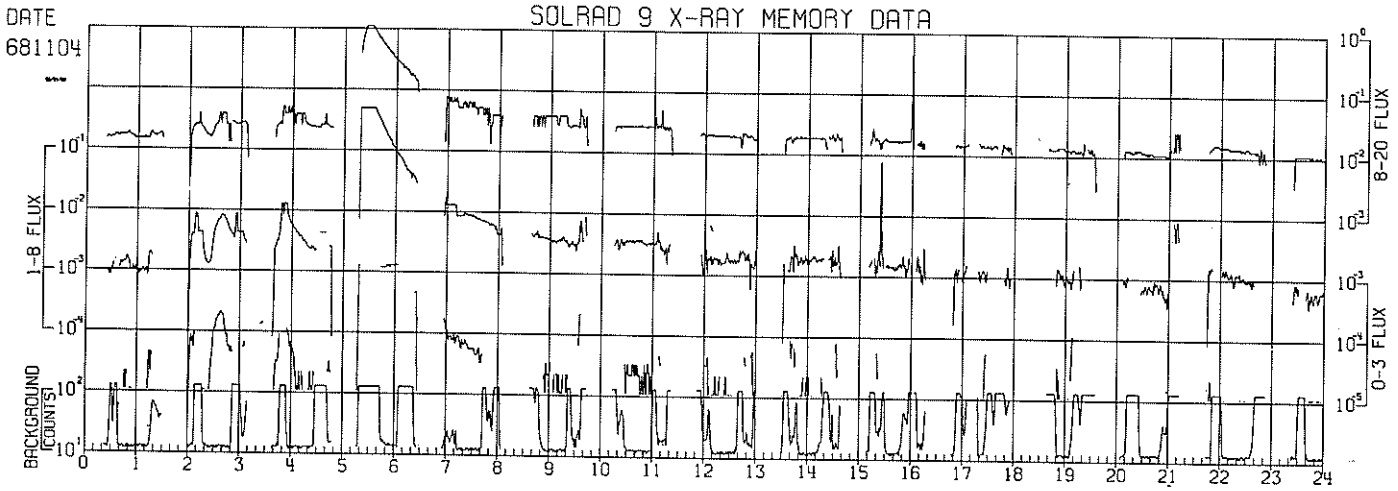

Fig. 10. Solar x-ray flux for November 4, 1968.

Conclusion

Perusal of solar x-ray data for the period March 15, 1968 to October 24, 1969 revealed no other ten-day period with solar x-ray activity comparable to that of October 26 through November 4, 1968. Seven times during this ten-day span the solar x-ray emission in the 1 to 8A band exceeded 1 x 10^{-1} ergs/cm^2/sec and on 18 additional occasions it exceeded 1 x 10^{-2} ergs/cm^2/sec. During the period February 20 through March 1, 1969 the 1 to 8A band emission exceeded 1 x 10^{-1} ergs/cm^2/sec five times and it exceeded 1 x 10^{-2} ergs/cm^2/sec 24 additional times. However, the events which occurred during this latter period were, on the average, considerably smaller. During July 5 - 12, 1968, which is another period of great interest, the 1 x 10^{-1} erg/cm^2/sec level was exceeded twice and the 1 x 10^{-2} erg/cm^2/sec level was exceeded seven times.

REFERENCES

ESSA 1969a "Solar-Geophysical Data", IER-FB 296, April 1969 (flare class and plage region for October 1968).

ESSA 1969b "Solar-Geophysical Data", IER-FB 297, May 1969 (flare class and plage region for November 1968).

KREPLIN, R. W. 1961 Ann. Geophys., 17, 2, 151-161.

7. SUDDEN IONOSPHERIC DISTURBANCES

"Sudden Ionospheric Disturbance Summary October 22-November 4, 1968 from WDC-A Archives"

by

J. Virginia Lincoln
Space Disturbances Laboratory
ESSA Research Laboratories, Boulder, Colorado

The following table groups the individual sudden ionospheric disturbance (SID) reports for this period as they have been published in "Solar-Geophysical Data" into a single event listing. The selection has been made subjectively. Preference for the times selected has been given to sudden phase anomalies (SPA) at VLF, whenever possible, followed by shortwave fadeout (SWF) times. The importance rating from 1- to 3+ has been made considering all the importances of the individual reports. The widespread index signifies the geographical extent of the event from 1 = single station reporting to 5 = many stations reporting. The final columns give the number of station reports per SID-type which were considered in formulating the event details. The SID associated with the major flares of the period are underlined. All of these are associated with McMath plage region 9740. The letter in the widespread column is the x-ray flare class for the SID associated with flares in region 9740 according to the following flux ranges:

$D = \Delta\Phi_m$ (0.5-8Å) $\approx 10^{-3}$
$E = 2\times10^{-3} \leq \Delta\Phi_m < 10^{-2}$
$M = 10^{-2} \leq \Delta\Phi_m < 10^{-1}$
$X = 10^{-1} \leq \Delta\Phi_m$
"+" or "−" means $\Delta\Phi_m$ was near the upper or lower end, respectively, of the flux range of a class.

The flux for each event was estimated from all the available satellite x-ray data and other SID data. If the flare associated with the SID is not in region 9740, the last two digits of the McMath region in which the associated flare occurred are given in the widespread index column. Parentheses indicate it was an unconfirmed flare in that region. Question marks indicate the region to associate with the SID is unknown.

The following table summarizes the number of SID per day per region from October 22-November 4, 1968:

	McMath Region										
Date	35	40	39	49	47	51	54	58	44	60	Unknown
October 22	5	4									
23	5	3	2								
24		1									
25		4									
26		3									
27		11									
28	2	2	1	1							
29		8		2							
30		8			1						2
31		2									1
November 1		7		1							5
2		8				1		2			1
3		7					1		1		3
4		2				1				1	1

Date	Universal Time Start	Max	End	Impt.	Wide-spread Index	No. of Stations Reporting for Type Listed
Oct. 22	0141	0145	0223	1	5 M-	2SWF, 3 SPA, 5 LF-SPA, 6 SES
	0444	0500	0523	1	5 35	1 SWF, 2 SPA, 4 LF-SPA, 5 SES
	0523	0528		1-	1 E	1 SPA and SES
	0729	0732	0757	2	3 35	1 SWF, 1 SES
	1319	1326	1436	1-	5 35	1 SEA, 2 SPA, 2 LF-SPA, 4 SES
	1656	1704	1708D	1+	5 35	4 SWF, 2 SPA, 2 LF-SPA, 5 SES
	1708	1718	1810			
	1858	1903	1914	1-	1 E-	1 SPA
	1929	1936	1950	1-	1 D	1 SPA
	2122	2132	2202	1-	3 35	1 SPA, 1 SES
Oct. 23	0012	0017	0045	1	5 35	1 SWF, 2 SPA, 4 LF-SPA, 4 SES
	0357	0407	0523	2	5 35	3 SWF, 1 SCNA, 1 SPA, 4 LF-SPA, 4 SES
	0857	0904	0907	1-	1 D	1 SWF
	1142	1145	1210	1-	1 35	1 SCNA
	1310	1312	1400	1-	5 39	1 SWF, 2 SPA, 1 SES
	1743	1749	1804	1-	5 39	3 SPA, 2 LF-SPA, 3 SES
	1837	1839	1843	1-	3 35	1 SPA, 1 SES
	1939	1940	2009	1-	5 M	3 SWF, 2 SPA, 2 LF-SPA, 3 SES
	2130	2133	2146	1-	1 35	1 SPA
	2350	0019	0055	2+	5 X-	2 SWF, 2 SPA, 2 LF-SPA, 3 SES
Oct. 24	2059	2125	2240	1	5 M	2 SWF, 1 SCNA, 2 SPA, 1 SES
Oct. 25	1534	1539	1600	1	5 35	1 SPA, 3 LF-SPA, 3 SES
	1907	1913	1922	1-	5 35	1 SWF, 2 SPA
	2317	2323	2346	1-	1 35	1 SPA
Oct. 26	0115		0145	1+	1 E	1 SWF
	1638	1646U	1646D	1	5 M	4 SWF, 2 SCNA, 4 SPA, 3 LF-SPA, 5 SES
	1646	1655	1707D			
	1849	1851	1852	1-	5 D	1 SPA, 1 SFD
	2017	2028	2140	1-	1 D	1 SPA
Oct. 27	0004	0015	0018D	1	5 E-	1 SWF, 3 SPA, 1 SES
	0018	0022	0114U	1	3 E-	1 SPA, 1 SES
	0112	0133	0258	2-	3 E	2 SWF
	1110	1112	1127	1+	5 E+	4 SWF, 2 SEA, 2 SPA, 1 LF-SPA, 2 SES
	1144	1148	1154	2	5 E+	4 SWF, 1 SEA, 2 SPA, 1 SES
	1230	1235	1302U	2+	5 M	5 SWF, 1 SCNA, 1 SEA, 2 SPA, 2 SES
	1305	1328	1435	2+	5 M+	2 SWF, 2 SCNA, 2 SPA, 2 LF-SPA, 3 SES
	1636	1638	1648	1-	1 D	1 SWF and SPA
	1911	1914	1918	1-	3 D	1 SWF, 1 SPA
	2142	2143	2145	1	1 D	1 SFD
	2206	2207	2209	1-	1 M-	1 SWF and SPA
	2211	2219	2235	1	5 M-	1 SWF, 3 SPA
Oct. 28	0203	0211	0245	1	5 39	1 SPA, 3 LF-SPA, 3 SES
	0507	0515	0555	1	5 E	1 SWF, 1 SPA, 4 LF-SPA, 4 SES, 1 SEA
	1240	1335	1600U	1+	1 49	1 SPA
	1349	1356	1522	1-	5 E	1 SWF, 1 SPA, 1 SES
	1631	1637	1656	1-	5 35	1 SWF, 2 SPA, 3 LF-SPA, 4 SES
	1945	1951	2002	1-	1 35	1 SPA
Oct. 29	0356	0359	0404	1-	1 49	1 SWF
	0546	0554	0603	1+	5 E	1 SWF, 3 LF-SPA, 3 SES
	0727	0737	0750	1	3 E	1 SWF, 1 SEA, 1 SES
	0900	0912	0952	1+	5 M-	4 SWF, 1 SCNA, 3 SEA, 1 SES
	0956	1000	1006	1+	5 M	3 SWF, 1 SEA, 1 SPA, 2 SES
	1218	1230	1328	2+	5 M+	5 SWF, 1 SCNA, 3 SEA, 3 SPA, 2 LF-SPA, 4 SES
	1413	1416	1443	1	5 E	1 SEA, 1 LF-SPA, 1 SES
	1711	1714	1733	1	5 49	1 SWF, 2 SPA
	1823	1834	1848D	1-	5 D	1 SWF, 2 SPA
	1848	1849	1853	1-	5 D	2 SWF, 2 SPA, 1 SES, 1 SFD

Date	Universal Time Start	Max	End	Impt.	Wide-spread Index		No. of Stations Reporting for Type Listed
Oct. 30	0134	0138	0230	1	5	E+	1 SWF, 2 SPA, 2 LF-SPA, 1 SES
	0215	0225		1	3	D	2 LF-SPA, 2 SES
	0752	0755	0810	1-	1	E	1 SWF
	0922	0935	1002	1	1	E	1 SWF
	1210	1215	1235D	1+	5		1 SWF, 1 SEA, 1 SPA
	1235	1300	1300D	2	5	M	5 SWF, 3 SEA, 1 SPA, 3 LF-SPA, 5 SES
	1335	1345	1500U	1	5		2 SWF, 1 SCNA, 1 SEA, 2 SPA, 2 LF-SPA, 2 SES
	1449	1516		1	3		2 LF-SPA, 2 SES
	1622	1624	1644U	1-	1	D	1 SPA
	1802	1809	1820	1-	1	?	1 SWF
	2023	2036	2112	1-	1	D	1 SPA
	2204U	2212	2240	1-	1	47	1 SPA
	2242	2248	2257	1-	3	?	1 SWF, 1 SPA, 1 SES
	2343	2355	0301	2+	5	X-	3 SWF, 3 SPA, 5 LF-SPA, 5 SES
Oct. 31	1434	1443	1526	1	5	?	1 SWF, 1 SCNA
	1714	1722	1750	1	3	D	1 SCNA, 1 SPA
	2247	2303	2349	1+	5	M+	4 SWF, 1 SCNA, 3 SPA, 1 SES
Nov. 1	0020	0025		1	5	?	5 LF-SPA, 6 SES
	0547	0550	0557	1-	1	E	1 SWF
	0828	0858	1012	2	5	M+	4 SWF, 1 SPA, 1 SEA
	1015	1030	1100	1	3	?	1 SWF, 1 SPA
	1208	1211	1233	1	1	E	1 SPA
	1405	1420	1504	1	1	(49)	1 SPA
	1511	1514	1518	1-	1	D	1 SPA
	1707	1708	1717	1-	1	?	1 SPA
	1808	1813	1847	1-	5	E	1 SPA, 1 LF-SPA, 1 SES
	1847	1848	1859	1-	1	?	1 SWF
	1905U	1906	1927	2	1	?	1 SWF
	1959	2010	2127	2	5	X-	3 SWF, 2 SCNA, 1 SEA, 5 SPA, 1 LF-SPA, 3 SES, 1 SFD
	2245	2250	2309	1	5	M	1 SWF, 5 SPA, 4 LF-SPA, 4 SES, 1 SFD
Nov. 2	0011	0023		1	3	?	6 LF-SPA, 6 SES
	0038	0046	0100	1-	5	D	1 SWF, 2 SPA, 2 LF-SPA, 3 SES
	0110	0115	0141	1-	5	M-	1 SWF, 2 SPA, 2 LF-SPA, 3 SES
	0331	0345	0423	1	5	E	1 SWF, 1 SPA, 3 LF-SPA, 2 SES
	0928	0938		1+	1	E	1 SWF
	0946	1003	1045	2+	5	X	2 SWF, 1 SCNA, 1 SEA, 2 SPA, 2 SES
	1049	1054	1100	2	1	(58)	1 SWF
	1518	1543	1620	1	5	E	3 SWF, 1 SEA, 2 SPA
	1700	1703	1715U	1-	5	D	1 SPA, 1 LF-SPA, 1 SES
	1715	1718	1723	1-	1	51	1 SPA
	1913	1917	1926	1-	5	D	1 SWF, 2 SPA
	1937	1943	1953	1-	5	D	1 SPA, 1 SES
	2158	2201	2215	1-	1	(58)	1 SPA
Nov. 3	0000	0001	0011D	1	5	?	1 SPA, 1 SES
	0259	0303	0312	1	5	E	1 SWF, 3 LF-SPA, 3 SES
	1234	1242	1328	1+	5	E	4 SWF, 1 SCNA, 4 SEA, 1 SPA, 2 SES
	1641	1642	1654	1-	5	54	1 SPA, 3 LF-SPA, 3 SES
	1714	1722	1744	1-	5	E	1 SWF, 1 SPA, 2 LF-SPA, 2 SES
	1809	1813	1829	1-	5	?	1 SWF, 2 SPA, 2 LF-SPA, 2 SES
	1938			1-	1	D	1 SPA
	1955		2030	1-	1	D	1 SPA
	2034	2039	2043	1	5	E+	3 SWF, 2 SPA, 2 LF-SPA, 2 SES, 1 SFD
	2105	2111	2124	1-	1	D	1 SPA
	2210	2220	2304	1-	5	44	2 SPA
	2323	2330	0012	1-	5	?	1 SWF, 3 SPA, 2 LF-SPA, 3 SES
Nov. 4	0202	0213		1	3	E	2 LF-SPA, 2 SES
	0346	0356	0417	1	5	(51)	1 SEA, 1 SPA, 2 LF-SPA, 2 SES
	0509	0527	0642	2	5	X	2 SWF, 1 SEA, 2 SPA, 1 SES
	2106	2109	2117	1	5	?	2 SPA
	2143	2152	2225	1-	1	60	1 SPA

"Panska Ves Observatory Sudden Ionospheric Disturbances October 21 - November 3, 1968"

by

Pavel Tříska
Geophysical Institute, Czechoslovak Academy of Sciences

[The records printed below for October 27 and 29, 1968 are examples of sudden ionospheric disturbances (SID) as recorded at the Panska Ves Observatory (N50.53° E14.57°) of the Geophysical Institute of the Czechoslovak Academy of Sciences. The types of SID reported are short-wave fadeouts (SWF), sudden enhancement of atmospherics at 27 kHz (SEA), sudden decrease of atmospherics at 5 kHz (SDA), and sudden phase anomalies on LF amplitude recordings (SFA). The latter are indirect phase measurements by the one-hop sky-wave interfering with the ground wave on 155 kHz and 164 kHz transmissions at 1000 km distance.

The records submitted to World Data Center A, Upper Atmosphere Geophysics are for:

October 21, 1100-1600 UT
22, 0600-1000 and 1200-1500
27, 1100-1500
29, 0800-1100 and 1100-1500
30, 1100-1500
November 1, 0800-1100
2, 0900-1300 and 1400-1700
3, 1200-1500.]

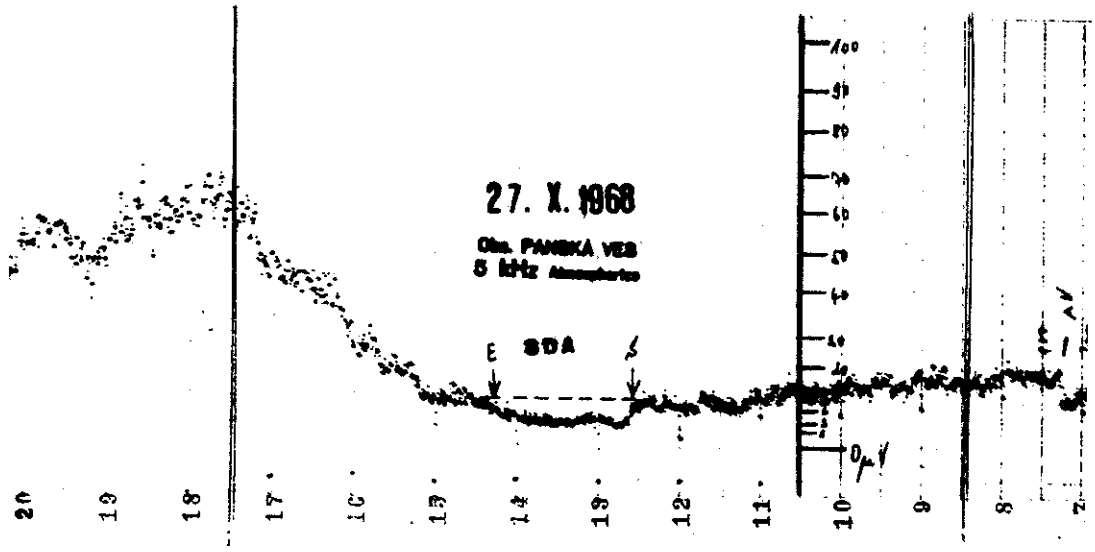

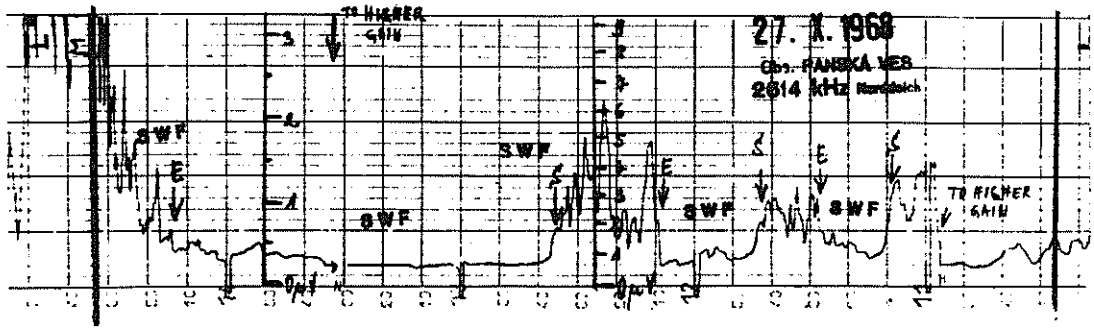
27. X. 1968
Obs. PANSKÁ VES
2614 kHz
SWF
E
TO HIGHER GAIN

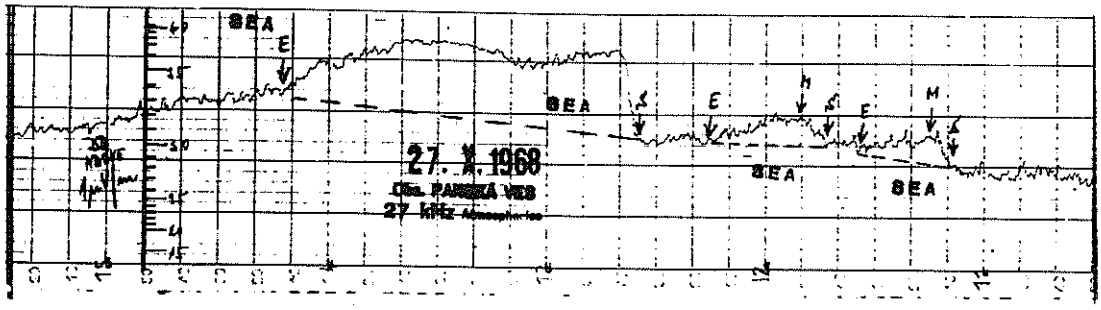
SEA
E
27. X. 1968
Obs. PANSKÁ VES
27 kHz

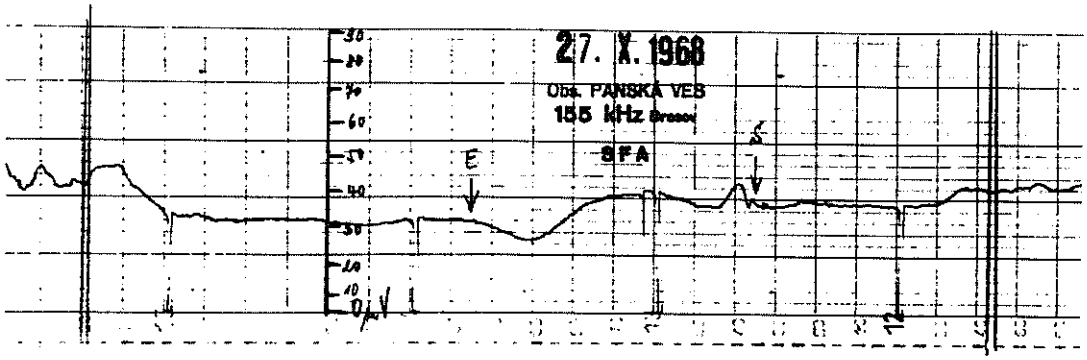
27. X. 1968
Obs. PANSKÁ VES
155 kHz
SFA
E

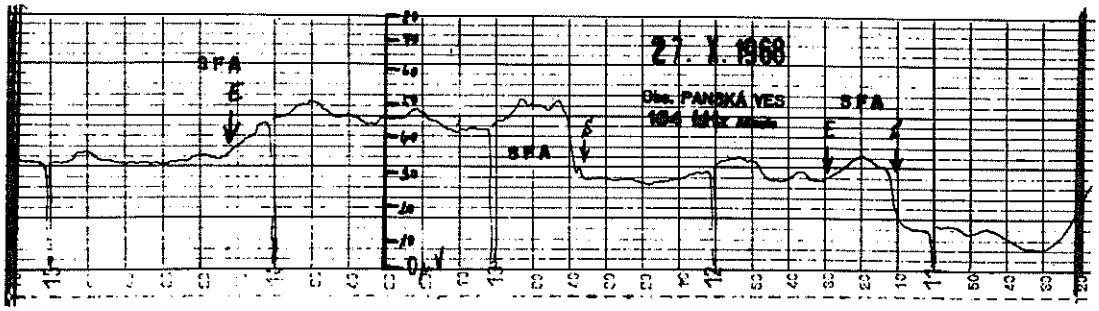
SFA
E
27. X. 1968
Obs. PANSKÁ VES
SFA

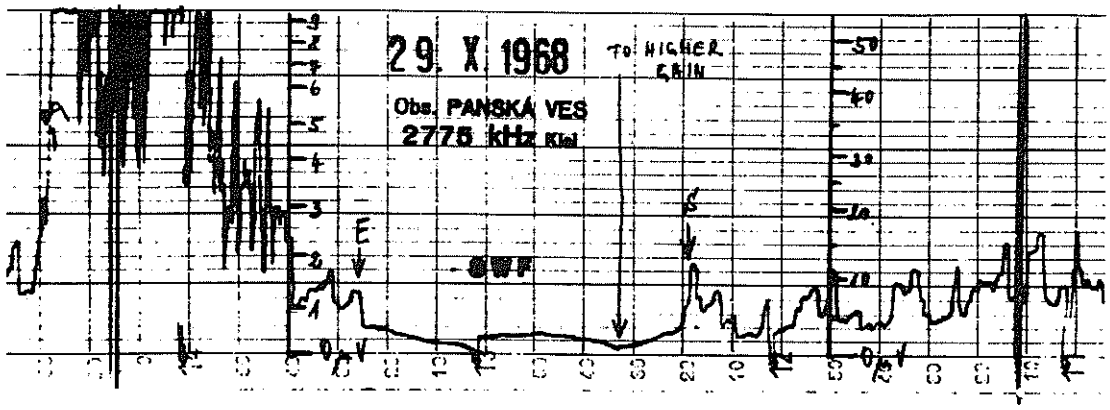
29. X 1968
Obs. PANSKÁ VES
2775 kHz Kiel
TO HIGHER FREQ.
E
S
SWF

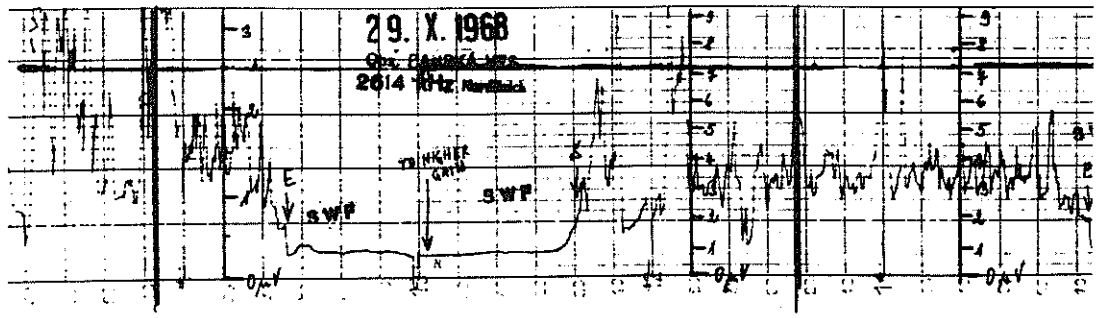
29. X. 1968
2614 kHz
E
SWF
SWF

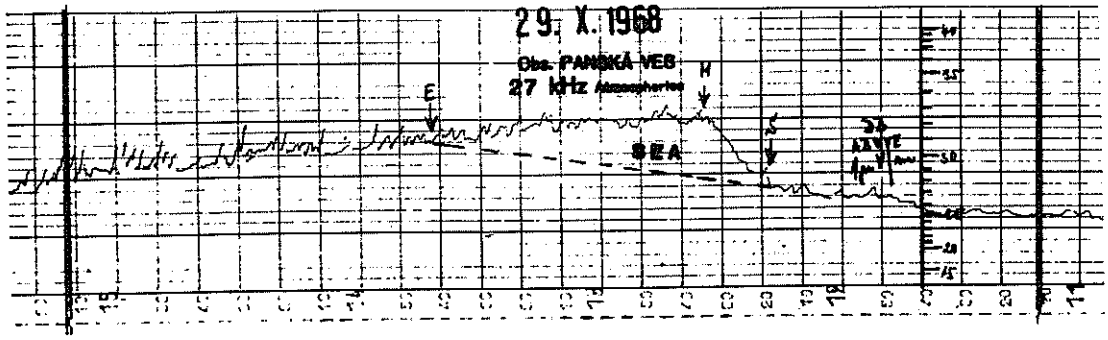
29. X. 1968
Obs. PANSKÁ VES
27 kHz
E
H
SEA

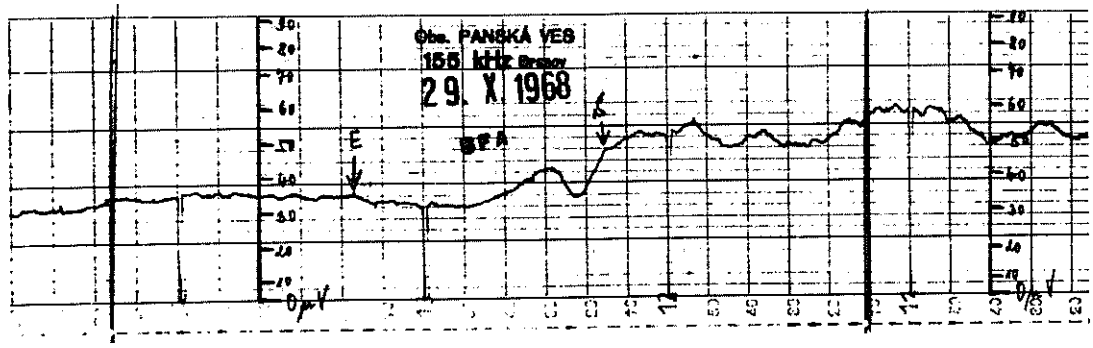
Obs. PANSKÁ VES
155 kHz
29. X 1968
E
SEA

"Solar Flare Effects in the Ionosphere Observed at Lindau
(51°39' N; 10°7.5' E) from October 27 to November 2, 1968"

by

H. Schwentek
Max-Planck-Institut für Aeronomie
Institut für Ionosphärenphysik
D3411 Lindau, Federal Republic of Germany

Introduction

During great solar flares occurring mainly in years of high and maximum sunspot number the electron density of the lower ionosphere (at heights between 65 and 100 km) increases considerably. On records of the signal strength of shortwave transmitters made simultaneously at different frequencies, the increase of solar radiation causes a more or less distinct decrease of signal strength (shortwave fadeout); and it is well-known that the higher the frequency of the transmitter, the weaker the effect. It should be mentioned that most of the solar flares observed in the light of Hα are not correlated with a shortwave fadeout. But nearly every shortwave fadeout can be correlated with a solar flare observed in Hα. Out of 295 shortwave fadeouts observed in the IGY, 280 were typically correlated with Hα; 12 were correlated with Hα activity occurring simultaneously but being of other than flare-type; the correlation for two fadeouts was uncertain, and was missing for one [De Mastus and Wood, 1960].

The increase of ionospheric absorption during a solar flare, as a function of time, is rather well associated with the increase of solar x-ray flux (in the wave-length band 1 - 12 Å). See Fig. 1 by Hartmann and Schwentek [1969]. One or two days later, caused by solar particles, still other important effects may - but often do not - occur: aurora and a geomagnetic storm.

At Lindau, for a couple of years, the signal strength of several shortwave transmitters has been recorded continuously on carefully selected circuits [Schwentek, 1958 and 1966]: Norddeich - Lindau (2.614 MHz; distance transmitter - receiver 296 km), Kiel - Lindau (2.775 MHz; 300 km), Luxemburg - Lindau (6.09 MHz; 339 km) [Timpe, 1968]. In addition, the cosmic noise at 27.6 MHz [Schwentek and Gruschwitz, 1970] has been recorded by the corner-reflector antenna of the riometer used directed to the Pole Star.

In the period October 27 until November 2, 1968, several solar flare effects occurrred, some of them being very great; they will be described in the following section. Concerning the aurora and the geomagnetic storm which appeared in that period see the paper of Czechowsky, Kochan, Lange-Hesse, Lauche and Möller of pages 296 to 309 of this Report.

Description of the solar flare effects

The data characterizing each effect are compiled in Table 1. They are listed as far as they could be derived from the records. It should be mentioned that such effects can be observed only between sunrise and sunset. Solar flares occurring when there is nighttime at Lindau can be recorded only by stations in daylight.

In order to obtain a complete picture of all the events in the period October 27 to November 2, 1968, all available observations have to be collected and analyzed. Here only a description of the effects as observed at Lindau will be given.

After October 21, when a weak solar flare effect was recorded, the next effect occurred on October 27. It was a heavy double effect; this can be recognized clearly only on the record of 6.09 MHz in Fig. 2. Also the cosmic noise record shows two maxima of absorption. However, on this day, the normal trend of cosmic noise was obscured by solar noise. The trend of signal strength recorded on 2.61 MHz and 2.77 MHz is rather curious, in fact unique. Very probably the signal strength between 1300 UT and 1400 UT is not due to the ground wave.

From the ionogram taken at 1330 UT a value of f-min = 2.6 MHz was derived. That is to say that there were no echoes from the E layer.

While October 28 was undisturbed, on October 29 three solar flares were recorded, one of them a rather great one. The weaker effects can be recognized clearly only on the records of the lower frequencies in Fig. 3. The cosmic noise record is very much disturbed and on it only the time of maximum absorption can be derived.

Table 1 Data of solar flare effects observed at Lindau in the period October 27 to November 2, 1968

(NL circuit = Norddeich-Lindau; KL = Kiel-Lindau; LL = Luxemburg-Lindau; N = a value cannot be derived; U = uncertain value; S-SWF = sudden shortwave fadeout; V-SWF = V-shaped shortwave fadeout)

Date 1968	Start UT	Maximum UT	End UT	Type	Absorption dB	Duration min	Circuit
Oct 27	1236	N	1424	S-SWF	> 27	108	NL
	1237	N	1430	S-SWF	> 28	113	KL
	1236	1242	1300	S-SWF	U 21	24	LL
	1300	U 1329	U 1430	V-SWF	U 22	90	LL
	N	1242	N	N	N	N	Riometer
	N	U 1333	N	N	N	N	Riometer
Oct 29	U 0904	0915	0927	V-SWF	27	23	NL
	0903	0909	0933	V-SWF	21	30	KL
	N	1000	1015	N	15	N	NL
	0936	0957	U 1015	V-SWF	15	39	KL
	1218	N	1353	N	> 35	95	NL
	1215	N	1420	N	> 39	125	KL
	1217	1235	1349	V-SWF	15	91	LL
	N	1232	N	V-SWF	N	N	Riometer
Oct 30	1242	1300	1315	V-SWF	26	33	NL
	1248	1300	1324	V-SWF	25	36	KL
	1248	U 1300	N	N	U 10	N	LL
	N	1301	N	N	N	N	Riometer
	1318	1354	1419	V-SWF	19	61	NL
	1327	U 1351	1421	V-SWF	18	54	KL
Nov 1	U 0836	N	1007	V-SWF	> 22	91	NL
	0836	N	1006	V-SWF	> 25	90	KL
	U 0839	U 0909	N	V-SWF	N	N	LL
	U 0848	0900 - 1000	N	N	0.53	N	Riometer
Nov 2	0948	N	1112	N	> 19	84	NL
	0948	N	1113	N	> 18	85	KL
	0949	N	1100	S-SWF	> 26	71	LL
	0950	1001	1057	S-SWF	2.27	67	Riometer

On October 30 a double effect occurred as shown in Fig. 4. The greater one can be recognized on all four records. This double effect is also seen on the record of the backscatter circuit Bielstein - Lindau [See Czechowsky et al. in this Report].

The solar flare effect which occurred on November 1 appears on the records of the two lower frequencies as usual. On 6.09 MHz it does not show up very distinctly and on 27.6 MHz it is irregular. After the decrease of the noise power the level remains constant for about one hour, and subsequently shows a burst of solar noise from 1000 UT to 1215 UT with maximum at 1040 UT.

The records taken during the night of November 1 to 2 indicate a greatly disturbed 1 F transmission. This is supported by applying transmission curves of the circuits to the ionograms of the Lindau station which show a largely decomposed F layer. Sometimes there is a 1 Es transmission. This can be deduced from strong increases of the signal strength, partly observed simultaneously on the circuits Norddeich - Lindau and Kiel - Lindau.

Very typical is the strong solar flare effect on November 2, 1968 in Fig. 5. The signal strength of the two lower frequencies is reduced to zero (ground wave on 2.614 MHz). Only the cosmic noise record at 27.6 MHz shows the complete trend of the effect due to the small absorption at such high frequencies as shown in Table 1.

REFERENCES

DE MASTUS, H. and M. WOOD	1960	Shortwave fadeouts without reported flares, J. Geophys. Res., 65, 609-611.
HARTMANN, G. and H. SCHWENTEK	1969	Solar X-ray intensities measured via SOLRAD satellites and their influence on the D and E region of the ionosphere; will be published in Space Research X, containing papers presented at the COSPAR Meeting at Prague 1969.
VAN ALLEN, J. A.	1969	Solar X-ray flares May 23, 1967, in Report UAG-5 of World Data Center A, Boulder, Colorado.
ESSA	1969	Report UAG-5 (1969), Data on solar event of May 23, 1967, and its geophysical effects, World Data Center A, Upper Atmosphere Geophysics, Boulder, Colorado.
SCHWENTEK, H. and E. H. GRUSCHWITZ	1970	Measurement of absorption in the ionosphere on 27.6 MHz at 52° N by means of a riometer and a corner reflector antenna directed to the Pole Star, J. Atmos. Terr. Phys., 32, in press.
SCHWENTEK, H.	1958	Bestimmung eines Kennwertes für die Absorption der Ionosphäre aus einer automatisch-statistischen Analyse von Feldstärkeregistrierungen, Arch. Elektr. Übertr., 12, 301-308.
SCHWENTEK, H.	1966	The determination of absorption in the ionosphere by recording the field strength of a distant transmitter, Ann. Geophys., 22, 276-288.
TIMPE, Ch.	1968	Bestimmung der Absorption der Ionosphäre aus Feldstärkeregistrierungen von 6,09 MHz über 339 km, Diplomarbeit, Max-Planck-Institut für Aeronomie, Lindau.

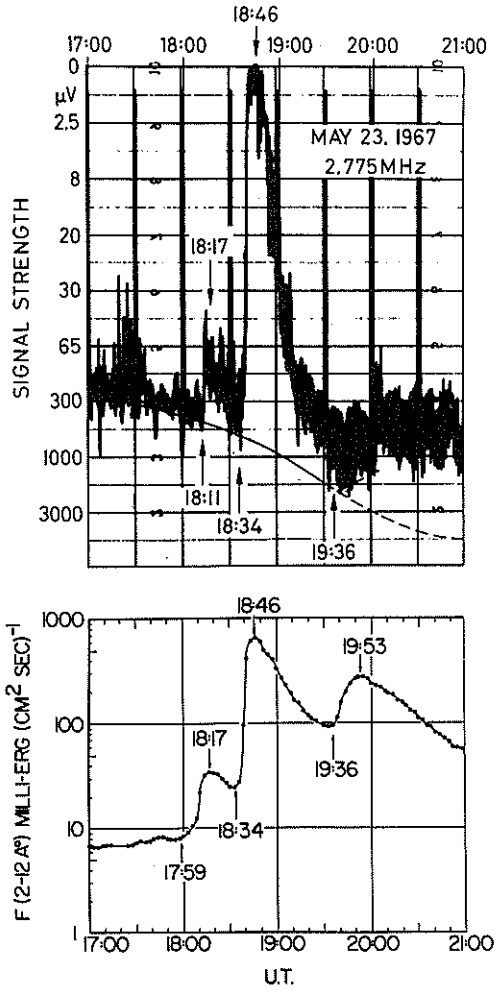

Fig. 1. Absolute solar x-ray flux observed with Explorer 33 (Van Allen, 1969), and signal strength of the transmitter Kiel recorded at Lindau (distance 300 km), as a function of time in the period 1700 - 2100 UT, May 23, 1967. The signal strength varies rather similarly with the solar flux. Shortly after 2000 UT (sunset), the 1 E transmission being the dominant mode in the daytime, is replaced by the 1 F mode (nighttime conditions), and then there is no more absorption in the D region. Due to sunset, the solar effect cannot be pursued longer than to about 2000 UT at Lindau.

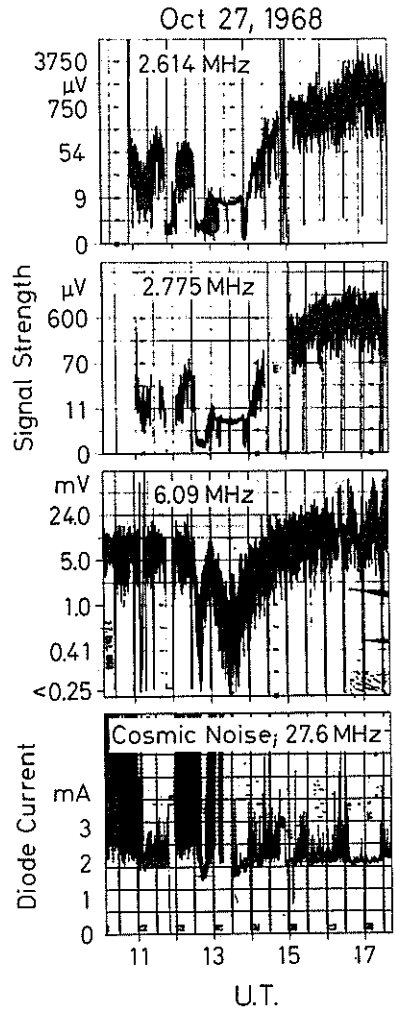

Fig. 2. Shortwave fadeouts on October 27, 1968. The gaps before 1200 UT are produced for timing; the small lines always indicate the interval 29 to 30 minutes, or 59 to 60 minutes, respectively, given by a crystal clock; E indicates periods for calibration.

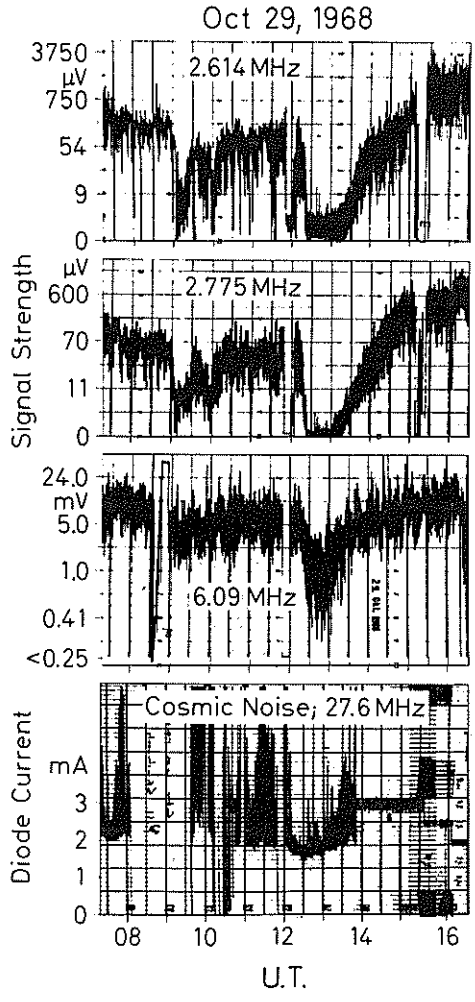

Fig. 3. Shortwave fadeouts on October 29, 1968. E = calibration. At 6.09 MHz calibration was carried out between 0830 UT and 0900 UT.

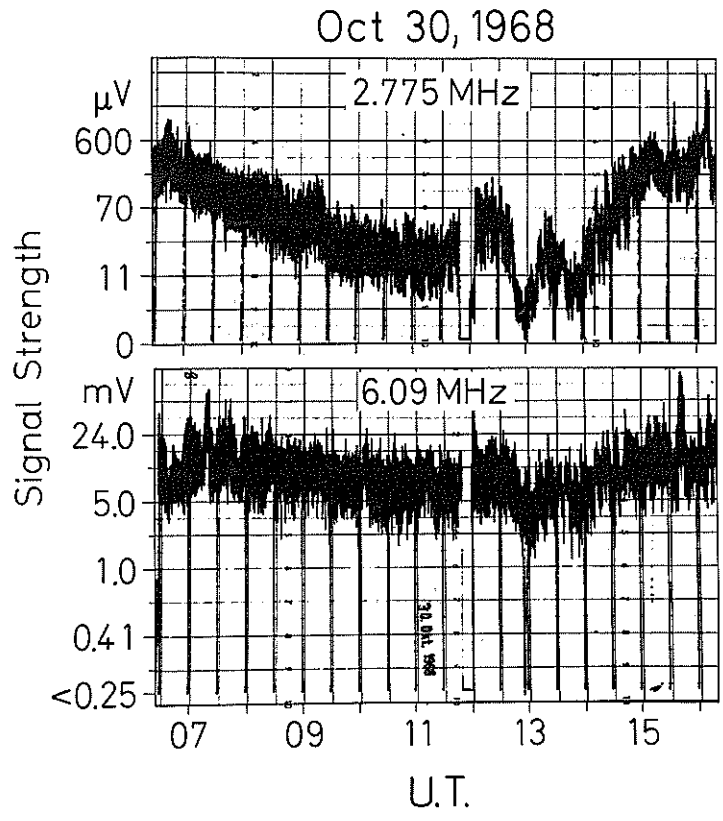

Fig. 4. Shortwave fadeouts on October 30, 1968.

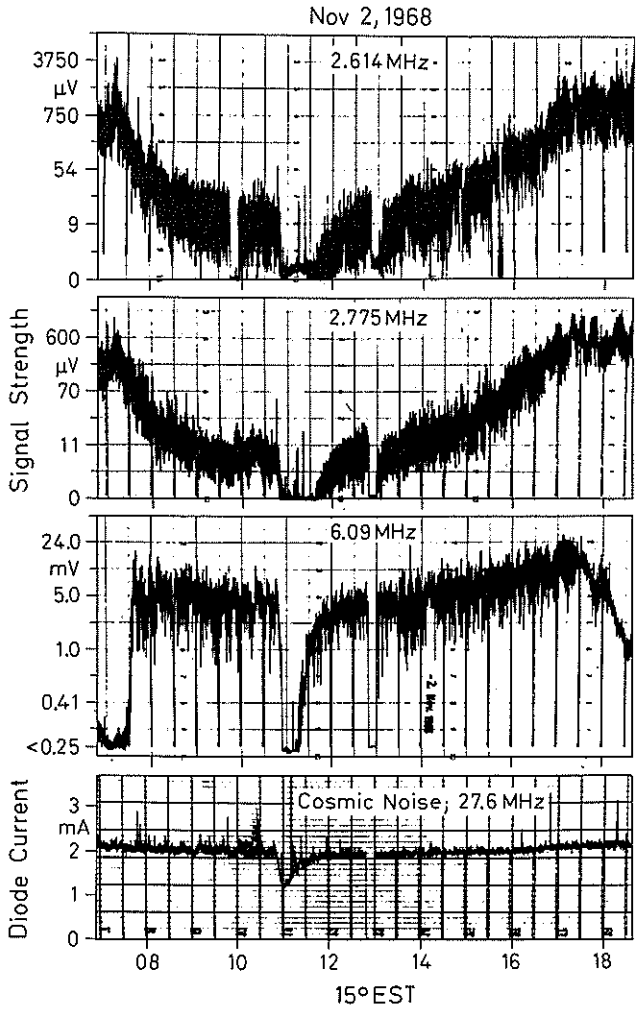

Fig. 5. Shortwave fadeout on November 2, 1968.

8. SPACE OBSERVATIONS - ELECTRONS, PROTONS, ALPHAS, INTERPLANETARY MAGNETIC FIELDS

"Explorer 34 Solar Proton Monitoring Experiment, Ep >10 Mev, October 21-November 10, 1968"

by

C. O. Bostrom
John Hopkins University Applied Physics Laboratory
and
D. J. Williams and J. F. Arens
NASA Goddard Space Flight Center

[The compiler has prepared the following paragraph and figure from the data routinely published in "Solar-Geophysical Data".]

In Figure 1 the proton intensities in the energy range Ep ≥10 Mev from the Solar Proton Monitoring Experiment (SPME) are presented for the period October 21-November 10, 1968. These data are from "Solar-Geophysical Data", No. 298, Part II, p. 163 and No. 300, Part II, p. 91. The Descriptive Text issued as IER-FB 294 (Supplement) to "Solar-Geophysical Data" describes these measurements on pages 64-69. The events are complex beginning on October 29 and continuing through November 5, 1968.

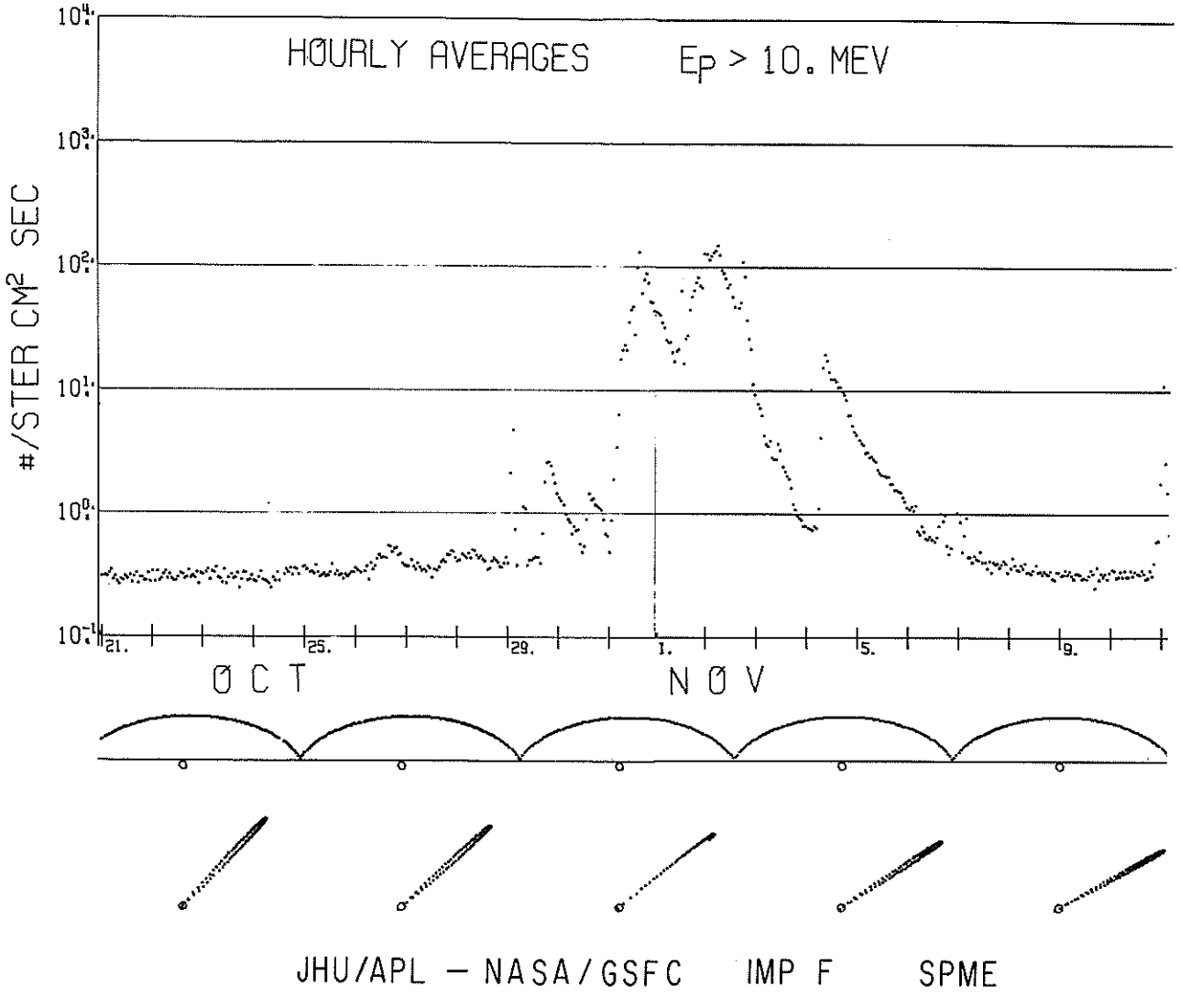

"Explorer 35 University of California Energetic Particles Experiment October 26 - November 22, 1968"

by

Robert B. Lin
Space Sciences Laboratory
University of California, Berkeley

Figure 1 consists of plots of one-hour averages of the detectors' count rates over the 28-day period beginning 26 October, 1968. The three curves never cross each other; detector GM2 is on top, GM1 is in the middle, and the IC is the lowest curve. At the top of the figure is the ecliptic longitude of the satellite position (sun-earth-satellite angle projected on the ecliptic plane, measured counter-clockwise as seen from the north pole). Fluxes can be derived from the counting rates by multiplying by the following factors after subtracting background:

$$\text{Particle Flux GM1 } (cm^{-2}sec^{-1}ster^{-1}) = \text{Count Rate GM1} \times 28$$
$$\text{Particle Flux GM2 } (cm^{-2}sec^{-1}ster^{-1}) = \text{Count Rate GM2} \times 3.5$$

Explorer 35 is a lunar orbiting spacecraft with aposelene of 5.42 R_L (1 R_L = lunar radius = 1738 km) and periselene of 1.46 R_L. The orbital period is 11.5 hours and the orbital plane is inclined 14° off the ecliptic plane. As the moon orbits the earth, Explorer 35 effectively traces out a circular orbit at the lunar orbital radius of ~60 R_E. Lunar effects, such as shadowing [Lin, 1968] are evident in the data, as well as terrestrial radiation in the Earth's magnetic tail (ecliptic longitude ~150°-210°).

The three curves denoted GM1, GM2 and IC refer to three detectors in the University of California experiment aboard Explorer 35 (AIMP-2). These are described in detail elsewhere [Lin, 1968]. Essentially GM1 and GM2 are Geiger-Mueller detectors sensitive to >45 keV electrons, and >22 keV electrons and >0.3 MeV protons, respectively. IC refers to an ionization chamber sensitive primarily to protons of ≥ 15 MeV energy, although energetic x-ray bursts are occasionally observed (identifiable by their rapid variation, usually less than 1 hour). Galactic cosmic ray background levels (bkd) for each detector are indicated on the left-hand side of the figure.

REFERENCES

LIN, R. P. 1968 Observations of Lunar Shadowing of Energetic Particles, J. Geophys. Res., 73, 3066-3071.

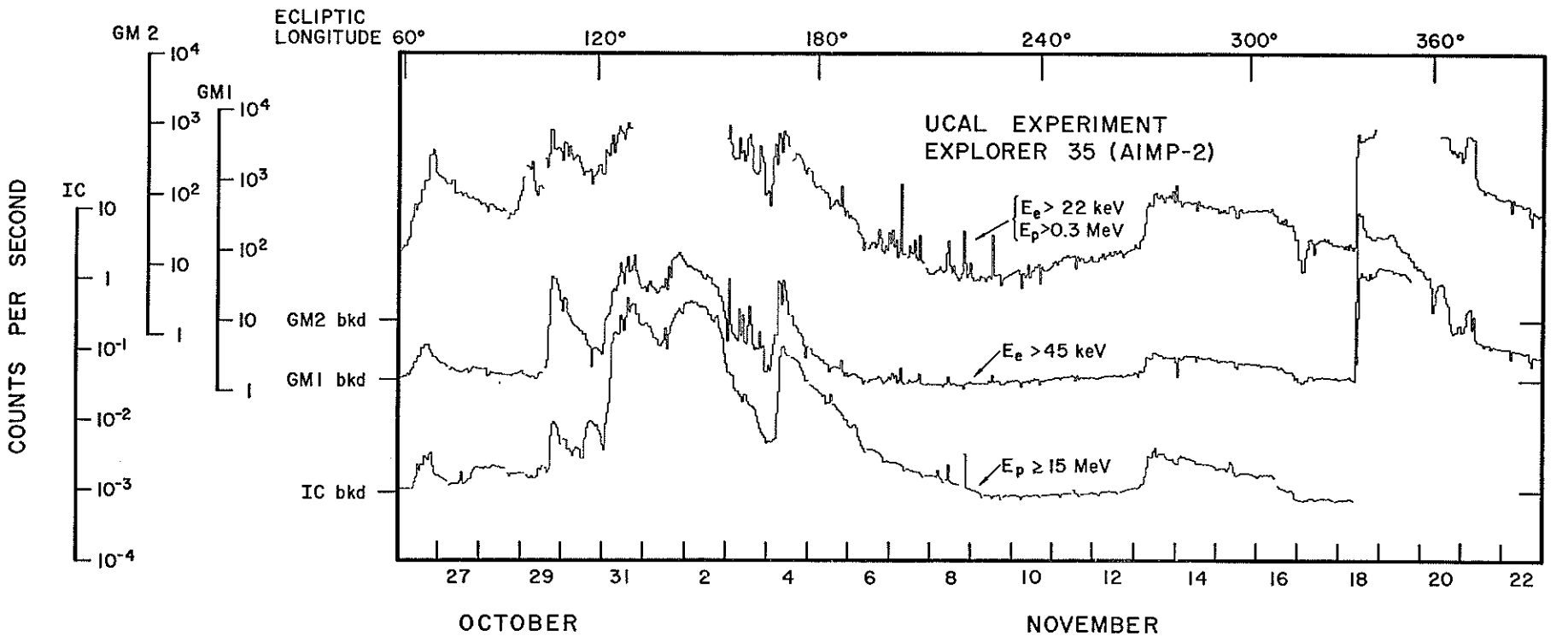

Fig. 1. One-hour averages of the count rates by detectors on Explorer 35, October 26 - November 22, 1968.

"Temporal Variation in the 100 kev to 8 Mev Solar Protons during the October/November 1968 Event"

by

F. Søraas and A. Gjerde
Department of Physics
University of Bergen, Bergen, Norway

This paper reports preliminary results from the S71C experiment (University of Bergen, Norway and Danish Space Research Institute, Denmark) for the October/November 1968 Event.

The experiment is flown onboard the ESRO I (Aurorae) satellite launched on October 3, 1968 into a near-polar orbit with inclination 94°, apogee 1540 km and perigee 260 km. During the period considered perigee was over the northern polar region. The satellite is magnetically stabilized.

The S71C experiment employs three totally depleted surface barrier detectors, two unshielded detectors D_1 and D_2, and one background detector D_3, shielded by 0.3 mm of aluminum. The detectors have the following orientation: D_1 along, D_2 normal and D_3 45° with the magnetic field. The orientation of the detectors in the northern hemisphere is such that D_1 detects particles that will be absorbed in the atmosphere, whereas D_2 responds to particles that mirror at the satellite altitude. A collimator restricts the solid angle of the detector to 0.074 sr. and the directional geometric factor is 0.037 cm^2 sr. Magnets in front of the apertures sweep away electrons with energy less than 500 kev. Each detector is followed by a charge-sensitive amplifier and a main amplifier. The signals from the amplifiers are fed to a six-channel differential pulse-height analyzer. In the first five channels both protons and alpha-particles will be recorded, while channel six will respond to alpha-particles only.

The different energy channels are counted sequentially taking two adjacent channels each time. The counting period being 0.345 seconds. A complete sample of all three detectors is obtained every 3.6 seconds. A complete description of the instrument is given by Søraas et al. [1969].

In order to study the time history of the solar protons, data from each pass above invariant latitude 78° were averaged. The results are shown in Figure 1 where the count rates of the energy channels (115-180)kev, the (475-880)kev and the (2900-8000) kev of precipitated protons are plotted versus time. The time period covered is from October 27, 1968 through November 4, 1968. In this report no interpretation of the data will be given and the variations in the count rates will not be related to flare activity on the sun. Comparing these data with the data obtained from the detector looking normal to the magnetic field, it appears that the proton pitch angle distribution below 1 Mev was peaked along the magnetic field. Above this energy the pitch angle distribution was isotropic. This seems to be the case for the whole time period covered in Fig. 2. To convert the count rates given in Fig. 1 to protons/cm^2 s sr. Mev the (115-180)kev, the (475-880)kev and the (2900-8000)kev channels must respectively be multiplied by the following factors 1200, 193, 15.4.

The count rates given in Fig. 1 are preliminary as they have not yet been corrected for background. The background corrections will be important for the time period after October 31. It can be of the order of 10%. No correction is either made for the possible "contamination" of auroral protons. In order to do the corrections the data must be looked into in great detail.

At the beginning of October 27 there was a fairly high flux of protons in the two lowest energy channels, but no detectable flux in the (2900-8000)kev channel. The intensity of the low energy protons decreases and reaches a minimum late in the evening on October 28. Around 0000 UT on October 29 there is a rapid increase in the two lowest energy channels reaching a maximum around 1200 UT. Late in the evening the fluxes are down to a minimum again. During October 30 there are some variations in the count rates in the two lowest energy channels. Around 0700 UT on October 31 there is an increase in the count rates in all three channels. This is the first time during the time covered in Fig. 1 that the flux in the (2900-8000) kev channel exceeds 15 protons/cm^2 s sr. Mev. The count rate in this energy channel has two pronounced maxima, during the days October 31 to November 2. The count rates in the two lowest energy channels have during that time period high and variable values. Early in the morning on November 4 there is an increase in the count rates in the two high energy channels. The increase in the (115-180)kev channel is delayed for some hours. The count rates reach a maximum around noon and then start to decay.

In Fig. 2 two sample energy spectra of the solar protons in the time period considered are shown. In order to obtain the energy spectrum, data from the background detector are used together with data from the detector looking normal to the magnetic field. The data points are fit fairly well by a power law differential energy spectrum.

REFERENCE

SØRAAS, F., K. AARSNES, H. R. LINDALEN and M. MØHL MADSEN 1969 "A satellite instrument for measuring protons in the energy range 0.1 Mev to 6 Mev", Department of Physics, University of Bergen, Norway, Report No. 8.

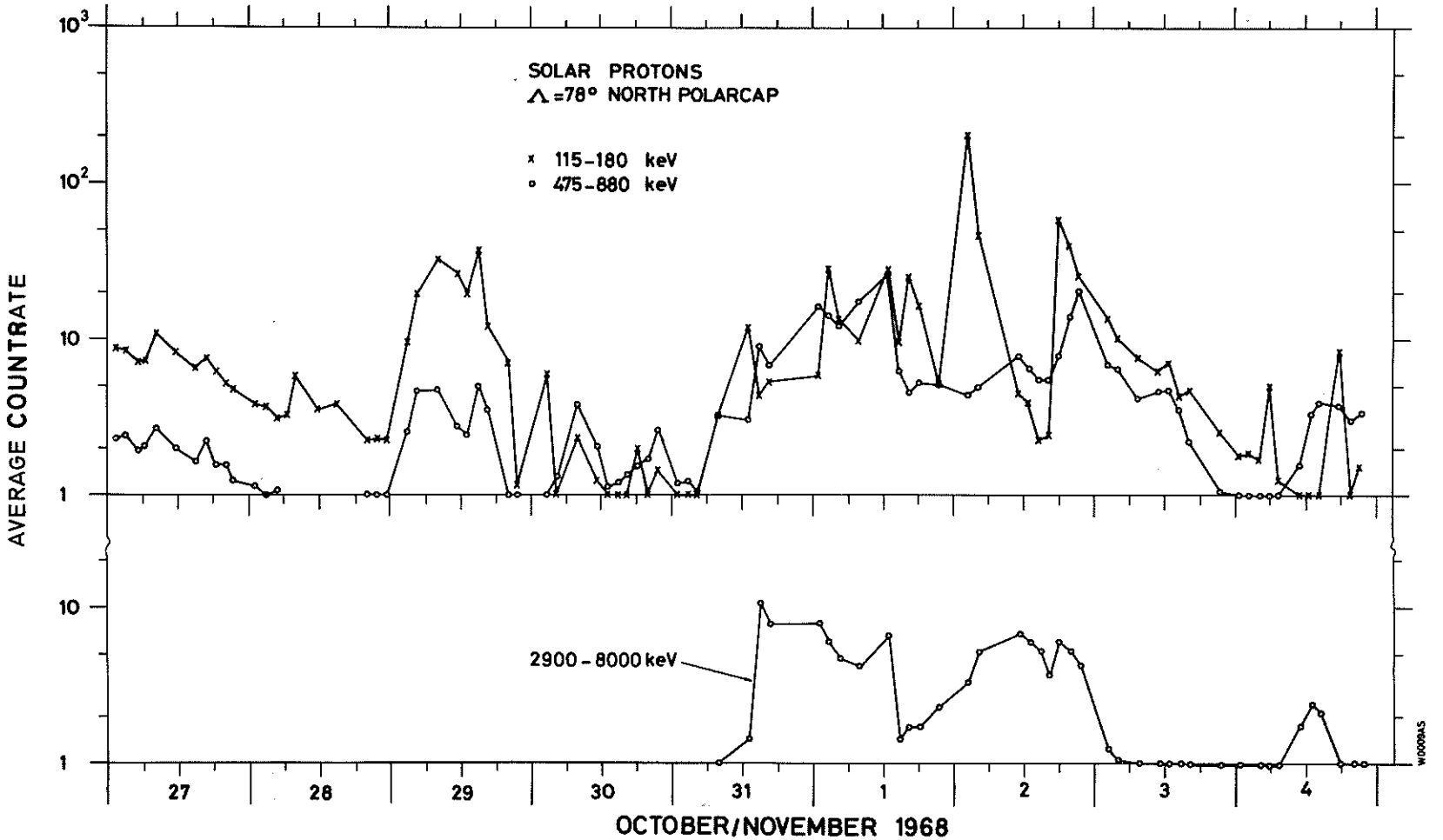

Fig. 1. Three channels of the detector looking along the magnetic field plotted versus time. The numbers indicating the dates are placed at 1200 UT.

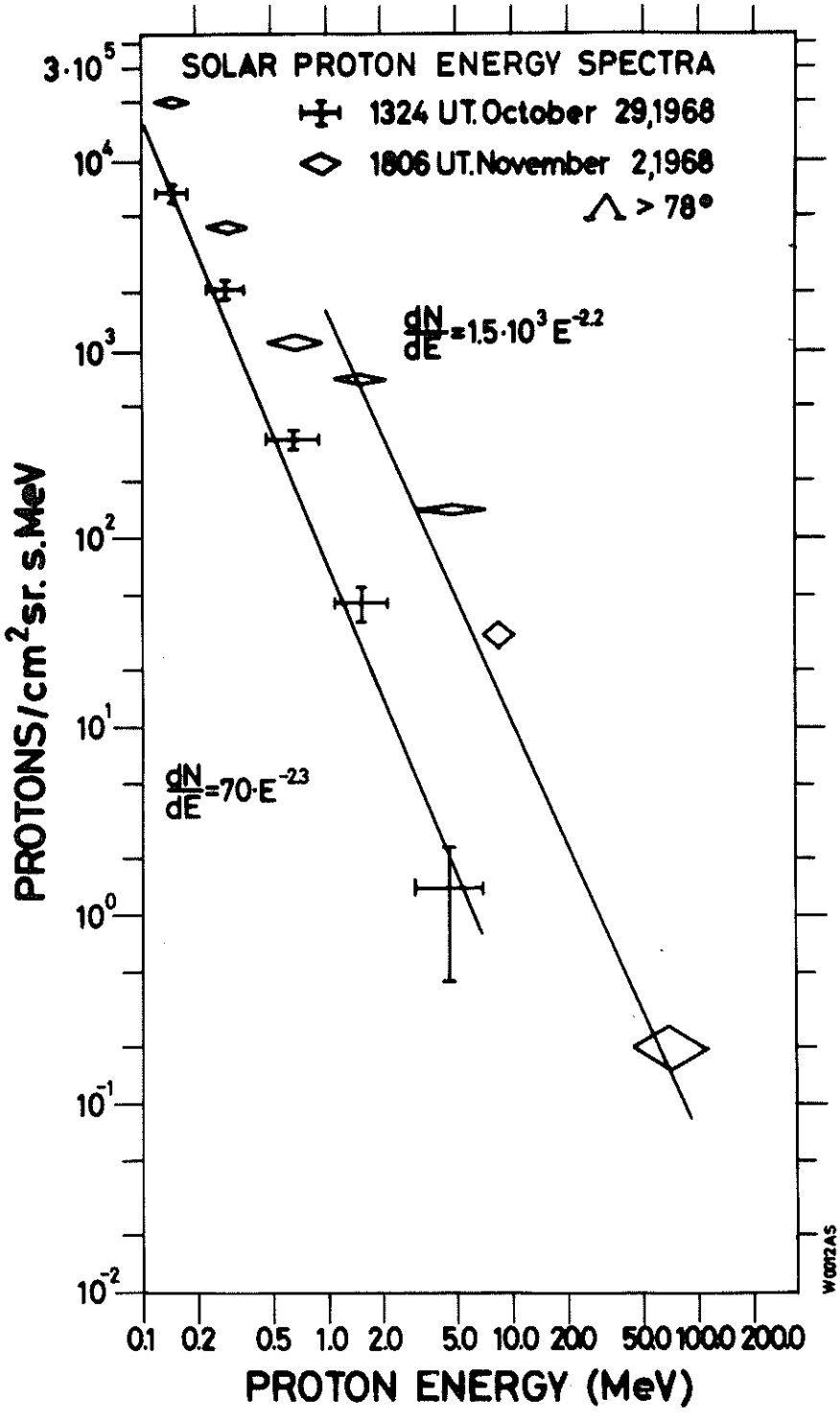

Fig. 2. Sample spectra from the S71C experiment are shown to be fairly well fitted by a law $dN/dE = NoE^{-\gamma}$.

"ATS-1 Energetic Proton Flux (5-70 Mev) at the Synchronous Orbit during the Proton Events of October - November 1968"

by

G. A. Paulikas and J. B. Blake
Space Physics Laboratory
The Aerospace Corporation, Los Angeles, California

The data in Figure 1 on the 5-70 Mev proton flux were obtained aboard the ATS-1 satellite. The 21-70 Mev flux at this orbit appears to be identical to the interplanetary flux. The 5-21 Mev flux departs in a complex way from the interplanetary flux because the measurement is made inside the magnetosphere. The flux may be attenuated by up to a factor of 10 for measurements near local noon and magnetic quiet. For other local times and disturbed magnetic conditions the flux of 5-21 Mev protons measured at ATS-1 approaches the interplanetary flux.

The measurements were made with an omnidirectional spectrometer. This instrument contains shielded solid state detectors. Pulse height analysis discriminates electrons from protons and, together with the shield thickness, determines the energy bites of the instrument.

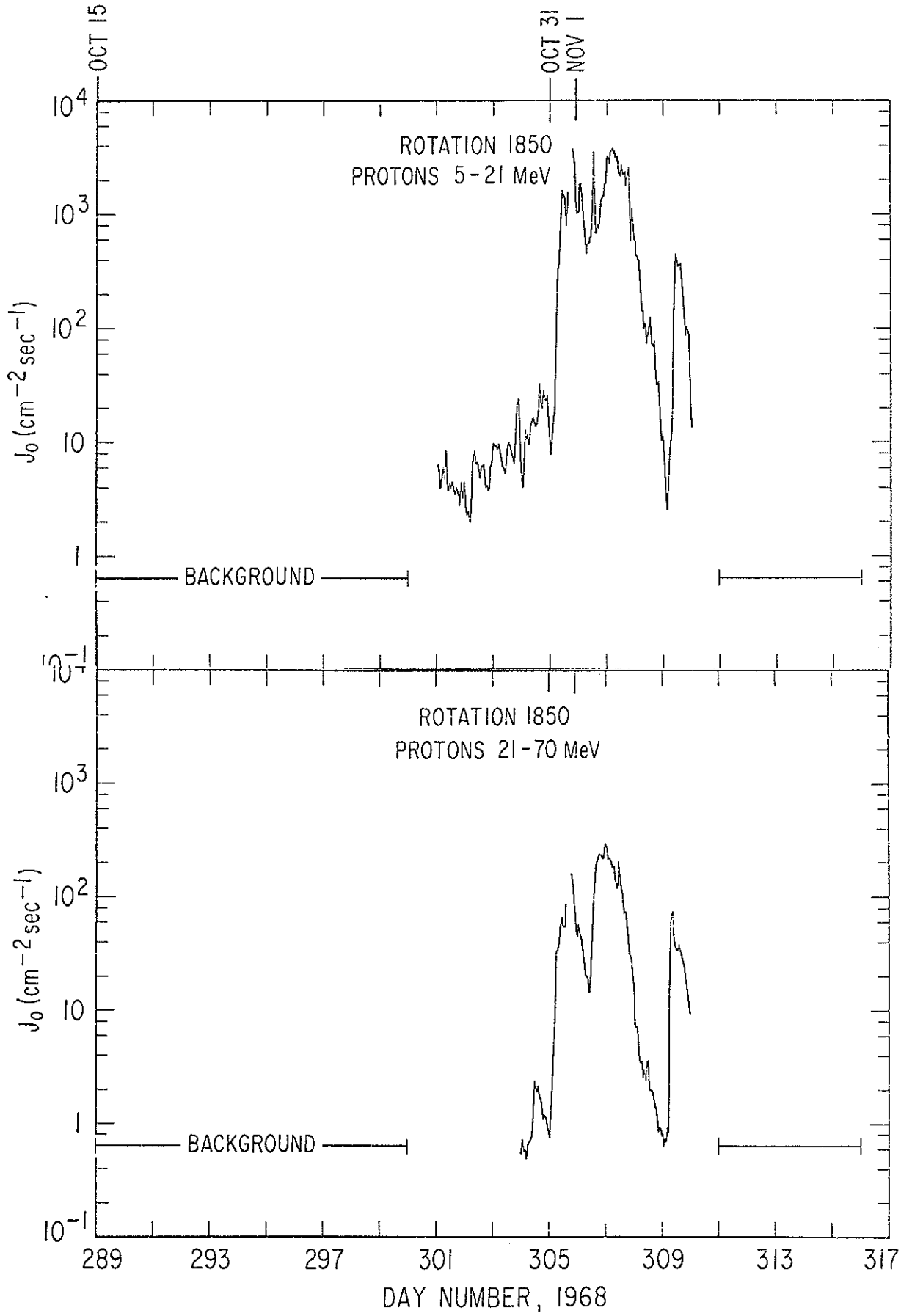

Fig. 1. Proton flux on ATS-1 satellite from October 15 - November 12, 1968

"Interplanetary Protons and Alphas: Days 300-313, 1968"

by

L. J. Lanzerotti and C. M. Soltis
Bell Telephone Laboratories
Murray Hill, New Jersey

Introduction

The period in late October and early November, 1968, represented an interval of time when the interplanetary medium was quite disturbed and heavily populated with low energy solar protons. The solar flare-produced disturbances in the solar wind caused at least five large sudden commencements (SC) to be recorded in the earth during the seven days from October 26 through November 1.

The interplanetary measurements reported here were made by the Bell Laboratories experiment on the Explorer 34 (IMP F) satellite. Explorer 34 was a spin stabilized (with spin axis perpendicular to the ecliptic plane) satellite with an apogee of approximately 34 R_E. The BTL experiment consisted of a four element solid state telescope oriented perpendicular to the spin axis. The half angle of the detector telescope defining collimator was 20°; the flux measured by the experiment was the spin averaged flux of particles in the ecliptic plane. Protons and alphas up to an energy of approximately 4 Mev/nucleon were distinguished by the energy deposited in the first two detectors of the telescope and subsequently measured in a five channel analyzer. Particle species above this energy were distinguished by the use of an on-board pulse multiplier [Lanzerotti, Lie, and Miller, 1969].

Interplanetary Observations - Protons

The interplanetary proton fluxes measured in four of the seven energy channels from day 300 to day 313 are plotted in Figure 1 together with the Alert neutron monitor counting rate. The time of the five sudden commencements (observed by more than 10 stations) are shown by inverted triangles on the neutron monitor plot [Solar-Geophysical Data, 1969a].

The data in Figure 1 suggest that the time interval shown could be characterized as consisting of four major solar flare enhancements. The first enhancement, beginning on October 26, extended through October 29; the second occurred almost entirely on October 30. The third enhancement, beginning on October 31, persisted for several days and decayed away until the sharp onset of the fourth on November 4. The initial two enhancements have quite soft spectra in comparison to the third enhancement.

A small cosmic ray decrease at the time of the SC on October 26 was measured by the Alert neutron monitor. The two low energy enhancements on October 29 were probably energetic storm particles associated with the interplanetary disturbances producing the SC's on October 28 and 29. The large Forbush decrease began within an hour or two of the SC on October 29. A decrease in the lowest energy solar proton fluxes was also observed at approximately the time of the SC and the beginning of the Forbush decrease.

The third interplanetary proton enhancement occurred during the large Forbush decrease and was characterized by extremely large modulations of the low energy particles. The contrast in the temporal development between the 0.56-0.60 Mev fluxes and the 1.2-2.4 Mev fluxes, for example, is quite striking. After the large energetic storm particle enhancement accompanying the SC on October 31, the proton fluxes (0.56-0.60 Mev) remained depressed for several hours while the proton fluxes (1.2-2.4 Mev) decreased in intensity for only approximately one-half hour before increasing again.

The proton flux enhancement beginning on November 4 has a temporal profile typical of a west limb flare; this is particularly true for the higher energy fluxes (Figure 1). McMath plage region 9740, on the extreme west limb of the sun, was quite active on November 4. A 1B flare (S15°, W90°) beginning at 0520 and having a maximum at 0527 [Solar-Geophysical Data, 1969b] was perhaps the source of the protons.

The time interval between the flare maximum and the initial observation of proton increases on November 4 are plotted in Figure 2 as a function of energy. Also shown in the figure are the predicted arrival times at the earth assuming the protons were injected into a 500 km/sec solar wind at the flare maximum with either a 0° or a 90° pitch angle [Winge and Coleman, 1968; C. R. Winge, Jr., private communication]. The data in the two lowest energy channels have two successive increases and, hence, a point is plotted for the beginning of each increase. The first flux increases in the two lowest energy proton channels appear to have occurred prior to the time expected if they resulted from the 0520 UT flare. Hence, it is possible that these initial increases could have been due to an earlier 1B flare that lasted from 0202 to 0334 UT [Solar-Geophysical Data, 1969b].

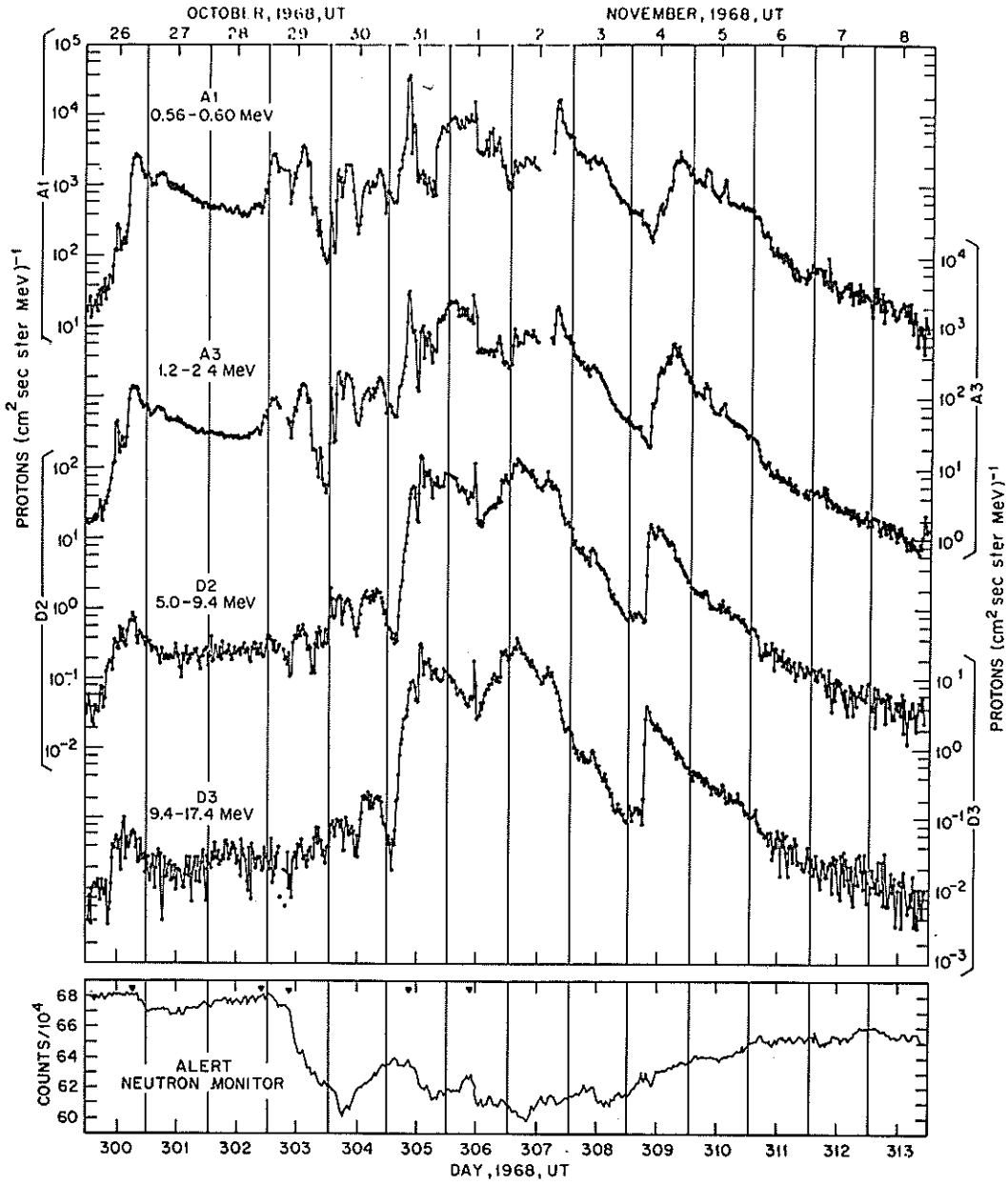

Fig. 1. Solar Proton Data from day 300 to day 314, 1968. The Alert neutron monitor counting rate is plotted at the bottom of the figure. The times of five sudden commencements are marked on the neutron monitor data.

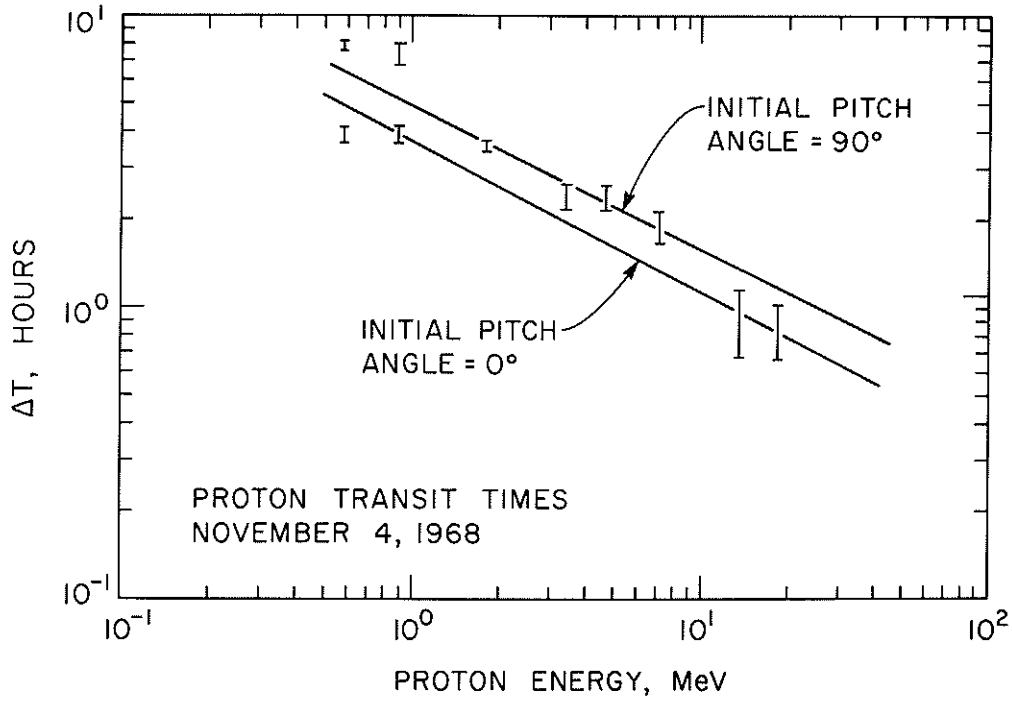

Fig. 2. Transit time for solar particle enhancements at the earth produced by a 1B flare (maximum at 0527 UT) on November 4, 1968. The two theoretical transit times for 0° and 90° initial pitch angle injections were computed by C. R. Winge, Jr.

Interplanetary Observations - Alpha Particles

Composition studies of solar cosmic rays are potentially powerful tools in unraveling source and propagation effects. The series of solar events in late October and early November were interesting in the fact that only the event commencing on October 31 contained appreciable fluxes of low energy/nucleon alpha particles. Alpha particle fluxes measured in two of the five experimental alpha channels are shown in Figure 3 for the period including the enhancement. The basic temporal history of the alpha particle fluxes during this time resembles that of the proton fluxes with the same energy/nucleon (Figure 1).

Energetic Storm Particles

Although much interesting temporal structure is seen in the data of Figure 1, there were no sharp, intense, less than one hour duration flux spikes at the time of the SC's as are sometimes seen in the low energy solar data [see, e.g., Lanzerotti, 1969]. The proton and electron counting rates measured during two time periods around the SC's on October 31 and November 1 are shown in Figures 4 and 5. Each data point corresponds to a 9.28 second counting average.

The data in Figure 4 show that a small enhancement in the lowest energy proton channel was observed approximately one minute prior to the October 31 SC at 0859 UT [Solar-Geophysical Data, 1969a]. No disturbances were seen in either the higher energy proton data or the electron data.

The data in Figure 5 show the proton and electron fluxes for the time period prior to and following the SC at 0916 UT on November 1 [Solar-Geophysical Data, 1969a]. Again the lowest energy fluxes increased in intensity prior to the SC. The higher energy proton fluxes and electron fluxes were unaffected by the interplanetary disturbance. An enhancement was observed in the proton fluxes beginning at ∿1200 UT and extending to ∿1240 UT. The flux enhancement was larger for the higher energy fluxes (as can be seen from the data in Figure 1). Almost one hour after the proton decrease at 1240, the electron fluxes increased in intensity.

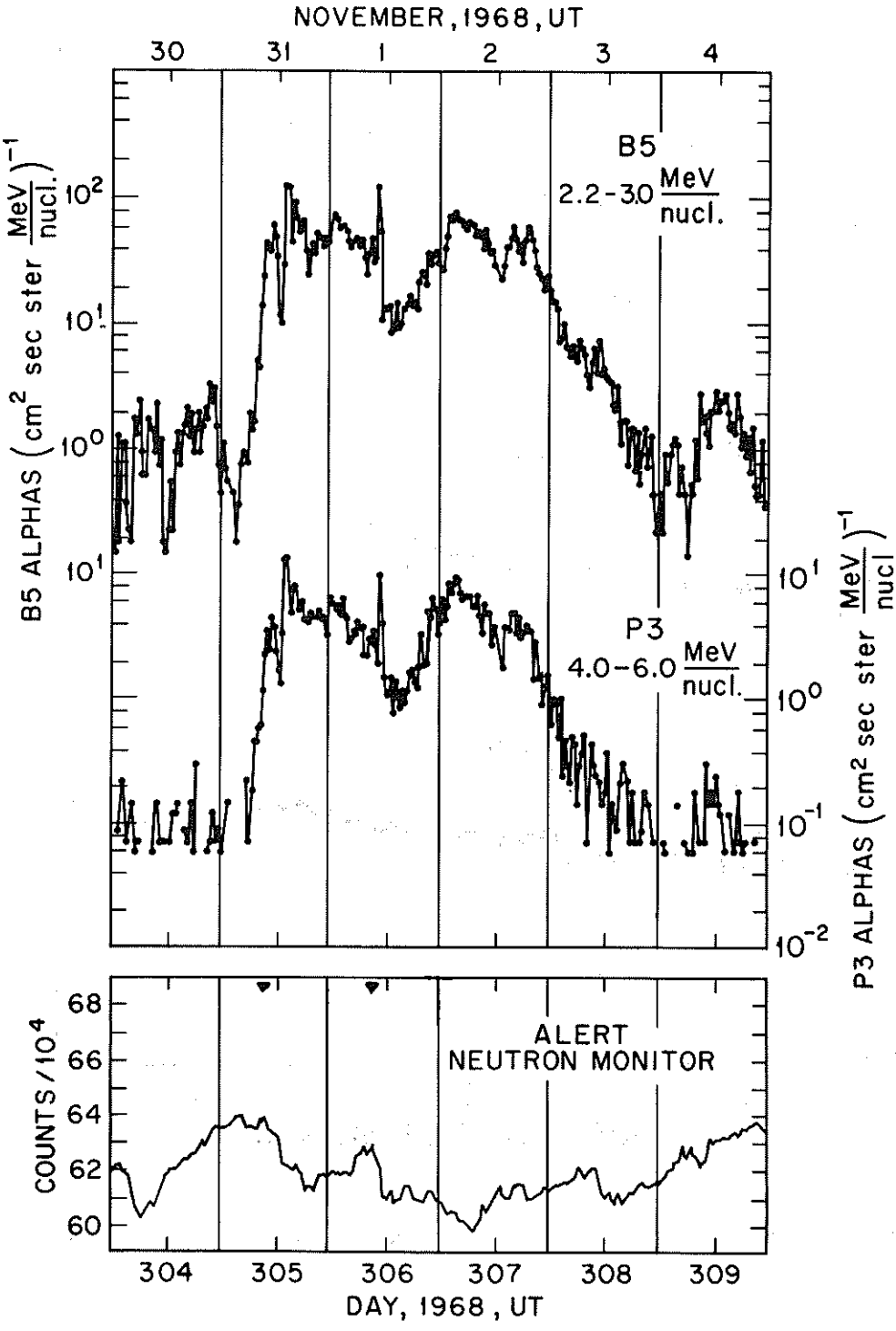

Fig. 3. Solar alpha particle fluxes during the October 31 enhancement.

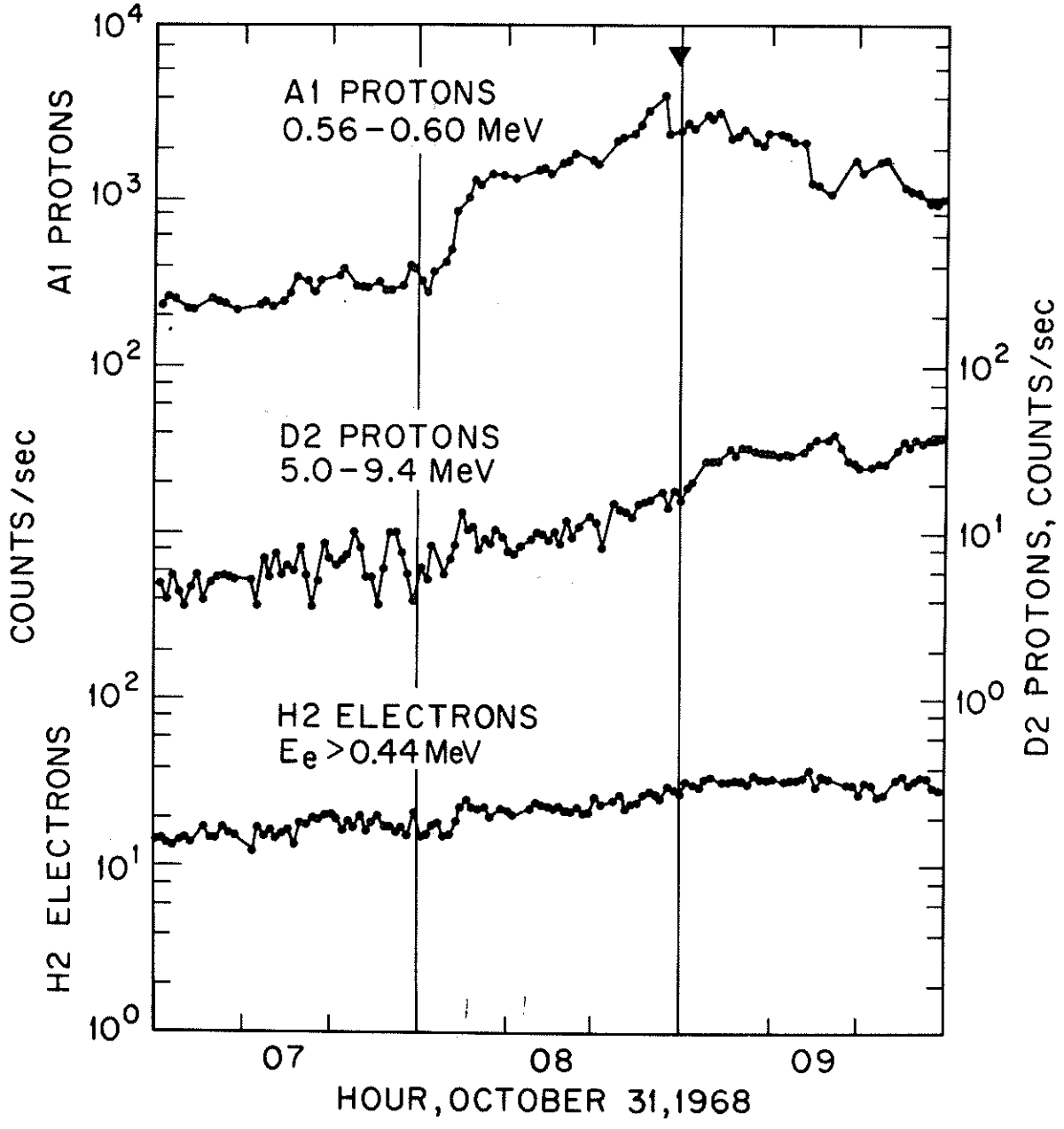

Solar particle fluxes during the time interval around the October 31 sudden commencement.

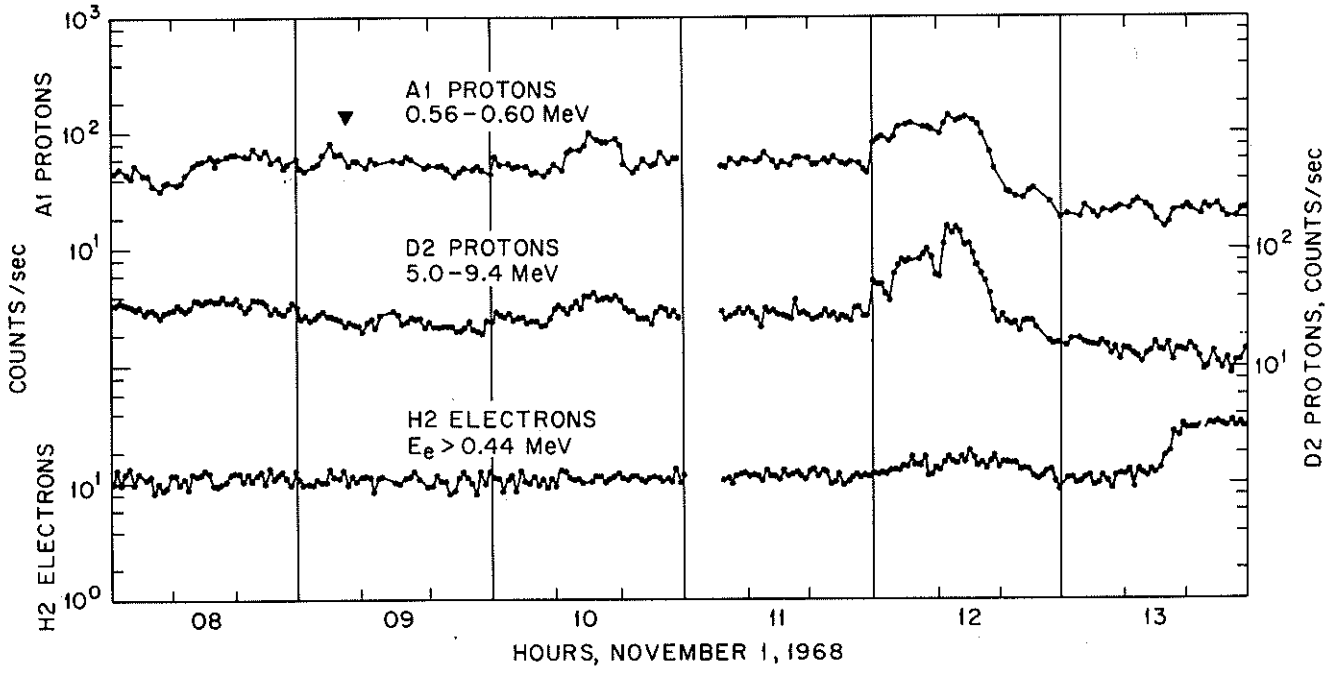

Fig. 5. Solar particle fluxes during the time interval around the November 1 sudden commencement.

REFERENCES

LANZEROTTI, L. J., H. P. LIE, and G. L. MILLER	1969	"A Solar Cosmic Ray Particle Spectrometer with on-Board Particle Identification," IEEE Trans. Nucl. Sci., NS-16, February 1969.
LANZEROTTI, L. J.	1969	"Low Energy Solar Protons and Alphas as Probes of the Interplanetary Medium: The May 28, 1967, Solar Event," J. Geophys. Res., 74, 2851.
ESSA	1969a	Solar-Geophysical Data, IER-FB-296, April 1969.
ESSA	1969b	Solar-Geophysical Data, IER-FB-297, May 1969.
WINGE, C. R., and P. J. COLEMAN, JR.	1968	"The Motion of Charged Particles in a Spiral Field," J. Geophys. Res., 73, 165.

"Synchronous Altitude Protons and Electrons: October 26 - November 8, 1968"

by

L. J. Lanzerotti and C. M. Soltis
Bell Telephone Laboratories
Murray Hill, New Jersey, 07974

Electron and proton data obtained from a particle telescope on the synchronous altitude ATS-1 satellite during the stormy geomagnetic period from October 26 through November 8, 1968 are presented here. The stormy period resulted in large flux changes and large diurnal variations in the ATS-1 electron fluxes. The solar protons resulting from the several solar flares during this period were also observed continuously at synchronous altitude.

The ATS-1 satellite (launched December 6, 1966) is a geostationary, spin-stabilized satellite (with the spin axis parallel to the local magnetic field) stationed at 158°W, 0°N (2.7°N, 278.7°E geomagnetic) and at a geocentric distance of $6.6R_E$. The Bell Telephone Laboratories (BTL) experiment flown on ATS-1 consists of a six-element solid-state detector telescope oriented perpendicular to the spin axis of the satellite. By use of the particle dE/dx characteristics and appropriate logic circuitry, the experiment is capable of distinguishing between protons, alphas, and electrons. The half-angle of the detector telescope collimator is 20°; the flux measured by the BTL experiment is the spin-averaged flux of those particles with pitch angles close to 90° [Lanzerotti, 1968a]. ATS-1 local time is obtained by subtracting 10 hours from the Universal time.

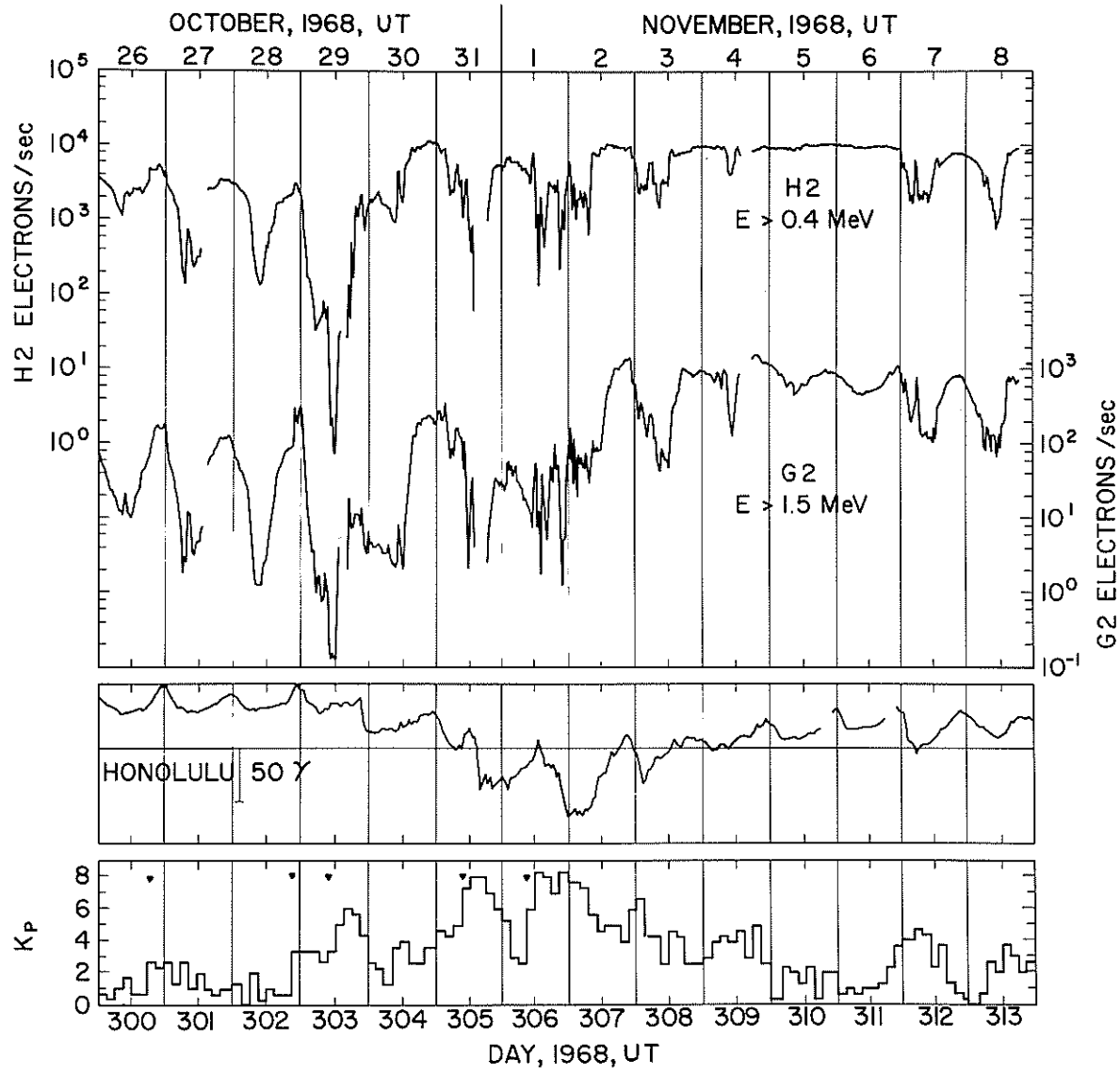

Fig. 1. Hourly average synchronous altitude electron fluxes, Kp, and the hourly value Honolulu H-component during October 26 - November 8, 1968.

The time history of the electron fluxes in two of the ATS electron channels is shown in Figure 1 together with the Kp index and the hourly value H-component of the Honolulu magnetic field (21.1°N, 266.5°E geomagnetic). The five largest SC's during this period are shown above the Kp data [Solar-Geophysical Data, 1969]. The measured electron flux intensities show the typical daily variations, with larger fluxes observed near ATS local noon than at ATS local midnight. These diurnal variations in the flux intensities arise because of the distortion of the magnetosphere from its dipolar shape by the solar wind. The ATS-1 satellite, in a circular orbit, effectively measures electrons on a higher drift shell at local midnight than at local noon. Since the ATS orbit is beyond the maximum of the outer electron belt, the fluxes are lower at midnight than at noon [Lanzerotti, et al., 1967; Brown, 1968; Paulikas, et al., 1968]. Furthermore, since the radial gradient of the higher energy electrons is larger than for the lower energies, the diurnal variation is larger in the higher energy fluxes.

The Kp and Honolulu field data of Figure 1 show clearly that on the days of greater magnetic activity (larger Kp and larger Honolulu field depression) the diurnal variations of the ATS electron fluxes become larger, less symmetrical, and undergo larger intensity variations on the scale of an hour (or less). Furthermore, on days 303-304 and days 305-307, for example, when Kp was quite large and the Honolulu H-trace indicated a field depression near local noon, the ATS electron fluxes near local noon were also strongly depressed.

The solar proton fluxes measured in two energy channels on ATS during the stormy period are shown in Figure 2. Previous work has shown that, in general, when a source of solar-originated particles is present in interplanetary space, comparable fluxes of these particles with similar spectral characteristics are usually observed inside the magnetosphere at synchronous altitudes.

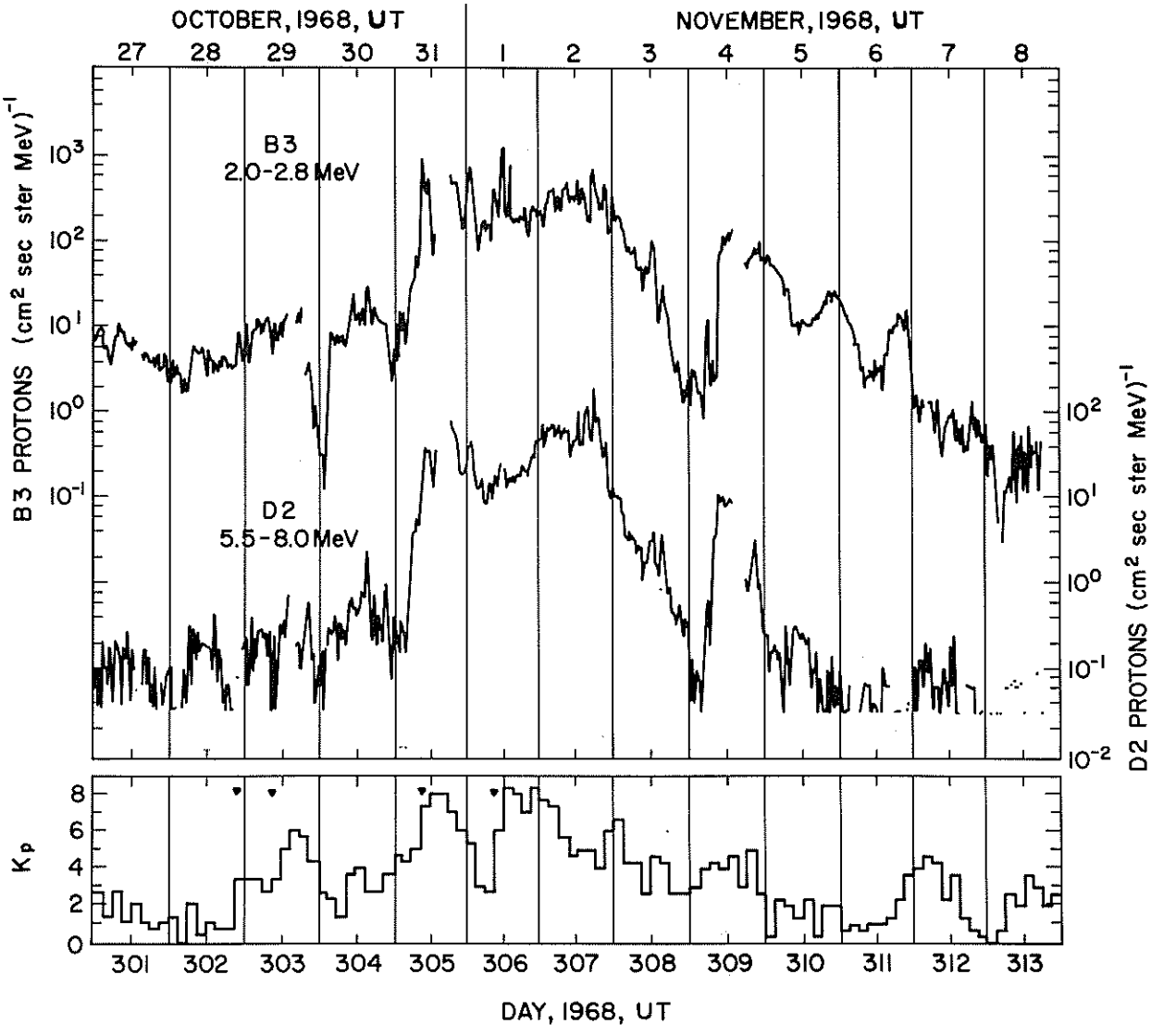

Fig. 2. Hourly average solar proton fluxes measured at synchronous altitude during October 26 - November 8, 1968.

Frequently, diurnal variations, opposite to the electron flux diurnal changes, are observed in the synchronous altitude solar proton fluxes [Lanzerotti, 1968; Paulikas and Blake, 1969; Lanzerotti, 1970]. It has been pointed out that these diurnal variations often resemble, temporarily, PCA mid-day recoveries [Leinbach, 1967; Lanzerotti, 1970]. During most of the time period, plotted in Figure 2, however, such variations were not strongly apparent.

An example of a rapid change in the synchronous altitude electron fluxes near local midnight during one of the stormy days (day 304), is shown in Fig. 3. This type of sudden increase in the fluxes near local midnight has been discussed previously by Leznick and Winckler [1969] and by Lanzerotti and Maclennan [1969] and is generally observed to accompany a simultaneous increase in the local magnetic field intensity. Although a complete understanding of such rapid flux variations requires the use of the local ATS-1 magnetic field data, the lack of time dispersions in the several small-amplitude electron enhancements plus the existence of larger increases in the higher energy fluxes than in the lower energy fluxes support the view that the changes in Figure 3 were predominately adiabatic. Occasionally, however, the occurrence of large, non-adiabatic relativistic electron enhancements with gradient drift around the earth are observed [Lanzerotti and Maclennan, 1969].

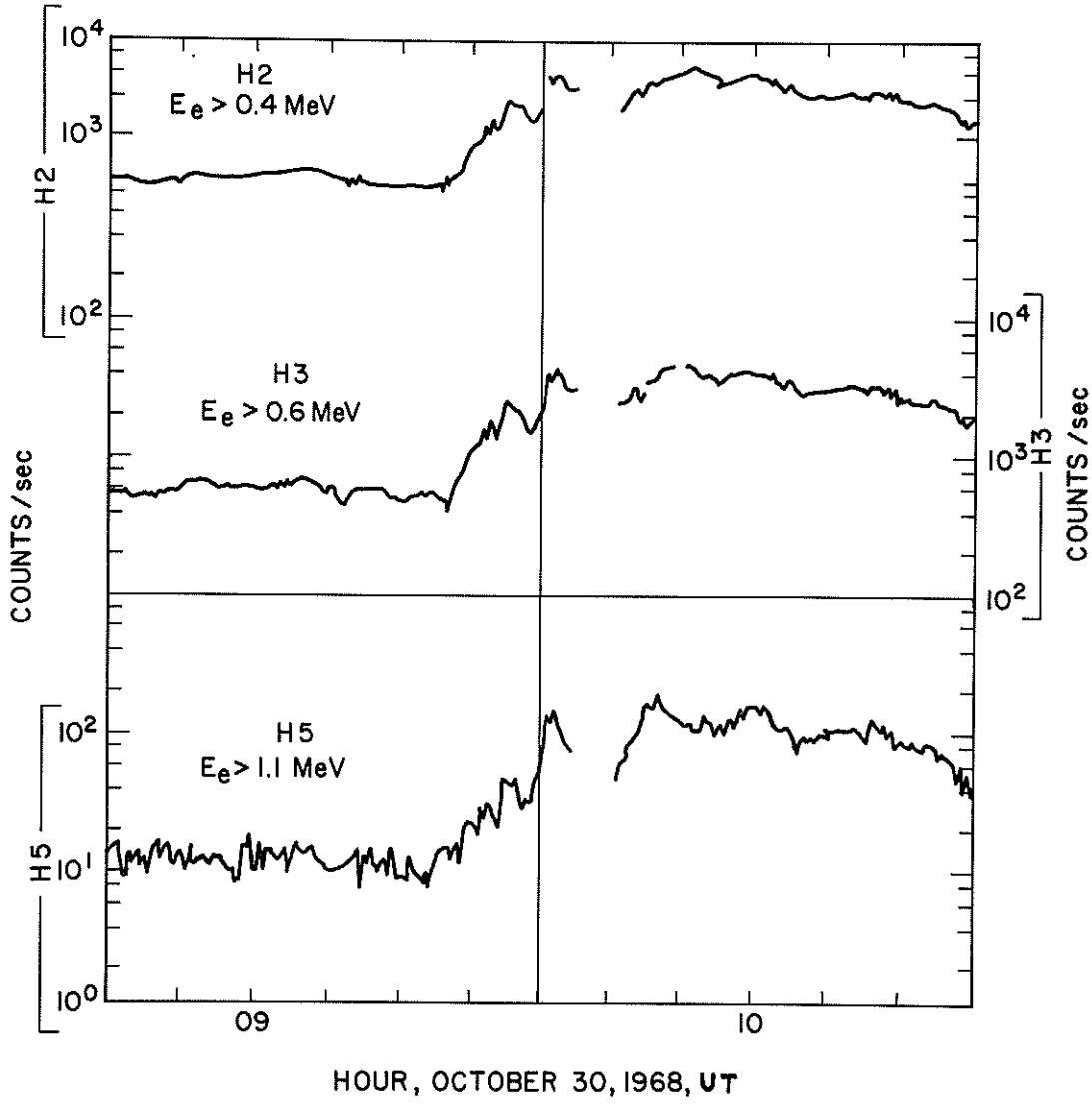

Fig. 3. Rapid time variations in the electron fluxes on October 30, 1968.

REFERENCES

BROWN, W. L.	1968	"Energetic Outer Belt Electrons at Synchronous Altitude", Earth's Particles and Fields, ed. by B. M. McCormac, Reinhold Book Corp., New York, 33-44.
LANZEROTTI, L. J.	1968a	"Calibration of a Semiconductor Detector Telescope for Space Experiments", Nucl. Instr. and Methods, 61, 99.
LANZEROTTI, L. J.	1968b	"Penetration of Solar Protons and Alphas to the Geomagnetic Equator", Phys. Rev. Letters, 21, 929.
LANZEROTTI, L. J.	1970	"Access of Solar Particles to Synchronous Altitude", Proc. Third ESRO Symposium on Intercorrelated Satellite Observations Related to Solar Events, to be published.
LANZEROTTI, L. J., and C. G. MACLENNAN	1969	"The Magnetospheric Substorm of August 25-26, 1967, Part 2: Relativistic Electron Accelerations at Synchronous Altitudes", (abstract) Trans. Am. Geophys. Union, 50, 287.
LANZEROTTI, L. J., C. S. ROBERTS, and W. L. BROWN	1967	"Temporal Variations in the Electron Flux at Synchronous Altitudes", J. Geophys. Res., 72, 5893.
LEINBACH, H.	1967	"Midday Recoveries of Polar Cap Absorption", J. Geophys. Res., 72, 5473.
LEZNIAK, T. W., and J. R. WINCKLER	1968	"Magnetospheric Substorm Effects on Energetic Electrons in the Outer Van Allen Belt" (abstract), Trans. Am. Geophys. Union, 50, 285.
PAULIKAS, G. A. and J. B. BLAKE	1969	"Penetration of Solar Protons to Synchronous Altitude", J. Geophys. Res., 74, 2161.
PAULIKAS, G. A., J. B. BLAKE, S. C. FREDEN, and S. S. IMAMOTO	1968	"Observations of Energetic Electrons at Synchronous Altitude, 1.General Features and Diurnal Variations", J. Geophys. Res., 73, 4985.
ESSA	1969	Solar-Geophysical Data, IER-FB 296, April 1969.

"Response of Electrons ($E_e \geq 0.28$ Mev) at $1.2 \leq L \leq 1.3$ to the November, 1968 Magnetic Storm"

by

J. C. Armstrong, C. O. Bostrom, and D. S. Beall*
Applied Physics Laboratory, The Johns Hopkins University
Silver Spring, Maryland

The magnetically active period in late October - early November, 1968, was unusual in that it was one of two periods over a five year time span that caused a major change in the electron population, $E_e \geq 0.28$ Mev, at L = 1.2 (the other period was May 26, 1967). A change in the flux levels of these electrons was observed during this period at all inner zone L-values covered by satellite 1963-38C. This satellite was in a near-circular, polar orbit with altitude ∿1100 km. It was magnetically aligned, and the detector of interest (silicon surface barrier) looked perpendicular to the field line, with a full angle of ∿13°. We wish to emphasize here the response of the electrons in the region L = 1.20 - 1.30. The B-values are limited to narrow bands for a given L-value and are within the interval 0.16 - 0.19 gauss. Exact ranges are given in Bostrom et al. [to be published]. Examples of the response of other inner zone particle populations in a more extended L-region can also be found in the cited paper. Approximate flux values can be obtained by multiplying the count rates by 450, but more precise procedures for determining flux are given in Beall et al. [1967].

The count rates obtained during the period of interest are shown in Figure 1, which shows the clearly recognizable responses at L = 1.2 to 1.3 of these electrons to geomagnetic activity as measured by ΣKp. A general feature of these electrons in this region of space is their response to even modest geomagnetic activity, as can be seen at day 276. For the period of interest here (day number ≥ 304), we can summarize the qualitative aspects of the response as follows:

(i) Geomagnetic activity produces an increase in count rates at all L-values between 1.2 - 1.3.

(ii) The magnitude of this increase is a maximum at L = 1.27.

(iii) Generally, both the rise and decay are slower at higher L-values.

Quantitatively, the percentage increase was a maximum at L = 1.20 (100%) and a minimum at L = 1.30 (200%). Rise time was a minimum of L = 1.20 (2.5 ± 1 days) and a maximum at L = 1.30 (8.0 ± 1 days). The decay time ranged from roughly 7.5 days at L = 1.20 to 55 days at L = 1.30.

REFERENCES

BEALL, D. S., C. O. BOSTROM, and D. J. WILLIAMS — 1967 — Structure and decay of the Starfish radiation belt, October 1963 to December 1965, J. Geophys. Res., 72, 3403-3424.

BOSTROM, C. O., D. S. BEALL, and J. C. ARMSTRONG — Time history of the inner radiation zone, October 1963 to December 1968, presented at the International Association of Geomagnetism and Aeronomy General Assembly, Madrid, Spain, September, 1969. Also accepted for publication in the Journal of Geophysical Research.

*Present Address:

University of Wisconsin
Department of Computer Sciences
Madison, Wisconsin

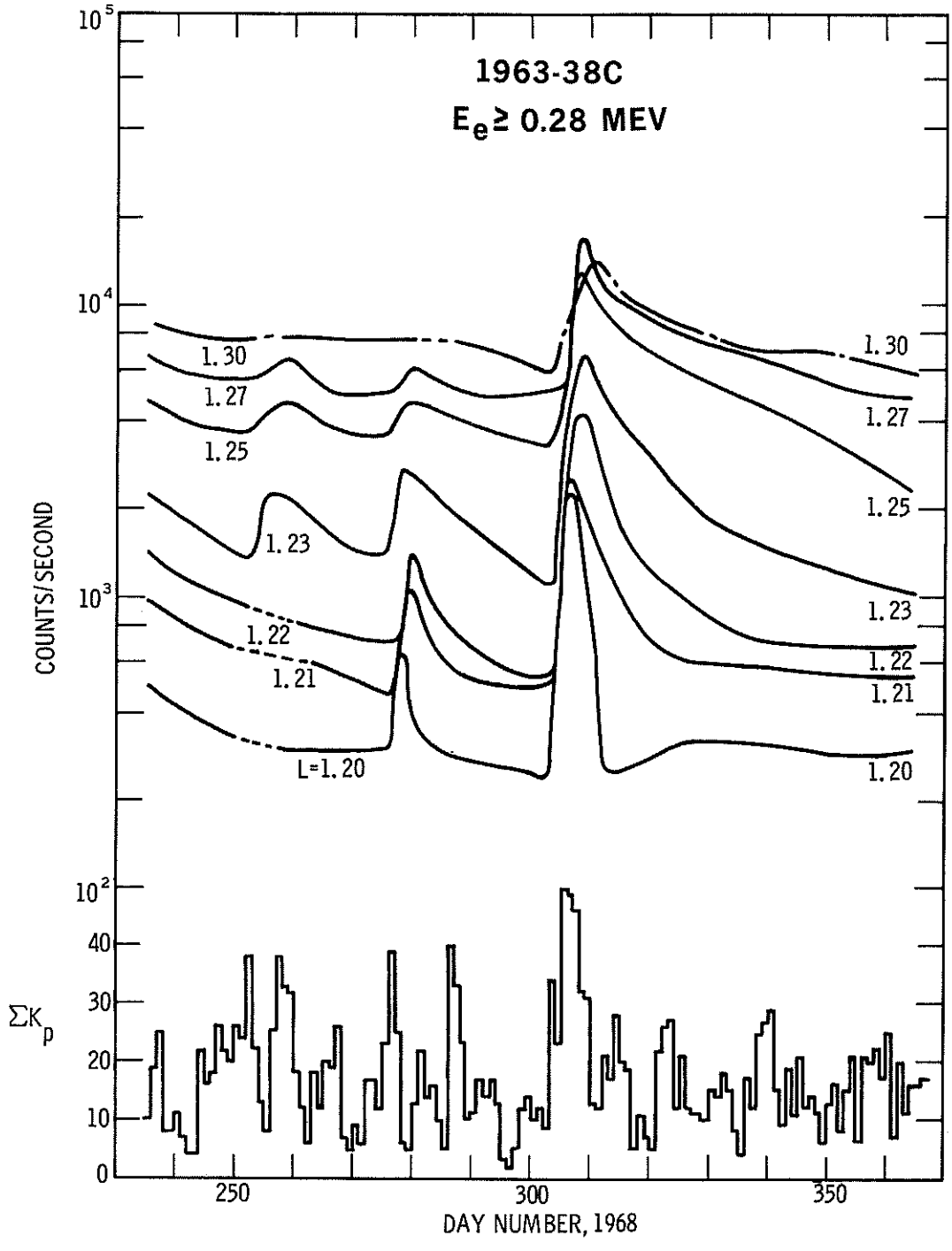

Fig. 1. Electron ($E_e \geq 0.28$ Mev) counting rates vs time for $1.20 \leq L \leq 1.30$ showing the low L response to the November 1968 storm. Kp daily sums are plotted below the data.

"Transverse Magnetic Disturbances due to
Field Aligned Currents on October 31 and November 1, 1968"

by

J. C. Armstrong and A. J. Zmuda
Applied Physics Laboratory
The Johns Hopkins University, Silver Spring, Maryland

Magnetic disturbances transverse to the local main field direction were observed at 1100 km. altitude by satellite 1963-38C on October 31 (day 305) and November 1, 1968. The satellite is magnetically aligned, and the magnetometer used to measure the disturbances is nominally perpendicular to the main field (for more details of the experiment, the reader is referred to the article by Zmuda, et al., 1966).

Figures 1 and 2 are examples of the raw data obtained with this experiment. The two alternating levels shown represent the magnetometer output as a function of time both with and without a 1390 γ calibration signal, and the difference between the two levels during undisturbed times can be used to scale the amplitude of the magnetic disturbance. The general level of the magnetometer output varies with time even when there is no magnetic disturbance, due to the oscillation (period $\approx$8 minutes, amplitude $\approx$6°) of the satellite about the field line. This kind of variation is shown by the dark line on Figure 1. Magnetometer levels which vary about this line represent the disturbances of interest here.

The magnetic disturbances shown in Figures 1 and 2 are probably due to field aligned currents (see, for example, Cummings and Dessler, 1967). Boström [1964] has studied models of the auroral electrojet, assuming them to be driven by magnetospheric electric fields and allowing vertical (i.e., field aligned) currents to flow. In one model (designated by Boström as Case 2) strong sheet currents flow into and out of the auroral arc, one along the equatorward edge and one along the polarward edge, the sheets bracketing the horizontally flowing auroral electrojet. The magnetic field due to such sheet currents would be transverse to the main field and would be contained between the current sheets. It appears that the disturbance field shown in Figure 1 between 1505:12 UT and 1505:57 UT (satellite local time $\sim$ 0851) can be interpreted as being produced by this type of current system. Following the model of Boström, this current system would be driven by a magnetospheric electric field associated with plasma flow from the tail around the morning side toward the sun. In this case the electric field in the equatorial plane is directed from the morning to the evening side of the magnetosphere, and an auroral electrojet flows westward in the region where the sheet currents close in the ionosphere. The noticeably constant amplitude of the disturbance between 1505:12 UT and 1505:57 UT is consistent with a steady, intense magnetospheric electric field. This interpretation of the data in Figure 1, while not unique, seems reasonable.

The data shown in Figure 2, actually taken approximately 25 hours earlier, but at approximately the same satellite local time, is more difficult to interpret. While the magnetic disturbance shown in this figure is probably also produced by field aligned currents, the highly structured nature of the disturbance field indicates either a strongly time-dependent current and/or one with considerable spatial structure. We defer a detailed analysis of this disturbance until a later time.

REFERENCES

BOSTRÖM, ROLF	1964	A model of the auroral electrojets, J. Geophys. Res., 69, 4983.
CUMMINGS, W. D. and A. J. DESSLER	1967	Field-aligned currents in the magnetosphere, J. Geophys. Res., 72, 1007.
ZMUDA, A. J, J. H. MARTIN, and F. T. HEURING	1966	Transverse magnetic disturbances at 1100 kilometers in the auroral region, J. Geophys. Res., 71, 5033.

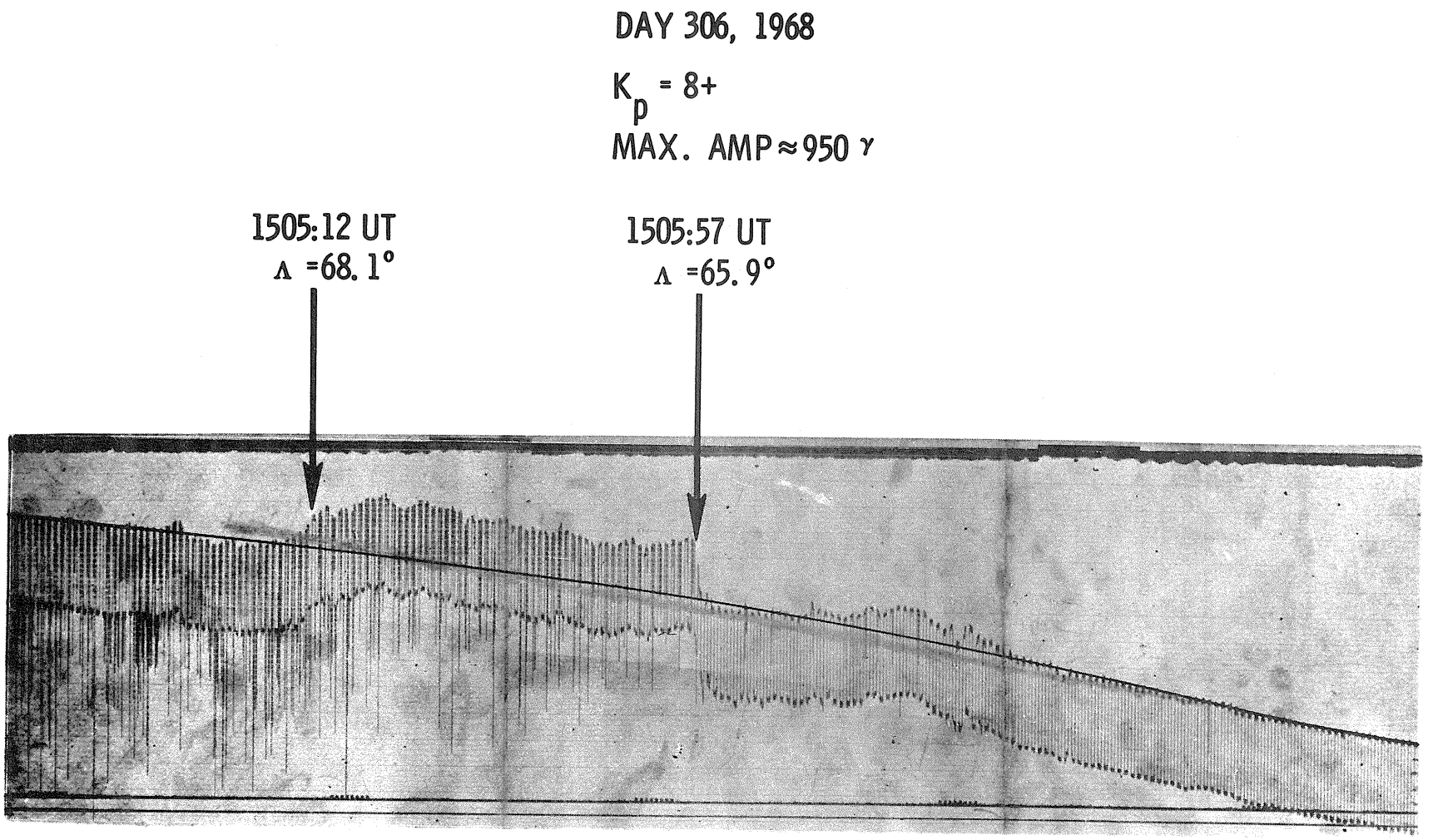

Fig. 1. Example of a transverse magnetic disturbance at 1100 km. taken on November 1, 1968. The alternating magnetometer levels represent the output with and without a calibration signal of 1390 γ. The dark line has been drawn to show the expected magnetometer output (along the portion without the calibration signal) which would be expected if no magnetic disturbance were present. Satellite local time for this pass is 0851. The latitudes shown are invariant latitude, i.e., $\Lambda = \text{Cos}^{-1} (1/L)^{\frac{1}{2}}$.

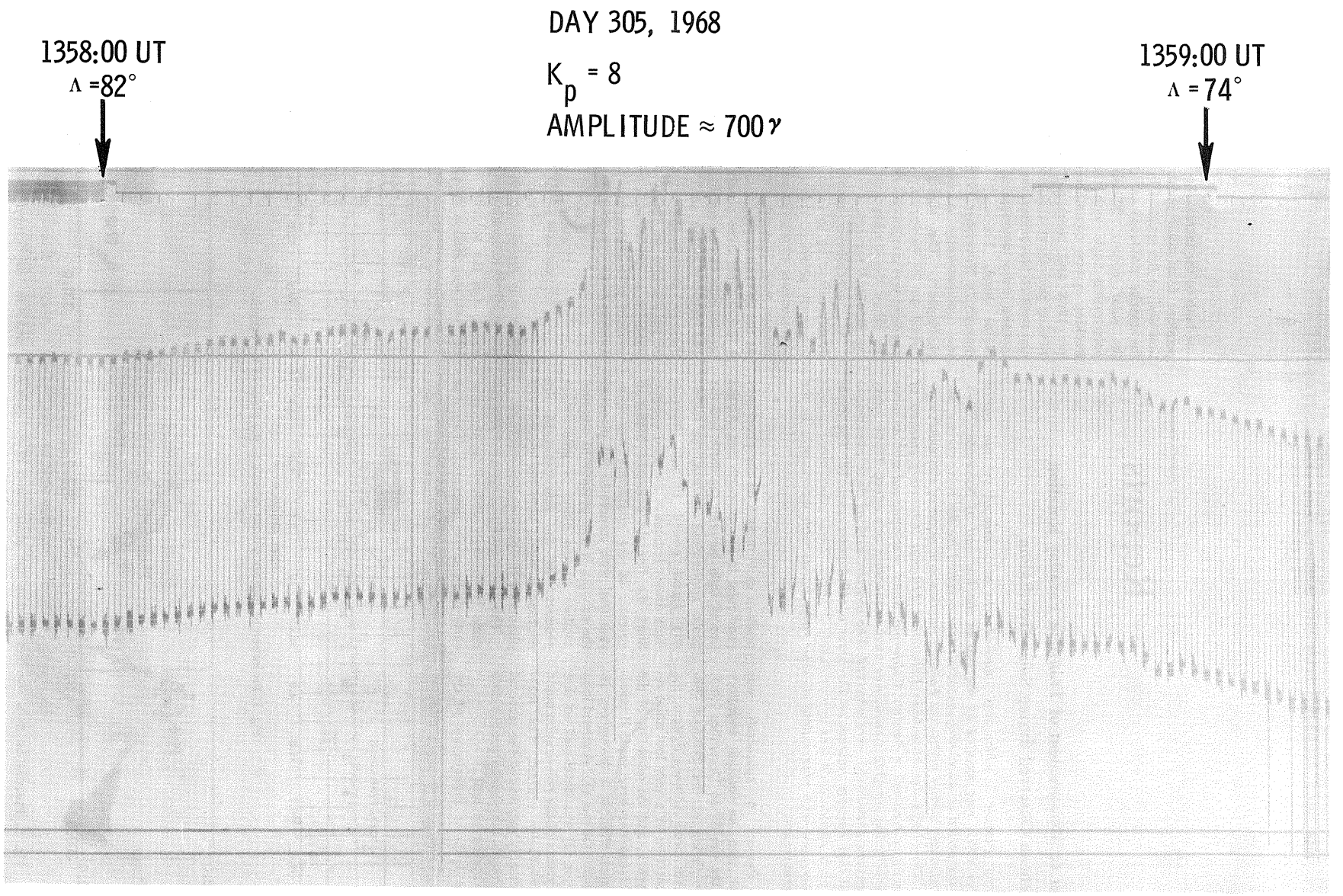

Fig. 2. Example of a transverse magnetic disturbance at 1100 km. taken on October 31, 1968. These data were taken approximately 25 hours earlier than that shown in Figure 1, with satellite local time of 0855.

Reports

Pioneer 6: Measurement of Transient Faraday Rotation Phenomena Observed during Solar Occultation

Abstract. *Pioneer 6, which was launched into orbit around the sun on 16 December 1965, was occulted by the sun in the last half of November 1968. During the period in which the spacecraft was occulted by the solar corona, the S-band telemetry carrier underwent Faraday rotation as a result of this anisotropic plasma. The NASA–Jet Propulsion Laboratory 210-foot (64-meter) antenna of the Deep Space Network at Barstow, California, which was equipped with an automatic polarization tracking system, was used to measure this effect. Three large-scale transient phenomena were observed. The measurement of these phenomena indicated that Faraday rotation on the order of 40 degrees occurred. The duration of each phenomenon was approximately 2 hours. These phenomena appear to be correlated with observations of solar radio bursts with wavelengths in the dekametric region.*

The Pioneer 6 spacecraft was launched into an orbital trajectory around the sun on 16 December 1965. The completion of the 210-foot (64-meter) Advanced Antenna System, the implementation of a very low noise receiver system, and the reliability of the vehicle transmitter have made it possible to track Pioneer 6 throughout its orbit around the sun (*1*). A closed-loop polarimeter (*2*) was developed so that the orientation of the polarization could be automatically tracked. The technique not only maximized the received signal strength but yielded precise data on polarization as well.

Figure 1 shows a projection of the position of Pioneer 6 on the plane perpendicular to the sun-earth line. As the line of sight between the earth and the probe approached the sun, the telemetry signal passed through increasingly denser regions of the solar corona. Since the linearly polarized high-gain antenna of the spacecraft was spin-stabilized with respect to the plane of the ecliptic, it was possible to measure rotation of the plane of polarization produced by the interaction of the microwave signal with the magnetized plasma of the propagation medium.

The polarization measurements became increasingly difficult as the sun-earth-probe angle decreased. This was due both to the increase in system temperature from solar microwave radiation and to the spectral broadening of the carrier produced by distortion in the solar corona. Measurements of polarization angle with the automatic tracking system commenced 26 October 1968 and continued during the viewing periods at Goldstone (California) until 16 November when the signal-to-noise ratio deteriorated below the useful level. From 21 November through 24 November 1968, Pioneer 6 was geometrically occulted by the photosphere. The signal was reacquired on 29 November, and the experiment was continued until 8 December when the station was assigned to the Apollo 8 mission.

A magnetoionic medium appears doubly refracting to radio waves; thus a linearly polarized signal is split into characteristic elliptically polarized components with different phase velocities. At the down-link frequency of Pioneer 6 (2.292 Ghz) these generally elliptical components can be considered circular. The relative phase shift suffered by these two components caused the plane of polarization of the resultant linear signal to be rotated with respect to the incident polarization (*3*). The Faraday rotation Ω (in rotations) is given by

$$\Omega = \frac{1}{4\pi^2} \frac{e^3 c}{m^2 f^2} \int_0^L H(s) N(s)\, ds$$

where e is the charge on an electron (1.6×10^{-20} in centimeter-gram-second units), c is the velocity of light (3×10^{10} cm/sec), $H(s)$ is the component of

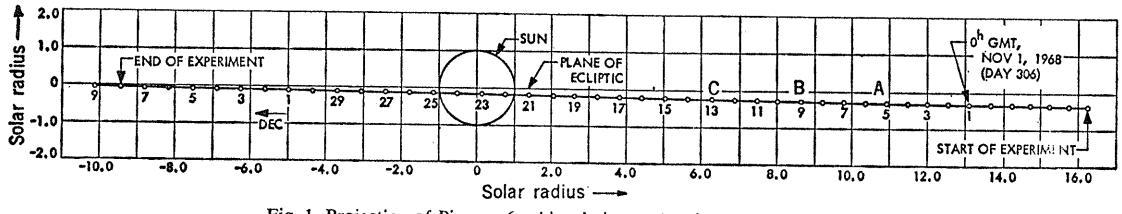

Fig. 1. Projection of Pioneer 6 orbit relative to the plane of the ecliptic.

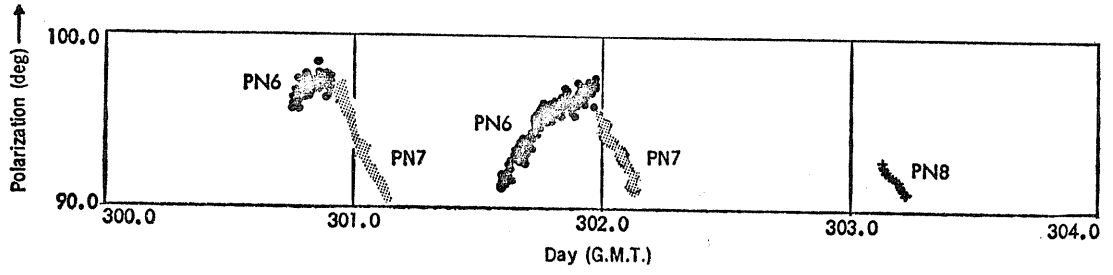

Fig. 2. Polarization as a function of time for observations of Pioneers 6, 7, and 8 in late October 1968.

the magnetic field along the line of sight at s (in gauss). $N(s)$ is the number of electrons per cubic centimeter at point s, m is the mass of an electron (9.1×10^{-28} g), f is the frequency of the radio waves in hertz, and L is the path length of the ray in centimeters.

Rotation can be expressed in terms of the integrated product of the columnar electron content and the magnetic-field component. At the Pioneer 6 down-link frequency, 1° of rotation is produced by 3.9×10^{12} electron-gauss/cm^2.

The polarimeter angle was digitally recorded every 10 seconds during actual observation. These data were transformed to an angle with respect to the plane of the ecliptic. Initially, a nominal 30-second time constant was used in the servo loop. The data from 26 through 29 October 1968 are shown in Fig. 2. In this figure, polarization angle is presented as a function of time for observations of Pioneers 6, 7, and 8. Each point is an average of 20 measurements for 200-second averaging. The most conspicuous feature of this graph is the diurnal variation due to the earth's ionosphere. The ranges of Pioneers 6, 7, and 8 (in astronomical units) were approximately 1.9, 1.2, and 0.4, respectively. The relative scatter of measurements increases with increasing range from the earth, thereby reducing the signal-to-noise ratio. In the case of Pioneer 6, the line of sight of the spacecraft was approximately 15 solar radii from the center of the sun; thus, there was also a slight increase in the noise temperature of the system due to microwave thermal radiation in the side lobes of the antenna.

In Fig. 3 polarization is plotted as a function of time for 4 November 1968. One measurement point for every 10-second period is shown. A time constant for the servo loop of 30 seconds was used. This polarization transient (labeled *A* in Fig. 1) occurred at a distance of 10.9 solar radii from the center of the sun. The next polarization transient was observed on 8 November (Fig. 4). The servo time constant had been increased to 300 seconds. This transient (labeled *B* in Fig. 1) occurred 8.6 solar radii from the solar center. The last observed polarization transient (Fig. 5) occurred 12 November. Unfortunately, there was a loss of data during the first 45 minutes of this transient as a result of operational problems. This transient (labeled *C* in Fig. 1) occurred at a distance of 6.2 solar radii.

In the first two events, the base line is approximately 97°. The positive direction of the base line above 90° can be interpreted as due primarily to the earth's ionosphere, with interaction between electrons and the longitudinal components of the magnetic field of the earth. Any increase in the electron content of the ionosphere would cause an increase in polarization angle; a decrease in the number of electrons could not reduce the angle below 90°. In order to produce the phenomena observed, there must have occurred either

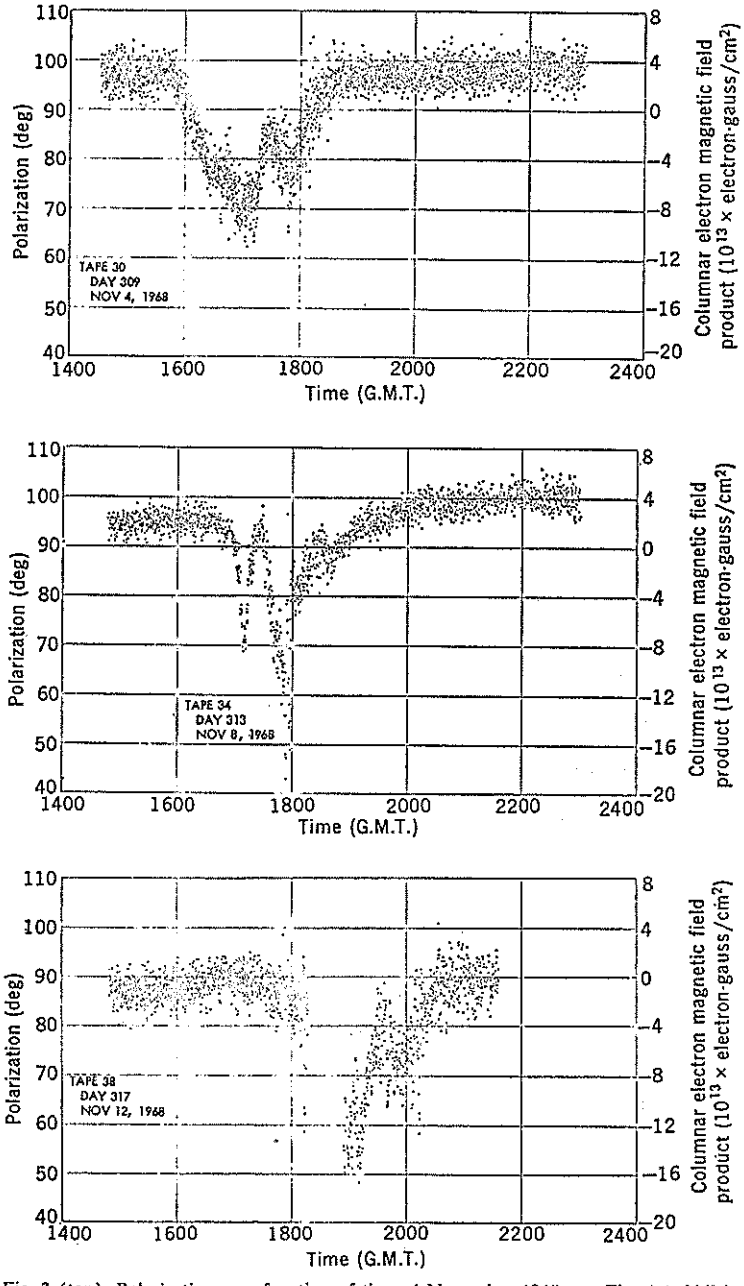

Fig. 3 (top). Polarization as a function of time, 4 November 1968. Fig. 4 (middle). Polarization as a function of time, 8 November 1968. Fig. 5 (bottom). Polarization as a function of time, 12 November 1968.

Table 1. Correlation of Faraday rotation transients and radio bursts in the dekametric range.

Dekametric noise burst* (U.T.)	Intensity†	Velocity (10^3 × km/sec)
4 November 1968 (1700 U.T.) (10.9 solar radii from solar center)		
1244		0.45
1305		.49
1457	2	.93
1502	2	.97
1522	2	1.17
8 November 1968 (1730 U.T.) (8.6 solar radii from solar center)		
1631	3	1.49
12 November 1968 (1900 U.T.) (6.2 solar radii from solar center)		
1643	3	0.44
1647	2	.43
1726	3	.64
1746	1	.82

* All bursts in the dekametric range were of type III. † Intensity scale: $3 > 2 > 1$.

a change in the sign of the particles in the ionosphere or a large concentration of electrons in a region where the longitudinal component of the magnetic field is in the opposite direction to the magnetic field of the earth. These considerations demonstrate that the phenomena were produced by plasma near the sun.

In the third event, the base line was approximately 87°. The reason for the change in base line appears to be an increase in the steady-state plasma density and magnetic field as the line of sight approached the sun. At the same time that these polarization measurements were being made, Goldstein (*4*) was using the same antenna to measure spectral broadening. Enhanced spectral broadening was observed during all three of the Faraday rotation transients. Enhancement of spectral broadening is consistent with an increase in the turbulence and density of the coronal portion of the line of sight.

Two possible explanations for the observed transient polarization effects are (i) a quasi-stationary structure which is probed as the line of sight is swept through, or (ii) a moving plasma concentration which is ejected by the sun. If we assume that we are seeing fairly stationary objects, then we can determine one dimension of these objects in terms of the time it took to sweep through them. Since the duration of each event was approximately 2 hours and the velocity of the line of sight relative to the plane containing the sun was approximately half a solar radius per day, the dimensions of these objects are of the order of 0.04 solar radius. If, on the other hand, we were observing a high-velocity concentration of plasma ejected from the sun, we would expect to find correlation with surface effects. On the 3 days that these transients were observed, there were active areas observed near the west limb where the observations were made. These areas were observed (*5*) by means of several mapping surveys at different radio frequencies. The events were poorly correlated with optical flares. However, in each case it appears that noise-burst events in the dekametric wavelength region preceded these transient Faraday rotation phenomena. On 8 November, the only events in the dekametric range that were reported prior to the Faraday rotation transient occurred between 1631 and 1632 and were classified, respectively, as intensity 1 and 3. On both 4 and 12 November there were many bursts. All bursts with wavelengths in the dekametric range which occurred within 11 hours before the Faraday rotation transient are listed in Table 1 along with the reported intensity (where available). Furthermore, we have calculated the velocity that the plasma clouds must have had if they were produced by the same mechanism that produced the noise bursts in the dekameteric range (Table 1).

Unfortunately, the locations of the origins of these noise bursts in the dekametric range on the photosphere were not known. Only three transients were observed in a period of high solar activity; thus the significance of the correlation with noise bursts is not known at this time. An effort is being made to see if other solar and interplanetary phenomena can be correlated with the Faraday rotation transients.

G. S. Levy, T. Sato
B. L. Seidel, C. T. Stelzried
Jet Propulsion Laboratory, California Institute of Technology, Pasadena 91103
J. E. Ohlson, W. V. T. Rusch
Department of Electric Engineering, University of Southern California, Los Angeles 90007

References and Notes

1. A. J. Siegmeth, *Space Program Summary 37–50* (Jet Propulsion Laboratory, Pasadena, Calif., 31 March 1968), vol. 2, pp. 17–27; Pioneer Project Office, *Pioneer 6 Mission* (Ames Research Center, National Aeronautics and Space Administration, Moffett Field, Calif., May 1967).
2. D. Bathker, T. Sato, C. T. Stelzried, in preparation; J. E. Ohlson, G. S. Levy, C. T. Stelzried, in preparation.
3. I. C. Browne, J. V. Evans, J. K. Hargreaves, W. A. S. Murray, *Proc. Phys. Soc. (London)* **69B**, 901 (1956); G. J. Aitchison and K. Weekes, *J. Atmos. Terrest. Phys.* **14**, 236 (1959); F. B. Daniels and S. J. Bauer, *J. Franklin Inst.* **267**, No. 3, 187 (1959).
4. R. M. Goldstein, *Science*, this issue.
5. *Solar Geophysical Data No. 293* (Environmental Science Services Administration, Washington, D.C., January 1969).
6. We acknowledge the cooperation and support of the personnel at the Pioneer Project Office and the Deep Space Network, and particularly of D. Girdner and the operational personnel at the Jet Propulsion Laboratory Mars site. We also thank D. Bathker, F. McCrea, and R. Cormack for their work in developing the microwave portion of the system. W. Peterschmidt supplied the servo electronics, and B. Parham assisted with the digital instrumentation. This paper presents the results of one phase of research carried out at the Jet Propulsion Laboratory under NASA contract NAS 7-100.

21 April 1969; revised 9 July 1969

Superior Conjunction of Pioneer 6

Abstract. *Spectrograms of the radio signals from Pioneer 6 were taken as the spacecraft was occulted by the sun. The spectral bandwidths increased slowly at first, then very rapidly at 1 degree from the sun. In addition, six solar "events" produced marked increases of bandwidth lasting for several hours. The received signal power seemed unaffected by the solar corona.*

The remarkable lifetime of the Pioneer 6 spacecraft, still operating 3.5 years after launch, has provided us with a rare opportunity to examine the solar corona. Pioneer 6 was injected into solar orbit 16 December 1965 and ever since has reliably transmitted to earth by S-band telemetry the results of its scientific experiments. Last November Pioneer 6 traveled directly behind the sun so that the telemetry signals passed through the interesting regions of the corona.

The corona is a very difficult object to study. The best data have been obtained only during the rare event of a total solar eclipse. Recently, radio astronomers have observed the scintillation of radio stars as they pass behind the sun, in order to draw conclusions about the corona. Radio stars are wide-band sources of radiation, and scintillation can be thought of as a manifestation of multipath phenomena. The Pioneer 6 signals, on the other hand, were extremely narrow-band (monochromatic) and give information of an entirely different kind about the corona.

During the superior conjunction of

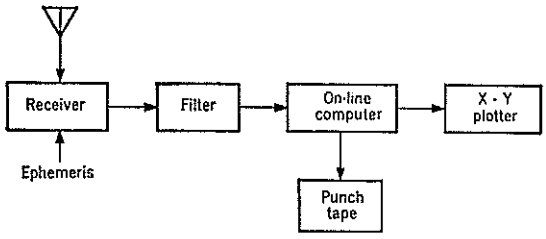

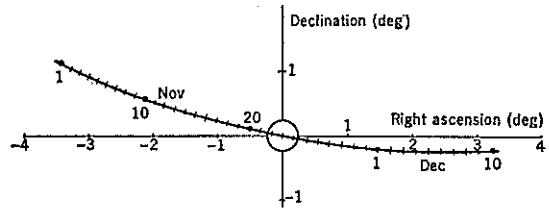

Fig. 1 (left). Block diagram of the experimental system. Fig. 2 (right). Angles made by Pioneer 6, the earth, and the sun as a function of date.

Pioneer 6 we observed the spectrum of the signal and its broadening as the rays passed close to the sun. We observed also a short-term (several hours) broadening of the spectra induced by certain solar events. During our measurements of the spectra of the signals, the direction of the polarization of the waves was monitored by Levy and his group (*1*). They observed Faraday rotation of the polarization which correlated strongly with the same events.

Pioneer 6 normally transmits telemetry composed of a spectrally pure carrier wave plus a set of modulation side bands. In our experiment, only the carrier wave (nominally at 2295 Mhz) was observed. The side bands, separated from the carrier wave by multiples of 2 khz, were removed by filtering.

A functional block diagram of the experiment is shown in Fig. 1. The 210-foot (64-m) antenna of the Jet Propulsion Laboratory was used. This remarkable antenna has a beam width of only 0.14 degree at 2300 Mhz (S-band). Such a narrow beam width was necessary for this experiment in order that we might be able to discriminate between the signal and the powerful radio noise emitted by the sun. Normally, the antenna-receiver system is extremely sensitive, having an equivalent noise temperature of only 25° K. As the angle made by Pioneer 6, the earth, and the sun diminished, the system temperature rose, until at 1 degree the temperature was between 200° and 300°K. The signal disappeared when this angle was less than 1 degree, apparently an effect of the corona. The signal-to-noise ratio would still have been adequate for detection at smaller angles.

Because of the orbital velocities of Pioneer 6 and the earth, the Doppler frequency of the signal shifted on the order of several hundred kilohertz. In addition, the earth's spin imparted an additional Doppler shift of 15 khz per day. In order to compensate for these effects, the receiver was tuned continuously according to an ephemeris. This automatic tuning was accurate to 0.05 hz.

A slight frequency instability remained, due to the spacecraft oscillator. A slow drift of 14 hz/day, presumably of thermal origin, was observed. In addition, a more erratic drift of up to 1 or 2 hz per 15 minutes was observed.

The frequency band which was observed, 100 hz, was the same for each spectrogram taken. This bandwidth was defined by a filter at the last stage of the receiver. A small computer (Scientific Data Systems model 920), programmed with a version of the fast Fourier transform, produced all of the spectrograms on-line. Each group of 1024 samples of the signal wave form was transformed to produce 512 points on the spectrum; this resulted in a frequency resolution of 0.2 hz over the 100-hz bandwidth. Averaged spectra were displayed on an *x-y* plotter and stored on punched tape for further processing.

Data were taken almost daily from 31 October to 8 December 1968. During that time, Pioneer 6 passed from an angular distance from the sun of 3.5 degrees, through geometric occultation, to a position 2.5 degrees on the other side of the sun. Figure 2 shows the angle made by Pioneer 6, the earth, and the sun during the time of interest.

All of the data were collected in the form of spectrograms. Each spectrogram is the result of about 15 minutes of

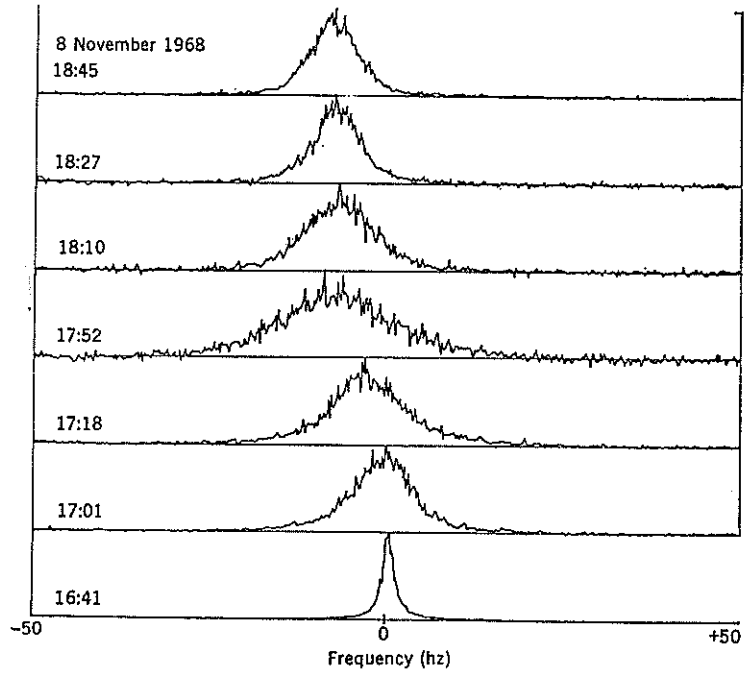

Fig. 3. Sample spectrograms taken on 8 November 1968, showing the effects of a solar event. Each spectrogram is the result of 15 minutes of averaging time.

Table 1. Times of observation.

Date (1968)	Time	Event
10/31	1800–2300	None
11/2	2211–2300	Event 2244
11/3	1622–1815, 1900–1950	None
11/4	1540–1645, 1840–1927	Event 1555–1645
11/5	1606–1720, 2104–2248	None
11/6	1635–1913	None
11/7	2110–2145	None
11/8	1641–2100	Event peak 1800
11/9	1653–1708, 1741–1940	None
11/10	1557–1817	None
11/11	1624–1915	Event peak 1707; gradual reduction to 1915
11/12	1613–2105	Events 1804–2105; peak at 1900
11/13	1640–2236	None
11/14	1648–1900, 1930–2050	None
11/15	1717–1915, 2022–2354	None
11/16	1538–1731	None, but no signal found 1923–2232
11/17	1539–1635	None
11/29	1747–1850, 1920–2100	None
11/30	1539–2005, 2130–2350	None
12/1	1533–1922, 2054–2204	None
12/2	1536–1753	None
12/3	1534–1860	Event peak 1700; gradual taper-off
12/4	1619–1800	Minor peak 1630; gradual taper-off
12/5	1555–1745	Minor peak 1710
12/6	1633–1800	None
12/7	1547–1800	None
12/8	1600–1800	None

observation. The actual schedule of observations each day was variable, depending on conflicting demands for the antenna as well as the results of the spectral measurements. During the occasions of unusual spectral activity, more observing time was made available. No data were taken when Pioneer 6 was closer than 1 degree from the sun as the signals there were not detectable. All together, over 450 spectrograms were taken during the experiment.

Each spectrogram was processed to provide three parameters of interest: signal power, center frequency, and bandwidth. The actual quantity measured $P(f)$ is the sum of the signal spectrum $S(f)$ and the noise spectrum N (assumed to be flat), both having passed through the system filter $H(f)$

$$P(f) = [S(f) + N]\,H(f)$$

Thus the first task in the data reduction was the subtraction of the noise spectrum and the removal of the effects of the system filter. To accomplish this, a calibration spectrum $Q(f)$ was measured, in which only system noise was measured with the receiver offset from the signal

$$Q(f) = aN\,H(f)$$

where a accounts for a possible change in system gain.

It can be seen from the equations above that

$$S(f)/N = P(f)\int_C P(f)df / Q(f)\int_C P(f)df - 1$$

where C is an interval which contains no signal. We used the first quarter plus the last quarter of the spectrum for this interval.

Signal power P_s was obtained by integration of the spectrum over the bandwidth and removal of the normalization N

$$P_s = \left(\int_0^{100} \frac{S(f)}{N}\,df\right) kT$$

where k is the Boltzmann constant and T is the system temperature, was measured separately by reference to a standard noise source. The measurement of P_s produced considerable scatter (± 2 db) caused primarily by the widely fluctuating system temperature. Minor side lobes of the antenna would rotate across the disk of the sun and cause tempera-

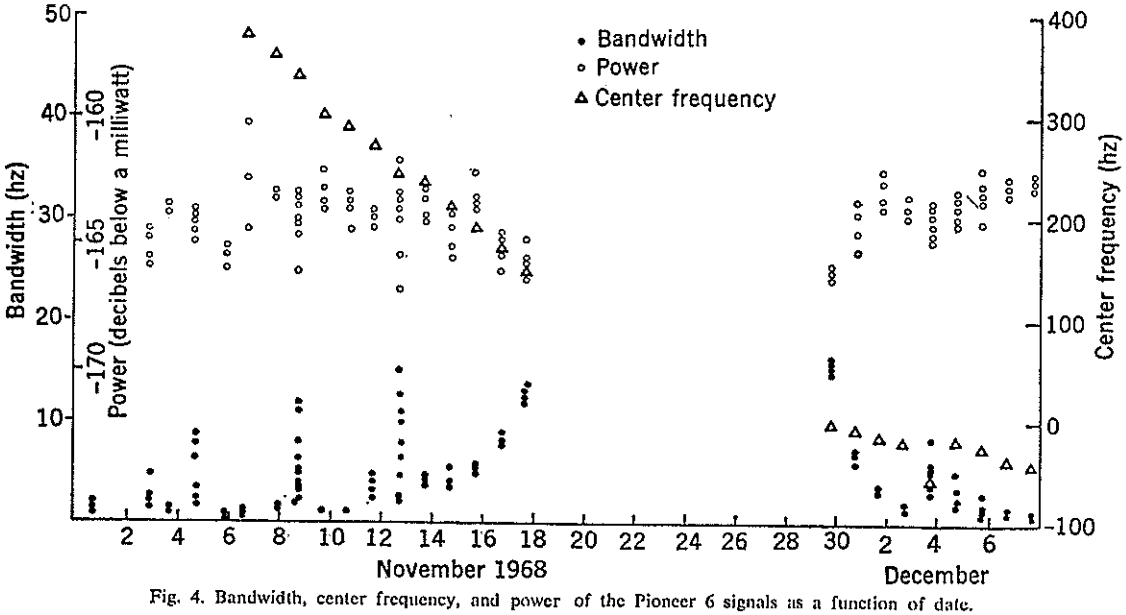

Fig. 4. Bandwidth, center frequency, and power of the Pioneer 6 signals as a function of date.

ture variations of up to several hundred degrees.

The center frequency f_c of each spectrum was estimated as that frequency which splits the received power into equal halves; that is

$$\int_0^{f_c} S(f)df = \int_{f_c}^{100} S(f)df$$

The bandwidth B of each spectrum was estimated, similarly, as that band which contains the central half of the signal power

$$\int_0^{f_1} S(f)df = 1/4\,P_s$$

$$\int_{f_2}^{100} S(f)df = 3/4\,P_s$$

$$B = f_2 - f_1$$

Figure 3 is a sequence of spectrograms taken on 8 November when Pioneer 6 was 2.4 degrees away from the sun and approaching the sun. This figure shows the effect of increased turbulence in the corona, presumably caused by some solar "event." The effects lasted several hours, the decay being much slower than the onset. Only six such events were observed. Most of the spectra were constant, showing only a slow thermal drift of the spacecraft frequency.

The results of the experiment are summarized in Fig. 4, where the bandwidth and power of each spectrum are plotted against the date. The average center frequency for each day is also plotted.

Two separate phenomena are manifested in Fig. 4. The first is the occasional marked increase in bandwidth caused by the solar events mentioned above. The second is a background bandwidth of about 1 hz, due to frequency instabilities of the system, which appeared when Pioneer 6 was far from the sun. This component increased slowly as the rays penetrated more deeply into the corona. Finally, the bandwidth increased very rapidly at about 1 degree from the sun, just before the signal disappeared. The effect is as though the solar radius were 1 degree at S-band.

The measurements of power do not seem to correlate with those of bandwidth. In particular, the power fluctuations do not correspond to the sudden increases in bandwidth induced by the solar events. Although there is considerable scatter associated with the power estimates, they are on the whole relatively constant throughout the experiment. The only exception would be the 2 days at 1 degree when the power appears to be somewhat smaller.

The nature of the solar events is not known. They do not appear to correlate well with solar flares or with the apparition of sunspots on the solar limb or with the S-band solar flux. They may be the result of streamers sweeping across the line of sight.

In the hope of establishing a correlation of the spectral broadening with other solar phenomena, I present in Table 1 the times and durations of the observed events. Table 1 also gives the times when spectrograms were taken but no events were observed. A full set of spectrograms will soon be available (*2*).

R. M. GOLDSTEIN
Jet Propulsion Laboratory, California Institute of Technology, Pasadena

References and Notes

1. G. S. Levy, T. Sato, B. L. Seidel, C. T. Stelzried, J. E. Ohlson, W. V. T. Rusch, *Science*, this issue.
2. R. M. Goldstein, *Jet Propulsion Lab. Tech. Rep. TR 32-1435* (1969).
3. This paper presents the results of one phase of research carried out at the Jet Propulsion Laboratory, California Institute of Technology, under NASA contract No. NAS 7-100.

24 June 1969

"Interplanetary Magnetic Field Measurements October 24, 1968 - November 23, 1968"

by

Norman F. Ness and K. W. Behannon
Goddard Space Flight Center
National Aeronautics and Space Administration
Greenbelt, Maryland

[The following figures and table were kindly supplied by Dr. Ness and his colleagues. The compiler has prepared the accompanying text from their description of the data.]

The interplanetary magnetic field measurements during October 24 through November 23, 1968, as recorded by Explorer 35 in lunar orbit, are presented in Fig. 1 and the Table. Because of the interplanetary disturbance around November 1, it has not been possible to identify with certainty the passage of Explorer 35 through the bow shock into the magnetosheath. The first contact with the shock may have been as early as October 30 at around 2300 UT. Since the major interest of this data compilation is in the interplanetary disturbance variations during this period, and since at the orbital distance of Explorer 35 the magnetosheath field is not greatly different from the interplanetary field in its gross features, data are included up to the hour of first contact with the magnetopause. Data during passage through the tail and traversal of the magnetosheath on the dawn side have been excluded. In addition the hours during passage of Explorer 35 through the lunar wake (twice each day) have been excluded since the wake field is generally different from the undisturbed interplanetary field.

The definitions of the values plotted and table column headings are as follows:

F = FHAV and AVF values (the darker lines are FHAV -- the values can be identified by using the table below)

Θ = THAV = Solar ecliptic (SE) latitude (+ north, - south)

Φ = PHAV = Solar ecliptic (SE) longitude (0° towards sun, 90° east, 180° away from sun)

RAD = Radial distance of spacecraft in earth radii (all trajectory data correspond to position of spacecraft at the center point of the hour)

XSE = Solar ecliptic X-coordinate of spacecraft

YSE = Solar ecliptic Y-coordinate of spacecraft

ZSE = Solar ecliptic Z-coordinate of spacecraft

YR = Year of data

DAY = Day of data on card (Jan. 1 = Day 000) --- Day 300 to Day 327 represent October 27, 1968 - November 23, 1968)

HR = Hour of data in UT

FHAV = Hourly average field magnitude (to 0.1 gamma)

THAV = Hourly average θ_{SE} (to nearest degree)

PHAV = Hourly average ϕ_{SE} (to nearest degree)

XEHAV = Hourly average BX_{SE} (X-component of field to 0.1 gamma)

YEHAV = Hourly average BY_{SE} (Y-component of field to 0.1 gamma)

ZEHAV = Hourly average BZ_{SE} (Z-component of field to 0.1 gamma)

XRMS = Standard deviation of BX (to 0.1 gamma)

YRMS = Standard deviation of BY (to 0.1 gamma)

ZRMS = Standard deviation of BZ (to 0.1 gamma)

AVF = Field magnitude computed from hourly average field components.

The table has been prepared from a punched card listing by selecting the values for 00 UT and 12 UT (or nearest to these times) for each day. The data for the intermediate hours can be requested from World Data Center A - Upper Atmosphere Geophysics or from Dr. Ness.

TABLE I

RAD	XSE	YSE	ZSE	YR	DAY	HR	FHAV	THAV	PHAV	XEHAV	YEHAV	ZEHAV	XRMS	YRMS	ZRMS	AVF
58.3	18.2	55.1	-5.5	68	300	0	6.0	59.0	345.0	2.3	-0.6	3.9	1.1	1.4	3.3	4.6
58.9	12.0	57.4	-5.5	68	300	12	2.9	-28.0	326.0	1.3	-0.9	-0.8	1.6	1.1	1.5	1.8
59.5	5.6	58.9	-5.3	68	301	0	1.6	31.0	123.0	-0.5	0.8	0.6	0.5	0.6	0.9	1.2
60.0	-0.9	59.8	-5.1	68	301	12	4.2	65.0	53.0	0.7	1.0	2.6	1.4	2.2	1.1	2.9
60.5	-7.3	59.8	-4.8	68	302	0	8.5	-42.0	319.0	2.4	-2.1	-2.9	2.9	5.8	3.0	4.3
60.9	-13.6	59.2	-4.5	68	302	12	16.8	39.0	295.0	3.0	-6.5	5.8	4.7	8.6	9.8	9.3
60.7	-20.0	57.2	-3.9	68	303	2	19.4	32.0	318.0	12.0	-11.0	10.2	2.4	3.3	2.9	19.3
61.2	-25.7	55.4	-3.5	68	303	13	7.3	-6.0	29.0	6.0	3.4	-0.8	0.6	0.4	0.5	7.0
61.7	-31.2	53.1	-3.1	68	304	0	9.1	-63.0	54.0	2.3	3.1	-7.5	2.6	0.8	3.7	8.5
60.6	-36.9	48.0	-2.2	68	304	14	38.9	-77.0	78.0	1.9	8.5	-36.3	11.7	4.2	8.9	37.3
61.7	-41.3	45.8	-1.9	68	305	0	20.5	-14.0	173.0	-13.5	1.6	-3.3	4.2	2.6	13.8	14.1
61.7	-45.7	41.3	-1.2	68	305	12	25.8	-57.0	107.0	-2.9	9.7	-15.6	3.3	5.3	17.2	18.7
61.6	-49.7	36.4	-0.6	68	306	0	11.5	-53.0	334.0	6.0	-2.9	-8.8	1.7	1.3	2.2	11.1
62.8	-41.7	-46.5	5.6	68	313	15	5.1	-18.0	176.0	-4.6	0.3	-1.5	0.6	0.9	0.4	4.9
62.9	-38.9	-49.1	5.5	68	314	0	4.3	16.0	165.0	-3.9	1.0	1.1	0.6	0.9	0.5	4.3
62.6	-33.8	-52.3	5.5	68	314	12	5.1	-34.0	120.0	-2.0	3.3	-2.7	1.0	0.9	1.3	4.8
62.2	-28.3	-55.1	5.3	68	315	0	4.2	-66.0	44.0	1.2	1.1	-3.7	0.6	1.0	0.5	4.1
61.9	-22.5	-57.4	5.2	68	315	12	6.3	-78.0	166.0	-4.6	1.1	-22.0	37.3	8.2	89.3	
61.6	-16.5	-59.1	4.9	68	316	0	3.8	-1.0	78.0	0.7	3.4	-0.1	0.9	0.4	1.0	3.5
61.3	-10.3	-60.2	4.7	68	316	12	2.8	-4.0	145.0	-2.2	1.5	-0.2	0.3	0.3	0.4	2.7
61.1	-4.0	-60.7	4.3	68	317	0	4.1	-6.0	143.0	-2.9	2.2	-0.4	1.4	0.9	0.8	3.7
60.9	2.4	-60.7	3.9	68	317	12	11.6	-14.0	311.0	7.2	-8.4	-2.8	0.7	0.6	1.2	11.5
60.8	8.6	-60.1	3.5	68	318	0	9.3	14.0	345.0	8.6	-2.4	2.3	0.3	0.4	0.5	9.3
60.8	14.7	-58.8	3.0	68	318	12	5.5	30.0	285.0	0.9	-3.4	2.0	2.8	1.3	1.7	4.1
60.6	20.4	-56.9	2.5	68	319	0	4.6	15.0	119.0	-2.1	3.9	1.2	0.4	0.3	0.2	4.6
59.0	25.7	-53.0	1.7	68	319	14	5.9	8.0	285.0	1.4	-5.4	0.8	0.7	0.8	1.3	5.7
59.4	30.8	-50.7	1.3	68	320	0	5.3	-17.0	302.0	2.5	-4.0	-1.4	0.8	0.9	1.5	4.9
57.9	35.7	-45.6	0.5	68	320	13	18.3	62.0	306.0	4.9	-6.8	15.8	1.8	4.1	1.1	17.9
57.2	40.2	-40.6	-0.3	68	321	1	12.5	-19.0	255.0	-3.0	-11.1	-4.0	1.1	1.0	2.4	12.2
56.9	44.1	-36.0	-0.8	68	321	12	12.7	-53.0	287.0	2.2	-7.2	-10.1	0.9	0.5	0.4	12.7
56.4	47.6	-30.1	-1.5	68	322	0	6.8	-69.0	209.0	-2.1	-1.2	-6.3	0.5	0.6	0.9	6.8
55.9	50.5	-23.8	-2.1	68	322	12	5.6	-11.0	308.0	3.2	-4.2	-1.0	0.8	0.6	1.4	5.4
55.6	52.7	-17.1	-2.7	68	323	0	5.4	-43.0	354.0	3.9	-0.4	-3.6	0.2	0.6	0.3	5.4
55.4	54.3	-10.3	-3.3	68	323	12	4.4	-31.0	328.0	3.2	-2.0	-2.2	0.3	0.6	0.4	4.4
55.4	55.1	-3.3	-3.8	68	324	0	4.6	39.0	309.0	2.0	-2.5	2.6	0.5	1.9	0.8	4.2
55.5	55.2	3.9	-4.2	68	324	12	15.9	-24.0	246.0	-5.0	-11.0	-5.5	3.7	3.8	6.2	13.3
55.8	54.5	10.9	-4.6	68	325	0	10.5	26.0	249.0	-3.4	-8.7	4.6	0.9	0.9	0.5	10.5
56.1	53.0	17.7	-4.9	68	325	12	6.4	-21.0	278.0	0.7	-5.3	-2.1	1.2	1.2	1.8	5.8
56.6	50.8	24.3	-5.1	68	326	0	4.7	-8.0	268.0	-0.1	-4.1	-0.5	1.3	0.5	1.8	4.1
57.1	47.9	30.5	-5.3	68	326	12	5.9	-25.0	291.0	1.8	-4.7	-2.4	0.8	0.6	1.3	5.6
57.6	44.3	36.3	-5.3	68	327	0	5.3	-4.0	332.0	3.8	-2.0	-0.3	1.4	1.8	2.2	4.3
58.1	40.2	41.5	-5.3	68	327	12	4.9	16.0	342.0	4.4	-1.5	1.3	0.3	0.7	0.6	4.8

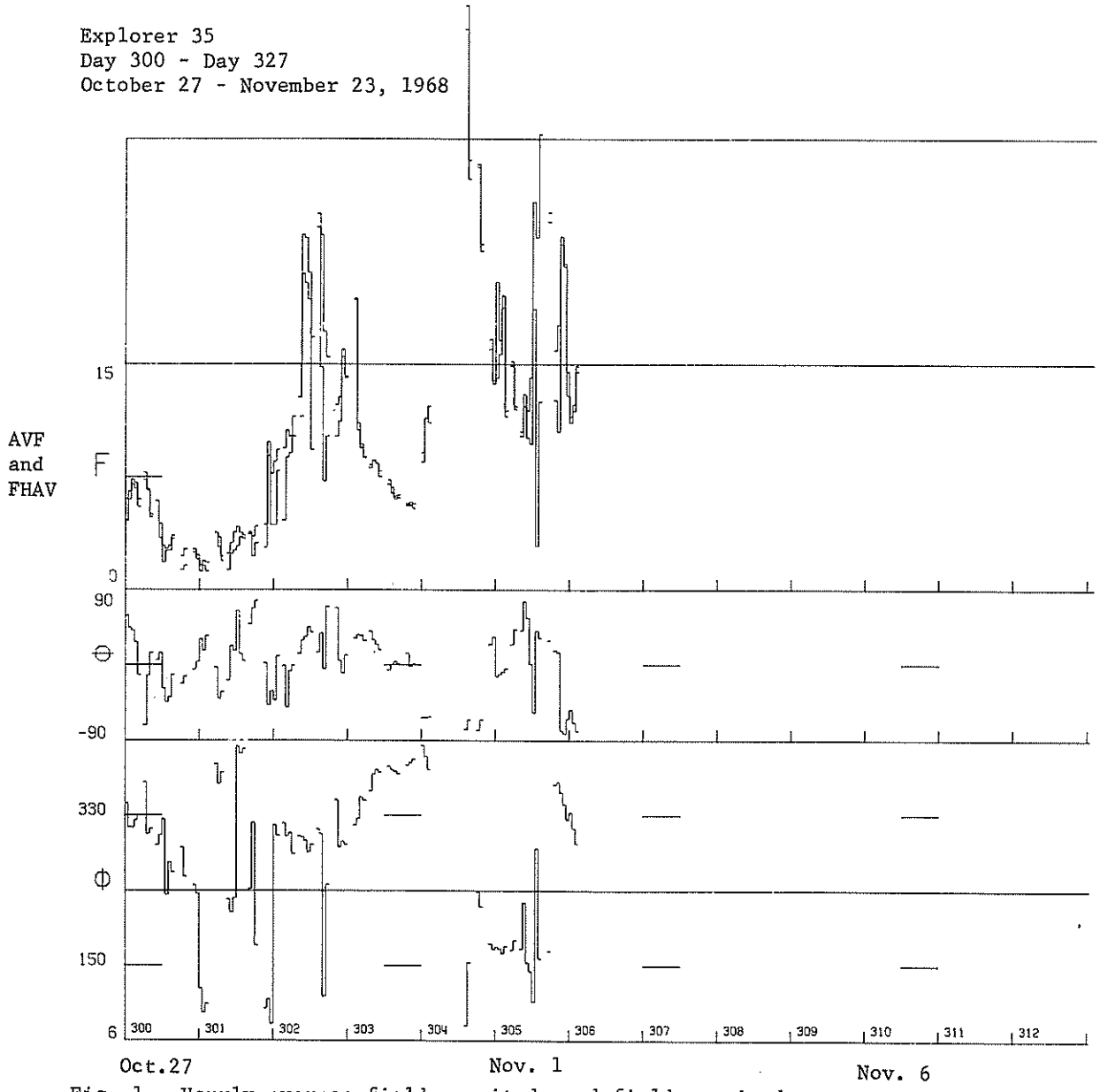

Fig. 1. Hourly average field magnitude and field magnitude computed from hourly average field components, hourly average solar ecliptic latitude and hourly average solar ecliptic longitude as observed by Explorer 35.

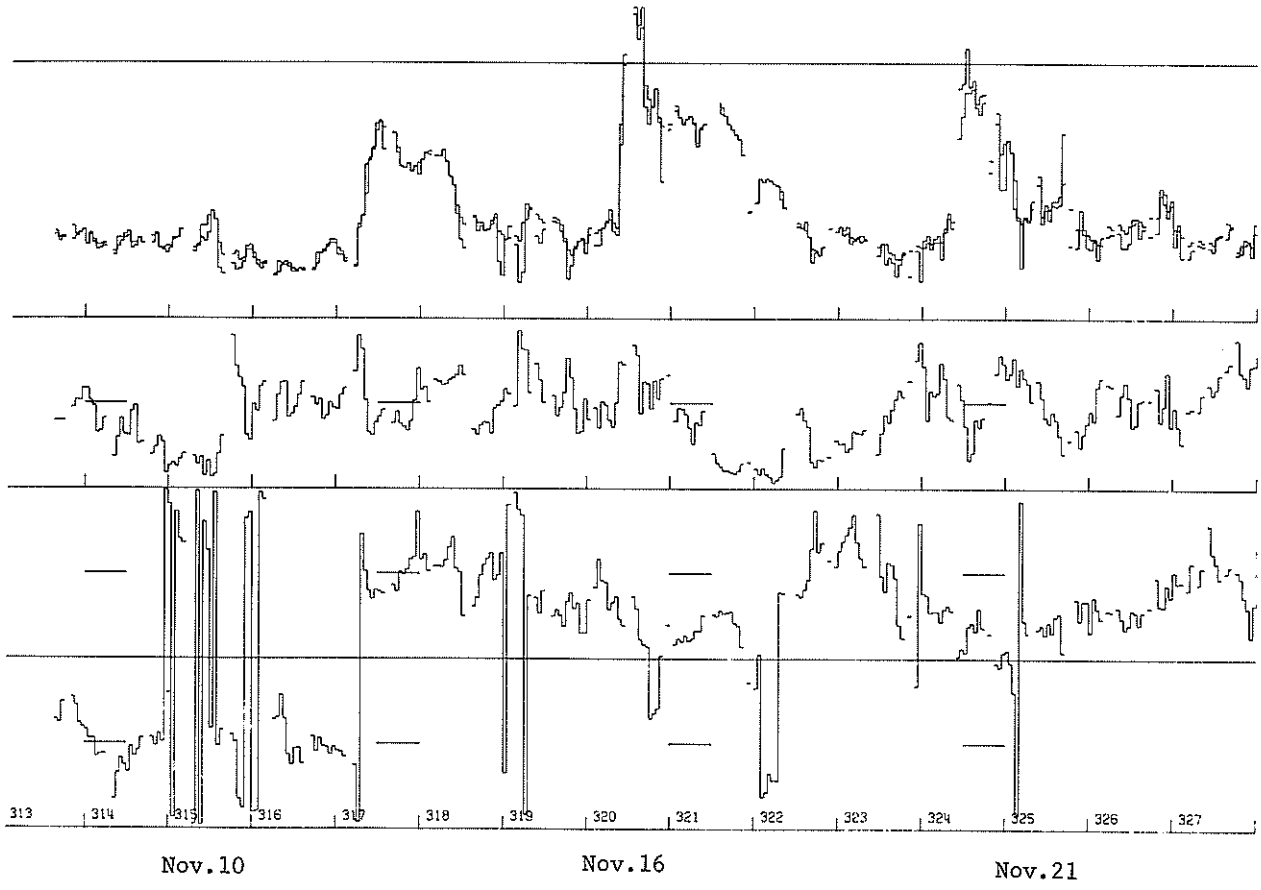

Fig. 1 (Continued)

9. COSMIC RAYS

"Events of October 28 to November 21, 1968"

by

John F. Steljes
Atomic Energy of Canada Limited
Chalk River, Ontario, Canada

Graphs of the cosmic ray neutron monitor stations operated in cooperation with Atomic Energy of Canada Limited have been plotted for the period October 28 to November 21, 1968 in Figure 1. The graphs are plotted as a percentage of the maximum rate attained during IQSY (actually the average for May 1965), if the station was operating at that time and as an estimated percentage if it was not. The vertical scale is 5 percent per division. The graphs are spaced an integral number of divisions apart so that adjacent graphs do not intersect. The percentage nearest the beginning of each graph is printed at the left hand side and the abbreviated station name at the right hand side.

The stations plotted are as follows:

Station		Country	Cutoff GV
Chacaltaya	CHAC	Bolivia	13.10
Kula, Hawaii	KULA	U.S.A.	13.30
Alert	ALERT	Canada	0.05
Deep River	D.R.	Canada	1.02
Goose Bay	G.B.	Canada	0.52
Inuvik	INUV	Canada	0.18
Resolute	RES	Canada	0
Sulphur Mountain	S.M.	Canada	1.14

The cosmogram is a projection of the cosmic ray intensity as a function of the spatial angle and time. The anti-solar direction is taken as 0° and the angle increases in the direction of rotation of the earth. The "garden-hose" angle lies between 90° and 180°.

The vertical thickness is proportional to the cosmic ray intensity, zero thickness being equal to the lowest intensity attained by any station during the entire period covered by the cosmograms. A scale of percent is given at the left hand lower corner. Time runs diagonally from the top right to the bottom left of the figure and there is a 12 hour overlap between the adjacent cosmograms.

Figure 2 starts at 1800 UT on October 28 at the top of the upper cosmogram and ends at 0600 UT on November 6, 1968 at the bottom of the lower cosmogram. Because of the large decrease on October 29, the upper cosmogram is plotted using half the vertical scale of the others. Part of the top of the second cosmogram (where it overlaps the first) is hidden by the near edge.

The paths of the stations are lines extending vertically downwards as is described in a previous publication. These paths have been omitted here because of the small size of the cosmograms.

The stations used are as follows:

Station	Operated by	Asymptotic angle
Oulu	Finland	4.31 hours
Tixie	U.S.S.R.	10.66
Inuvik	Canada	15.70
Churchill, Canada	U.S.A.	19.01
Goose Bay	Canada	22.43

The stations are those of the "Northern Ring", five in all, and the angles between them are filled in by linear interpolation between simultaneous readings at each station. This type of interpolation is valid if the event is assumed to occur simultaneously at each station as is the case with a Forbush decrease. Each interpolation is judged to be valid for an angle of 30° (2 hours) on each side of the station (after rounding off to the nearest hour). If the separation is greater than this, the intervening portion of the cosmogram is dotted. One dotted portion occurs over Reykjavik and the other over Noril'sk, U.S.S.R.

After interpolation, the data are passed through a triangular filter in the time direction, having weights 1, 2, 3, 2, 1 (operating on hourly values) in order to reduce statistical fluctuations.

REFERENCE

CARMICHAEL, H. and JOHN F. STELJES 1969 Forbush Decrease and Cosmogram May 25-26, 1967, Data on Solar Event of May 23, 1967 and its Geophysical Effects, World Data Center A, Report UAG-5, February 1969.

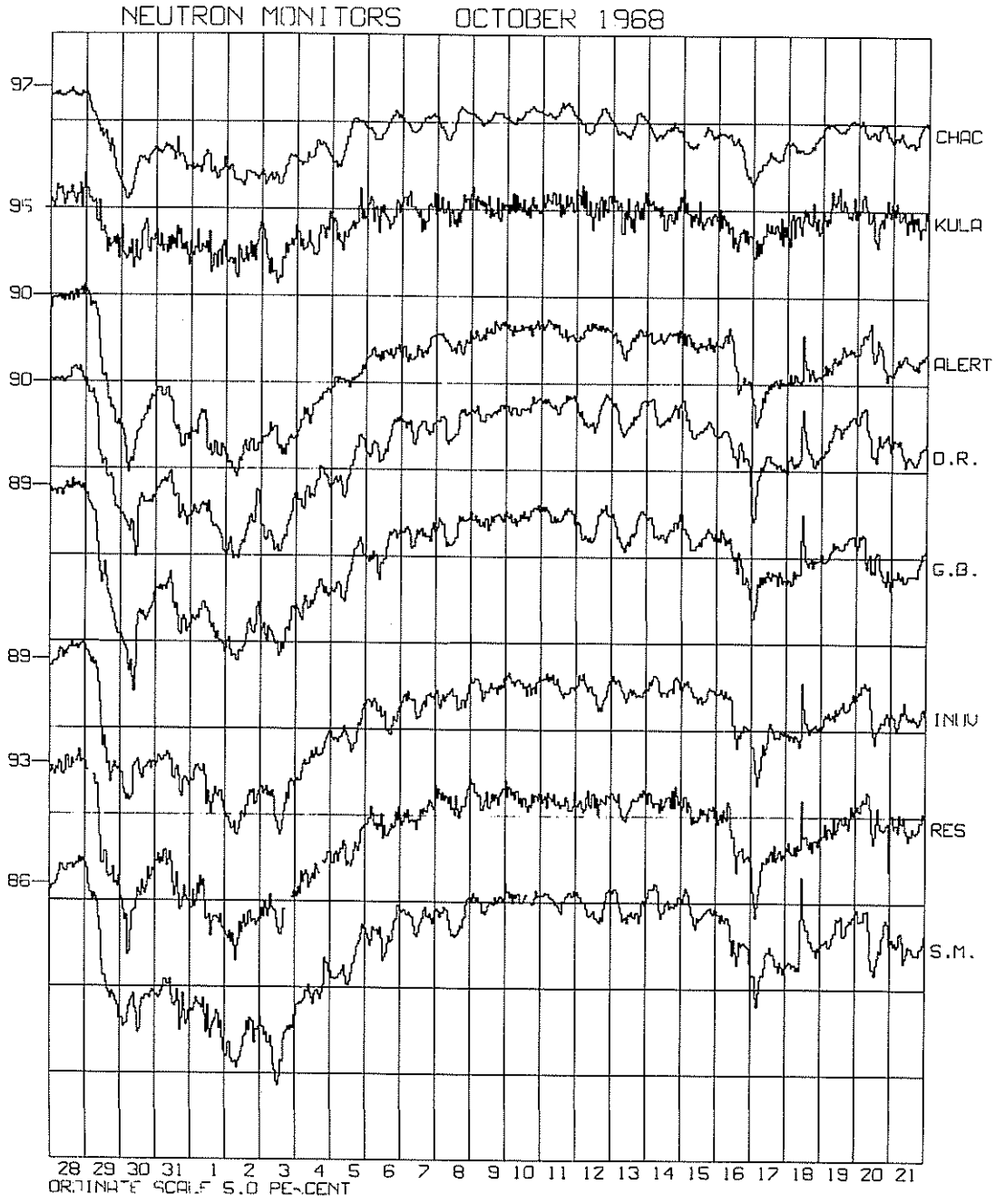

Fig. 1. Neutron monitor rates as percentages of the maximum rate during IQSY, plotted for the period October 28 to November 21, 1968.

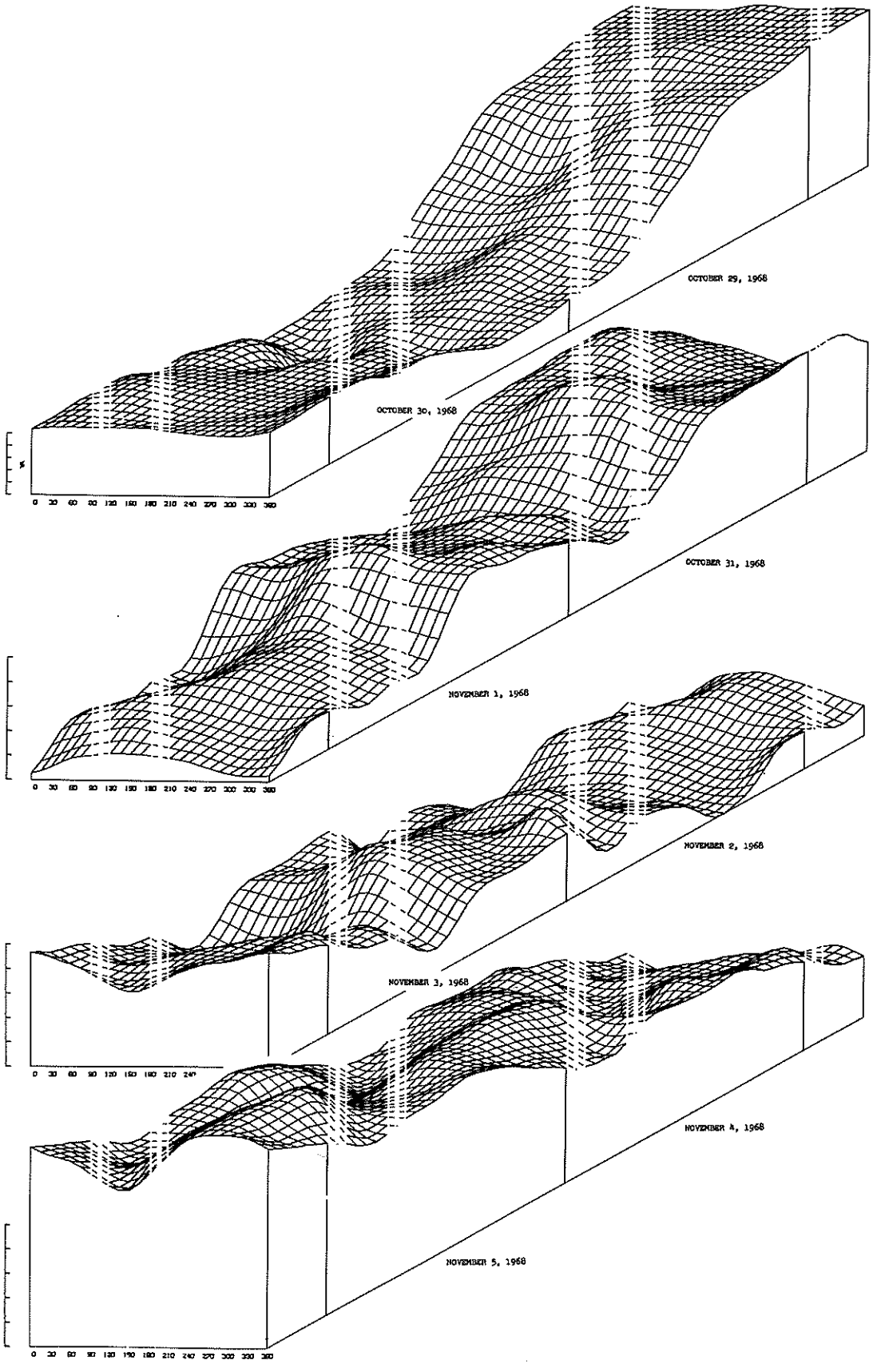

Fig. 2. Cosmograms for the period October 29 to November 5, 1968. The top cosmogram is plotted on half the vertical scale of the others.

"Editorial Comments on Cosmic Ray Data Available at World Data Center A, Upper Atmosphere Geophysics"

by

J. Virginia Lincoln
World Data Center A - Upper Atmosphere Geophysics
ESSA Research Laboratories, Boulder, Colorado

Special contributions of cosmic ray data have been made in addition to the usual daily-hourly tabulations sent to World Data Center A, Upper Atmosphere Geophysics.

G. Milleret of the Laboratoire de Physique Cosmique, Verrières, France has supplied 15 minute corrected tabular values from October 28 to November 6, 1968 for the neutron monitor stations of Pic du Midi and Kerguelen, and graphs of hourly corrected values from October 17 to November 15, 1968.

M. Galli of the Istituto di Fisica "A. Righi" of the University of Bologna, Italy sent data from the scintillation detector of the IGC Cosmic Ray Station Bologna B-237 for October 26 through November 20, 1968.

Prof. J. Van Mieghem supplied the hourly neutron monitor 9 NM 64 counts and air pressure values for October 27 through November 5, 1968 from Dourbes.

G. Valas, Central Research Institute for Physics of the Hungarian Academy of Sciences, sent the Budapest underground meson telescope data and corresponding 200 mb meteorological data for October 25 through November 7, 1968. The telescopes are a semi-cubical vertical one, and narrow-angle inclined ones.

10. GEOMAGNETIC DATA

"Geomagnetic Indices"

by

J. Virginia Lincoln
ESSA Research Laboratories, Boulder, Colorado

The musical note diagram of Kp and the C9 figures as published by IAGA for 1968 reproduced below indicate that the storm period of October 29 - November 4, 1968 was the greatest of the year, but did not reach the magnitude of the storm period of May 25-31, 1967.

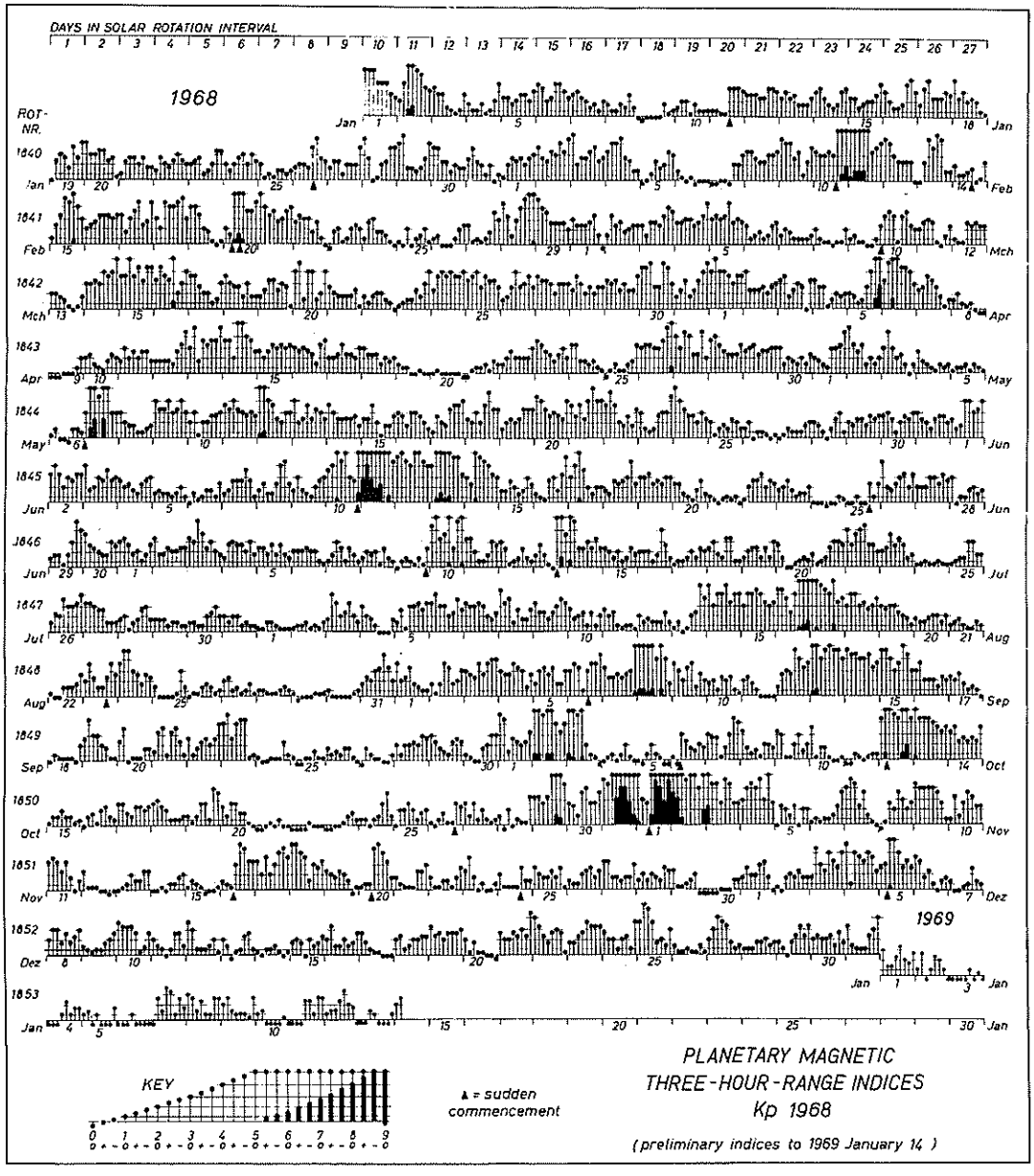

DAILY GEOMAGNETIC CHARACTER FIGURES C9 AND 3-DAY MEAN SUNSPOT NUMBERS R9

For explanation and previous years see J. Bartels, Abhandlungen der Akademie der Wissenschaften zu Göttingen, Beiträge zum I.G.J., Heft 3 (1958) (may be requested from Institut für Geophysik, Postfach 876, 34 Göttingen, Germany).

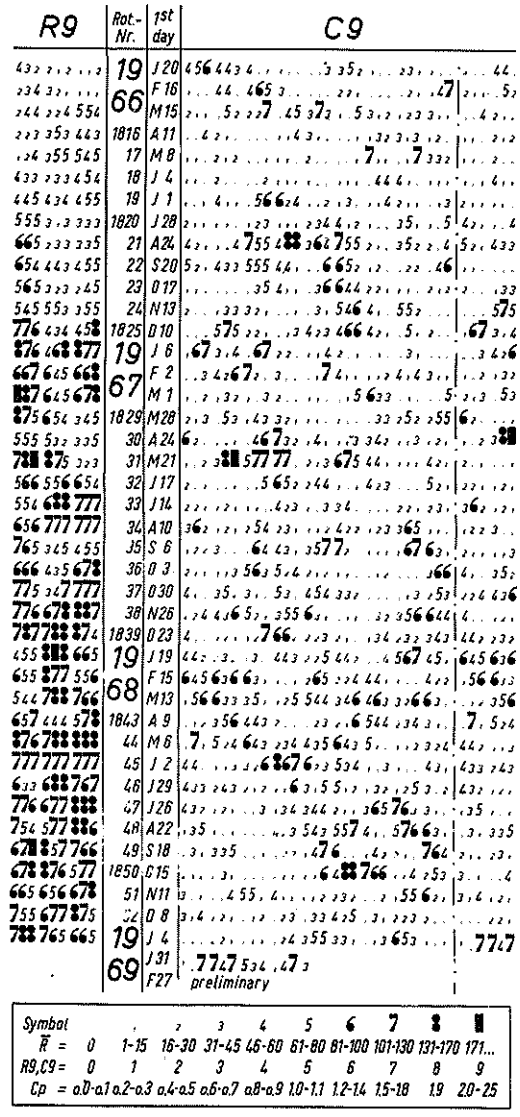

The Kp and Ap indices were as follows:

1968		Kp								Ap	
Oct.	27	3-	1+	3-	1o	2o	1o	1-	1o	6	
	28	1+	0o	2o	0+	1o	1-	1-	3+	5	
	29	3+	3+	3-	3+	5o	6o	6-	4+	37	D
	30	3-	2+	1+	4-	4o	3-	3-	4-	15	
	31	5-	4+	5o	7+	8o	8o	7o	6o	112	D
Nov.	1	5+	3o	3-	6o	8+	8o	7o	8+	122	D
	2	8-	7+	6-	5-	5o	5o	4o	6+	82	D
	3	7-	4+	4+	3-	5-	4+	3-	3-	35	D
	4	3o	4o	4+	4o	5-	3o	5o	3-	27	D
	5	0+	2+	2o	1+	2+	0+	2o	2o	6	
	6	1-	1o	1-	1o	1o	1+	2+	4-	7	

According to IAGA the storm sudden commencements (ssc) were:

October 28, 2132 UT from 12 stations
October 29, 0909 UT from 50 stations (ssc; 46[A:26; B20]; si: 3; sfe:NI)
October 30, 0838 UT from 2 stations
October 31, 0859 UT from 35 stations (ssc: 32[A:17; B:13; C:2] si: 2; pi 2: 1)
November 1, 0916 UT from 30 stations (ssc: 29[A:12; B:15; C:2] si: 1)
November 1, 1206 UT from 3 stations
November 5, 0659 UT from 2 stations.

"On the Solar and Geomagnetic Events of October - November 1968"

by

M. C. Ballario
Osservatorio Astrofisico Arcetri

Introduction

In examining the Special Events of March 1966 [Ballario 1969a] we have found that the recorded geomagnetic disturbances and other terrestrial phenomena (aurorae, ionospheric F-layer disturbances, absorption) were due to different causes:

a) the CMP of particular recurrent plages, labelled positive plages;
b) the occurrence of particular flares, primarily proton flares.

Plages - For positive plages we mean the plages of low or moderate activity which before the meridian transit are never associated with spot-groups type C or greater. Their CMPs are generally correlated with geomagnetic disturbances and other terrestrial phenomena. Particularly interesting are the recurrent active regions which before and during the meridian transit do not show chromospheric-photospheric phenomena, or only very small plages, and reveal themselves in the western hemisphere (labelled pa plages). Their CMPs are also correlated with geomagnetic disturbances [Ballario 1967-1969b].

On the contrary the recurrent plages of high activity associated before the meridian transit with spot-groups type C or greater, show "Sunspot negative effect" and their CMPs, as well as the CMPs in the subsequent rotations, are generally followed by quiet or slightly disturbed geomagnetic conditions (negative plages).

Also the non-recurrent plages are geomagnetically negative plages [Ballario 1967].

Thus during a year of minimum solar activity, like 1964, in the absence of big importance 2 or 3 flares, the recorded geomagnetic disturbances are generally correlated with the CMPs of positive plages [Ballario 1967]. In particular the geomagnetic storms and other terrestrial disturbances recorded when the Sun is completely quiet, are often correlated with the CMPs of recurrent pa plages rising in the western hemisphere some days later. These regions although not visible during the meridian transit are geomagnetically active and might be identified with the so-called "M solar regions" [Ballario 1969b].

Exceptions, described in detail in a previous paper [Ballario 1969a], to the positive and negative geomagnetic effects of the CMPs of positive and negative plages, may occur. However none of them are observed during the period under examination: Oct. 23 - Nov. 30, 1968.

Flares - It is well known that not every flare of importance 2 or 3, even if a proton flare, is followed by geomagnetic disturbance.

In a general survey of the flares recorded during the year 1968, we have found that only 19 of the 51 observed importance 2-3 flares are followed by geomagnetic storms having the Kp maximum value $\geq 5+$; 8 are followed by geomagnetic disturbances with Kp max 4+ or 5 and the others by fluctuations or by quiet and very quiet geomagnetic conditions (time delay 1-2 days).

We have to add that many of these storms and disturbances are also correlated with CMPs of positive plages.

The characteristics of the flares which are correlated with geomagnetic storms are not at present completely defined.

In a research in progress we try to obtain some other indications on these characteristics, bearing in mind that a flare may be judged entirely responsible for the subsequent storm only when there are no CMPs of positive plages correlated with the storm itself. Thus, according to our hypotheses, in order to interpret the behaviour of the Kp geomagnetic index during a year of high solar activity it is necessary to take into consideration both the CMPs of positive plages and the occurrence of particular flares.

On the basis of these data we shall examine the solar and geomagnetic phenomena recorded during the proposed period.

The events of October 27 - November 1968.

We have taken into consideration a more extended period: October 23 - November 30 in order to compare the solar phenomena occurring in correlation with very quiet or very disturbed geomagnetic conditions.

In Fig. 1 are given:

A) The CMPs of all the recurrent and non-recurrent plages observed in this period, as given in the McMath calcium plage list are presented in Table 1.

Table 1

Characteristics of plages recorded during the period Oct. 23 - Nov. 30, 1968

McMath Data					Characteristics		Remarks
1968 CMP	Lat.	McMath plage number	Return of Region	Age			(Fraunhofer solar maps)
Oct.							
23.9	N17	9735	(5)	2&3	recurrent	negative	associated with eastern E groups
25.9	S16	9739	New	1	rec.	"	Eastern H groups
26.4	N04	9752	New	1	non-rec.	"	--
27.1	N19	9741	9687	3	rec.	"	C,D groups in the preceding rotation
28.1	N13	9762	New	1	non-rec.	"	--
28.4	S15	9740	9692	3	rec.	"	Eastern D groups
30.0	S24	9745	New	1	non-rec.	"	--
30.7	N28	9744	9710(3)	2	rec.	"	C,D groups in the preceding rotation
31.5	S27	9750	New	1	non-rec.	"	--
Nov.							
1.0	N15	9761	New	1	non-rec.	"	--
2.0	N17	9746	9700 9705	6&2	rec.	"	E,C,D groups in the preceding rotation
2.2	N05	9747	9701	2	rec.	"	E groups in the preceding rotation
2.9	S16	9749	9724 9725	2	rec.	"	Eastern D groups
4.6	N18	9751	9705	2	rec.	"	E groups in the preceding rotation
4.8	S22	9755	New	1	non-rec.	"	--
4.9	S13	9753	New	1	rec.	positive	Eastern A,B groups
6.9	N33	9766	New	1	rec.	positive	Rising on Nov. 10 in western hemisphere
7.1	N35	9756	New	1	non-rec.	negative	--
7.5	N11	9754	New	1	rec.	positive	Eastern A,J groups
7.6	S23	9767	New	1	non-rec.	negative	--
7.9	S09	9757	New	1	non-rec.	"	--
8.5	N17	9770	New	1	rec.	positive	Probably recurrent at the third transit. Return of the NE part of plage 9660 (map of Sept. 15) and of the NE part of plage 9723 (map of Oct. 12)
9.5	S24	9759	9717	6	rec.	negative	E,G,D groups in the preceding rotations
10.1	S15	9758	9722	5	rec.	"	E,D groups in the preceding rotations
11.5	N18	9760	9736	2	rec.	"	Eastern H groups
12.4	S16	9763	9728	2	rec.	"	C groups in the preceding rotation
14.4	S11	9764	9737	2	rec.	"	Eastern C groups
14.8	N27	9765	9726	2	rec.	"	Eastern C groups
15.2	N02	9774	New	1	non-rec.	"	--
16.1	N11	9768	New	1	non-rec.	"	--
16.1	N17	9775	New	1	rec.	positive	Rising on Nov. 17 in western hemisphere
16.4	S24	9782	New	1	non-rec.	negative	--
17.1	S05	9771	9743	2	rec.	"	D groups in the preceding rotation
18.3	S16	9776	9733	3	rec.	doubtful	Probably negative as the fourth transit of plage 9646 associated with western groups C
18.4	S14	9773	New	1	non-rec.	negative	--
19.4	N15	9772	9735	3	rec.	"	Eastern C,D groups
21.8	S31	9778	New	1	non-rec.	"	--
22.2	N15	9779	9741 9735	2&4	rec.	"	E,D,C groups in the preceding rotations
22.3	S20	9777	9739	2	rec.	"	H groups in the preceding rotation
25.2	S18	9780	9740	4	rec.	"	Eastern D groups
26.8	S18	9783	New	1	non-rec.	"	--
27.2	S07	9785	New	1	rec.	"	Eastern D,E groups
27.3	N27	9784(3)	9744	3	rec.	"	C groups in the preceding rotations
28.1	N07	9787	9747	3	rec.	"	E groups in the preceding rotations
29.1	N04	9789	9747	3	rec.	"	E groups in the preceding rotations
30.1	S18	9790	9749	3	rec.	"	D groups in the preceding rotation
30.2	N20	9792	9746	3	rec.	"	E,D,C groups in the preceding rotations

McMath footnotes:

(5) Region 9735 is a return of regions 9678, 9683, 9687 and 9690

(3) Region 9784 is a return of region 9744, which was incorrectly identified in last month's report. It should have been listed as a return of region 9710

B) The CMPs of the recurrent positive plages only. The discrimination between positive and negative plages depending on the associated spot-group type, is based on the Fraunhofer Institut solar maps.

C) The Kp geomagnetic index (Bartels map).

D) The importance 2-3 flares and the importance 1 proton flares. The data, deduced from the Quarterly Bulletin on Solar Activity, are given in Table 2.

Table 2

Importance 2 and 3 flares and importance 1 proton flares observed during the period Oct. 23 - Nov. 30, 1968

Solar flares (Quarterly Bull. on Solar activity)							Geomagnetic storms (Bartels map)				
Date 1968	Max. UT	Position	Imp.	Area Corr.	Remarks	Active Region	Date	Kp max UT	Kp max value	Δt_h	Remarks
Oct.							Oct.				
23	2404 2421	16S-59E	2B	9.7	KLU	9740	-	-	-	-	
27	1322	18S-17E	2N	5.3	Z	"	29	∿1630	6	∿51	
29	0902	14S-08W	1B	4.2	IJKUZ	"	31	∿1330	8	∿52	
29	1223 1234	16S-12W	2B	7.9	IJKMTZ	"	31 Nov.	∿1630	8	∿52	
30	1252 1346	18S-26W	2B	7.6	IJKOUZ	"	1	∿1330	8+	∿48	
30	2358 2412	14S-37W	3B	-	FHUZ	"	1	∿2230	8+	∿46	
31	2244 2302	14S-49W	2B	10.2	FH	"	2	∿2230	6+	∿47	
Nov.											
1	0843 0903	16S-47W	2N	-	EHKLWZ	"	3	∿0130	7-	∿41	
2	0957 1012	15S-65W	2B	-	HKZ	"	4	∿1330	5-	∿51	Also correlated with the CMP of a rec. positive plage at 13S
2	1659 1708	20N-26E	2N	-	GKL	9751	4	∿2230	5	∿53	
3	1237	19S-82W	2B	-	EH	9740	-	-	-	-	
12	1426	05N-72W	2N	-	EI	9754	-	-	-	-	
18	1035	21N-87W	1B	-	AHY	9760	20	∿1330	5-	∿51	Revised as proton flare
20	0131	21S-63E	1N	-	U	9780				∿12	

From Fig. 1 it results that:

1) During the very quiet geomagnetic period Oct. 23-28 the Sun is very active, but only CMPs of non-recurrent plages or of recurrent negative plages are recorded (Table 1). The "Sunspot negative effect" is thus confirmed (Fig. 2a).

2) To the very quiet geomagnetic conditions of the preceding interval, there follows a series of big geomagnetic storms lasting Oct. 29-Nov. 4. According to the sunspot group types given in the Fraunhofer maps, there are no CMPs of recurrent positive plages during this period (Table 1 and Fig. 1B). The storms are thus entirely due to the observed series of importance 2 and 3 flares.

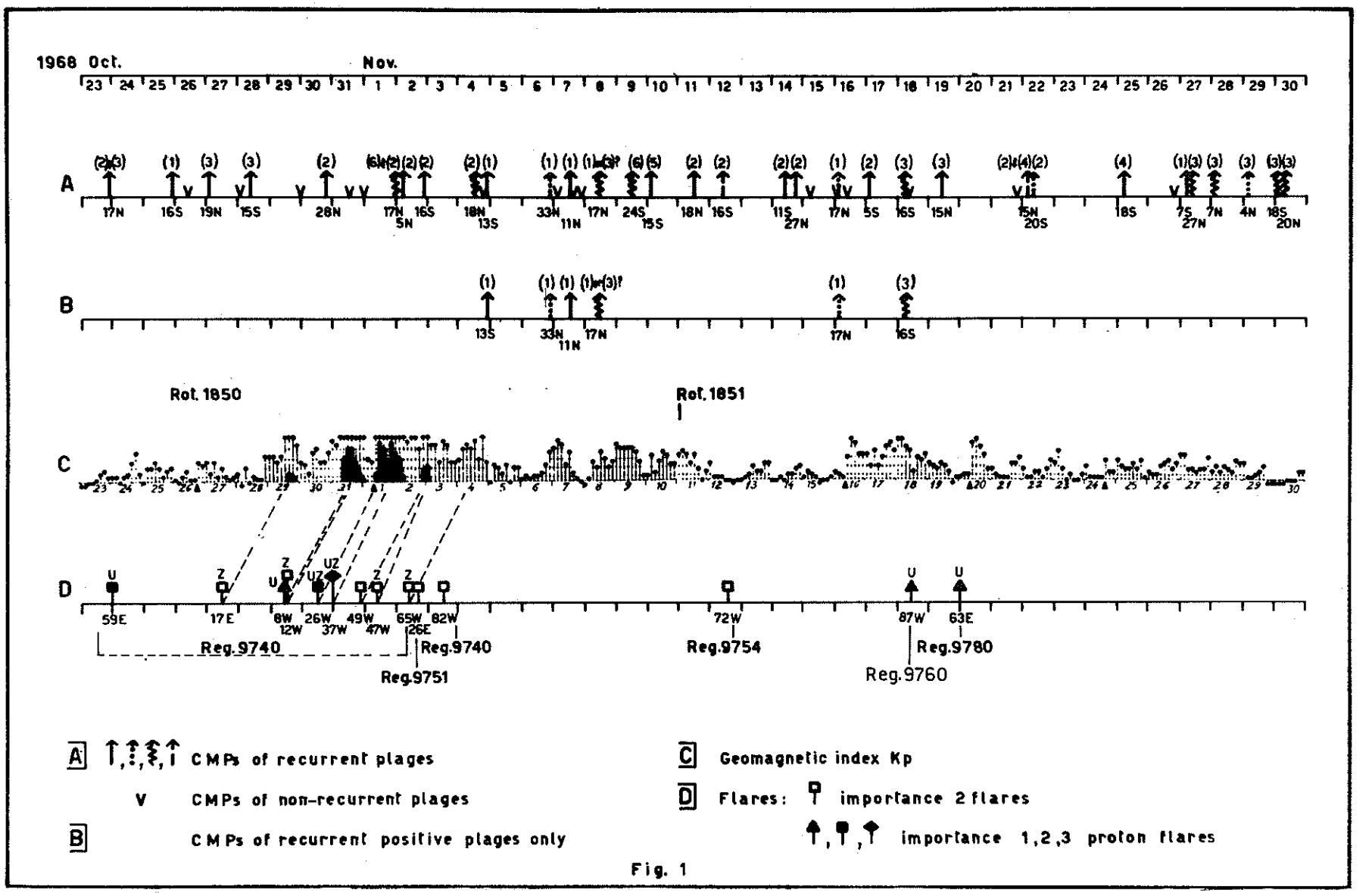

Fig. 1

Fig. 1. CMPs of the recurrent and non-recurrent plages (A), CMPs of recurrent positive plages only (B), Kp (C), and importance 2-3 flares and importance 1 proton flares (D) for October 23 - November 30, 1968.

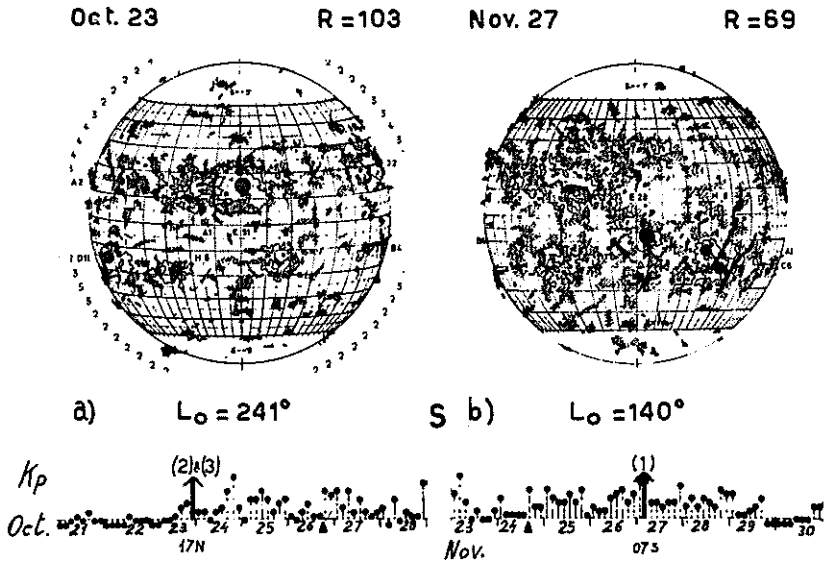

Fig. 2.- The quiet geomagnetic conditions correlated with the CMPs of recurrent negative plages:
a) at 17 N associated with the spot-group type E51
(McMath data: No. 9735 - 17N - CMP: 23.9 Oct.-age 2 & 3)
b) at 07 S associated with the spot-group type E28
(McMath data: No. 9785 - 07S - CMP: 27.2 Nov.-age 1)

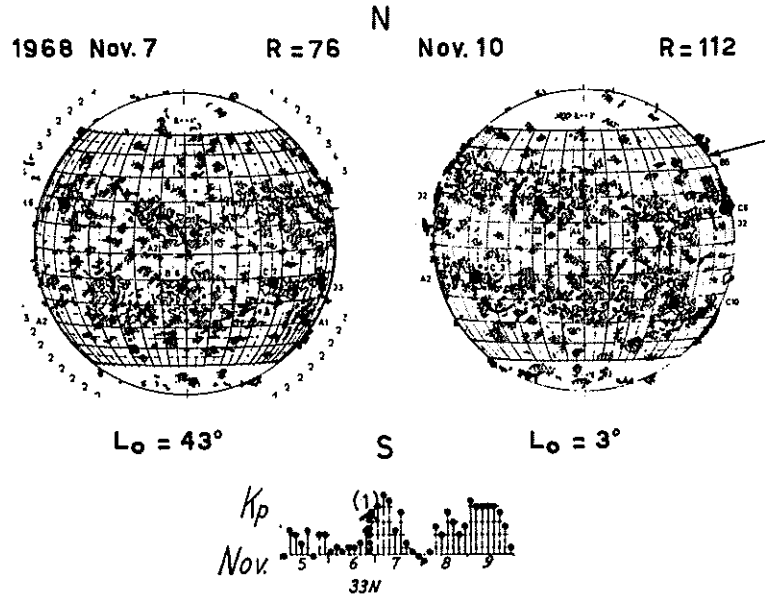

Fig. 3.- The moderate disturbance of Nov. 7 is correlated with the CMP, on Nov. 6.9, of a typical pa recurrent positive plage rising in the western hemisphere on Nov. 10 at 33N - 47W, (L = 50°), associated with a spot-group type B5.
(McMath data: No. 9766 - 33N - CMP: 6.9 Nov.-age 1)
The plage at 23S (No. 9767 - CMP: 7.6 Nov.) is a non-recurrent one.

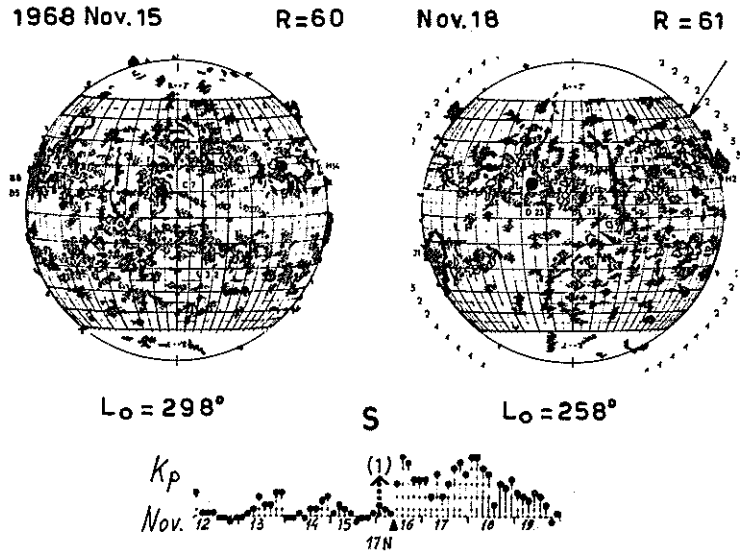

Fig. 4.- The sc geomagnetic disturbances of Nov. 16-17-18 are correlated with the CMP, on Nov. 16.1, of a typical pa recurrent positive plage at 17N and L = 292°, rising in the western hemisphere on Nov. 17 at 17N - 20W, associated with a spot-group type A4 which changes into C8 on Nov. 18.
(McMath data: No. 9775 - 17N - CMP: 16.1-age 1)

Some characteristics of these flares are:

- they belong (except the flare of Nov. 2 at 20N) to the same southern recurrent negative plage (McMath No. 9740) at its third transit, but we have to note that a resurgence takes place in this region after the second transit;
- most of them have the remark Z (major spot umbra covered by flare) and three have the double remark Z and U (proton flare);
- if we attribute the greatest storms of the series (Nov. 1: Kp max at 13 and 22 UT), to the UZ flares of Oct. 30 (max at 13 and 24 UT) we have a time delay of about two days. (Almost the same time delay is found for the UZ importance 3 flare of May 23, 1967 and the subsequent geomagnetic storm of May 25 [Akasofu and Perreault, 1969]. On this assumption other importance 2 and 3 flares of the series under examination may be related to a Kp maximum occurring about two days later (Fig. 1 and Table 2). However, other associations with different time delay may be proposed.

A CMP of a positive plage (McMath No. 9753) occurs on Nov. 4.9. It may be correlated with the last part of the geomagnetic disturbances.

3) After the West limb passage of region No. 9740, no big flares are recorded until Nov. 12, but geomagnetic disturbances are observed during the period Nov. 6-20. These disturbances are correlated with CMPs of recurrent positive plages (Fig. 1 and Table 1) the most interesting of which are plages No. 9766 at 33N (Fig. 3) and No. 9775 at 17 N (Fig. 4) rising in the western hemisphere. The positive geomagnetic effects of the CMPs of the recurrent pa plages is again confirmed.

The importance 2 flare of Nov. 12 is followed by very quiet geomagnetic conditions. On the contrary the sc geomagnetic disturbance of Nov. 20 may be due to the importance 1 proton flares of Nov. 18 or/and of Nov. 20, since there are no correlated CMPs of positive plages.

4) There follows another very quiet geomagnetic interval, Nov. 21-30, during which only CMPs of negative plages are observed (Table 1, Fig. 1 and Fig. 2b).

Conclusion

The behaviour of the Kp geomagnetic index during the period Oct. 23-Nov. 30 may be interpreted as follows:

- the series of great geomagnetic storms Oct. 29-Nov. 4 is well correlated with a series of importance 2 and 3 flares rising in the same negative plage No. 9740 and having mostly the characteristic Z and UZ. Probably the Kp maxima follow the flare occurrences after about two days. No CMPs of positive recurrent plages are correlated with the storms.
- The other geomagnetic disturbances are well correlated with CMPs of recurrent positive plages, some of which rise in the western hemisphere and, at their meridian transit, may be considered as "M solar regions".

No big flares are responsible for these geomagnetic disturbances.

- The very quiet or slightly disturbed geomagnetic conditions, recorded when the Sun appears to be very active (Oct. 24-28) or moderately active (Nov. 21-30), are associated with CMPs of negative plages.

These results are in good agreement with those obtained in examining the solar and terrestrial phenomena during the year 1964, and for other intervals of 1966 and 1968.

The unlike geomagnetic effects related to plages of different activity have been also pointed out by Bumba and Howard. The authors compare the recurrent geophysical disturbances with solar active regions and with the persistent low-latitude background field pattern in the magnetic fields on the solar surface and conclude that "around the maximum the geophysical disturbances tend to avoid active regions and around the minimum they tend to be associated with the zone of moderate activity" [V. Bumba, R. Howard, 1969].

REFERENCES

AKASOFU, S.-I. and P. D. PERREAULT	1969	The geomagnetic storm of May 25-26, 1967, World Data Center A - Upper Atmosphere Geophysics Report UAG-5, 92-105.
BALLARIO, M. C.	1967	The Quiet Sun Year 1964. Relationship between the CMP's of solar recurrent plages and terrestrial phenomena, IQSY Notes, 21, 36-48.
BALLARIO, M. C.	1969a	On the special events of March 1966. Correlation beween solar and terrestrial phenomena, Ann. Geophys., 25, fasc. 1, 135-146

BALLARIO, M. C. 1969b The IQSY 27-day recurrence sequence for 1964. Solar and terrestrial activity, Mem. SAIt., 40, fasc. 3.

BUMBA, V. and R. HOWARD 1969 On the solar sources of recurrent geophysical effects, Bull. Astr. Inst. Csl., 20, 61-62.

"Short Description of Geomagnetic Activities Observed in Greenland During the Events 30 October - 3 November 1968"

by

K. Lassen
Danish Meteorological Institute, Charlottenlund, Denmark

[The following notes were supplied by Dr. Lassen from interpretation of the records from the magnetometers measuring H, Z and D components at Narssarssuaq (61.2N 45.4W), Godhavn (69.2N 53.5W) and Thule (76.6N 68.8W). The coordinates are geographic and the times are all UT.]

Magnetic disturbances 30 October - 3 November 1968

Narssarssuaq. Activity starts around 2300 on 30 October. Substorm around 0000 on 31 October with negative bay in H about 500γ and positive in Z about 250γ. Thereafter the activity increases with a negative bay in H around 0800 31 October (600γ) followed by a positive bay in H and a negative bay 1000-1200 October 31 (120γ). On 1 November there is a substorm at 0100-0200 with negative bay in H (900γ) and a negative bay in Z (600γ). Thereafter it is rather quiet until noon. On 1 November there is a SSC at 0917 followed by continuous activity to 1000 on 2 November. On 1 November there are negative bays in H of about 1000γ at 1330 and 1500. Moderate negative bays in H occur on 3 November at 0000-0200 and 0600-0800.

Godhavn. Moderate substorms give negative bays in H on 31 October 0000-0100, 0300-0400 and 0700-0830. On 1 November there is a moderate substorm at 0200 with a positive bay in Z (negative bay in Z at Narssarssuaq at the same time). On 1 November there are negative bays in H 1100-1200 (600γ) and 1400 (400γ), thereafter slow recovery with several small bays. There is a negative bay at 1400 (1800γ) and positive in H at 1430 (1000γ). SSC is seen 1 November at 0917 in H and D. Storm activity from SSC follows until about 0600 on 2 November. Disturbed conditions occur again from 1700 on 2 November to 0400 on 3 November with substorms at 2200-2300 on 2 November and at 0100-0230 on 3 November.

Thule. The SSC on 1 November at 0917 is only clearly seen in H. There is SD variation in H and D after SSC. On 1 November there are negative bays in H at 1100-1330 (500γ) and at 1430-1530 (400γ). There is a positive bay in H at 1330-1430 (300γ).

"Some Specific Features of the Perturbed Period October 27 - November 2, 1968"

by

E. Selzer and J. Roquet
Service et Laboratoire de Magnétisme
et d'Électromagnétisme Terrestres
Institut de Physique du Globe, Paris

In general this period is characterized by an unusual continuity in the display of any kind of aspect of geomagnetic disturbances. Any detailed report of these -- as detected by our registrations in CHAMBON-LA-FORET (and its side-station, of GARCHY, 100 km away) -- would require dozens of pages. Therefore we will limit our contribution to three very specific particularities which were observed from October 31 to November 2 which, although having being observed on some other occasions, never have followed each other, so far, in such a clear intense manner.

The three particular phenomena we are referring to are:

1. Two very isolated (but close to each other) cases of storm pulsations.
2. A very spectacular case of giant pulsation.
3. A very unusual series of a great number of pi 2 + pi 1, IPDP-like events.

We are going to examine these three type of events, successively.

Type 1 Storm pulsations events.

By this term "storm pulsation" we refer to some very regular, quite monochronomatic micropulsations, of a few seconds in period, which have appeared on a few other occasions in the middle of the most perturbed and intricate part of a few huge worldlike storms. (Other known cases refer to the storms of July 8, 1958, and to the one of July 15, 1959). In the present case, these "storm pulsations" appear in two separated but closely following groups.

The first group from 16.07.50 UT to 16.09.00 UT on October 31 consists of a little more than 20 oscillations (the last ones are lost in the magnetic background noise), is very monochromatic, of period 3.0 seconds with a regular increase, then decrease of the amplitude after having reached a maximum amplitude of about 0.35γ.

The second group from 16.13.13 UT to 16.14.06 UT on the same day (a little more than 5 minutes later). There is the same general morphology, same period (3.0 seconds) as for the first group. The maximum amplitude is a little bigger, about 0.4γ.

These two groups have been registered, nearly identically, at the two stations of CHAMBON-LA-FORET and GARCHY (about 100 km apart) on both magnetic and telluric registrations, H and D for the magnetics and the two orthogonal directions for the tellurics. The oscillations seem to be linearily polarized (further investigations are in progress). The study has been confined, so far, to paper records (30 mm/minute of paper speed), but magnetic tape registrations exist at Chambon.

Examination of similar equatorial records at ADDIS-ABABA distinctly shows these two groups of pulsations. Other equatorial records gave negative results, the traces being strongly perturbed by regional electric-storm effects. A study on the exact limits of the geographical domain of these storm pulsations is badly needed.

Type 2 Giant pulsations.

Giant pulsations occur between 2145 and 2300 UT the same day (October 31, 1968), during a lull of the storm. (In fact, the lull extends from 2110 to 0045 on November 1, but the giant pulsations do not fill all the duration of this lull).

Period: about 7 minutes (not very constant, nor regular)

Amplitude: greater than 10γ (will be more exactly determined subsequently).

About same appearance at CHAMBON-LA-FORET and at GARCHY.

Polarization: elliptically polarized (exact determination in progress).

Geographical domain: These giant pulsations do not seem to appear on our equatorial records. A study on the limits of the geographical domain of their manifestation is highly desirable.

Type 3 Series of IPDP-like events.

These series appear on November 1 and November 2.

So far, only graphical determinations by direct observations of the wave-form have been made.

Each event consists mainly of two parts: a "SIP-like" event of confused oscillations (with no distinct periods - a mixture of pi 2 and pi 1) lasting about 3 to 5 minutes, and following this a pi 1 event of much shorter period lasting also a few minutes. This double structure, constitutes the schematic elements of a IPDP event. For a confirmation of this, spectral analyses are needed. (They are planned for the CHAMBON-LA-FORET records where magnetic-tape registrations of the events exist).

Because of the inclusion of these successive individual events in the general complexity of the other kind of perturbations constituting the overall activity of the storm, it has not been easy to determine the beginning and the closing times of each one of these events. Therefore, the following list is given here only tentatively.

Event No.	I :	Between 2210	and	2222	on November 1
	II :	" 2227	"	2236	"
	III :	" 2311	"	2317	"
	IV :	" 2328	"	2335	"
	V :	" 2357	"	0002	Nov. 1 to Nov. 2
	VI :	" 0007	"	0030	on November 2

This list is not exhaustive, but more precise measurements are required. Just as for the other types of events, the world-domain of these has to be determined.

"Hourly Equatorial Dst Indices for the Magnetic Storm Beginning on October 29, 1968"

by

M. Sugiura and S. J. Cain
Laboratory for Space Physics
Goddard Space Flight Center, Greenbelt, Maryland 20771

The figure presents the hourly equatorial Dst indices for October 16 through November 15, 1968. The Kp indices for the same period are also plotted on the figure, and the sudden commencements are indicated.

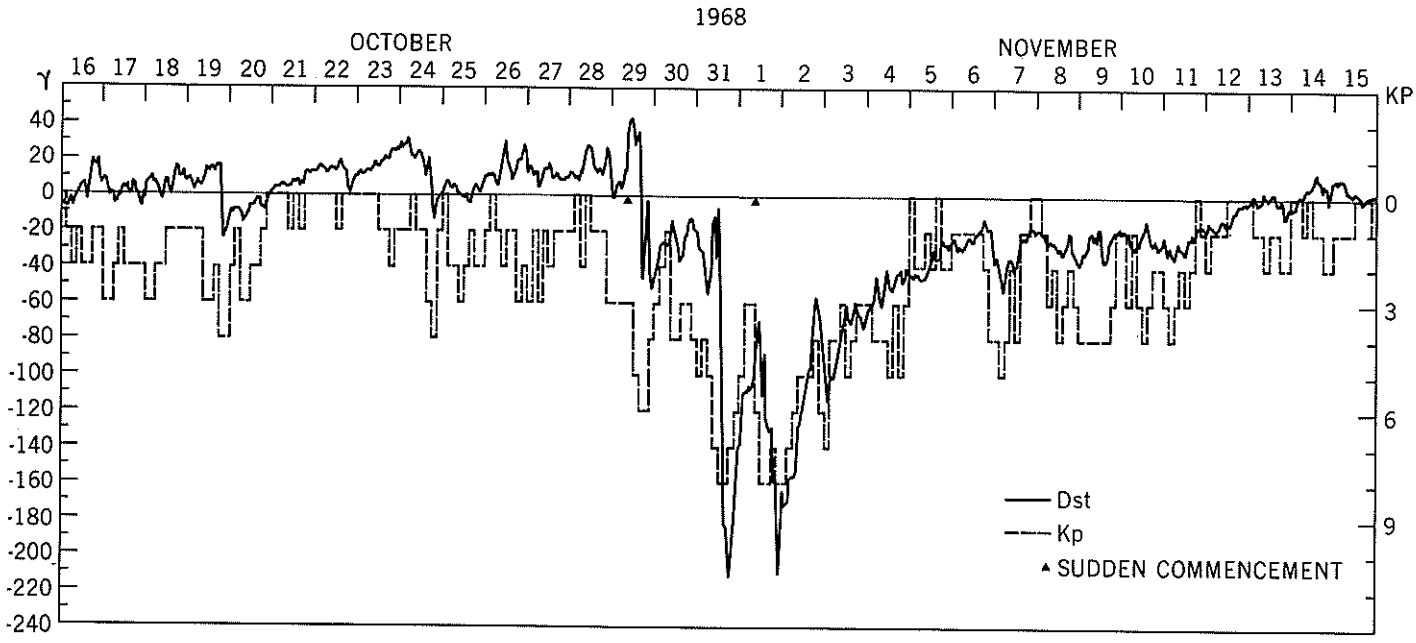

"Geomagnetic Disturbances (October 26 - November 5, 1968)
Associated with the McMath Plage Region 9740"

by

S.-I. Akasofu and K. Kawasaki
Geophysical Institute, University of Alaska
College, Alaska 99701

ABSTRACT

Geomagnetic disturbances primarily associated with the McMath plage 9740 which traversed the sun during the latter part of October and early November of 1968 were studied. As the flare-producing plage region passed through the central meridian of the sun from the eastern to the western limbs, systematic changes in the characteristics of the geomagnetic storms were observed, although somewhat complicated by the presence of flares produced by the McMath region 9739.

The magnetic records from a number of low and high latitude stations widely distributed in longitude are presented for the period of major storms.

A series of complex geomagnetic disturbances in the latter part of October and also in the early part of November 1968 were caused by an active region (McMath Plage region 9740) which was first observed on October 21 on the eastern limb, passed the central meridian on October 28 and disappeared at the western limb about November 4. There is also an indication that some of the disturbances during this period were caused by other active regions, such as the McMath Plage region 9739.

October 22 was the quietest day of that month, the Kp indices being 0o, 0o, 0o, 0o, 1-, 0+, 0+, 0+ (Σ Kp =2-). A similar situation also existed in the early half of October 23, the Kp indices being 0o, 0o, 0+, 0+.

Weak si activity began in the latter half of October 23, with the Kp indices rising to 1-, 1+, 2-, 1o. A number of weak si's were recorded during this period and also in the early half of October 24 (1o, 1o, 0+, 1o). A weak magnetic disturbance began at 1500 UT on October 24 and lasted until the end of the day; the Kp indices in the latter half of this day were 1+, 3-, 4-, 1+. Magnetic activity on October 25 and in the earlier half of October 26 was also characterized by weak si activity; the Kp indices during this period were 0+, 2o, 2o, 3-, 2o, 1o, 2-, 2o, and 1-, 0+, 1o, 2-.

Between October 21 and 26, the McMath Plage region 9740 (hereafter abbreviated as the M9740 region) shifted from the eastern limb to about the central meridian distance E25. During this period, the M9740 region was relatively quiet, although there occurred a few intense flares, such as those during 2356-0009 UT, October 23/24 and at 2057, October 24.

Fig. 1 shows the H component magnetic records from Honolulu for the period between October 26 and November 5, 1968; the major flares which occurred in the M9739 and M9740 regions are also indicated. The figure also includes major si's during the period under study.

The first magnetic storm associated with the M9740 region began at 1833 UT on October 26, with a distinct ssc. It is likely that either or both solar flares on October 23 and 24 mentioned above were responsible for the storm. The storms had typical features associated with flares in the eastern (helio) hemisphere; that is, a distinct ssc and an initial phase with a very weak main phase [Akasofu and Yoshida, 1967; Akasofu, Perreault and Yoshida, 1969]. The storm ended by 09 UT on October 27 and was followed by a quiet period which lasted for more than 24 hours.

During the period when the M9740 region was located near the central meridian and west of it, it became quite active and produced a number of intense solar flares. They are indicated in Fig. 1.

It seems quite likely that the second storm was associated with the flare which occurred at 1240 UT on October 27. The M9740 region was at S15, E19 at that time. Again, the storm had characteristics of being associated with an eastern flare. It began with a distinct ssc and initial phase, without a significant main phase.

The third storm began with a double ssc which occurred at 0640 and 0909 UT on October 29; however, only the latter ssc is reported in Solar-Geophysical Data. The storm had all the major characteristics of being associated with a western flare. It exhibited very intense si activity which lasted for more than 12 hours and which was then followed by a relatively weak main phase. Some other such examples were discussed by Akasofu, Perreault and Yoshida [1969]. It is suggested that the flare at 0200 UT on October 28 in the M9739 was responsible for the storm. This particular region was located at S19 W29 at that time.

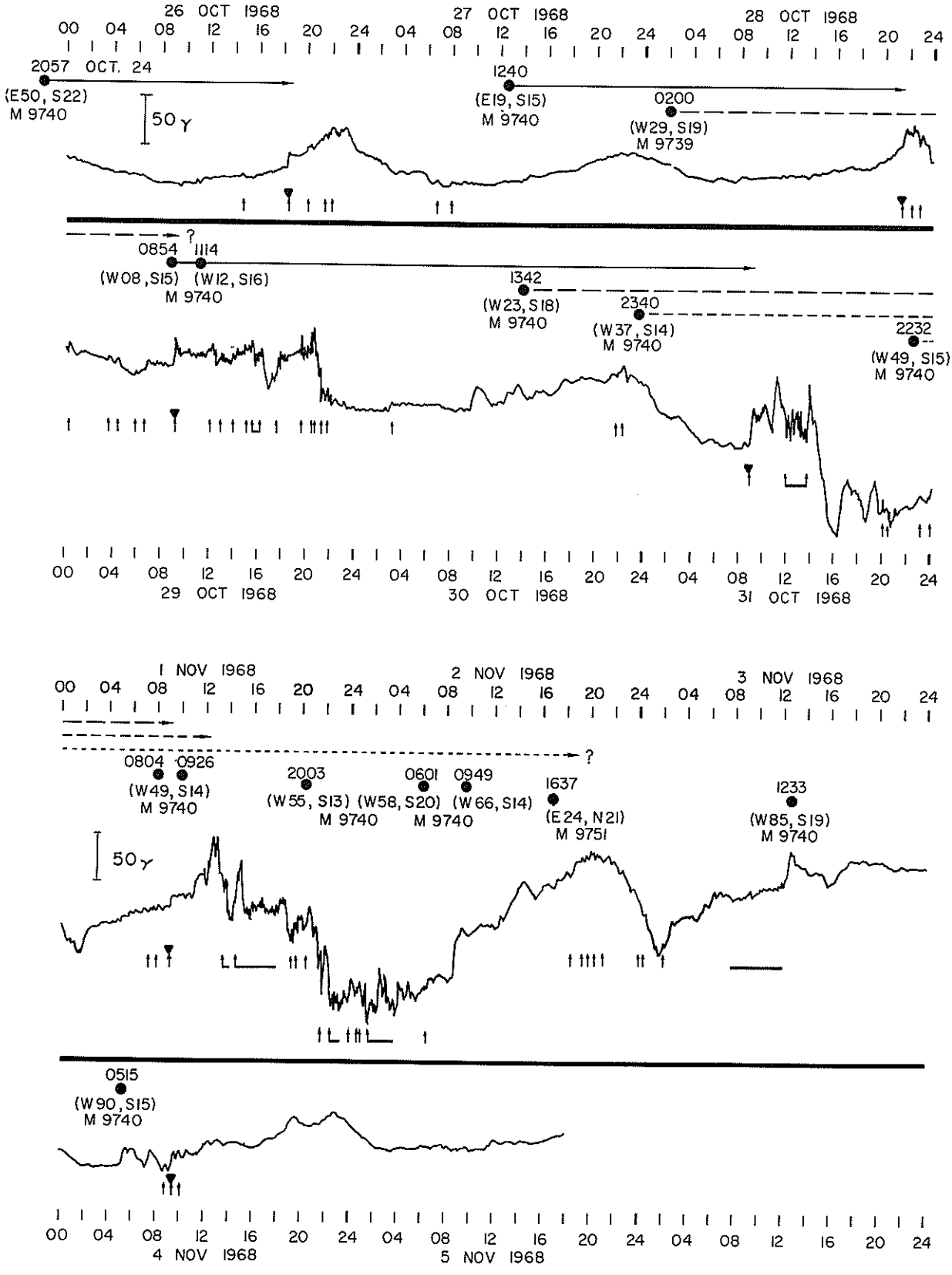

Fig. 1. The H component magnetic record from Honolulu for the period between October 26 and November 5. The McMath Plage region 9740 was facing the earth during this period. The occurrence times of the major solar flares (importance greater than 2) and their inferred association with the corresponding geomagnetic storms are indicated. The major si's are indicated by arrows and reported ssc's by triangles over arrows.

In order to show details of the development of the storm, Fig. 2a shows a collection of magnetic records from six low latitude stations which are distributed in all longitudes, and Fig. 2b shows the collection of the records from six high latitude stations. Unfortunately, magnetic records from Siberia were not available during the preparation of the paper. However, it may be inferred from Fig. 2b that there occurred at least two major polar substorms during the storm, one a little after 16 UT and the other at about 20 UT. A weak brief main phase developed during the first substorm. Also it was greatly asymmetric and was most intense in the afternoon and the evening sectors (see the Tashkent, M'Bour and San Juan records), but there was only a little indication of it in the early morning sector (see the Honolulu and Kakioka records). The substorm subsided by 19 UT; the main phase was also recovering at that time. A complex series of si activity began at about 1930 UT which was then followed by another weak main phase depression (Fig. 2a). The second substorm took place during this period.

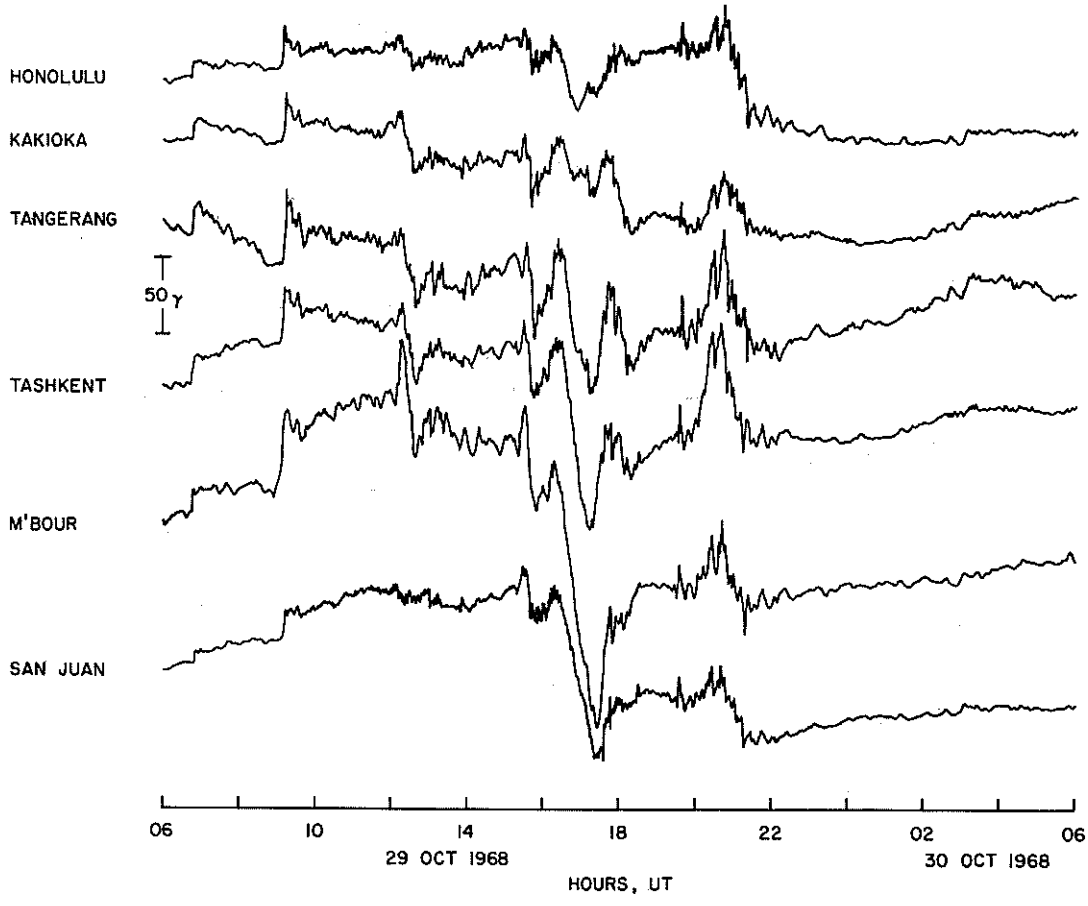

Fig. 2a The collection of the H component magnetic records from six low latitude stations for the storm of October 29/30, 1968.

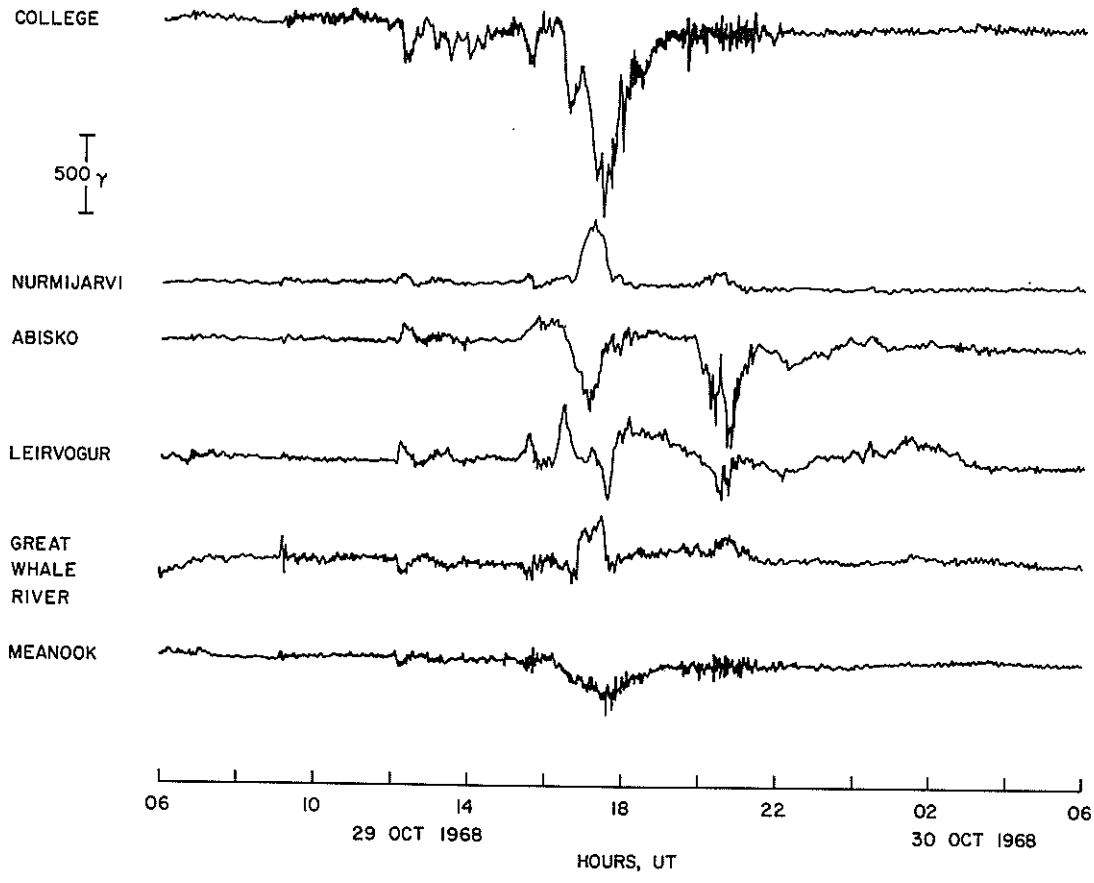

Fig. 2b The collection of the H component magnetic records from six high latitude stations for the storm of October 29/30, 1968.

The fourth storm had characteristics of being associated with a central meridian flare. It began with a large ssc at 0859 UT on October 31 and developed a large main phase. Figs. 3a and 3b show a collection of magnetic records from six low latitude stations and ten high latitude stations. The ssc was soon followed by a weak main phase and a single polar substorm which occurred between 1000 and 1150 UT. Then, an intense si activity followed, lasting from 1150 UT to 1340 UT. A series of polar substorms began at about 1340 UT. An intense main phase developed during the substorm activity (Figs. 3a and 3b). The main phase was also quite asymmetric, being most intense in the evening sector. Only a moderate disturbance was recorded at Honolulu, since the station was in the forenoon sector during the growth period of the storm.

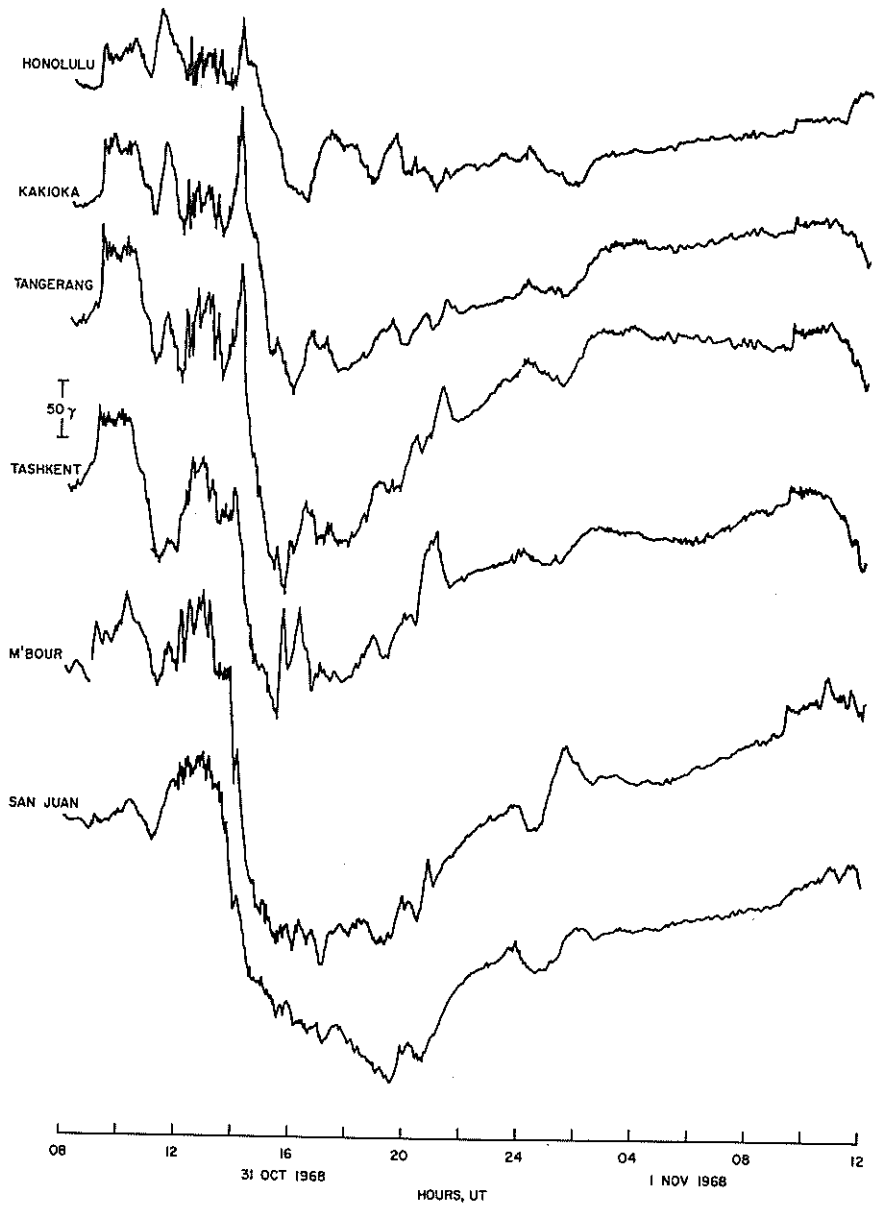

Fig. 3a The collection of the H component magnetic records from six low latitude stations for the storm of October 31/November 1, 1968.

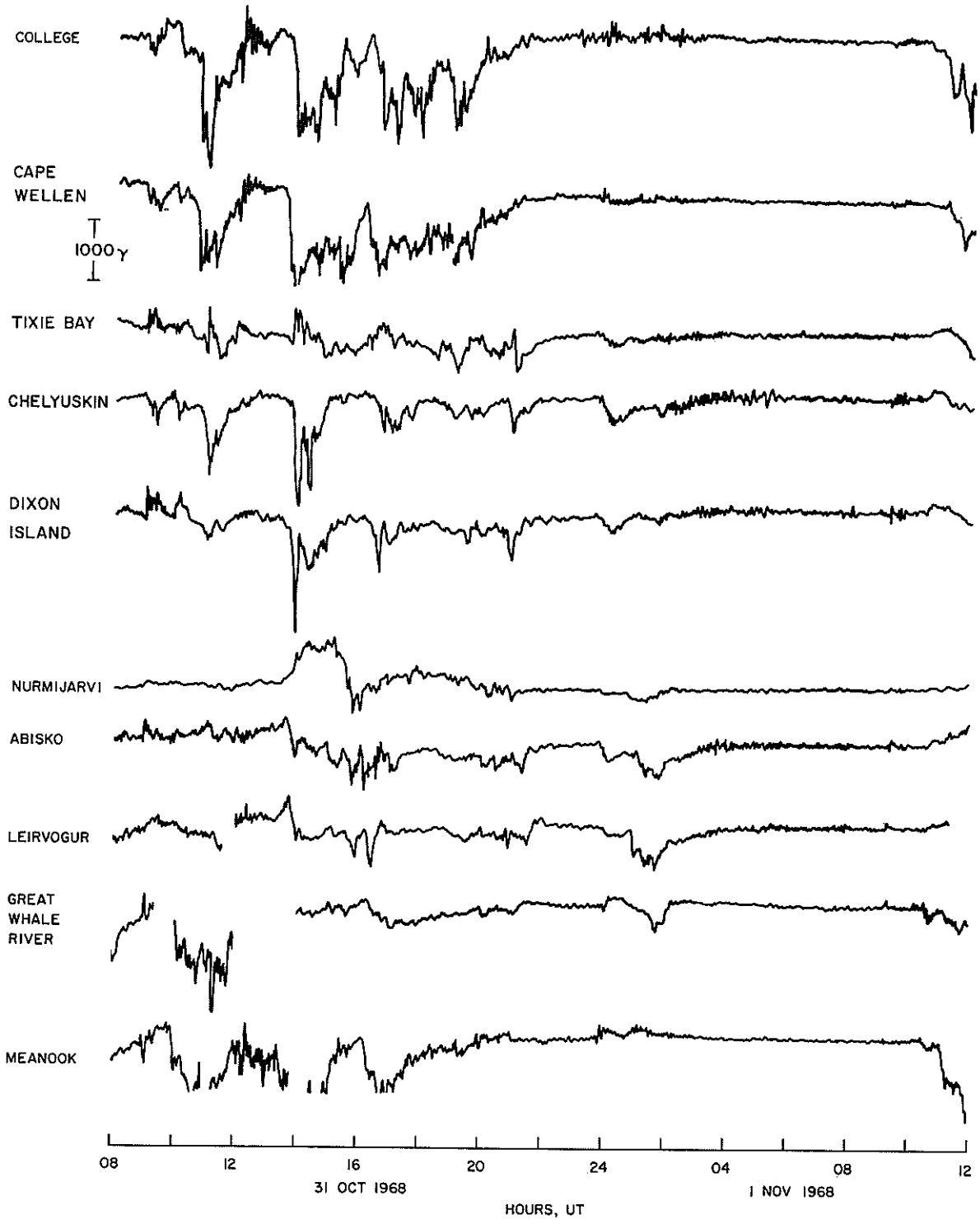

Fig. 3b The collection of the H component magnetic records from ten high latitude stations for the storm of October 31/November 1, 1968.

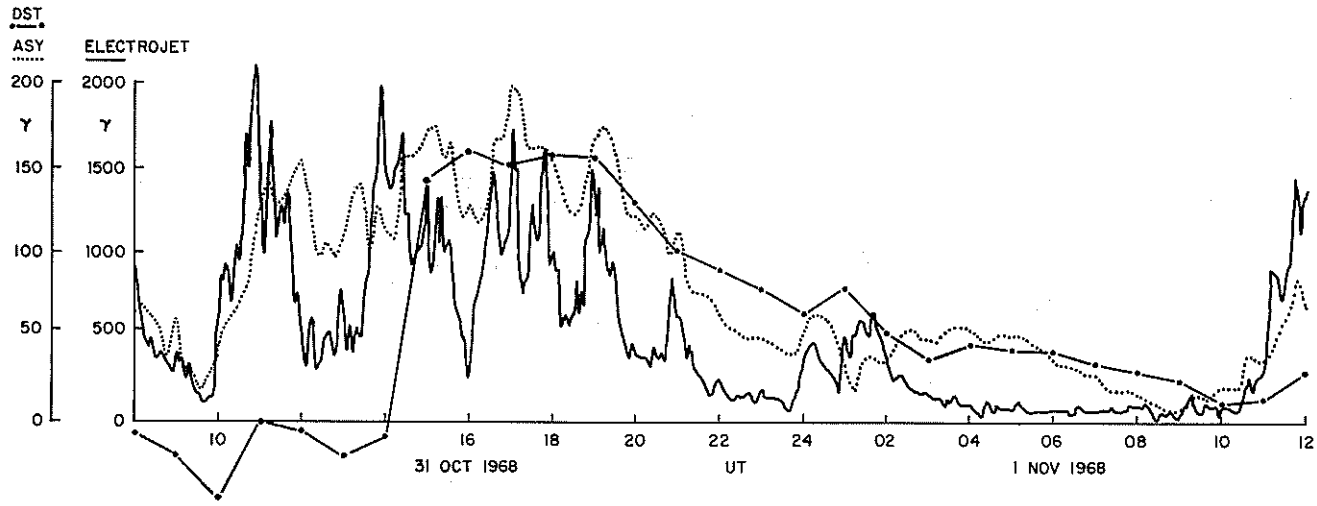

Fig. 3c The Dst, asymmetry and electrojet indices for the October 31/ November 1, 1968 storm.

Fig. 3c shows the Dst index, the asymmetry index and the electrojet (AL) index for the storm. For the procedures for obtaining those indices, see Solar-Geophysical Data; May 1969, pp. 148-149. It can be seen that the asymmetry and the electrojet index had a similar time variation.

The fifth storm began with a distinct ssc at 0917 UT on November 1. This storm also had typical characteristics of being associated with a western flare. A very intense si activity was present during the storm period. Figs. 4a and 4b show a collection of magnetic records from six low latitude and nine high latitude stations. The main phase was weak. In Fig. 1, the November 1 storm appears as intense as the October 31 storm; this is, as mentioned earlier, because Honolulu was located in an unfavorable local time sector to observe the former storm, but in a favorable sector during the latter storm.

In high latitudes, there occurred two intense substorms (Fig. 4b) during an early phase of the storm. This activity was followed by a series of weak substorms for more than 24 hours.

The M9740 region became quite active after the end of October 31. There occurred at least six flares by 12 UT on November 2. It is likely that either or both the flares at 2232 UT on October 31 and 0804, 0926 UT on November 1 were responsible for the sixth storm which began with a series of weak si's between 1830 UT and 2130 UT on November 3 which was then followed by an appreciable main phase decrease.

However, the flares at 2003 UT on November 1 and those at 0601, 0949 UT on November 3 appeared to produce only a very minor disturbance which consisted of an ssc at 0927 UT, followed by an si. It is quite likely that this is at least partly due to the large central meridian distance of the flares [Akasofu and Yoshida, 1967]. By November 5, effects from the M9740 region became unrecognizable. The Kp indices on November 5 and 6 were (0+, 2+, 2o, 1+, 2+, 0+, 2o, 2o) and (1-, 1o, 1-, 1o, 1o, 1+, 2+, 4-), respectively.

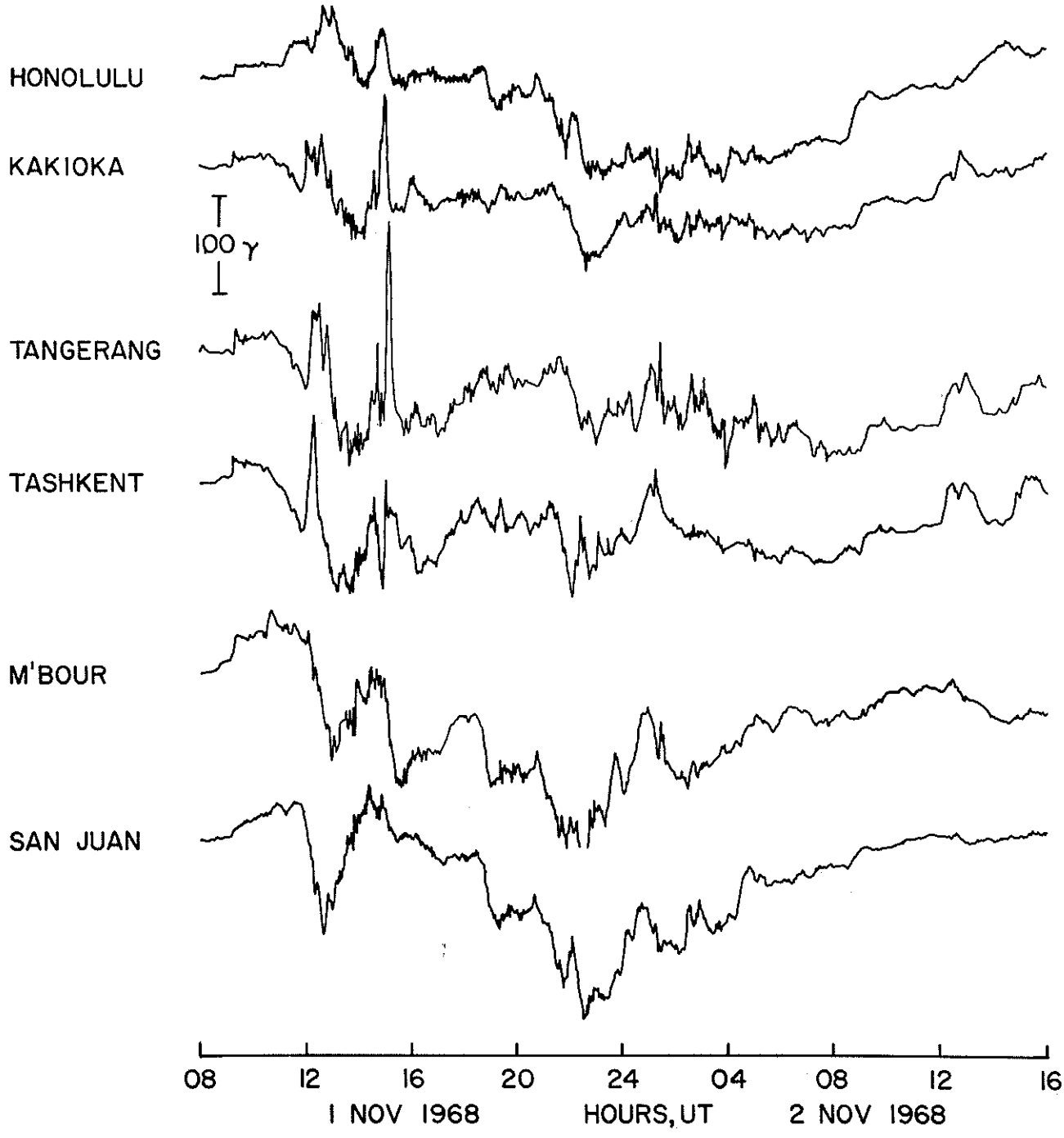

Fig. 4a The collection of the H component magnetic records from six low latitude stations for the storm of November 1/2, 1968.

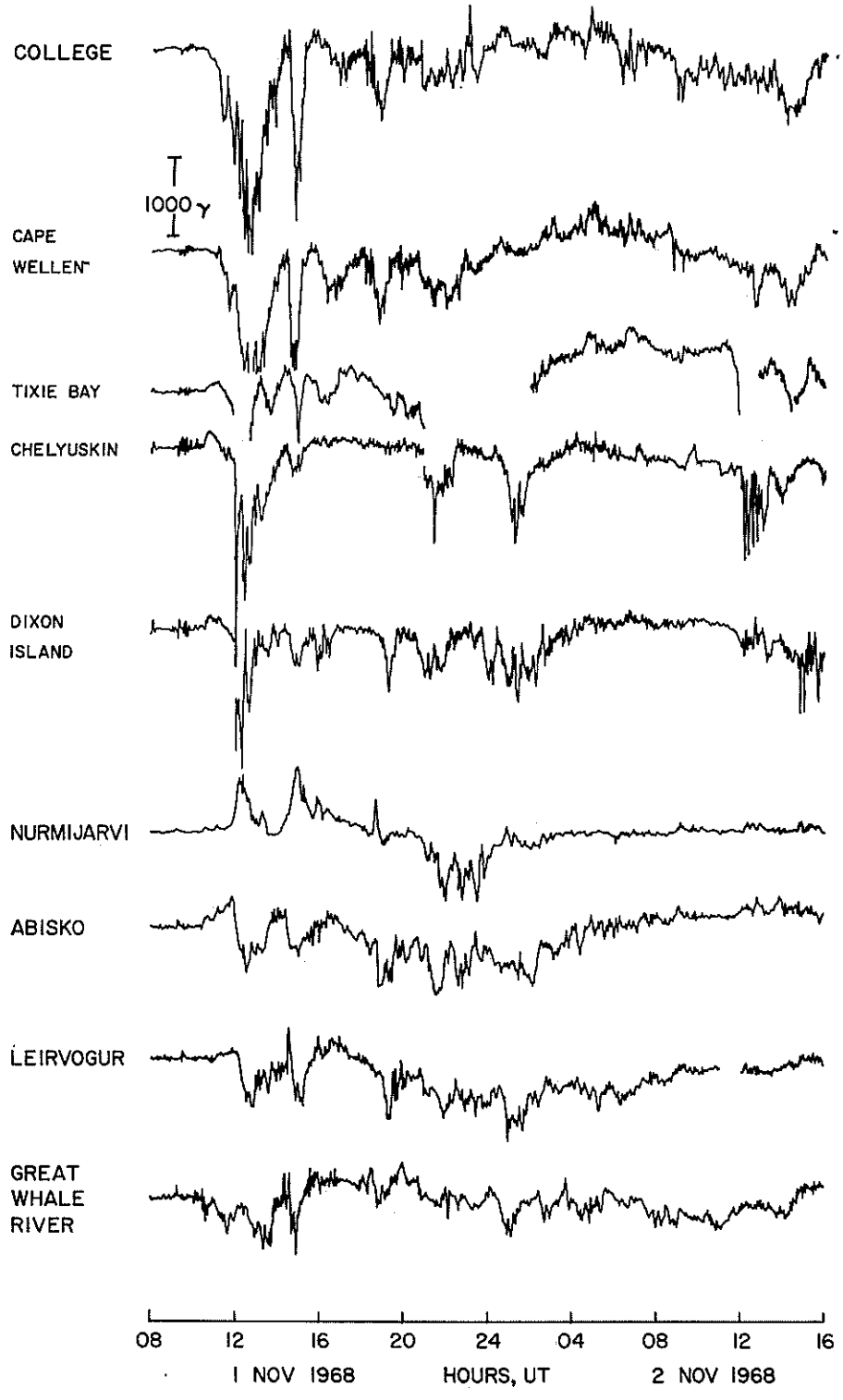

Fig. 4b The collection of the H component magnetic records from nine high latitude stations for the storm of November 1/2, 1968.

REFERENCES

AKASOFU, S.-I., P. PERREAULT and S. YOSHIDA — 1969 — The geomagnetic and cosmic ray storm of May 25/26, 1967, Solar Physics, 8, 464-476.

AKASOFU, S.-I., and S. YOSHIDA — 1967 — On the three-dimensional structure of the solar plasma flow generated by solar flares, Plan. Space Sci., 15, 942-944.

Acknowledgement

This study was made possible by the National Science Foundation GA-1703. A special thanks to Mr. W. Paulishak for efficient service in providing the magnetograms for this work.

11. AURORAL PHENOMENA

"Auroral Activity in Western Europe October 27-November 2, 1968"

by

J. Paton
University of Edinburgh, Edinburgh, Scotland

[Dr. Paton has supplied the following statements which are expanded versions of the Abbreviated Calendar Record statements published in STP Notes No. 7. All times are Universal time.]

1968 October 27-28 No unusual auroral activity.

28-29 Auroral glow on horizon visible to latitude 60°.

29-30 Cloudy conditions but interference filters showed aurora present from 1720h, and visible to about 20° above horizon in latitude 59°. Thereafter cloud too thick to allow any useful observations but clearance between 0300h and 0600h showed no aurora in latitude 59°.

30-31 Overcast conditions prevent observations.

31-Nov. 1 Overcast south of latitude 60°. A rayed arc with base overhead just to the north of Shetland after sunset, broke up about 1930h into several rayed bands, one showing striations. Pulsation occurred just before the forms began to recede northwards about 2130h. The active phase of this display was completed by about 2200h.

November 1- 2 Brighter and more active than the display of the previous night and activity persisted all night. Rayed arcs and bands were overhead from latitude 60° to at least 70°. It was overcast over Western Europe south of latitude 60° but a glow on the horizon was seen to latitude 49° over the Western Atlantic.

2- 3 Auroral light visible to latitude 56° at 0050h.

"Ascaplots for Greenland Stations October 30-November 2, 1968"

by

K. Lassen
Danish Meteorological Institute, Charlottenlund, Denmark

[Dr. Lassen has kindly supplied ASCAPLOTS for October 30-November 2, 1968 for Thule, Nord, Godhavn, S. Strømfjord, Kap Tobin, and Narssarssuak. The symbols are as described in Annals of the Geophysical Year, Vol. XX (Part I), 1962. Total cloudiness is marked by vertical lines through the middle of square 1, 2 or 3. Partial cloudiness is marked by a dot in the middle of square 1, 2 or 3. No operation is indicated by a thick horizontal line. Start and stop are marked by a thick vertical line. Twilight is indicated by an arrow at the end of the horizontal line. Filled in squares represent the following:

Line 1 = Aurora in north range, 80°-60°N zenith distance
Line 2 = Aurora in zenith range, 60°N-60°S zenith distance
Line 3 = Aurora in south range, 80°-60°S zenith distance
Line 4, Line 5 = Brightness according to scale 0-3, only in the zenith range.]

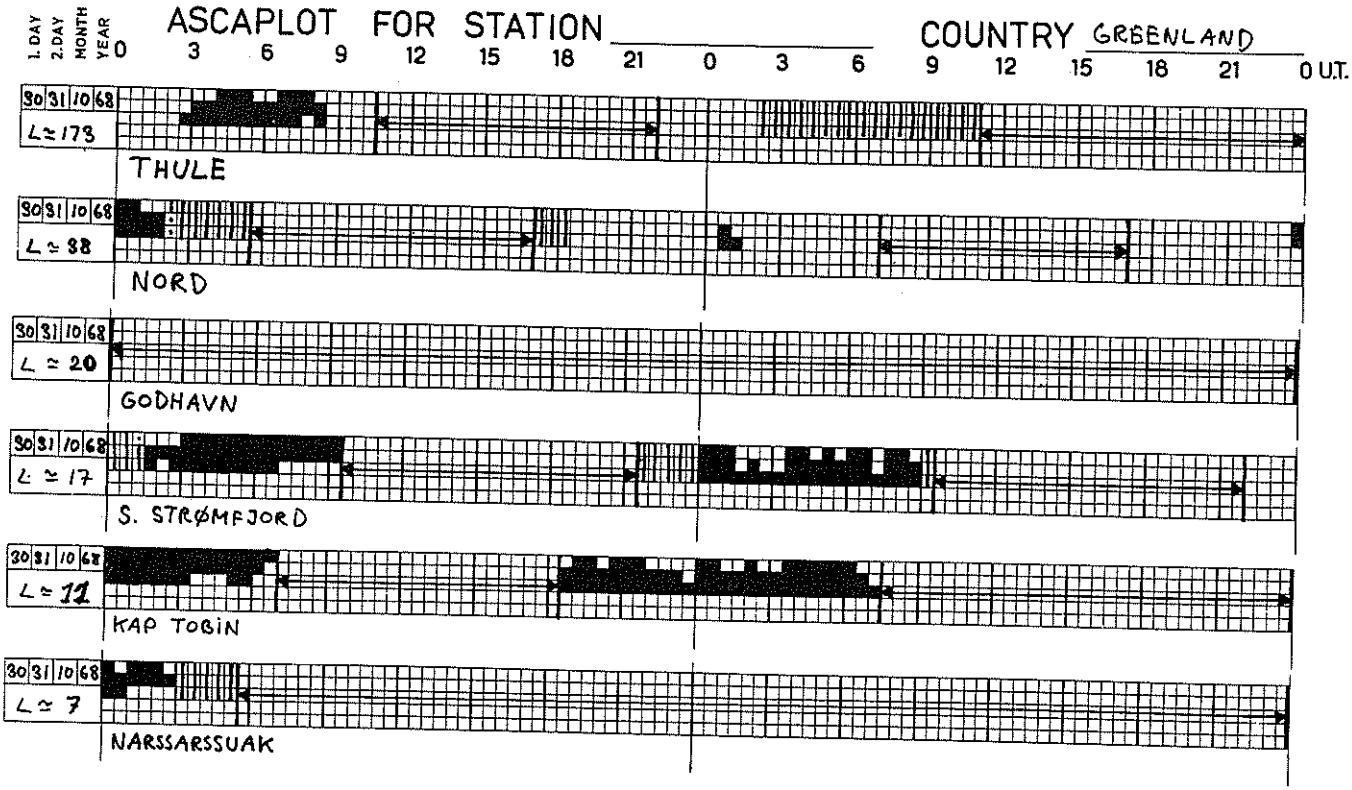

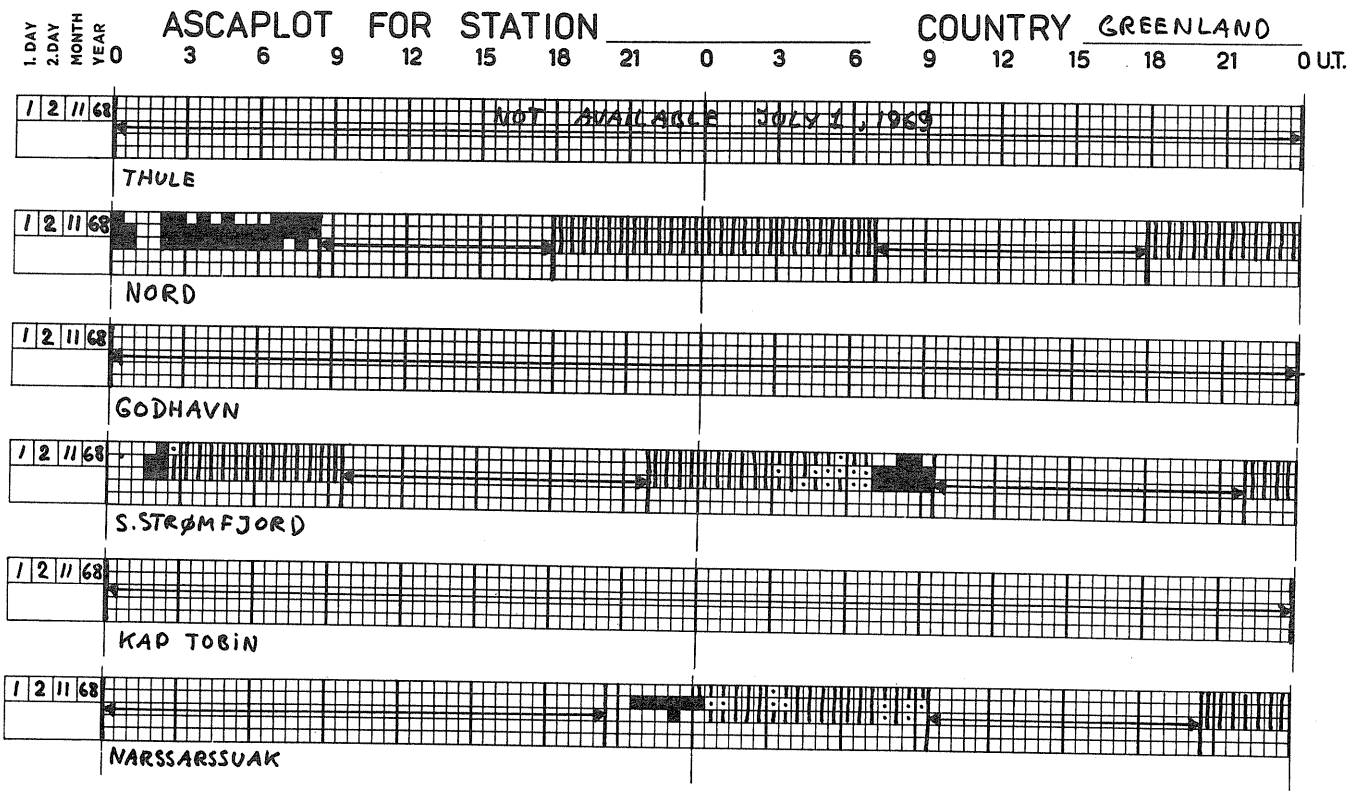
1. DAY
2. DAY
MONTH
YEAR
ASCAPLOT FOR STATION
COUNTRY GREENLAND
0 3 6 9 12 15 18 21 0 3 6 9 12 15 18 21 0 U.T.
1 2 11 68
NOT AVAILABLE JULY 1, 1969
THULE
NORD
GODHAVN
S.STRØMFJORD
KAP TOBIN
NARSSARSSUAK

12. IONOSPHERIC PHENOMENA

"Dourbes f-plots 27 October-5 November 1968"

by

L. Bossy
Institut Royal Météorologique de Belgique

[These f-plots as furnished by M. Bossy are included as indicative of the type of ionospheric data available in the archives of World Data Center A - Upper Atmosphere Geophysics for this time interval. These are particularly interesting since in addition to plots of the values of foF2, foE, foES, f min and ES type, photographs of the variation of ftE are included. Among other effects shown is evidence of the SID of October 27 at 1230 UT, October 29 at 1218 and November 2 at 0946 UT by the increases in f min. The foF2 values are depressed November 2-3 after the magnetic storm of October 31, 1968.]

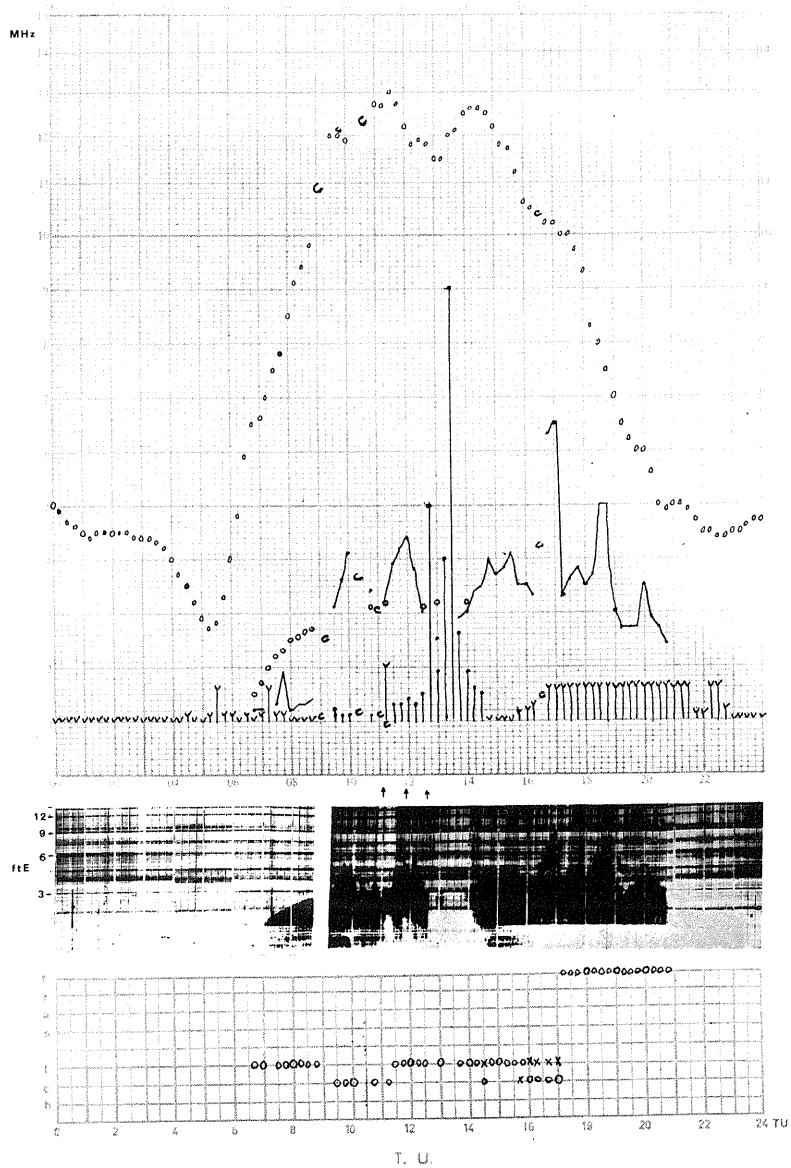

f-PLOT

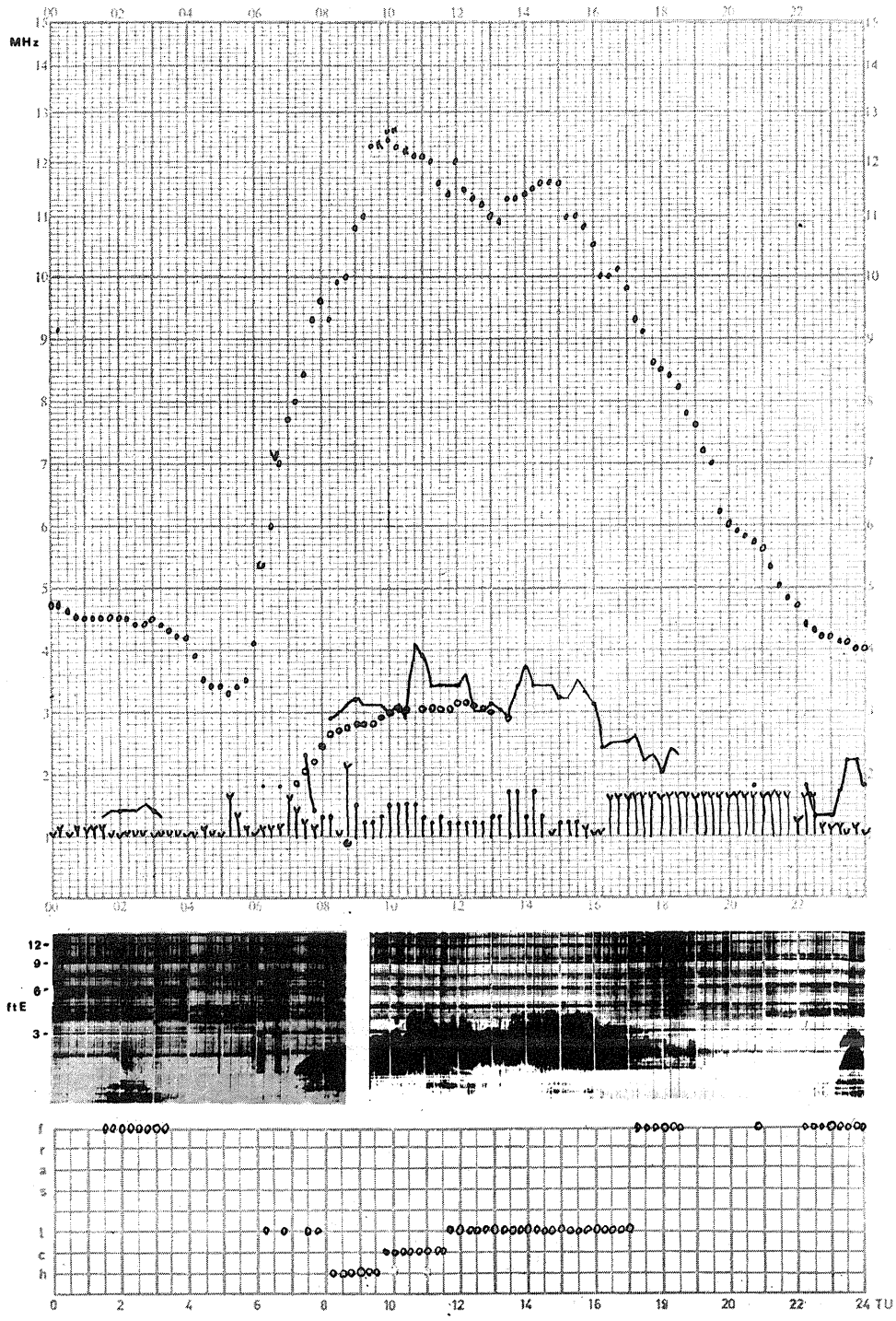

STATION : DOURBES

DATE : 28 OCTOBRE 1968

f-PLOT

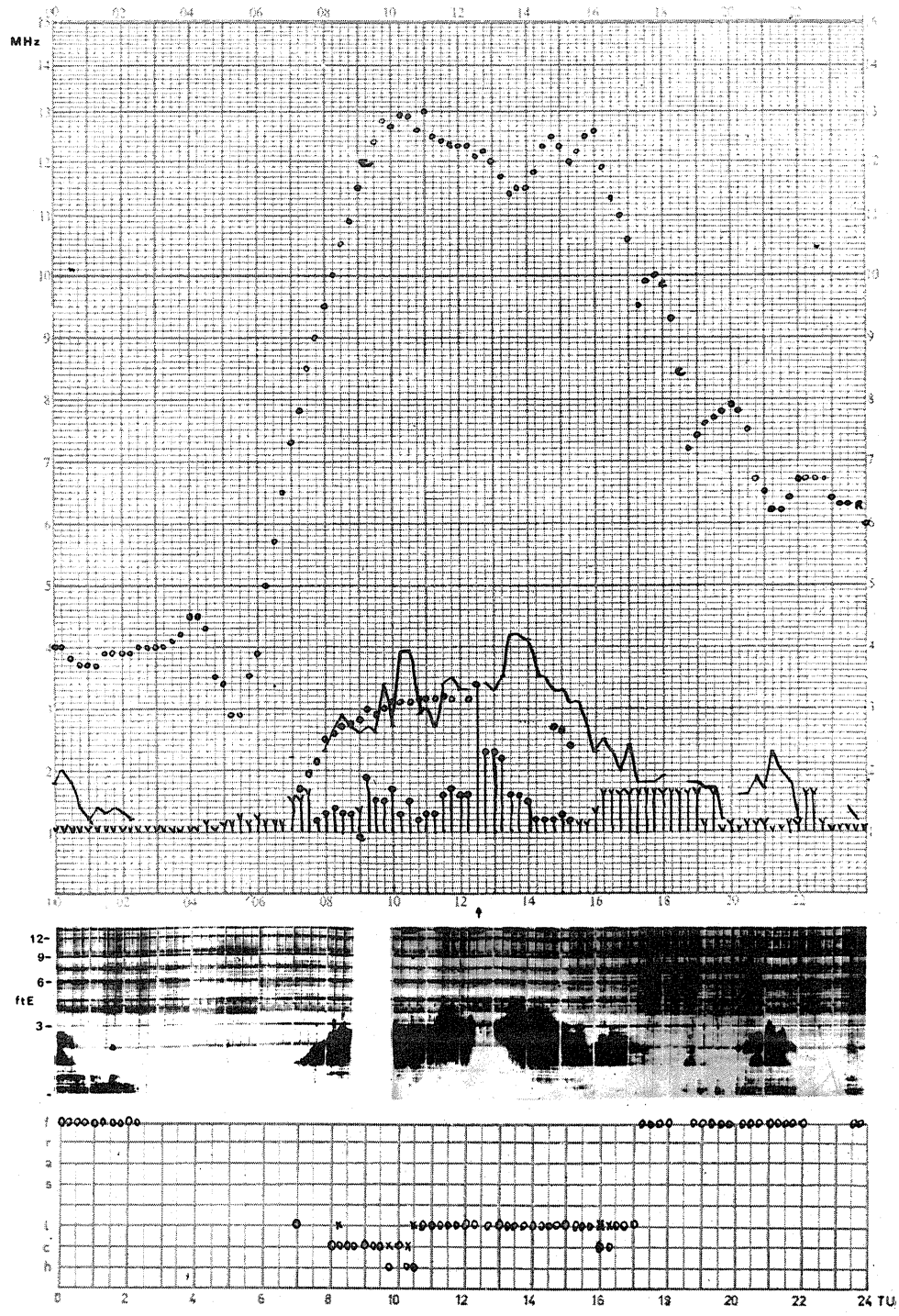

T. U.

STATION : DOURBES

DATE : 29 OCTOBRE 1968

f-PLOT

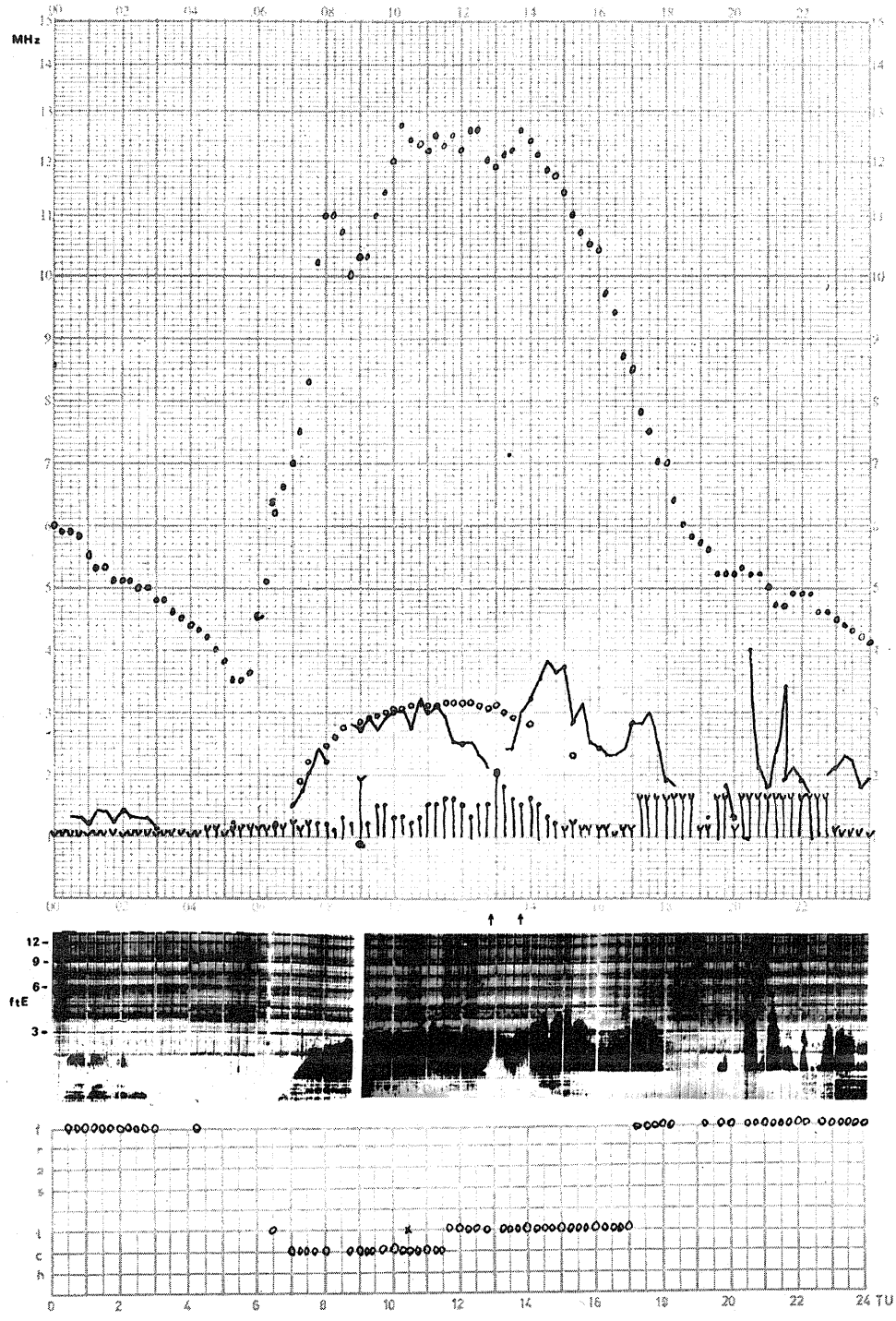

STATION : DOURBES

DATE : 30 OCTOBRE 1968

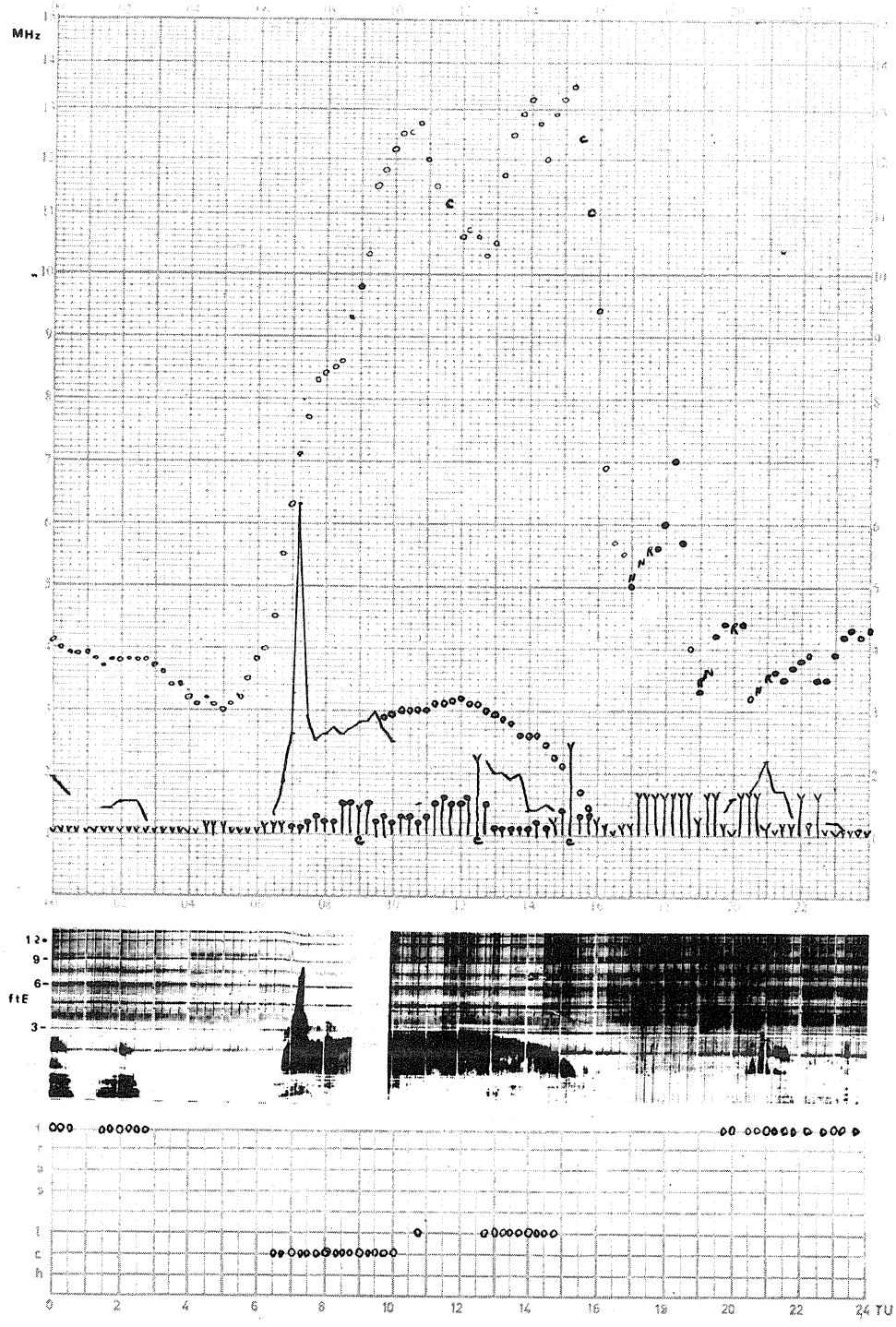

T. U.

STATION : DOURBES

DATE : 31 OCTOBRE 1968

f-PLOT

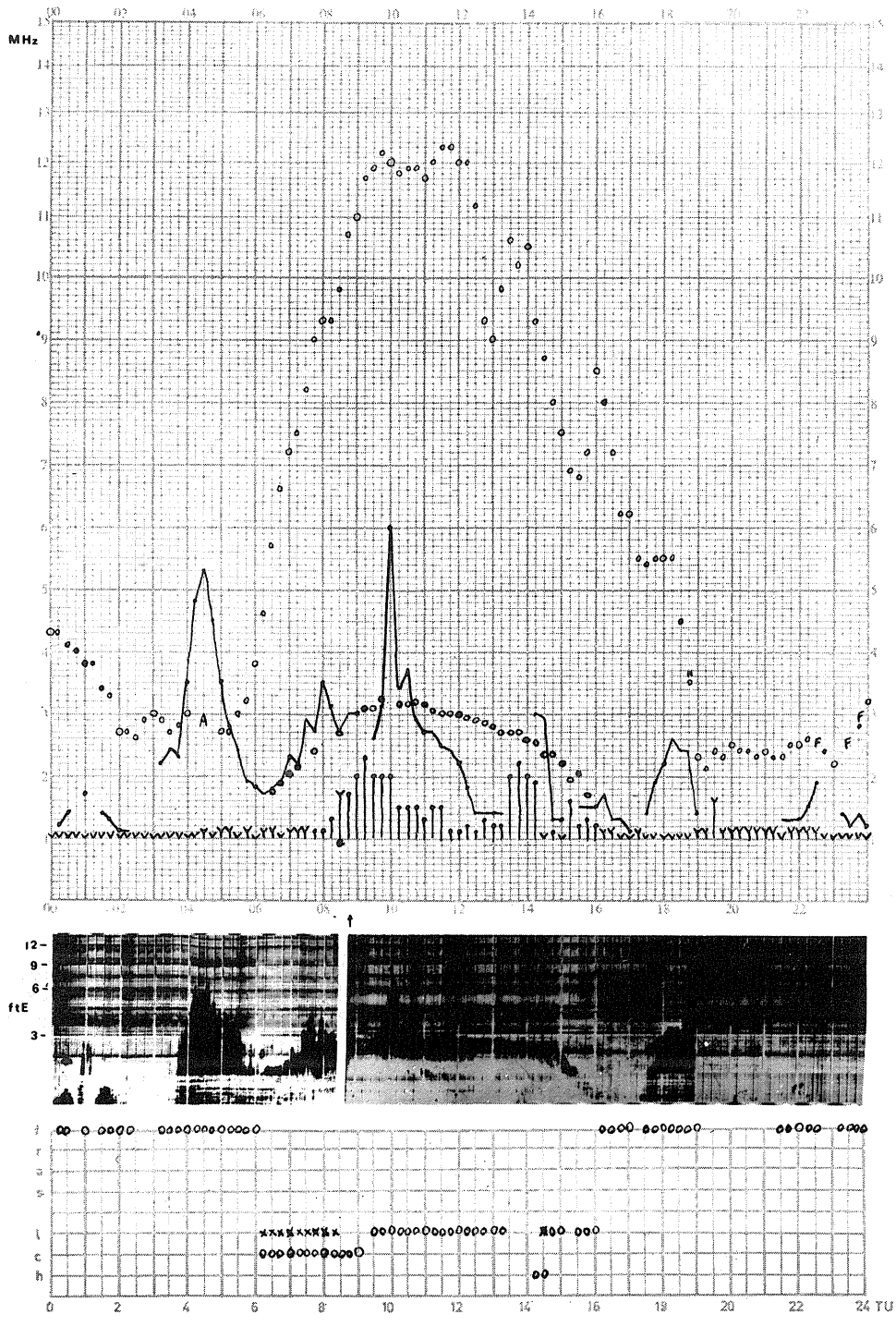

STATION : DOURBES

DATE : I NOVEMBRE 1968

f-PLOT

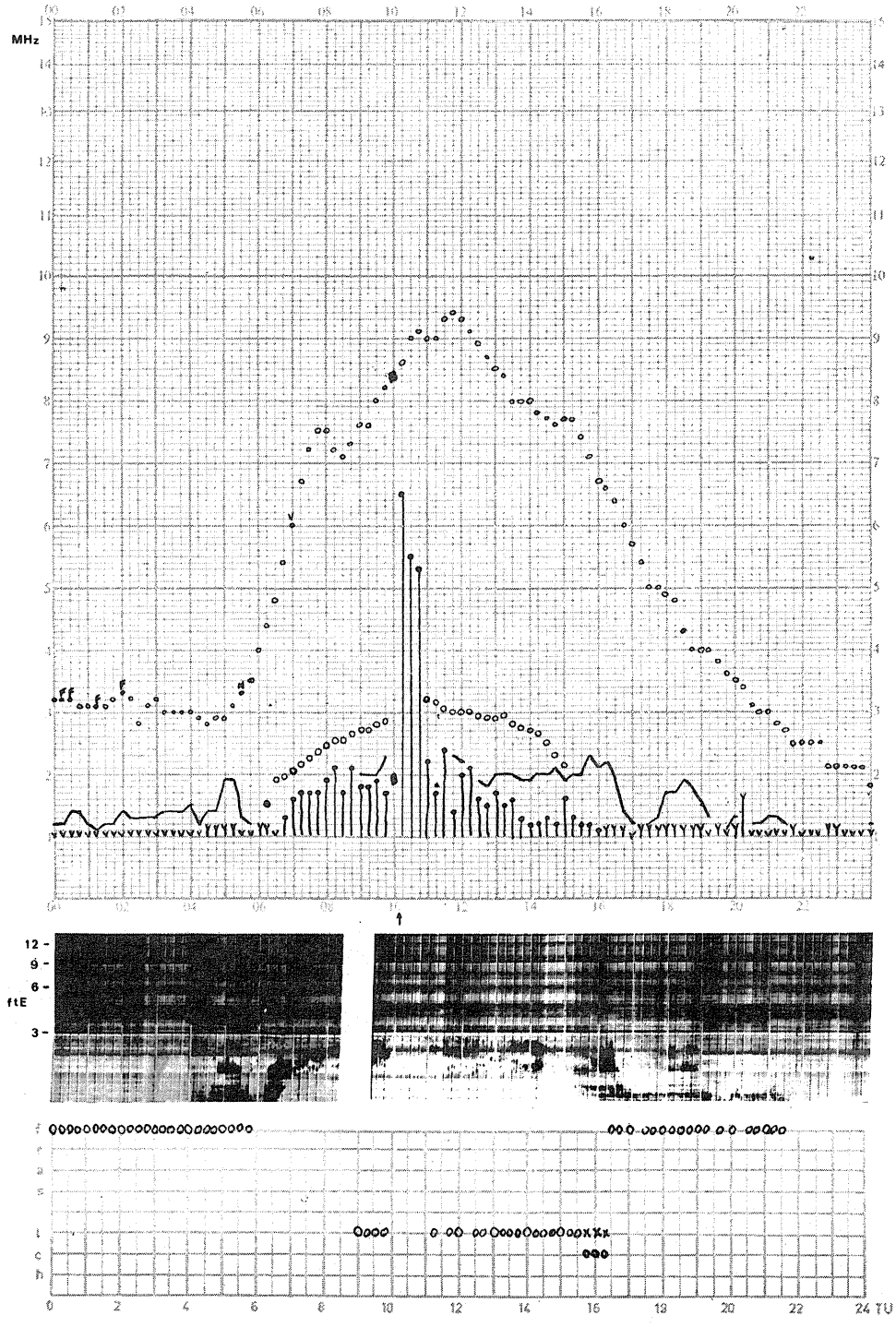

T. U.

STATION : DOURBES

DATE : 2 NOVEMBRE 1968

f-PLOT

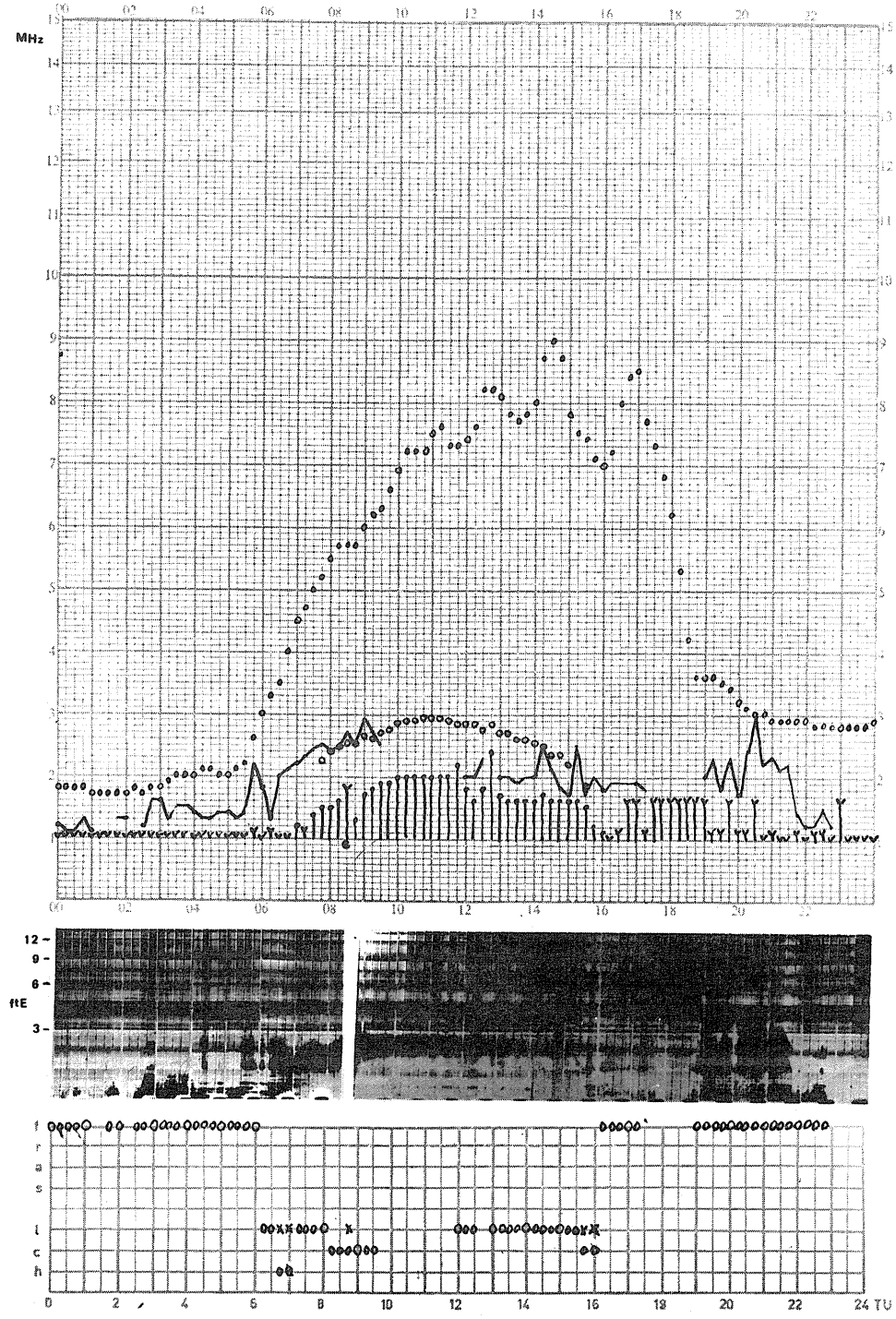

T. U.

STATION : DOURBES

DATE : 3 NOVEMBRE 1968

f-PLOT

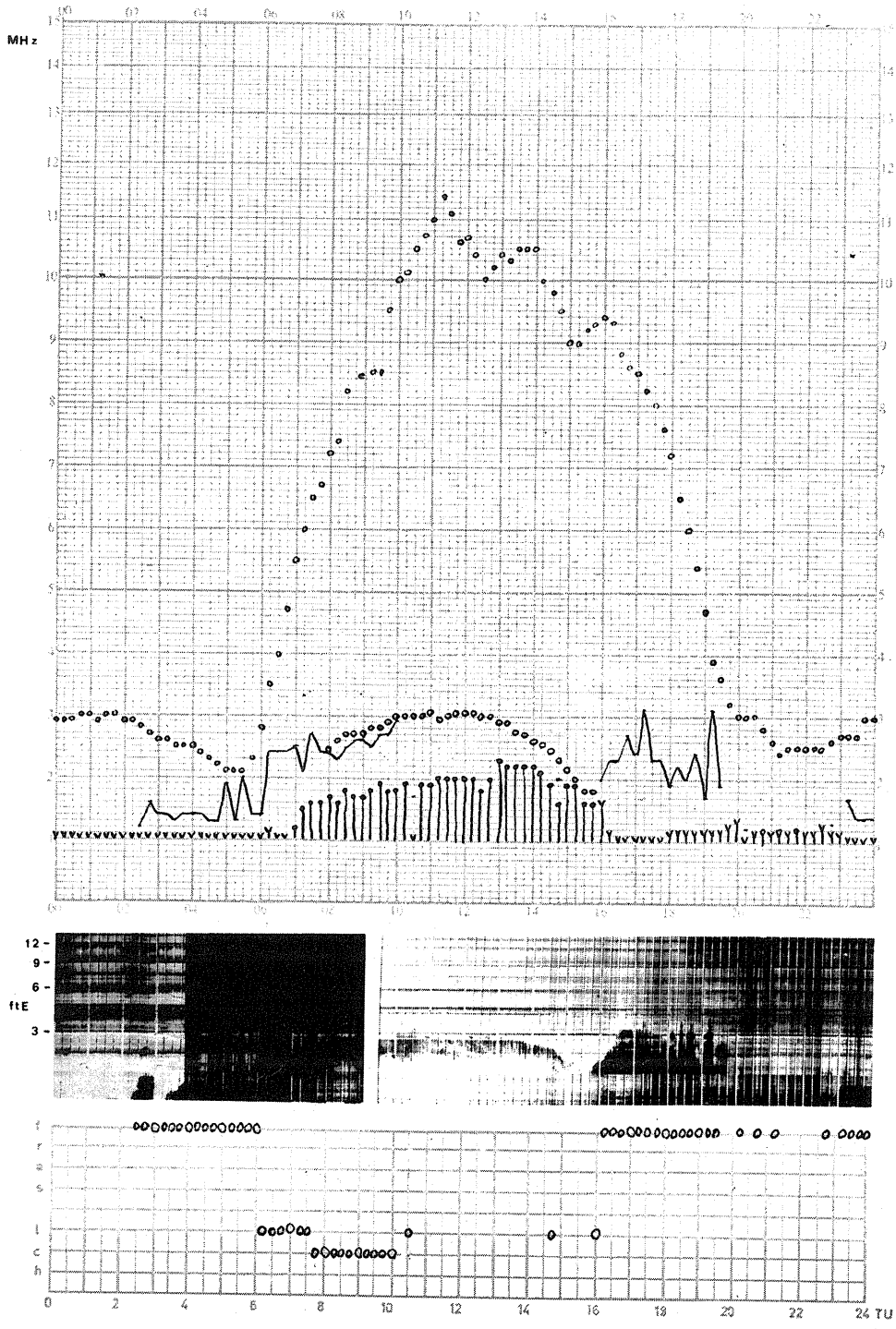

T. U.

STATION : DOURBES

DATE : 4 NOVEMBRE 1968

f-PLOT

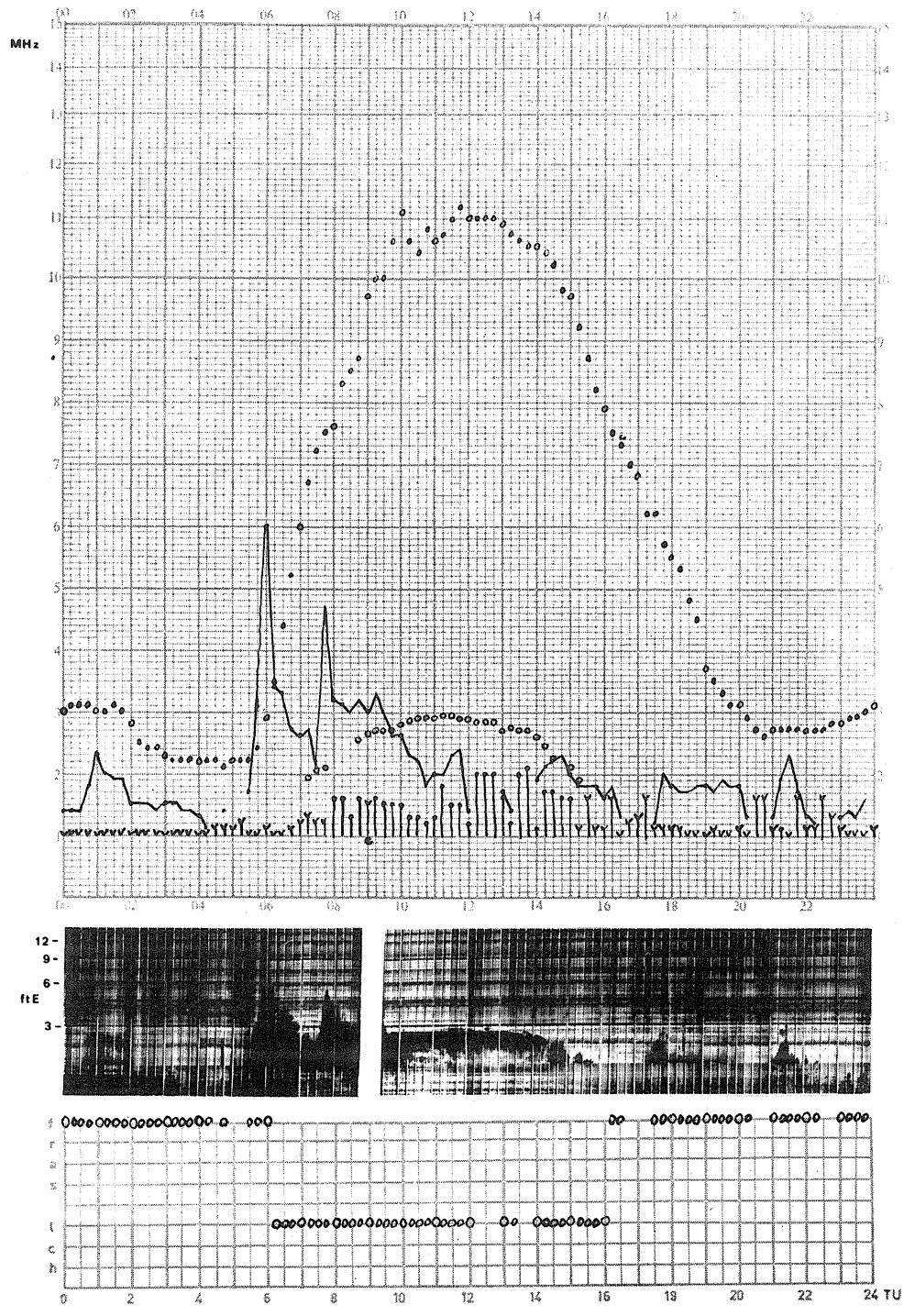

T. U.

STATION : DOURBES

DATE : 5 NOVEMBRE 1968

"Radio Propagation Quality Indices"

by

B. Beckmann
Fernmeldetechnisches Zentralamt
Deutsche Bundespost, Darmstadt, G.F.R.

The table presents radio propagation quality indices prepared from observations of the transmission frequency ranges at three azimuths for both day and night. The observations were made at Lüchow 53.0°N, 11.2°E from selected transmitters located in the three areas: U.S.A., South America and East Asia. The indices are computed as follows:

$$BK = (MUF - LUF + 1) \cdot \overline{F}$$

In this equation MUF and LUF are the observed ionospheric propagation parameters of maximum usable frequency and lowest useful frequency and $\overline{F}$ the mean logarithmic field strength on the path. From this the relative band characteristic figure BK_r is found.

$$BK_r = \frac{\overline{BK}}{\overline{BK}_{rot}}$$

where $\overline{BK}$ is the average of BK over a day or night period for the propagation path and $\overline{BK}_{rot}$ is the average of $\overline{BK}$ over the preceding 27 days or solar rotation. Thus, $BK_r > 1$ represents quiet, $BK_r = 1$ represents normal, and $BK_r < 1$ represents disturbance. To form values cooresponding to the 1-9 scale used for forecasts of radio propagation quality, the radio propagation indices published in the tables are 6 times the BK_r for the day or night period of the circuits in each of the three areas.

Radio Propagation Quality Indices

derived from observations of the transmission frequency range

October 1968

Date	USA - Germany		South America - Germany		East Asia - Germany	
	Day	Night	Day	Night	Day	Night
1	6.4	5.0	7.0	5.6	7.0	6.2
2	5.0	3.8	5.6	5.0	6.0	4.6
3	4.8	5.0	5.6	5.2	6.0	4.8
4	6.4	6.2	6.4	6.0	7.0	6.0
5	6.0	6.6	5.6	5.4	7.2	5.6
6	6.8	6.2	5.2	5.6	6.4	5.0
7	6.2	5.6	6.2	5.8	6.6	6.0
8	6.2	5.2	5.4	5.8	6.2	5.2
9	6.2	5.4	5.8	6.0	6.6	5.2
10	6.6	6.4	6.0	5.8	7.2	5.6
11	7.0	5.8	6.2	5.6	7.8	5.6
12	5.4	3.8	5.8	5.4	6.6	5.6
13	5.0	4.8	5.2	5.8	6.2	5.6
14	5.4	4.4	5.6	5.0	6.0	4.4
15	6.8	6.2	6.0	5.8	6.6	5.4
16	6.2	6.6	6.4	5.8	6.8	5.6
17	6.2	6.0	6.4	6.0	6.8	6.2
18	6.2	6.0	5.8	5.8	7.0	5.4
19	6.4	6.2	5.6	5.4	7.0	6.4
20	6.2	6.8	5.4	5.6	6.4	5.6
21	6.6	7.0	6.2	5.8	6.2	6.4
22	6.6	7.2	6.4	6.0	7.2	5.6
23	7.6	8.0	6.2	6.0	7.2	6.4
24	6.8	6.6	6.4	6.6	7.2	6.6
25	6.6	5.6	6.2	5.8	6.8	6.8
26	6.4	7.0	6.2	5.2	6.8	6.2
27	7.0	7.4	5.4	6.4	6.4	6.8
28	7.2	7.6	6.6	6.0	6.4	6.0
29	6.2	6.0	6.2	7.4	6.4	5.2
30	5.6	4.8	6.2	5.8	6.6	7.0
31	3.4	3.0	5.2	5.2	6.2	5.6

November 1968

Date	USA - Germany		South America - Germany		East Asia - Germany	
	Day	Night	Day	Night	Day	Night
1	3.0	2.0	5.0	4.8	5.4	4.0
2	3.2	2.8	5.0	4.2	4.2	4.2
3	3.2	2.0	4.6	3.8	5.0	4.0
4	4.2	2.4	4.6	4.4	4.8	5.0
5	3.8	3.0	5.0	3.8	5.0	3.8
6	4.6	4.0	5.8	5.2	5.4	4.8
7	4.4	4.2	5.2	5.0	5.4	5.0
8	4.8	3.8	5.4	5.6	6.4	5.8
9	4.8	3.8	5.2	4.6	6.2	4.6
10	5.0	4.8	5.2	5.8	5.6	4.6
11	6.0	4.6	6.0	5.0	6.6	5.6
12	5.6	4.0	5.2	5.0	6.2	5.0
13	5.8	5.4	5.4	6.0	6.2	5.4
14	6.2	5.4	5.8	5.8	6.4	5.4
15	6.6	7.0	5.8	5.6	6.2	5.0
16	7.2	8.0	6.2	6.2	5.6	6.4
17	5.6	5.0	5.4	6.0	5.4	5.6
18	4.6	4.4	5.2	4.6	5.6	5.0
19	6.2	5.0	6.0	4.8	5.4	5.0
20	7.0	6.4	6.6	7.0	6.6	6.4
21	6.6	6.8	7.0	7.4	6.4	5.6
22	6.8	7.0	7.2	6.2	6.4	5.8
23	7.8	7.8	6.8	6.4	6.6	5.6
24	8.2	9.0	6.2	6.2	7.4	6.8
25	8.2	9.0	7.4	7.6	6.6	5.8
26	8.0	7.6	7.4	7.6	6.2	6.2
27	7.6	7.6	7.0	7.2	7.0	6.8
28	7.0	6.8	8.0	7.2	6.4	7.2
29	8.0	7.6	6.8	7.0	6.2	5.6
30	7.0	6.6	6.6	6.4	6.4	5.2

"Some Absorption Changes at South Uist 29 October - 1 November 1968"

by

W. R. Piggott and E. Hurst
Radio Research and Space Station
Slough, U.K.

The following abstracts from a report on the operation of a riometer operating at 27.6 MHz at the Rocket Range at South Uist (57°23'N 7°25'W) summarize the most important changes during the period 29 October - 1 November 1968. In general interference on the operating frequency prevented observation during the daytime on most days.

Some very large absorption events were observed during the analysis, the most important of which are reproduced in the Figure 1. This shows the departure of the current, Δi, from its quiet day value as a function of time. The normal current varied from about 4 ma near 1000 to about 6 ma near 1800 for this period so that the absorption losses were of order 10 dB. This period was associated with an important proton flare followed by a PCA and accompanied by a major magnetic and ionospheric storm. It appears that the geomagnetic cutoff latitude decreased sufficiently to allow protons to enter above South Uist on this occasion. The nighttime auroral events are also exceptionally large, very much bigger than is usual near the auroral zone.

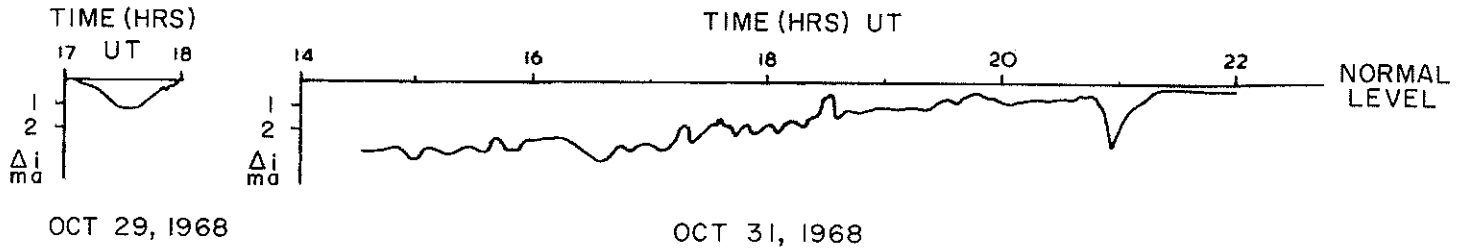

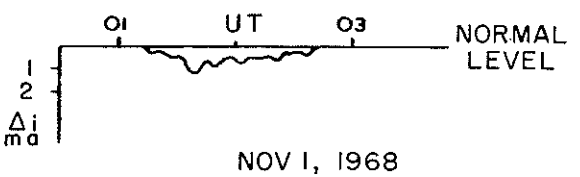

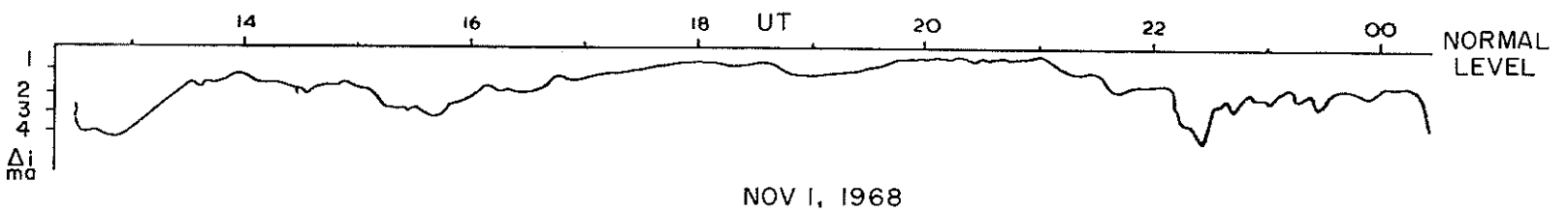

RIOMETER DATA - SOUTH UIST - 27.6 MHz

"Disturbances in the Lower Ionosphere (Solar Proton and High Energy Electron Precipitation) Observed at High Latitudes in Canada During the Period 26 October to 9 November 1968"

by

J. S. Belrose, D. H. Jelly, D. B. Ross and R. Bunker
National Radio Propagation Laboratory
Communications Research Centre
Department of Communications
Ottawa, Canada

Introduction

During the past 8 years or more the Communications Research Centre (formerly the Defence Research Telecommunications Establishment) has been investigating the properties of the lower ionosphere (below the 100 km level) by a number of techniques: (1) low and very low frequency propagation over a number of paths; (2) riometer absorption measurements at Resolute Bay (Λ = 84.2°), Churchill (Λ = 70.5°), Great Whale River (Λ = 68°), Moosonee (Λ = 64.2°), Val d'Or (Λ = 61.3°) and Ottawa (Λ = 58.2°); and (3) the partial reflection experiment at Ottawa, Churchill and Resolute Bay. The geographic locations of the experiments are shown in Fig. 1 (geographic and magnetic shell latitudes are indicated).

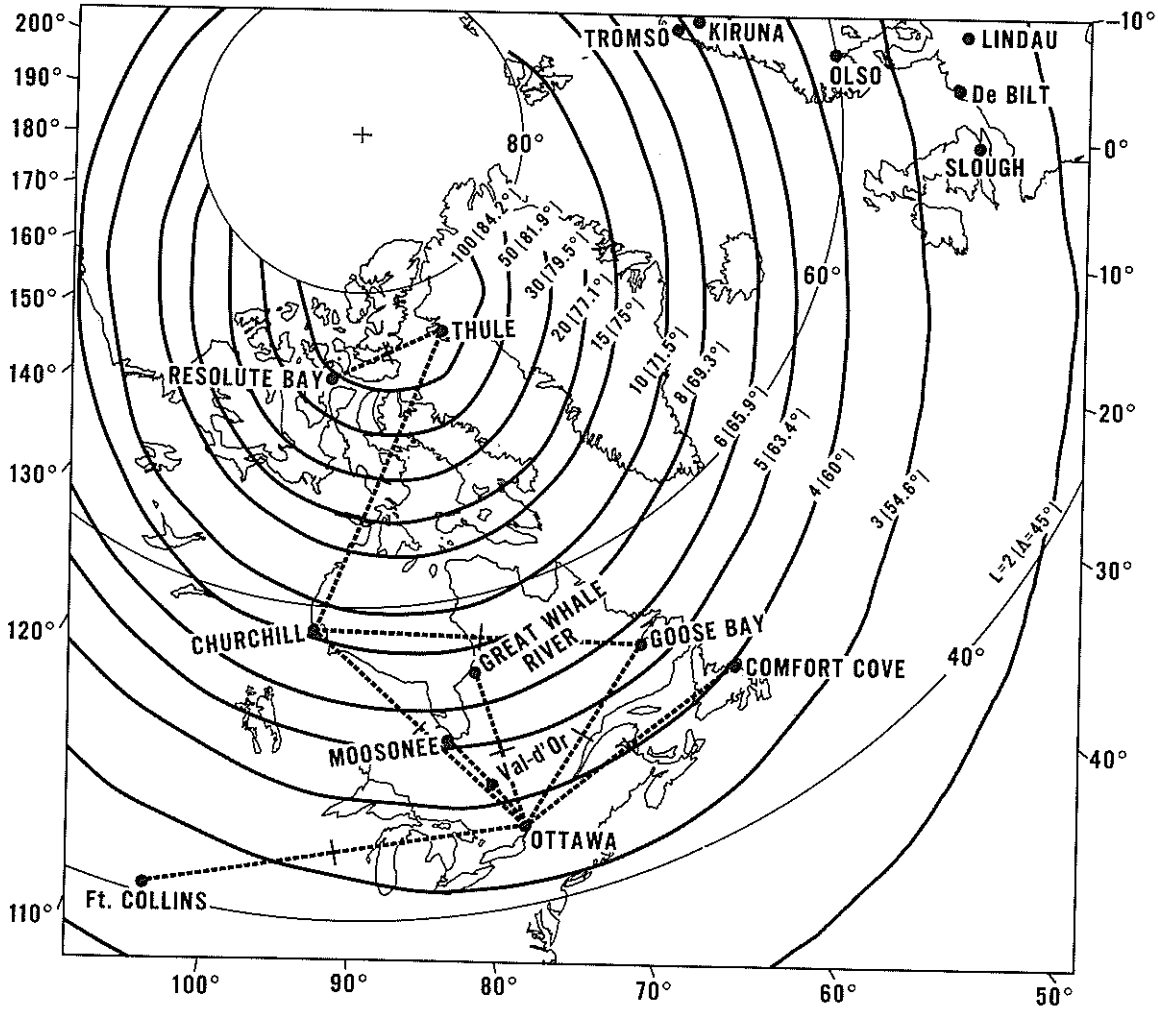

Fig. 1. Northern polar map shows the various long wave propagation paths. Locations of riometers and partial reflection experiments are also marked (see text). Geographic and magnetic shell latitudes (at 100 km) are shown.

The riometers employ 5-element circularly polarized (crossed elements) yagi-antennas which are directed at the zenith or at the polar star. The details of the long wave propagation paths of interest to this paper are listed in Table 1, and those of the partial reflection installations in Table 2.

Table 1

TRANSMITTER LOCATION	RECEIVER LOCATION	FREQUENCY kHz	DISTANCE km	LATITUDE OF MIDPOINT (Λ°)
Ottawa	Churchill	80	1920	65.2
Thule	Churchill	77	2210	79.6
Rugby	Churchill	16	~5300	---

Table 2

LOCATION	TRANSMITTER FREQUENCY MHz	TRANSMITTER POWER kW	ANTENNA	BEAM WIDTH (°)	BEAM POWER MW
Ottawa	2.66	1000 (usually ~350)	40-dipole	28	200
Ottawa	6.275	100	128-dipole	14	72
Churchill	2.66	100	4-dipole	50	(1)
Churchill	6.275	100	144-dipole(2)	13	29
Resolute Bay	2.66	100	4-dipole	50	1.6
Resolute Bay	6.275	100	40-dipole	28	20

(1) No ground screen is employed and so the gain is undoubtedly less than at Resolute Bay.
(2) Not put into operation until August 1969.

The low frequency propagation experiments and riometer experiments are useful in detecting lower ionosphere disturbances, they well compliment each other, and are operated on a continuous basis. The measurement of high latitude LF propagation, principally phase recordings, provides a continuous monitor for various geophysical disturbances, in particular solar cosmic ray (SCR) disturbances [Belrose and Ross, 1962; Belrose, 1968], and the sensitivity for detection of such events is a maximum if they occur at night; whereas the associated polar cap absorption (PCA), because of the strong diurnal variation of absorption, can be observed by a 30 MHz riometer only during the daytime, except for large events. The LF propagation provides in addition some indication of the lowest height where the ionization enhancement occurs (cf. the paper by Belrose and Ross [1962] which provided for the first time indirect evidence on the height of the base of the disturbing layer); whereas the magnitude of riometer absorption gives a very useful measure of the magnitude of the disturbance.

The partial reflection experiment is the most valuable of the three techniques, since it provides information on the electron number density - height distribution during the disturbance, as well as an estimate of the collision frequency near the base of the ionosphere (~60km), cf. Belrose and Burke [1964]. Unfortunately, the reduction of the partial reflection experimental data has been a time consuming tedious task and regular observations, until recently were limited to a half hour period at local noon and more continuously during disturbances. In 1967/68 a digital recording method was developed [Belrose, 1970] which eliminated this problem, and the continuous acquisition of data became a practical proposition. The partial reflection method is the most sensitive ground-based experiment for detection of SCR-events [Hewitt, 1969], but unless two or more frequencies and rather large antennae arrays are employed, the experiment provides only limited information on the electron distribution for PCAs where the absorption is >1dB on a 30 MHz riometer, and even with the most elaborate instrumentation the data are not very useful if the absorption is >5dB (or so). This is in part because of off-vertical reflections, which are particularly troublesome when the ionization density is abnormally high (radio wave absorption for waves travelling in the D-region is very high), and in part to the limited height range from which backscatter can be observed. The observation of partial reflections is possible because of the electron density irregularity of the lower ionosphere, and echoes are normally detected in the height range 50-85 km. This is the height range where there is a negative temperature gradient with height, and the ionosphere is apparently sufficiently turbulent to cause the partial reflection of radio waves. Below (and above) this height range, the temperature gradient is positive, and it becomes increasingly difficult to detect partial reflections for heights <50 km unless very large antennas (e.g. 40-dipole arrays) and large transmitter powers (~350 kW) are employed. Therefore, if the ionization density increase at heights <50 km is very great, the partial reflection experiment can in fact be "blacked-out" (no echoes are detected), or no echoes from the base of the ionosphere and weak O-wave echoes only from some higher height (the X-wave being already absorbed).

The purpose of this paper is to collocate the various data recorded during the period 25 October through 8 November 1968 and to describe the disturbances that were observed during this period.

The Observational Data

The various geophysical data are shown in Fig. 2* (curves a to i) which are from top downward: a) phase record of the Thule-Churchill (77 kHz) transmission; b) phase record of the Ottawa-Churchill (80 kHz) transmission; c) phase record of the Rugby-Churchill (16 kHz) transmission; d) ratio $(Ax/Ao)_{88km}$ at 2.66 MHz at Resolute Bay (this ratio is inversely proportional to the average electron density below the reference height); e) riometer absorption (zenith directed antenna) at Resolute Bay; f) riometer absorption (pole-directed antenna) at Churchill; g) riometer absorption (pole-directed antenna) at Ottawa; h) solar protons for E_p>10Mev by Explorer 34 (1967-51A) satellite (from "Solar-Geophysical Data", published by ESSA Research Laboratories); and i) magnetic index a_p-figure. The dates are with respect to Universal Time (UT).

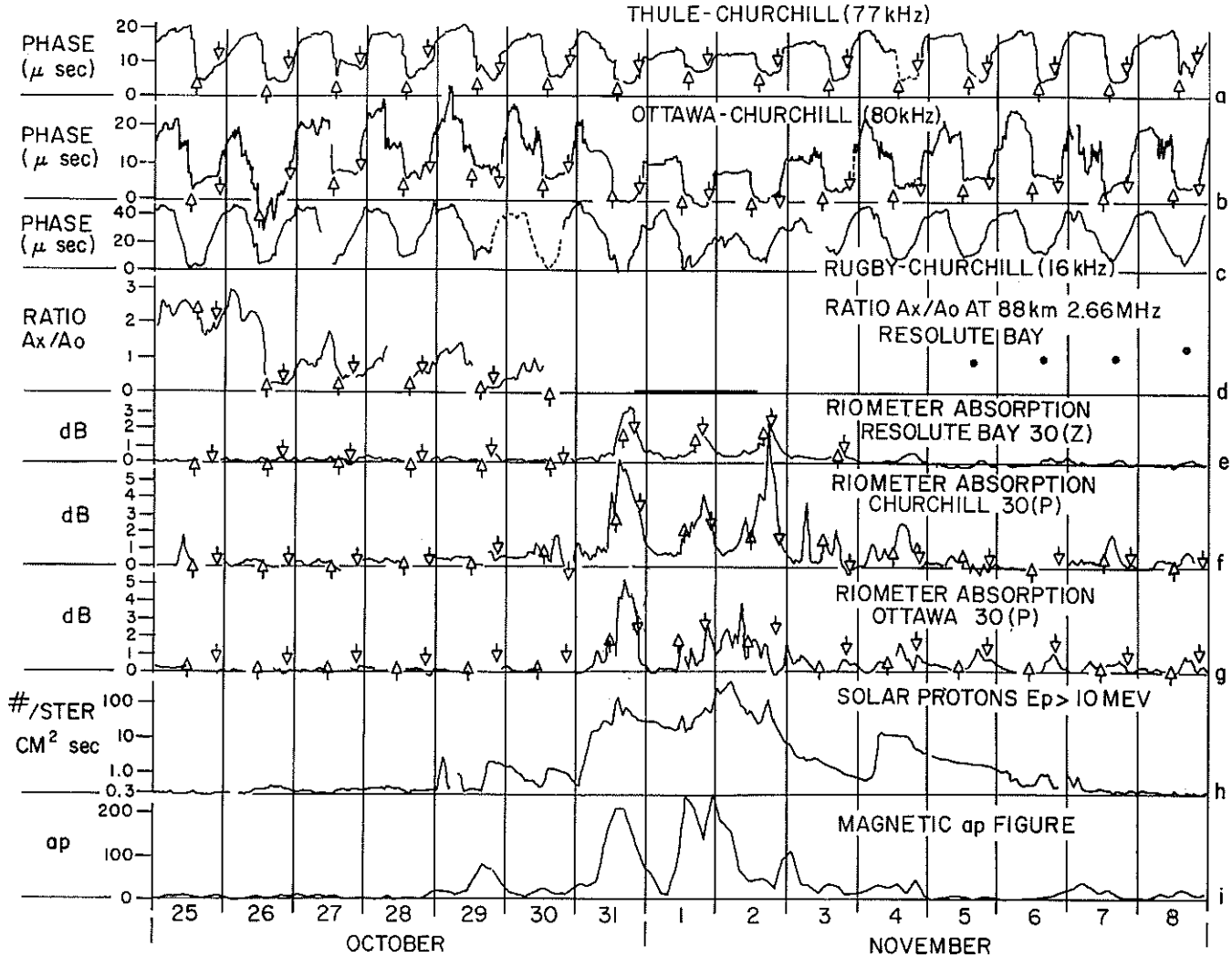

Fig. 2. Collocation of various geophysical data for the period 25 October to 8 November 1968 (Universal Time). See text for further details.

* A copy of the original of this figure is available from the authors on request.

The Partial Reflection Experiment

The partial reflection data will be described first since this experiment is the most sensitive and showed some early disturbances, prior to the main SCR event on 31 October 1968. Digital equipment, recording the partial reflection data on incremental magnetic tape, was installed at Resolute Bay in the early summer of 1968, and beginning on 1 August, the experiment was operated continuously (24 hours per day) until 30 October 1968 in anticipation of an SCR event. The equipment was turned on again late in the evening of 31 October (UT day), since it was realized that a major SCR-event was in progress, and it was operated continuously until mid-afternoon of 2 November. This period is indicated by the horizontal line, and while data were obtained during this period, no echoes were detected from heights of 88 km (lower echoes were detected but the waves were absorbed below 88 km). A preliminary study of these data has been given previously [Belrose et al., 1969]. No records were taken (for reasons unknown) on 3 and 4 November, and, beginning on 5 November local midday records only are available (indicated by the bold dots).

The 25th October 1968 was a typical quiet day for this time of the year. The sun rises barely above an elevation angle of 0°. The times when the sun rose and set for this elevation angle are indicated by the upward and downward directed arrows. There is a clear diurnal variation; minimum ratio occurs at local noon, but the magnitude of the diurnal change is hardly outside the range of variation of the nighttime values. During the dawn twilight period on the morning of 26 October, the ratio suddenly decreased, and remained below normal until 10 November (not shown), followed by subsequent decreases, beginning on 13 and 18 November 1968. The disturbance on 26 October 1968 was identified as an SCR-event [Belrose et al., 1969] before satellite proton data became available. The event can be clearly detected in the satellite data but it is scarcely outside the scatter of values for the undisturbed background.

The great sensitivity of the partial reflection experiment for detection of very small SCR-events is further emphasized in Fig. 3, which shows results for August 1968. Here the diurnal variation was larger (even though the sun never set). The bold dots indicate the midnight values that would have been recorded, judged from the long sequence of data, in the absence of a disturbance. Clear decreases in Ax/Ao ratio can be seen for the period 6-13 August, 14-16 August, 20-21 August (equipment failure prevented the observation of the decay of this event); as well as can be seen by the insignificant small event of 4 August 1968. Again these events were identified before satellite data became available, which, when it did, confirmed that these disturbances were small proton events, since each can be seen as a small increase in proton counts above the background.

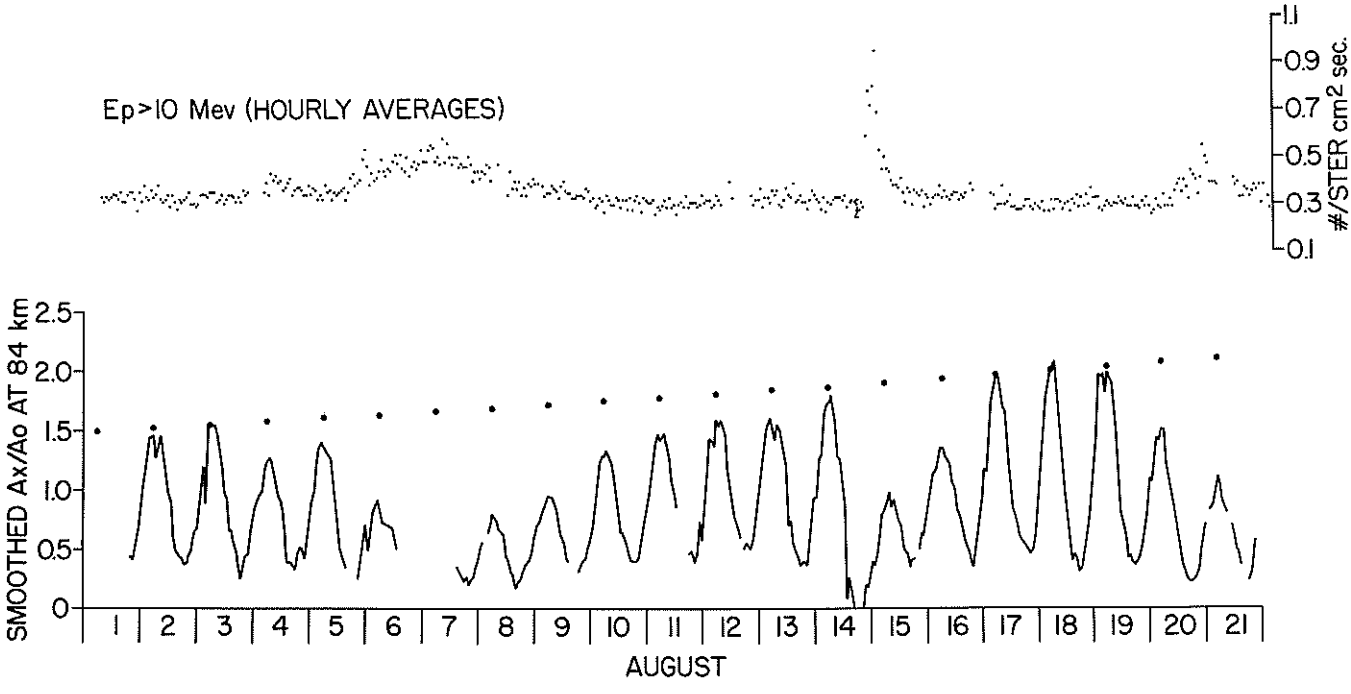

Fig. 3. Variation of the amplitude ratio Ax/Ao at 84 km for 2.66 MHz observations at Resolute Bay during 1-21 August 1968, superimposed with proton counting rate from Explorer 34 (IMP-F) UT.

Referring again to Fig. 2, it is interesting to note that the solar proton count rate has increased significantly above background during the pre-dawn period of 26 October 1968, yet the event was not detected by the partial reflection experiment until the solar zenith reached ~98°, whereas during the following nighttime period of 26 to 27 October, even though perhaps somewhat smaller rates of proton precipitation were recorded, the ionization density in the D-region remained higher than normal. It is difficult to be certain of the significance of this feature, since the proton fluxes were very nearly at the background level, but if significant then this fact leads to important inferences. For these very small events, solar illumination at the outset is apparently required before the ionization density can increase significantly; but once the ionosphere has been illuminated during proton bombardment, the enhanced ionization takes a very long time to decay (e.g. it does not decay during the course of a single night). The event of 29 October is seen as a further decrease in the Ax/Ao ratio. There were unfortunately no observations at the time of the onset of the main event on 31 October 1968.

Partial reflection data at Ottawa were available (not shown) for noons only for the period 25-30 October, and continuously during most of the day of 31 October 1968. These data, in particular the electron number density-height profiles, will be published in a later paper. The main event of 31 October 1968 began more or less coincident with a large geomagnetic storm: a_p reached a peak of >200 gammas during the afternoon of 31 October 1968 (due presumably to a previous disturbance on the sun), and because of this a PCA was observed as far south as Ottawa. PCA are not normally observed at Ottawa, except weakly during very large events*, unless, as in this circumstance, the earth's magnetic field is disturbed allowing the solar protons to penetrate to the D-region. The absorption was in excess of 4dB during the daytime of 31 October over Ottawa. Excellent partial reflection data were obtained, in particular the details of the decrease in D-region ionization (note the decrease in riometer absorption) over sunset on 31 October. Since Ottawa is near the southern extent of the disturbance, however, it makes the study of SCR effects difficult, since one has to be certain that the ionization decrease, which may be due to sunset, is not due in part to changing cut-offs during the sunset period when the a_p-figure was decreasing.

Long Wave Propagation

Long wave propagation, in particular transpolar VLF propagation, has long been thought to be a very sensitive method to detect the penetration of solar protons into the earth's upper atmosphere, and indeed it is. The polar cap disturbance (PCD) was, however, not clearly detected in the Rugby-Churchill transmission until the night of 1-2 November, except for a brief period on 31 October during the daytime when the signal amplitude was so weak the phase could not be tracked reliably. The LF transmissions Thule-Churchill (77 kHz) and Ottawa-Churchill (80 kHz) clearly showed effects earlier: a gradual decrease in phase height on the Thule-Churchill transmission and a sudden cessation of nocturnal fading on the Ottawa-Churchill transmission, beginning at about 05 UT on 31 October 1968. The diurnal variation was quite abnormal during 31 October - 3 November, particularly the 1-2 November. The depressed phase heights at midday on 31 October, and 1-3 November for the Ottawa-Churchill path is normal for PCDs (the fact that a similar decrease was not observed for the Thule-Churchill transmission is thought to be instrumental). The daytime phase was up to 10 microseconds below normal, which corresponds to a decreased phase height of 10 km. If the normal phase height of reflection is about 65 km, the phase height of reflection during the peak of the disturbance on 1 November 1968 was approximately 55 km.

The further increase of solar proton count rate during the early morning hours of 4 November 1968 clearly resulted in a decrease in nighttime phase on both the Thule-Churchill and Ottawa-Churchill transmissions.

The Thule-Churchill diurnal phase change is much more regular than the Ottawa-Churchill transmission. The latter traverses the auroral zone. Note in particular the irregularity typical of auroral disturbances during the daytime of 26 October and during early morning hours of 28, 29 and 30 October 1968.

Riometer Absorption

A PCA was not definitely detected until about sunrise on 31 October. The absorption observed on 29 and 30 October at Churchill and Ottawa is undoubtedly auroral absorption, since absorption was not strongly detected at Resolute Bay. A small daytime peak in absorption (~0.5 dB) on 29 October at Resolute Bay** is undoubtedly a PCA. The peak in absorption at 16 UT at Resolute Bay on 2 November, and in part the very strong peak in absorption at Churchill at 15 UT is clearly coincident with a peak in solar proton flux at about the same time. The effect of the SCR event of

* For example, the SCR event of 2 November 1969, which was distinguished by the exceptionally strong PCA at high latitudes; riometer absorption at Churchill was ~15 dB; was hardly detected at Ottawa (absorption was ~0.7 dB on the zenith riometer). The earth's magnetic field was quiet (A_p = 10).

** The daytime peak is not evident in the Figure, but is clearly seen in the full size copy of the Figure.

4 November can be clearly seen in the absorption over Churchill, and also at Resolute Bay where the effect is not so strong because of the higher solar zenith angles there. On 4 November the solar zenith angle was >90° over Resolute Bay (note that the arrows marking the times when $\chi = 90°$ are absent on 4 November and days following.)

Discussion

The ionization changes associated with the increases in solar proton count rates on 26, 29, 30 and 31 October can be detected in the high latitude geophysical data presented in this paper, as well as the intensity increase of the event on 1-2 November and the further increase on 4 November 1968. The minor enhancement of the background proton fluxes beginning on 26 October and continuing until the onset of the larger events is very clearly detected by the partial reflection experiment at Resolute Bay, which is the most sensitive ground-based technique for detection of SCR disturbances.

The fact that the SCR event of 31 October began more or less coincident with a large geomagnetic storm (a_p>200 gammas) resulted in a PCA of unprecedented magnitude at low latitudes for this solar cycle (4-5 dB on a pole-directed riometer being detected as far south of Ottawa). Electron density profiles over Ottawa, Churchill and Resolute Bay will be given in a later paper. A preliminary discussion of the partial reflection data at Resolute Bay and electron number density-height profiles have been published [see Belrose et al., 1969].

Acknowledgements

We thank our colleagues who made the observations at Resolute Bay, the first time we have attempted such a long series of continuous observations by the partial reflection experiment, and Mrs. Allison Morrison who scaled and plotted the riometer data.

REFERENCES

BELROSE, J. S. 1968 Low and very low radio propagation, AGARD Lecture Series XXIX on Radio Propagation, Technical Editing and Reproduction Ltd., London W 1.

BELROSE, J. S. 1970 Radio wave probing of the ionosphere by the partial reflection of radio waves (from heights below 100 km), J. Atmosph. Terr. Phys., 32, to appear in April 1970.

BELROSE, J. S. and D. B. ROSS 1962 Observations of unusual low frequency propagation made during polar cap disturbance (PCD) events, J. of Phys. Soc. (Japan), 17 (Suppl. A-1), International Conference on Cosmic Rays and the Earth Storm, 126.

BELROSE, J. S. and M. J. BURKE 1964 Study of the lower ionosphere using partial reflections. 1. Experimental technique and method of analysis, J. Geophys. Res., 69, 2799.

BELROSE, J. S., L. W. HEWITT and R. BUNKER 1969 Regular and irregular diurnal variations of electron number density in the lower ionosphere over Resolute Bay. The Polar Ionosphere and Magnetospheric Processes (ed. G. Skovli), Gordon Breach Pub. Co., N.Y.

HEWITT, L. W. 1969 Ionization increases associated with small solar proton events of 5 February 1965 and 16 July 1966, Can. J. Phys., 47, 131.

"Interpretation of Ionospheric Forward-Scatter Observations in Alaska During the Solar-Terrestrial Disturbances of Late October and Early November 1968"

by

D. K. Bailey and K. W. Sullivan
Space Disturbances Laboratory
ESSA Research Laboratories, Boulder, Colorado

Introduction

This report is similar in scope and form to a previous one [Bailey and Sullivan, 1969] concerning the geophysical effects which followed the solar events of 23 May 1967. In the present case data for seven rather than ten days are examined. Also, in the present case, forward-scatter observations are available only from one forward-scatter path rather than three. The present report is therefore simpler.

Observations

The hourly forward-scatter signal-intensity observations for the Alaskan path from Barrow to Anchorage at 23.19 MHz are shown at the top of the data plotted in Figure 1 for the period 30 October through 5 November 1968. The background noise levels, though rather unreliable at times, are shown immediately below. In the same figure the periods of full sunlight, $\chi<89°$, twilight, χ between 89 and 101°, and darkness, $\chi>101°$, are shown for the path midpoint region at L = 5.7. The latter two conditions are indicated by open and filled or black bars respectively. Below these indications are plotted the 3-hourly Kp figures. Lastly and just above the time scale the sc magnetic storm onsets are shown with the conventional triangle mark. The time of the principal solar flare in the 7-day period is also shown.

In addition to the basic data described above certain reference data are also shown. The fine continuous lines associated with the plots of signal intensity and background noise represent approximately the values that might have occurred in the absence of disturbance. In the data points representing signal intensity an "x" replaces the black dot whenever Es propagation occurred during the hour. If the Es propagation was sufficiently intermittent the position of the "x" represents a fair estimate of the signal intensity received by the forward-scatter mode. "x's" well above the normal trend are probably unreliable as indicators of the forward-scatter signal. The letter "S" replaces a value of signal intensity when Es propagation caused saturation of the received signal recording. The letter "m" is shown above a plotted value of signal intensity to indicate that the usual spikes of strong signal propagated via meteor trails are missing owing to heavy absorption above the scattering stratum. The symbol is usually shown when the signal intensity is otherwise normal or shows some enhancement. Eight consecutive hourly values of signal intensity are missing in the 3 - 4 November period. They are replaced by the letter "T" to indicate the cause, transmitter difficulties.

Interpretations

Because absorption of ionospherically scattered signals as revealed by signal-intensity decrease is only observable by day, and is replaced at night by enhancement of signal intensity [Bailey, 1964], it is necessary to know the position of the sun at all times with respect, for example, to the zenith at the midpoint of a scatter path. It is for this reason that the bar symbols, previously explained, are shown in Figure 1. The absence of a bar plot indicates full daylight, $\chi<89°$.

SID

As the sun was very low at the time of the 3B flare which began at 2339 UT on 30 October, the absorption effects in both signal intensity and background noise were small. The hourly observational points plotted for 0030 UT on 31 October show the effect.

Solar Protons, 31 October - 5 November

The most intense absorption resulting from solar protons (PCA) was observed during the daylight period of 1 - 2 November, nearly two days after the 3B flare which probably signalled the emission of the protons from the sun. The preceding daylight period showed distinctly less absorption and exhibited a trace of midday recovery [Leinbach, 1967]. These observations suggest that the intense fluxes of the softer protons were rather long delayed, perhaps as a result of the highly disturbed conditions that must have existed both in the magnetosphere and in the interplanetary space at this time. The PCA was much reduced during the daylight period of 2 - 3 November, and we cannot state whether it was still present on the following day because of the transmitter difficulties, but the observations early in the daylight period suggest still further reduction in intensity. During the

daylight period of 4 - 5 November the PCA increased to a level comparable with that of the 2 - 3 November daylight. No subsequent evidence of PCA was seen.

Nighttime signal enhancement during periods of PCA is normally observed, but during the present period the presence of much auroral substorm activity (see below) has obscured the normal nighttime behavior.

Electron Precipitation, 30 October - 4 November

In the period plotted in Figure 1, 30 October through 5 November, there was considerable auroral activity during the periods of darkness on all except the last day, and there must have been particularly fine auroral displays, as evidenced by the observed Es propagation [Bailey, 1968], during the periods of darkness. The periods before magnetic midnight on 31 October, 2 and 3 November, should have been particularly noteworthy. A less spectacular display probably occurred on 4 November. On 30 October and 1 November the main electron precipitation took place after midnight and was probably represented by a harder spectrum.

There seems to have been some relativistic electron precipitation (REP) activity during the period of study particularly in the dawn and early post-sunrise hours of 31 October and 1 November.

Discussion

Throughout the period plotted in Figure 1 there was a prolonged Forbush decrease in cosmic-ray intensity. It began early on 29 October according to the Alert and Deep River neutron monitors [Steljes, 1970, see page 226 of this Report]. By the end of 5 November recovery was nearly complete.

The Explorer 34 observations of solar protons reported by Lanzerotti and Soltis [1970, see page 199 of this Report] and by Bostrom *et al.* [1970, see page 190 of this Report] seem to be in good agreement with the deductions made above as to the relative intensities of absorption during the brief daylight periods in Alaska. In particular the square roots of the hourly averages of $E_p > 10$ Mev given in the second reference immediately above are closely proportional, during the brief periods of daylight at the midpoint of the Barrow-to-Anchorage path, to the maximum absorption values observed each day, as would be expected [Bailey, 1964].

REFERENCES

BAILEY, D. K. 1964 Polar-cap absorption, Planetary Space Sci., 12, 495-541.

BAILEY, D. K. 1968 Some quantitative aspects of electron precipitation in and near the auroral zone, Rev. Geophys., 6, 289-346.

BAILEY, D. K. and K. W. SULLIVAN 1969 Interpretation of ionospheric forward-scatter observations in high latitudes during the solar-terrestrial disturbances of late May 1967, World Data Center A, Upper Atmosphere Geophysics Report UAG-5, 71-78

BOSTROM, C. O., D. J. WILLIAMS and J. F. ARENS 1970 Explorer 35 Solar Proton Monitoring Experiment, Ep > 10 Mev, October 21-November 10, 1968, World Data Center A, Upper Atmosphere Geophysics Report UAG-8, 190.

LANZEROTTI, L. J. and C. M. SOLTIS 1970 Interplanetary Protons and Alphas: Days 300-313, 1968, World Data Center A, Upper Atmosphere Geophysics Report UAG-8, 198-204.

LEINBACH, HAROLD 1967 Midday recoveries of polar-cap absorption, J. Geophys. Res., 72, 5473-5483.

STELJES, J. F. 1970 Events of October 28 to November 21, 1968, World Data Center A, Upper Atmosphere Geophysics Report UAG-8, 225-227.

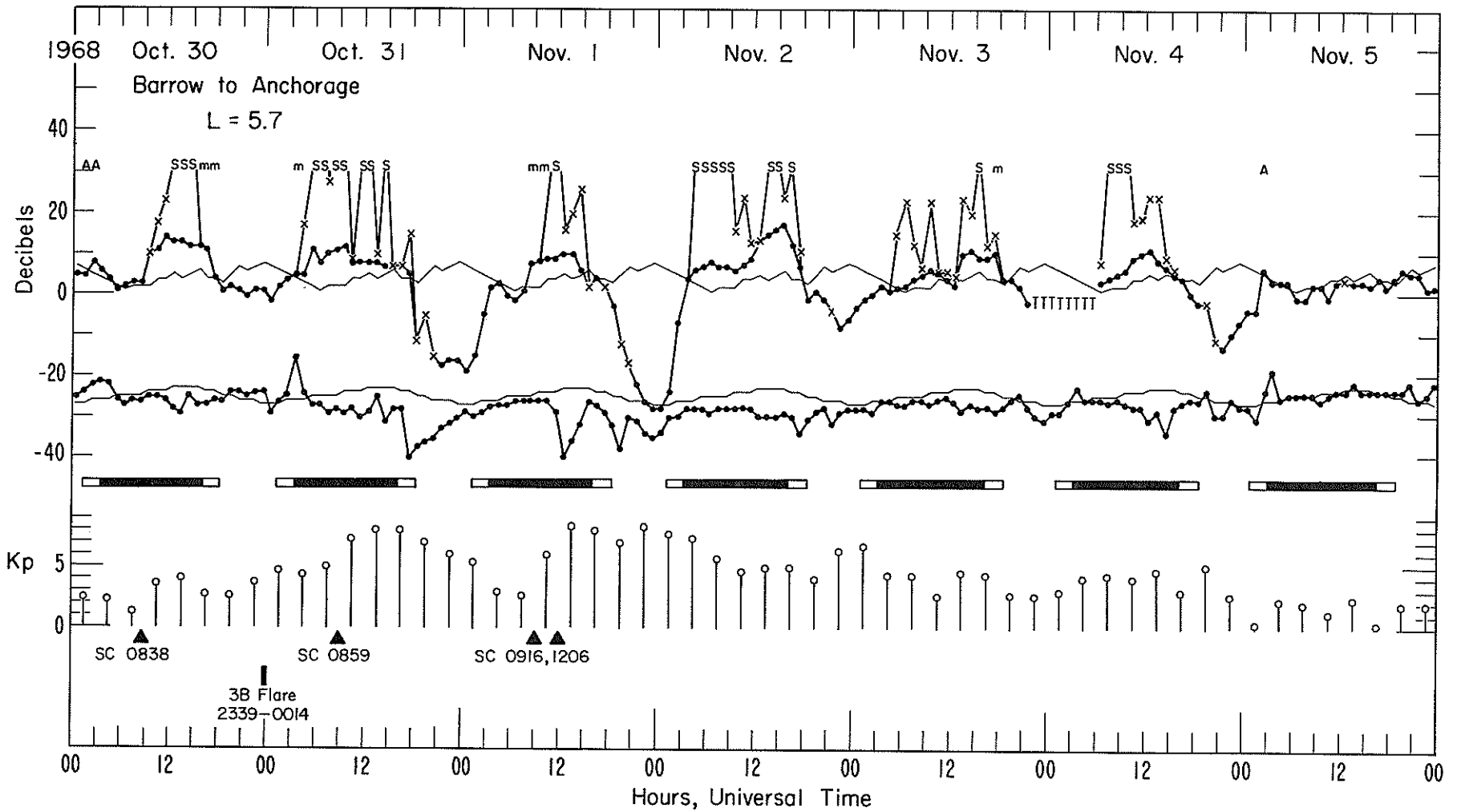

Fig. 1. Ionospheric forward-scatter observations from Alaska showing effects of solar protons and electron precipitation at L = 5.7.

"VLF Phase and Amplitude Measurements During the PCA Event October 31 - November 6, 1968"

by

T. R. Larsen*
The Auroral Observatory
Box 387, 9001 Tromsø, Norway

This paper gives a presentation and short discussion of very low frequency (VLF) phase and amplitude variations observed at Tromsø, Norway (corrected geomagnetic coordinates: Φ_c= 66.3°N, λ_c = 105.4°) during the polar cap absorption (PCA) event starting October 31, 1968. This event followed a 3B flare occurring at 2339 UT on October 30, 1968 [Solar-Geophysical Data, IER-FB 291, November 1968] and is superposed on a weaker PCA already in existence from October 29. The latter event, however, will not be discussed here.

The three VLF paths to be considered are as follows:

1. NPG (18.6 kHz), Seattle to Tromsø. The path is 6500 km long and crosses the northern tip of Greenland.
2. Hawaii (10.2 kHz) to Tromsø. Pathlength: 9700 km.
3. Trinidad (10.2 kHz) to Tromsø. Pathlength: 8700 km.

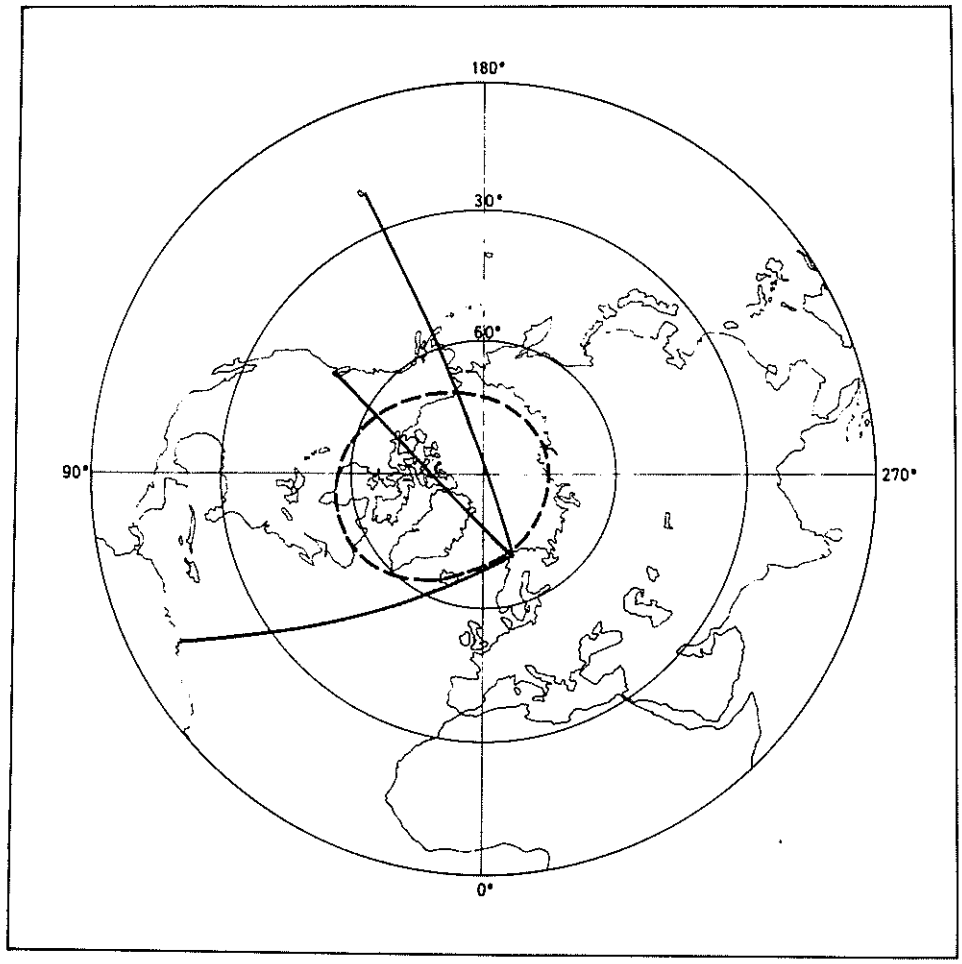

Fig. 1. The map shows the three VLF paths discussed in this paper.

* Seconded from Norwegian Defence Research Establishment.

These paths are shown in Figure 1 as solid lines. The auroral zone is marked by a broken line. Notice that the two northernmost paths cross the auroral zone twice, while the Trinidad path is nearly parallel to the auroral zone from Iceland to Tromsø. At Tromsø a Rubidium standard was used as local frequency reference. In addition to the VLF data magnetometer and riometer (27.6 MHz) data from Tromsø will be discussed.

The phase and amplitude curves for the event are shown in Figure 2. The shaded area in the phase curves represents instantaneous phase deviation from "normal" conditions. It is thus immediately seen that most phase effects on the transpolar paths have disappeared by noon on November 6.

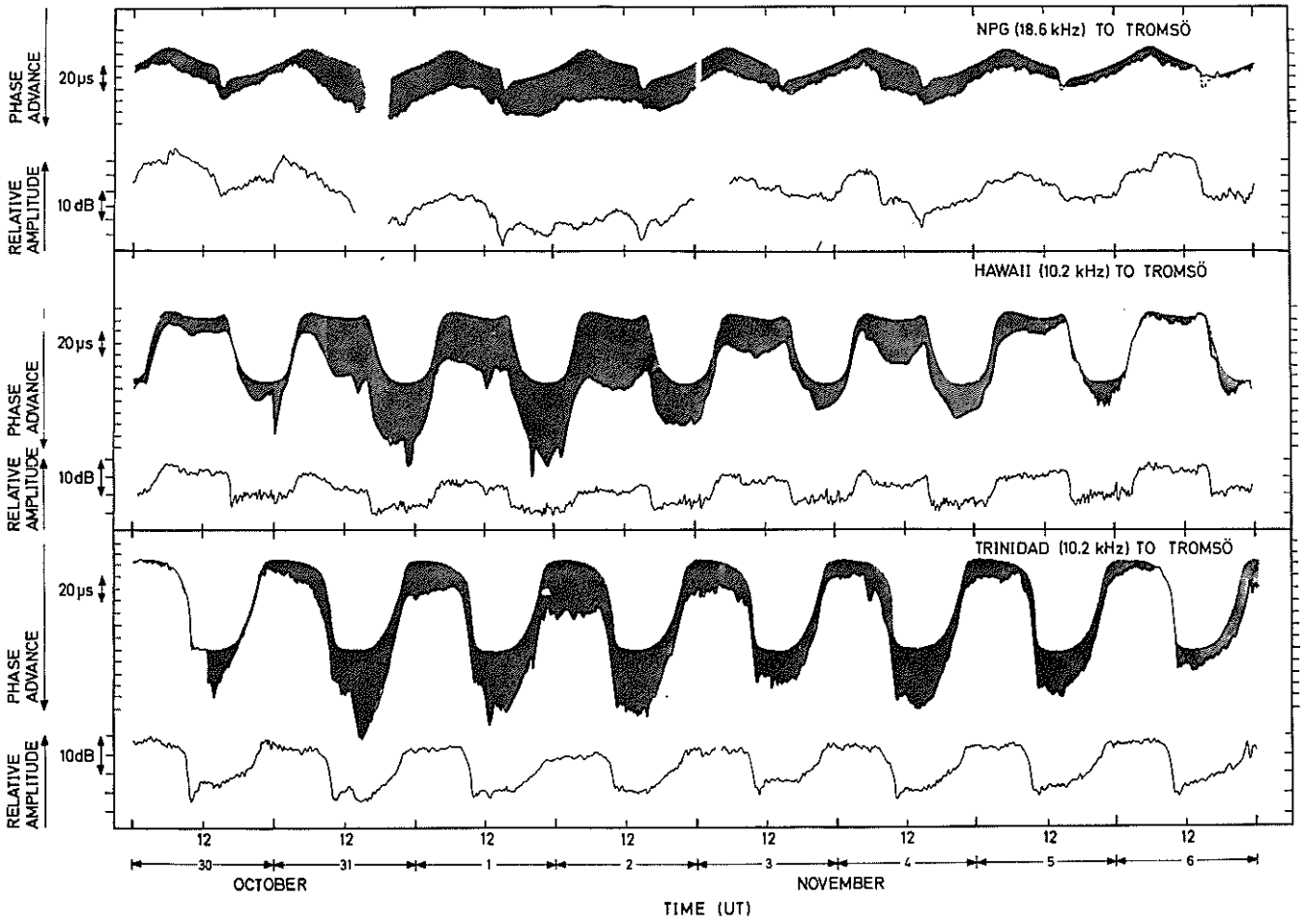

Fig. 2. Phase and amplitude variations during October 30 - November 6, 1968. Shaded areas show deviations from normal phase variations.

A few comments on the "normal" phase variations are appropriate. For the NPG and Hawaii paths the average phase values were calculated using the days October 26, 27 and 28, and the resulting curve subsequently slightly smoothed. For the Trinidad path the smoothed curve of October 30 was chosen to represent normal propagation conditions. Of these averaged phase curves the NPG curve is inadequate between 1400 - 1600 for the last days of the event, but this effect will be discussed later.

It is noticed that both transpolar paths exhibit some phase deviation (10 - 15 μs) on October 30. This is due to the PCA that started the day before.

The trigger flare for the PCA under consideration here was detected on the Hawaii path, 60% of which was in daylight when the event occurred. The VLF onset was 6 ± 1 min. after the start of the optical flare, but the major disturbances became clearly apparent with increasing phase deviation at 0400 - 0600 hrs. the next day. From 1300 - 1700 the magnetic field at Tromsø was much disturbed and at the same time the southernmost path (Trinidad) experienced greatly enhanced disturbances. Strong riometer absorption (5 - 6 dB) was observed with a midday recovery between 0900 - 1330.

The major magnetic storm started about 1145 on November 1 and was enhanced at 1900, 36 and 43 hrs., respectively, after the flare. These two periods mark arrival of low energy plasma from the sun and are also reflected in the VLF curves as periods of enhanced phase deviation and signal attenuation. Then in the course of November 1/November 2 the PCA reached its peak. During this time the diurnal phase variation of NPG was reduced from 35 to 15 μs and the night-time phase was typically 10 μs lower than average day-time values. Night-time phase of Hawaii was also below normal day-time level.

It should be noticed that the deep minimum in the normal phase of NPG at about 1500 occurs when the complete path for a short time is in sunlight. This condition does not prevail till November 6, therefore the "normal" curve between 1400 - 1600 is not appropriate for the complete duration of the PCA.

Table 1 give approximate values for the maximum PCA disturbance for day and night conditions on the paths.

TABLE 1

path	time(UT)	path condition	phase advance	ampl. attenuation
NPG	Nov 1 1500	path day-time	22 μs	15 dB
	Nov 2 0600	night-time	45 μs	25 dB
Hawaii	Nov 1 2300	path day-time	65 μs	5 dB
	Nov 2 1000	night-time	65 μs	10 dB
Trinidad	Nov 2 0300	path night-time	50 μs	5 dB
	Nov 2 1500	day-time	50 μs	3 dB

It is noticed that the NPG - Tromsø path, which crosses Greenland suffers the largest signal attenuation. This is in accordance with findings of e.g. Westerlund, Reder and Åbom [1969].

The VLF curves suggest that a new injection of particles took place on November 4 at about 0500. The riometer at Tromsø showed increased absorption (2 - 6 dB) between 0500 - 1100 while the magnetometer was relatively quiet.

At noon on November 6 only minor disturbances remain on the VLF circuits. However, a new event, believed to be a minor PCA event, started late night on the same day.

Acknowledgement

The VLF work in Tromsø is carried out in cooperation with the Norwegian Institute of Cosmic Physics. Mr. L. A. Fletcher at the Omega Systems Project Office is thanked for having provided part of VLF receiving equipment.

REFERENCES

ESSA 1968 Solar-Geophysical Data, IER-FB 291, November 1968.

WESTERLUND, S., F. H. REDER, and C. ÅBOM 1969 Planet. Space Sci., 17, 1329-1376.

"Long Path VLF Observations of the Ionospheric Disturbances Resulting from the Solar Proton Event of October - November 1968"

by

T. B. Jones
University of Leicester, England

Long path VLF propagation is severely affected by ionospheric disturbances associated with solar flares, solar proton events, magnetic storms and high altitude nuclear detonations. As part of the program for investigating the ionospheric disturbances caused by flare enhanced radiations [Burgess and Jones, 1967; Jones and Wand, 1967a; Jones and Wand, 1967b] the phase and amplitude of the following long path VLF transmissions are continuously monitored at Leicester. These are: (a) 12.0 kHz. Omega/Trinidad; (b) 18.6 kHz NLK, Jim Creek, Washington; and (c) 21.4 kHz NSS Annapolis.

After certain flares polar cap disturbances are observed as a result of enhanced D-region ionization which is probably caused by solar protons and other charged particles trapped in the earth's magnetic field. These solar proton events affect the whole polar cap and disturbances can occur down to magnetic invariant latitudes (Λ) of about 55 degrees [Belrose et al., 1956]. The duration of these events are dependent on the magnitude of the solar proton event and also on the magnetic latitude [Bates and Albee, 1965; Egeland and Naustvik, 1967]. The VLF propagation paths monitored at Leicester are particularly interesting in this respect since they cover a wide range of magnetic latitude.

During the solar proton event of October - November 1968 all three circuits were monitored and in addition some data was also available for the 17.8 kHz (NAA) Cutler, Maine, transmission received at Leicester.

On 29 October sudden phase anomalies (SPAs) were observed as shown below:

29 October 1968

Transmitter	Time of SPA (UT)		
	Start	Maximum	End
Ω/Trinidad	1216	1300	1400 ?
	1402	1420	1515
	1850	1855	?
NSS	1200	1250	?
NLK	?	1240	?
NAA	1215	1245	1400
	1850	1855	?

(? denotes events difficult to observe due to (a) records poor or missing, or (b) a second SPA occurring during the recovery phase of the first one).

On the following day, 30 October, two well defined SPAs were recorded, the second event starting before the first had fully recovered. Details of these two anomalies are given below:

30 October 1968

Transmitter	Time of SPA (UT)		
	Start	Maximum	End
Ω/Trinidad	1230	1255	
	1330	1350	1500
NSS	1240	1300	
	1330	1345	?
NLK	1230	1300 ?	
	1330	1345	?
NAA	1240	1300	
	1330	1345	1500

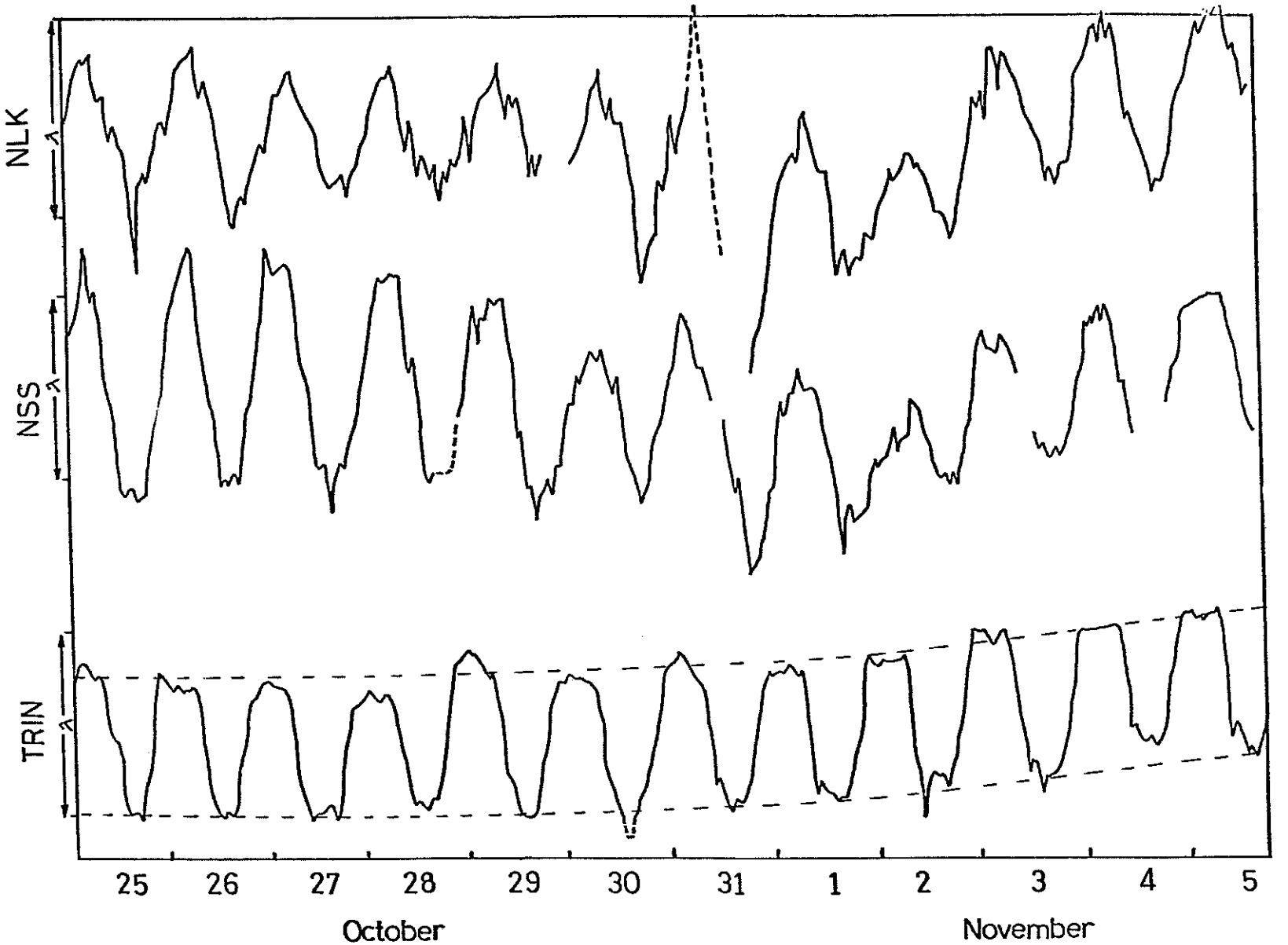

(Dotted line indicates Oscillator Drift)

Fig. 1. Phase records of NSS(21.4 kHz), NLK(18.6 kHz), and Ω/Trinidad(12.0 kHz) during a PCA event; October/November, 1968.

No SPAs were detected on 31 October but further activity occurred on 1 November with small SPAs on all paths starting about midday with maximum phase advance at 1245 UT.

The diurnal phase variations of the Trinidad, NSS and NLK transmissions during the period 25 October to 5 November are reproduced in Fig. 1. The first feature of interest is the shift in the night-time phase of the NSS signals during the night of 29-30 October. This feature is not well defined for the NLK results and is not present in the Trinidad data. During the morning of 30 October the night and day change of the NLK phase is greater than normal and the phase remains at this anomalous value throughout the day. In contrast, the day time phase of the NSS and Trinidad signals are normal throughout 30 October.

The phase for all three transmissions appears to be normal during the night of the 30-31 October although a marked drop in the NPG signal strength made observations difficult at this frequency. The following day both NSS and NPG transmissions show large phase disturbances, and the phase variations from the night of the 30-31 to day on 31 are about one and a half times the normal change. During the night of 31 October - 1 November the phase returns to its normal value although some minor disturbances are evident.

The following night, however, (1-2 November) exhibits a marked storm after effect, the night-time phase retardation being only about half its normal magnitude and considerable phase fluctuations are present throughout this night. After 2 November the diurnal phase pattern slowly recovers although it is difficult to determine when recovery is complete due to the slow drift of the reference oscillator.

No disturbances were observed on the Trinidad transmissions during the proton event apart from the SPAs associated with the flares. This indicates that the ionospheric disturbances resulting from the proton event were limited to magnetic latitudes greater than those of the Trinidad to Leicester path. The receiver is at $\Lambda \simeq 50°$ but Λ is less than $\Lambda \simeq 40°$ for about half of this path. The NSS to Leicester path, which lies between $\Lambda \simeq 45°$ and $\Lambda \simeq 60°$, did, however, show considerable disturbances during the event.

The VLF observations have enabled the time and latitude variations of the ionospheric disturbance produced by the proton event to be investigated. Particularly interesting features of this event are the dissimilar effects observed on the high latitude paths during the initial phase of the disturbance, the well defined storm after effect, and the disappearance of the ionospheric disturbance at geomagnetic latitudes below about 45 degrees.

REFERENCES

BATES, H. F. and P. R. ALBEE — 1965 — J. of Geophys. Res., 70, 2187.

BELROSE, J. S., M. H. DAVENPORT, and K. WEEKES — 1956 — J. of Atmos. and Terr. Phys., 8, 281.

BURGESS, B. and T. B. JONES — 1967 — Radio Science, 2, 619.

EGELAND, A. and E. NAUSTVIK — 1967 — Radio Science, 2, 659-667.

JONES, T. B. and I. C. WAND — 1967a — Proceedings 13th AGARD Symposium, Ankara (Ed. K. Davies).

JONES, T. B. and I. C. WAND — 1967b — I.E.E. Conference Proceedings, No. 36, 16, London.

Radio noise from the ionosphere on 225 MHz during a great ionospheric disturbance

G. ERIKSEN & L. HARANG
Institute of theoretical astrophysics, Blindern, Oslo

Eriksen, G. & Harang, L. Radio noise from the ionosphere on 225 MHz during a great ionospheric disturbance. *Physica Norvegica*, Vol.4, No.1, 1969.

During a great geomagnetic disturbance and at the end of a polar cap absorption (PCA) event, emission of radio noise on 225 MHz was observed at Oslo with a 7.5 m paraboloid directed towards the lower northern horizon and thus covering part of the auroral zone. The flux of the observed radio noise was of the order of 1×10^{-22} W/m²Hz.

L. Harang, Institute of theoretical astrophysics, Blindern, Oslo, Norway

1. OCCURRENCE OF THE 225 MHz EMISSION

Solar radio noise is recorded regularly at the Oslo Solar Observatory situated 50 km north of Oslo. The equipment used is a converted Würzburg antenna and a recording receiver operating on 225 MHz with a band-width of 1 MHz. The parabolic mirror has a diameter of 25 feet and is fed by a vertical dipole. The antenna beam has a width of approximately 13° by 15° between half power points.

It was decided to utilize this equipment during night hours in a search for noise radiation which might be emitted from the polar ionosphere at times of heavy disturbances. After sunset, the antenna was pointed 20° west of north at an elevation of 11°. Between half power points the antenna thus covers a height interval from 150 to 450 km in the auroral zone some 500 to 800 km west of Tromsø.

Almost every night from October 1968 to March 1969 cosmic noise was recorded from sunset to sunrise. Records were made with a recording time-constant of 3–5 seconds. During this 6-month period, emission in addition to the regular pattern arising from the Milky Way crossing the antenna beam was observed only once, and the highly disturbed condition of the ionosphere on this occasion indicates that the emission recorded is to be associated with this disturbance. The 225 MHz records from the three nights 31.10 to 2.11. 1968 are shown in Fig. 1. The upper trace, from 31.10, gives a typical example of the undisturbed radiation from the galactic background. The spike at the extreme left is the deflection caused by a calibrating noise generator. The lower trace, on the other hand, shows from the start of the record at 1528 UT, additional emission varying in intensity and fading away towards 1900 UT. The galactic background radiation expected is indicated by the broken line. The peaks of radiation received at 1540 UT and 1810 UT correspond to an excess flux of approximately

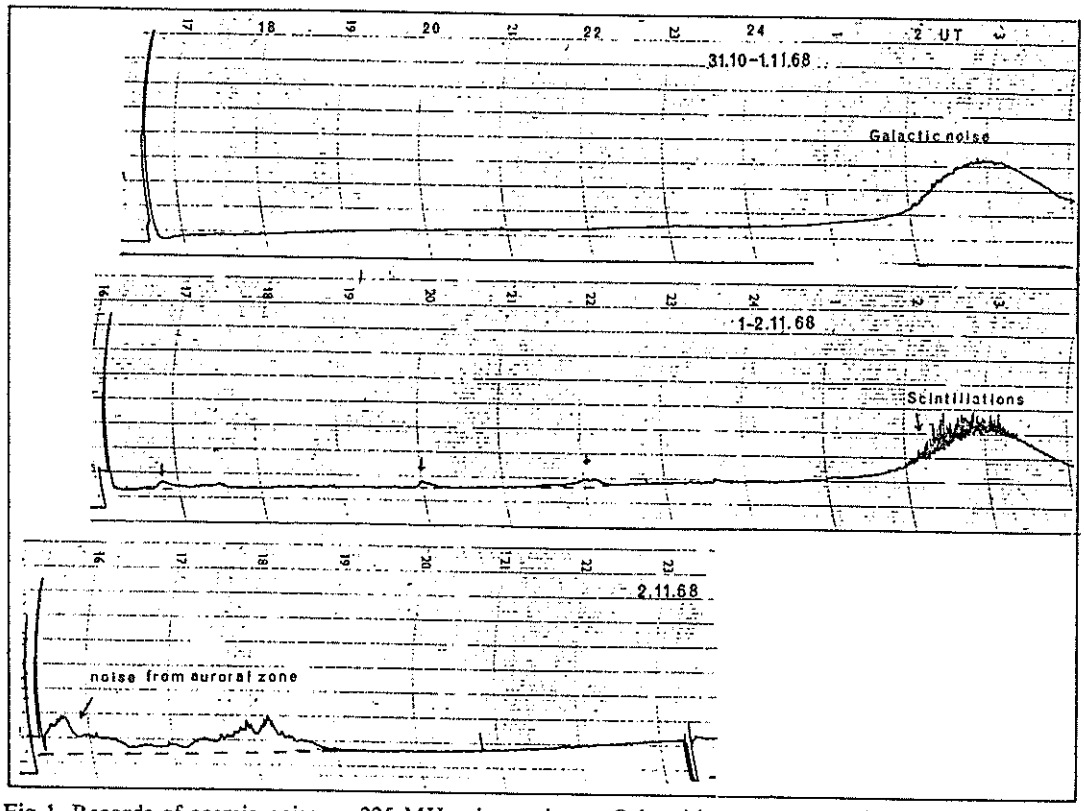

Fig. 1. Records of cosmic noise on 225 MHz observed near Oslo with an antenna pointing towards north at an elevation of 11°.

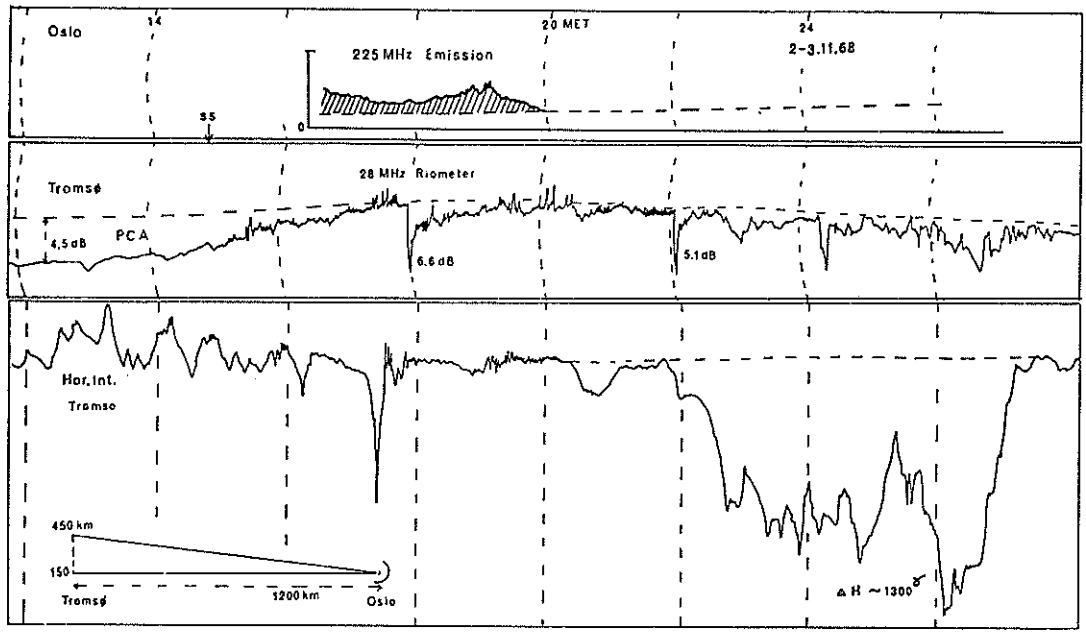

Fig. 2. Appearance of ionospheric noise on 225 MHz during the disturbance illustrated by the riometer records and *H*-records from Tromsø. A PCA of medium strength precedes the noise emission.

1×10^{-22} W/m²Hz. Inspection of the record from the preceding day reveals three smaller deflections, whereas the curve two days earlier is completely smooth. The heavy scintillations in the record of the galactic noise in the morning hours of 2.11 are signs of very strong irregularities in the ionosphere. As is evident from the geomagnetic *H*-records from Tromsø shown in Fig. 3, a series of geomagnetic storms appeared in the period 31.10. 1968 to 2.11. 1968.

In Fig. 2 are given, from top to bottom, the 225 MHz emission measured at the Oslo Solar Observatory (observations starting at 1628 MET), 28 MHz riometer observations, and geomagnetic *H*-records from Tromsø on 2.11 and 3.11. The polar cap absorption event (PCA) of medium strength had a magnitude of 4.5 dB at Tromsø and 4.3 dB at Lycksele.

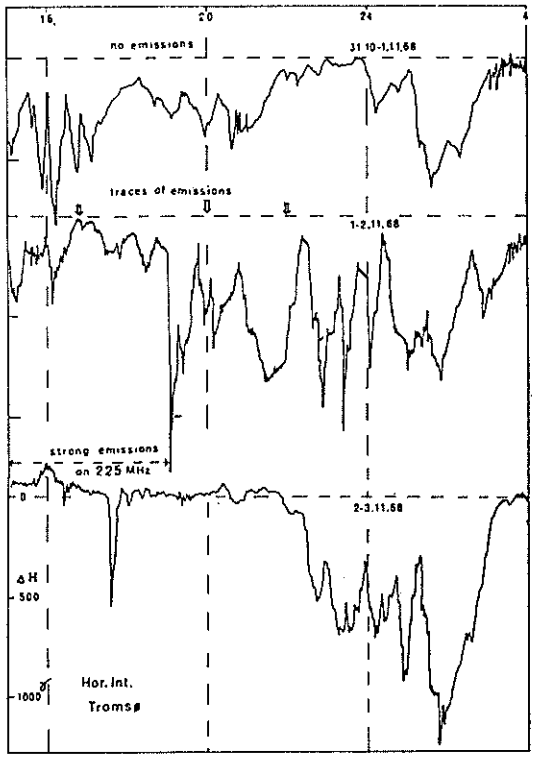

Fig. 3. Geomagnetic *H*-records from Tromsø on the three consecutive days. The night of greatest geomagnetic activity was 1–2.11. 1968, during which only faint traces of emission are present. On the last day, 2–3.11. 1968, the geomagnetic storm is declining, but a PCA appeared in day-time.

It might seem surprising that the riometer record from Tromsø in the evening of 2.11. 1968 (Fig. 2) shows only weak traces of emission, e.g. at 1730 MET, during the event on 225 MHz. One should bear in mind, however, that the beam of the Würzburg antenna crosses the ionosphere 500 to 800 km west of the riometer position at Tromsø. As is demonstrated in a subsequent paper (Harang 1969), emission events recorded by riometers are rather rare and have a geographic extent of just a few hundred kilometres. Simultaneity of events recorded on 225 MHz and 28 MHz may thus be expected only if the antenna beam points to the same region of the ionosphere.

From the 225 MHz observations nothing can be said about the spatial extent of the emission volume. More elaborate investigations are planned incorporating a scanning paraboloid operating on 225 MHz close to the auroral zone at Tromsø. Further, the antenna at the Oslo Solar Observatory will be pointed in the correct direction to cover the ionosphere above Tromsø.

2. SIMULTANEOUS OCCURRENCE OF EMISSIONS ON 225 MHz AND IN THE kHz-RANGE

In previous papers (Harang 1965, 1969) it has been shown that bursts of VLF-emission on 8 kHz at Tromsø may occur simultaneously with emission spikes on 28 MHz. The VLF records from the 8 kHz chain Tromsø–Lycksele–Oslo and Middle Europe showed no signs of emission in this frequency range during the 225 MHz event. Further, the riometers in Tromsø and Lycksele showed only weak, if any, spikes on 28 MHz. Parallel with the chain of VLF stations in Scandinavia and Middle Europe, however, there are a number of stations in Japan recording on 4–6 kHz. A preliminary comparison of the VLF records on 8 kHz from Middle Europe and the records from the Japanese station Moshiri on 4–6 kHz has revealed that there is often a coincidence of occurrence of the burst activity in these two distant chains of stations.

Now the VLF record on 4–6 kHz from Moshiri (the records from Moshiri were kindly put at our disposal by Dr. H. Ishikawa at the Research In-

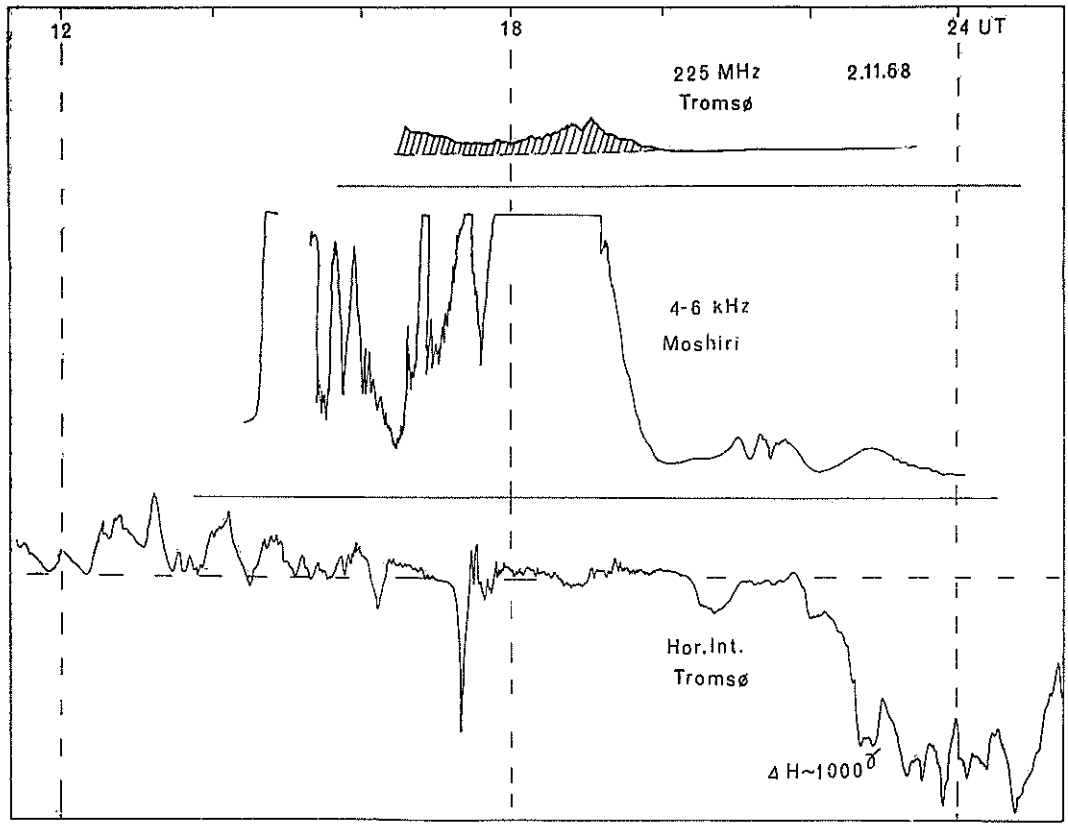

Fig. 4. Emission on 225 MHz at Tromsø–Oslo and on 4–6 kHz at Moshiri, Japan, occurring simultaneously.

stitute of Atmospherics, Nagoya, Japan) during the strongly disturbed days 1–2.11. 1968 showed a series of VLF emissions, and in Fig. 4 is shown the position in time of the VLF emission at Moshiri and the 225 MHz emission at Tromsø–Oslo. There is a remarkable coincidence between the occurrence of the main period of emissions and the fading-out of the emissions at the two stations. It must be emphasized, however, that VLF emission of the same character may occur at Moshiri without any emission occurring on 225 MHz at Tromsø–Oslo. It is therefore not possible to draw any definite conclusions generally concerning this simultaneity.

REFERENCES

1. Harang, L. & Larsen, R., *J. Atmosph. Terr. Phys.*, *27*, 481 (1965).
2. Harang, L., *Planet. Sp. Sc.* (1969) in press.
3. Harang, L., *Physica Norvegica* (1969) in press.

Received 23 June 1969

"High Latitude Scintillations During the October 30-November 4 Magnetic Storm"

by

Jules Aarons and Herbert Whitney
Air Force Cambridge Research Laboratories
Bedford, Massachusetts

Introduction

In an earlier paper we have advanced the hypothesis that a boundary exists during periods of magnetic quiet for the F region irregularity structure noted by scintillation studies [Aarons et al., 1968]. The boundary is frequently sharp shortly after sunset and very diffuse during early morning hours. The latitude of the boundary is a function of local time with the lowest equatorward position noted at 2200. In this preliminary report we would like to examine the boundary concept for highly disturbed conditions to determine the diurnal control as well as localized and temporal effects.

The period of interest is Oct. 30-Nov. 4 when two magnetic storms were recorded; one started on Oct. 30 at 23-24 UT and ended on Nov. 1 at 03 UT. The second portion of the storm period started on Nov. 1 at 0917 and ended on Nov. 3 at 17 UT.

Effects at Four Observatories

Using similar methods of data reduction, we have compared amplitude records of four stations simultaneously observing 137 MHz transmissions from the synchronous satellite, ATS-3. Indices using the method of Whitney et al. [1969] were obtained for each 15 min. period for the observatories listed in Table 1.

Table 1

	Elevation Angle	350 km Sub-ionospheric Intersection Lat.	350 km Sub-ionospheric Long.
Thule, Greenland	3.9°	73N	57W
Narssarssuaq, Greenland	21°	64N	46W
Rude Skov, Denmark	8°	52N	4W
Sagamore Hill, Hamilton, Mass.	35°	50N	68W

Both the Narssarssuaq and the Rude Skov stations are operated by the Danish Meteorological Institute; the other two sites are operated by AFCRL.

Thule: Even during periods of magnetic quiet, fading of ATS-3 signals was never less than 3-4 dB; during a larger portion of the quiet days fades to noise (peak to null of 15 dB) were observed. During the storm periods fades of 3-4 dB were not observed; only at rare times were the fades as low as 10 dB. A typical storm record is shown in Figure 1 along with a record of 41 MHz signals from BE-B showing deep scintillations over the polar cap. During quiet periods overhead passes of 41 MHz show frequent moderate scintillation indices; during this period signals of the type shown in the illustration were typical. The data clearly shows evidence of widespread enhanced polar cap scintillations during the storm period.

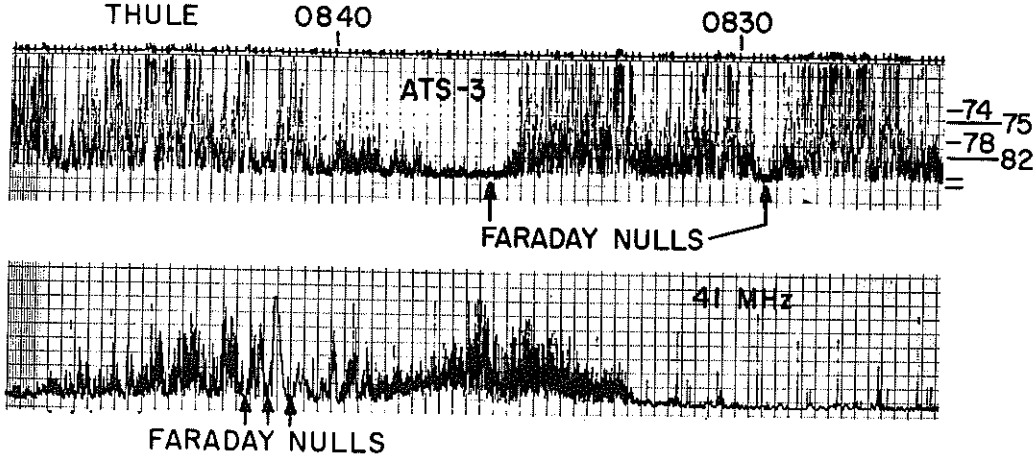

Fig. 1. High scintillation indices typical of storm period. 137 MHz signals fade to noise on top scale as do the 41 MHz BE-B transmissions almost through this pass.

From recent observations of other satellites, ESRO I and ISIS, it is known that the quiet day high angle scintillation indices (at 137 MHz) over the polar cap are much lower than the synchronous satellite observations. The consistent high amplitude scintillations (observations have been made of ATS-3 from Thule for approximately one year) are due to the low angle of the observations and to the intersection of the propagation path with the auroral oval with probable emphasis on the long length of the propagation path.

Narssarssuaq: Throughout the storm period moderate to high indices were recorded. For comparison of the diurnal pattern of Narssarssuaq and the two other stations, Figure 2 has been constructed. Hourly values are used. A nighttime maximum is seen for Nov. 1 and 2. Peak scintillation activity occurred between 00-10 UT on Nov. 2 somewhat later than the peaks of the second magnetic storm which were between 12-15 UT and 21-24 UT on Nov. 1. However, the 13-16 UT peak scintillation activity is correlated with the first peak of magnetic activity during the storm.

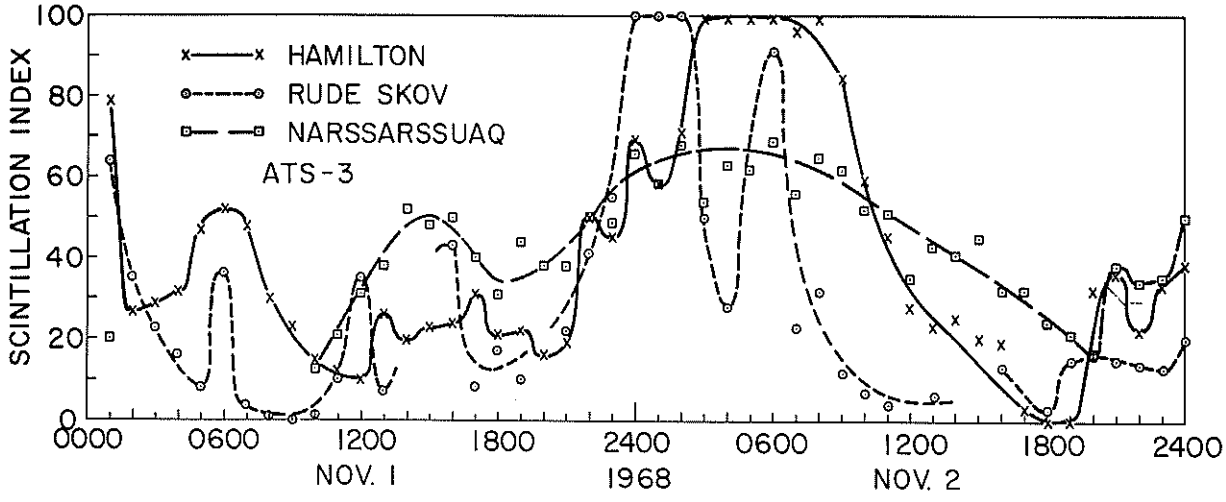

Fig. 2. Hourly scintillation indices for Narssarssuaq, Greenland, Rude Skov, Denmark and Hamilton, Mass. There is approximately 5 hours time difference between sub-ionospheric propagation path intersections of Hamilton and Rude Skov.

Rude Skov: Scintillation activity increased with magnetic activity from 15-16 UT but some data are missing from this period. On finer scale plots a clear maximum in index can be noted from 2200 (Nov. 1) to 0300 (Nov. 2) with peak activity from 2330-0200 UT.

Sagamore Hill, Hamilton: Peak scintillation indices were observed between 0300 and 0800 UT on Nov. 2 although a short period of high scintillation was recorded around 2200 (Nov. 1).

Taken with the Rude Skov data Hamilton observations indicate that the maximum activity occurs at each station as a function of local time although large scale simultaneous increases are also noted. Between Rude Skov and Hamilton one would expect a five hour time difference. Narssarssuaq appears to peak between the other two maxima.

The magnetic activity enhancement from 12-15 UT produced a moderate enhancement at Hamilton, a considerable enhancement at Narssarssuaq, and a possible enhancement at Rude Skov. It should be noted that for all three stations the quiet day indices during this time period are very low. 2200 UT indices were momentarily high on all records.

However, while intense magnetic activity appears to have a simultaneous large scale effect, the scintillation boundary maintains its diurnal pattern. Peak indices were noted at Hamilton on Nov. 2 between 03-08 UT, after the peak magnetic activity noted at Fredericksburg.

Effects at Sagamore Hill, Hamilton, Mass.

At Sagamore Hill Radio Observatory many types of ionospheric data were being taken during this period. These included recording amplitude fluctuations of LES-6, a synchronous satellite transmitting at 256 MHz, radio star tracking of Cassiopeia at frequencies ranging from 62 to 400 MHz as well as riometer measurements at 30 and 50 MHz.

A dramatic ionospheric effect occurred around 2200 UT on Nov. 1. At 2157 UT a rapid decrease in total electron content began. The measurement [Mendillo, et al., 1969] utilizing Faraday rotation observations of ATS-3 showed a 60% decrease in total electron content of the ionosphere between 2157 and 2214 UT. The timing of this and other events are shown in detail in Figure 3.

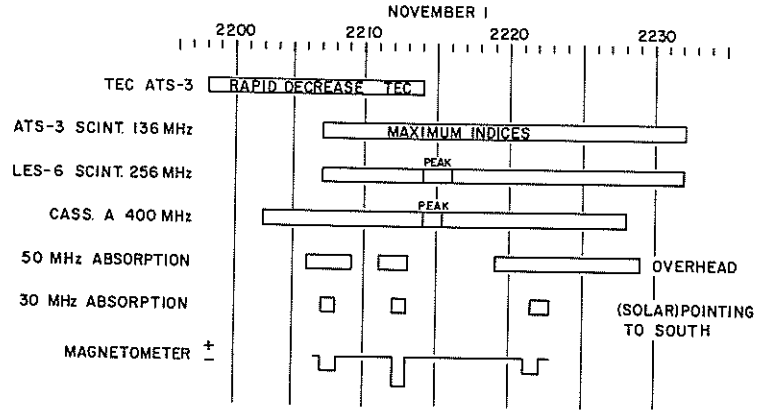

Fig. 3. Sequence of Events of Sagamore Hill Observations

When Faraday rotations increased in rate, ATS-3 scintillations were relatively low in amplitude. Scintillation index increased dramatically at 2207 UT; LES-6 scintillations started at the same time. The two synchronous satellites had approximately the same geomagnetic intersection latitudes. Cass A scintillations at 400 MHz (with the intersection latitude at 56° G.N.) started at 2202 and stopped at 2228 UT. LES-6 scintillations decreased at 2232 UT.

The time scale of the phenomena indicated that after the reduction of a large portion of the total electron content scintillations commenced on the same propagation path. Even earlier, however, scintillations were observed to the north. A motion of the scintillation boundary from north to south took place in the early stages of these events and then from south to north.

In addition to the total electron content decrease and the scintillation brusque start and stop, an absorption event was noted. On a riometer looking to the south, absorption increased sharply at 2207-2208, 2212 and 2222 UT. 50 MHz absorption on a large antenna observing Cygnus upper transit (almost directly overhead) was recorded somewhat earlier at 2206, 2211 and 2219 UT again indicating a motion from north to south in the early portion of this short period.

Magnetometer records taken at Bedford, Mass., show sharp negative impulses at the same time as the absorption events.

The data are not clear on mechanisms involved in this rapid sequence of events but the large scale latitude motions are quite consistent. Considerations of the polar characteristics of scintillations indicate that high latitude scintillations are probably produced directly or indirectly by precipitation of energetic particles of a few hundred electron volts. From the polar cap characteristics of the BE-B satellite scintillations, it appears as if more of the low energy electrons were precipitated during this period. From the local time control during the magnetic storm it would appear that the normal magnetospheric control of the boundary is maintained. However, during short periods of time within relatively small areas precipitation proceeds from higher L values to lower L values and then moves again back to high latitudes.

REFERENCES

AARONS, J., J. P. MULLEN and H. E. WHITNEY — 1969 — "The Scintillation Boundary", J. Geophys. Res., 74, 884-889.

MENDILLO, M., M. D. PAPAGIANNIS and J. A. KLOBUCHAR — 1969 — "A Seasonal Effect in the Mid-Latitude Slab Thickness Variations During Magnetic Disturbances", presented at the AGU Meeting, Washington, D. C.

WHITNEY, H. E. and C. MALIK — 1969 — "A Proposed Index for Measuring Ionospheric Scintillations", Planet. Space Science, 17, 1069-1073.

"Ionospheric Disturbances in the Northern and Southern Hemispheres in October and November 1968"

by

R. Knuth and H. Gernandt
Zentralinstitut für solar-terrestrische Physik (HHI) der
Deutschen Akademie der Wissenschaften zu Berlin, GDR,
Observatory Neustrelitz

The strong interplanetary and geomagnetic disturbances starting at the end of October 1968 also caused extremely pronounced effects in the lower ionosphere at medium latitudes. This behaviour shall be shown on the basis of LF-A3-measurements and Radar-Aurora-observations [Geophysikalische Beobactungsergebnisse] in Kühlungsborn, GDR (ζ = 54° 07' N, λ = 11° 46' E, Φ = 54.4°N) and LF-field-strength-measurements in Mirny, Antarctica. These latter observations have been performed during a 12-months stay of one of us (H.G.) as a member of the GDR-group at this Soviet Antarctic station.

Table 1 indicates the general behaviour of absorption anomalies in LF- and VLF-propagation for certain periods of the day as recorded with a large net of different frequencies in Kühlungsborn Observatory (HHI).

TABLE 1. Station: K ü h l u n g s b o r n — October/November 1968
Geogr.coordinates: 54°07'N; 11°46'E

Night-Time Disturbances in the Lower Ionosphere
(as observed in the LF and VLF range)

Date Night/Month		P-Effects VLF	P-Effects LF	Excessive Absorption SS	Excessive Absorption N	Excessive Absorption SR	Remarks (Time in UT)	p'
25-26	Oct.	-	-	-	-	-		0
26-27		-	-	-	-	-		0
27-28		-	-	-	-	-		0
28-29		-	-	-	-	-		0
29-30		-	P_1	-	S_1	-	P and S from 1840	3
30-31		x	-	-	A_1	-		1
31- 1		P_1	P_2	S_2	S_2	A_0	storm from 1430	8
1- 2	Nov.	P_1	P_1	S_3	S_2	A_2	repeated storm commencement 1515	9
2- 3		-	P_0	P_1	A_0	A_1	P from 2000	4
3- 4		-	P_0	A_0	-	A_0	P from 2050	2
4- 5		-	-	A_0	A_1	A_1		3
5- 6		-	P_0	A_1	-	A_1	P from 1730	3
6- 7		-	-	-	A_2	A_2		4
7- 8		-	-	A_2	A_2	A_0		5
8- 9		-	-	A_1	A_2	A_1		4
9-10		-	-	A_2	A_0	A_1		4
10-11		-	-	A_0	A_0	A_1		2
11-12		x	P_0	A_2	A_1	-	P from 1750	4
12-13		-	P_0	-	-	-	P from 1800	1
13-14		-	-	-	-	-		0
14-15		-	-	-	-	-		0
15-16		-	-	-	-	-		0

Symbols A_{0-3} characterize the excessive absorption in the lower ionosphere due to invading high-energy particles, P_{0-3} gives the increased fading rate in the VLF or LF range probably due to stormlike disturbances in the lower ionosphere, S_{0-3} characterizes sudden enhancements of night-time absorption. The night-time disturbance index p', ranging from 0 - 9, is a well proved character figure for corpuscular activity in the lower ionosphere. As can be seen from this table some indications of small disturbances had already occurred during the nights of October 29/30 and 30/31, but very pronounced effects started with an ionospheric storm on October 31, 1430 UT. A repeated storm commencement took place on November 1 at 1515 UT. Both these storm-effects in comparison with the normal behaviour are shown in Fig. 1. The excessive ionization in the lowermost parts of the ionosphere led to an almost total blackout of the LF-skywave for about 100 min., followed by a long lasting period of additional absorption. This well known after-effect in low frequency propagation [Lauter, 1950; Bracewell et al., 1951; Lauter and Knuth, 1967] lasted till November 11 and was one of the strongest events in the new solar cycle.

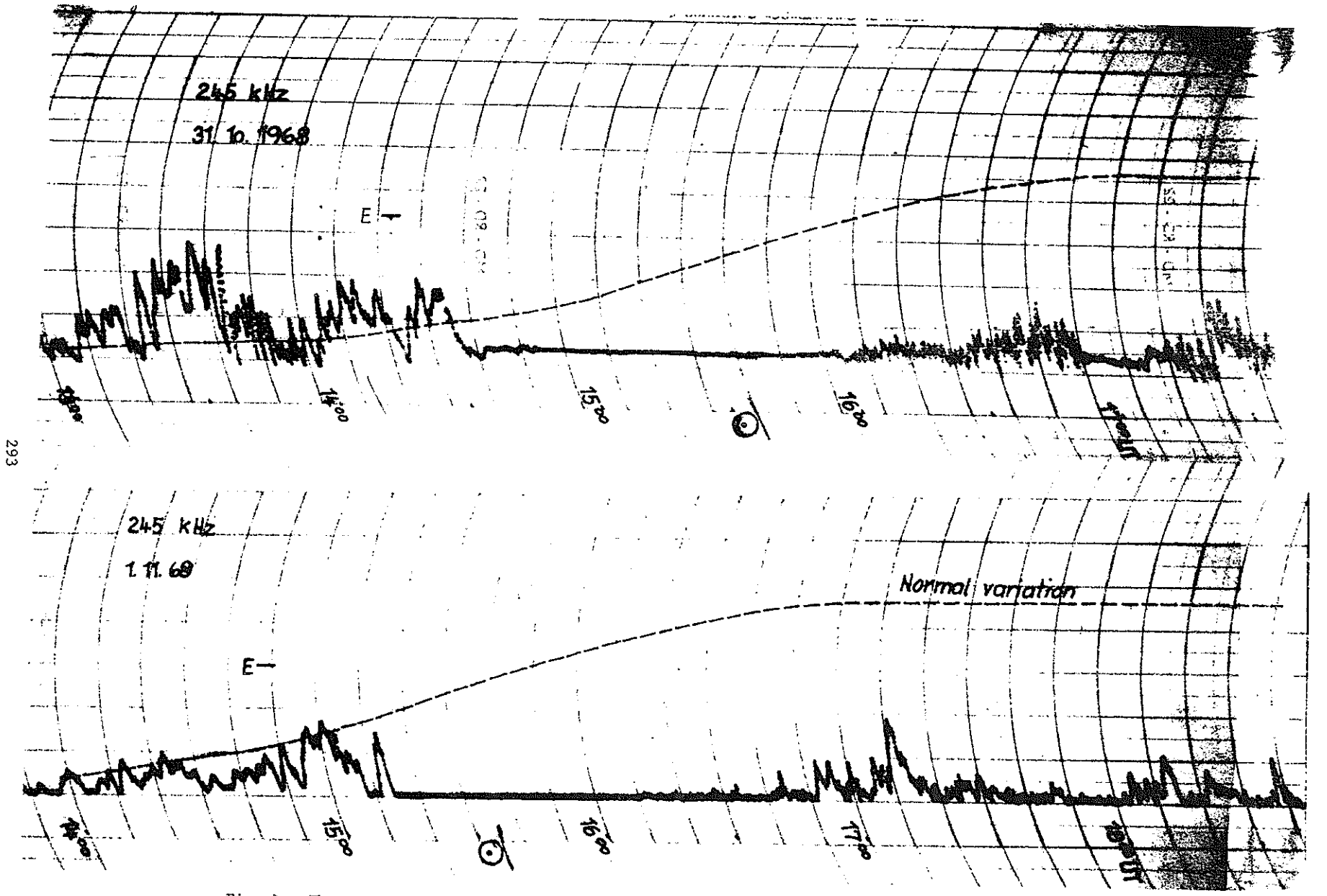

Fig. 1. The primary storm effects of October 31 and November 1, 1968, in LF-propagation.

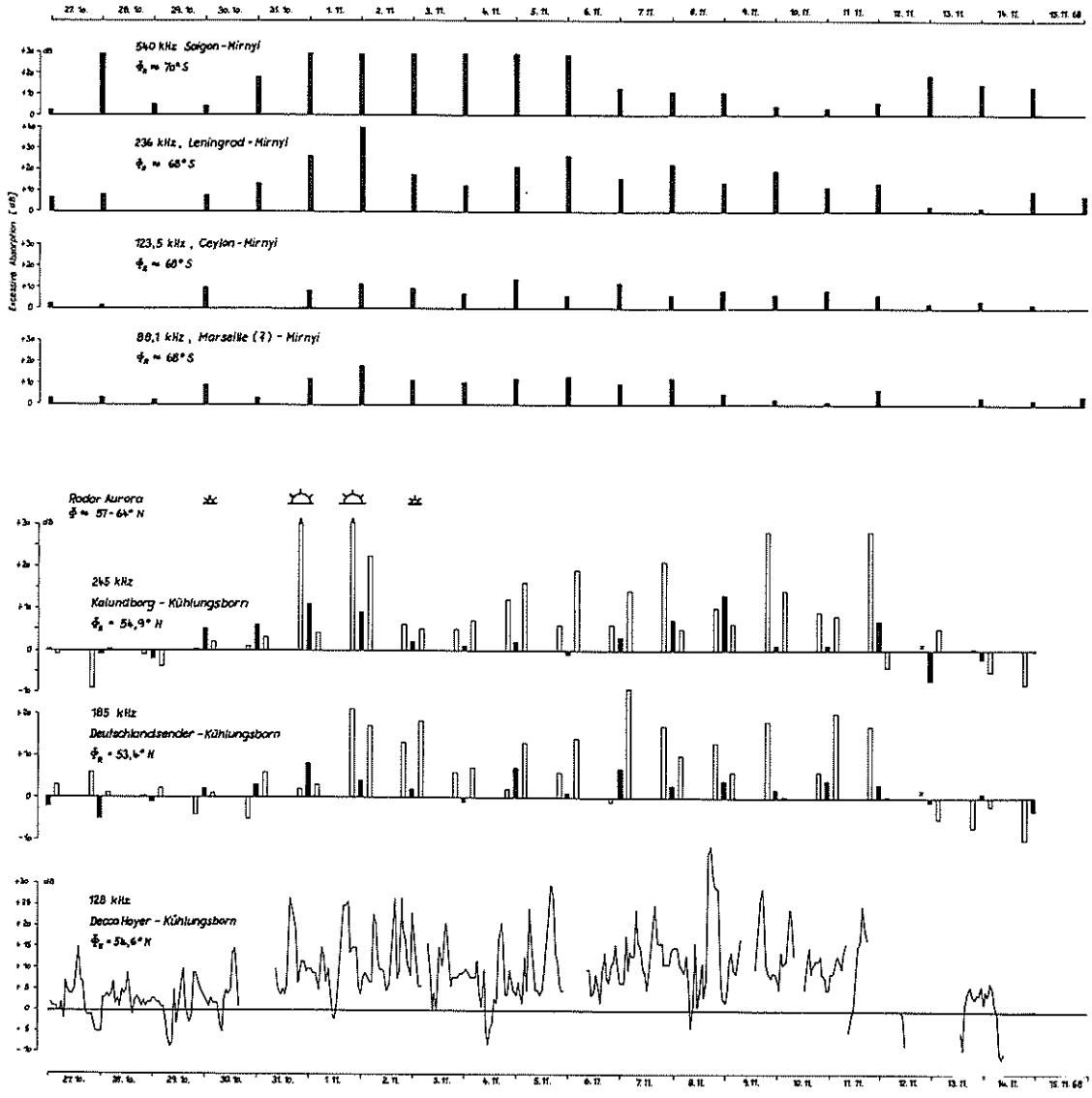

Fig. 2. Excessive LF-absorption in medium high southern and northern geomagnetic latitudes
(■ = night-time values,
(▭ = absorption during sunset and sunrise)

As known from many papers on this LF-after-effect the absorption anomalies are most pronounced during the periods of sunrise and sunset, certainly due to the important role of photodetachment processes on the ionization of the mesospheric D-region. For northern medium latitudes between 50° and 57° it could be proved, that in general the night-time absorption is influenced only during strong events. In the first 6 rows of Fig. 2 are given the excessive absorption values in dB in regard to the normal undisturbed median values for sunset, night and sunrise respectively. Unfortunately for the field-strength measurements in Mirny the absorption behaviour can clearly be interpreted only during the night, therefore we have shown only these values. Obviously the absorption anomalies also started about October 29, reaching maximal values in the night of October 31/ November 1 and then an after-effect with excessive night-time absorption between 15 and 20 dB lasted till about November 12. As known from some earlier investigations in Mirny [Glode 1969] the main influence on LF-propagation over very long ranges comes from the region of the last reflection point. Therefore in Fig. 2 are indicated the geomagnetic latitudes Φ_R of these points and probably the very marked absorption effects during the night are due to an enlarged influence of precipitating magnetospheric particles in these higher latitudes after the strong refilling processes of the magnetic storm.

But also the LF-measurements in northern geomagnetic latitudes between 53N and 55N indicate very well the primary absorption disturbances during the magnetic storm and the after-effect absorptions especially during sunrise and sunset. It can also be stated, that the general correlation between these similar observations in northern and southern hemisphere regarding the intensity and duration of the event is quite good.

In the lowermost part of Fig. 2 the hourly values of excessive absorption for a third LF-path in Kühlungsborn are drawn and it can be seen, that the strong after-effect-period has influenced not only the night-time but also the day-time propagation of the skywave indicating a persisting disturbance of the lowermost ionosphere. In Fig. 2 is also indicated the occurrence of radar-aurora in intensity and time from observations with a 33 MHz-Backscatter in Kühlungsborn. The strongest displays are again in coincidence with the main phases of the magnetic storms and indicate together with the very high excessive LF-absorption an equatorward shifting of the belt of invading high energy particles. A more extensive paper on this event taking into account much more different observations is in preparation.

REFERENCES

	1968	Geophysikalische Beobachtungsergebnisse (Geophysical Data), Heinrich-Hertz-Institut für solar-terrestrische Physik, 19, Nr. 10 and 11.
BRACEWELL, R.N., BUDDEN, K. G. and J. A. RATCLIFFE	1951	The ionospheric propagation of low- and very-low-frequency radio waves over distances less than 1000 km, Proc. IEE, 98, 221 - 236
GLODE, P.		Exzessive ionosphärische Absorption von Lang- und Mittelwellen bei Ausbreitung über sehr große Entfernungen nach Beobachtungen in der Antarktis, Monatsberichte der DAW zu Berlin, in press
LAUTER, E.-A.	1950	Zur Statistik der nächtlichen abnormalen E-Schicht, Zs. f. Met. Bd. 4, Heft 7/8, 234-240.
LAUTER, E.-A. and R. Knuth	1967	Precipitation of high energy particles into the upper atmosphere at medium latitudes after magnetic storms, J.A.T.P., 29, 411 -417.

"Simultaneous Observations of Various Ionospheric Phenomena During the Geomagnetic Storm from October 31 to November 2, 1968"

by

P. Czechowsky, H. Kochan, G. Lange-Hesse, H. Lauche and H. G. Möller
Max-Planck-Institut für Aeronomie, Lindau/Harz, Germany

Abstract

At times of strong geomagnetic storms so-called radio aurorae appear as well as visual and subvisual aurorae especially in the polar ionosphere. These radio aurorae are caused by inhomogeneities of electron density which give rise to scattering of radio waves from the HF- (3 - 30 MHz) to the UFH-band (300 - 3000 MHz) in a very characteristic manner. During the magnetic storm from October 31 to November 2, 1968 it was possible for the first time to record back-scatter echoes from radio aurora with a chain of transmitting and receiving stations which was completed in autumn 1967. The frequencies used were in the HF- (3 - 30 MHz) and the VHF-band (30 - 300 MHz). Echoes from the E as well as from the F region of the ionosphere were received from the area between approximately 55° and 65° geomagnetic north. For the times when the most southerly transmitting and receiving line (Bielstein - Lindau) showed strong echoes equivalent current systems were computed from the disturbance vectors of the magnetograms of ten geomagnetic observatories. The magnetic recordings and the backscatter-amplitudes show very similar variations, sometimes even in detail. During the magnetic storm the position of the polar electrojet (PEJ) changed continuously. The individual station received strong echoes at times when the PEJ lay in the area of the backscatter-curve which was computed for this station. The beginning and the end of the scattering-process as well as the amplitude of the scattered signals also depend on the strength of the PEJ (threshold-value). This confirms the theory of D. T. Farley and O. Buneman, that the electrojet produces the inhomogeneities of electron density (plasma-waves) in the E-region which give rise to scattering of radio waves. The echoes from field-aligned irregularities in the F-layer are associated with high positive values of Δ H. The disappearance and the reappearance of the F2-layer of the ionosphere during this magnetic storm is observed by means of 2xF-scatter propagation. The backscatter measurements were complemented by optical observations as photometer recordings of the red (6300 Å) and green (5577 Å) oxygen lines and by visual aurora observation from German ships.

Introduction

Since 1963 the Max-Planck-Institute for Ionospheric Physics at Lindau/Harz (W. Germany) carries out HF auroral backscatter observations. In 1967 these investigations were extended to the VHF-band and a network of beacon transmitters and receiving stations was established. The aim of these investigations is to study the auroral phenomena in middle latitudes and the interrelation between visual aurora, radio aurora and the polar electrojet (PEJ). At present the following stations are in operation:

transmitters:	DLØAR (Bielstein)	on	29.0 MHz,
	DLØPR (Garding)	on	145.971 MHz,
	SM4MPI (Borlänge)	on	145.960 MHz;

and the receiving equipments:

Lindau	on	29.0, 145.960 and 145.971 MHz,
Norddeich	on	145.960 MHz,
Kjeller near Oslo	on	145.960 and 145.971 MHz.

The stations with the beam directions of their antenna systems are shown in Figure 1. (The HF output of the transmitters is of about 150 W. The cw-signal is interrupted once in a minute by the call sign. The antenna gain is 12 dB.)

Theory

Models of the backscatter mechanism of VHF radio waves from aurora were developed by Booker [1956], Moorcroft [1961], Buneman [1963] and Farley [1963]. In this paper the observations of the time interval from Oct. 31 to Nov. 2, 1968 are compared with these theories.

The Booker model describes the electron density distribution in the auroral irregularities by means of a three dimensional autocorrelation function. These inhomogeneities are field-aligned and statistically distributed. An important feature of the scatter geometry is the so-called "aspect sensitivity". This means the dependence of the scattered signal strength on the angle between the

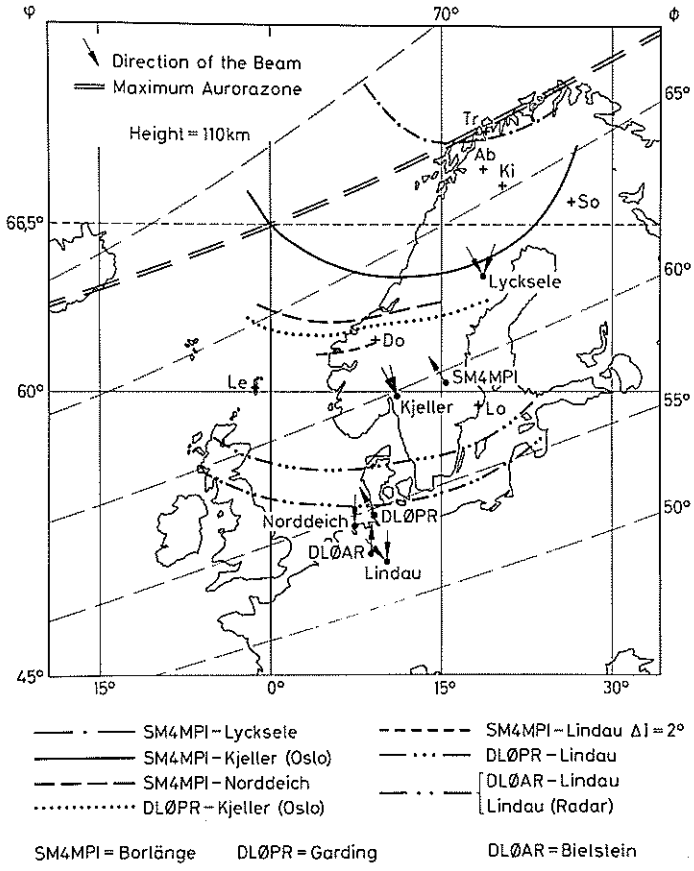

Fig. 1. Backscatter-curves calculated for a height of 110 km of the pairs of stations which are listed at the lower border of this figure. The arrows indicate the directions of the antenna beams of the transmitting and receiving stations. The transmitters are: DLØAR (29.0 MHz), DLØPR (145.971 MHz) and SM4MPI (145.960 MHz).

wave normal of the incident ($\underline{k}_o$) and scattered ($\underline{k}_1$) waves and the direction of the geomagnetic field lines. Optimum conditions for the scattering of HF and VHF radio waves are given, if the direction cosine of the wave normals $n_o(\underline{k}_o)$ and $n_1(\underline{k}_1)$ are equal with respect to the direction of the geomagnetic field lines. The geometrical locations where this condition $n_o(\underline{k}_o) = n_1(\underline{k}_1)$ is fulfilled are defined as backscatter curves. More details about the calculation of the backscatter curves are given by Chapman [1952], Millman [1959] and Czechowsky [1966]. These curves are shown in Figure 1 for all pairs of stations of our network.

The consequences of the Booker theory show in comparison with the measurements a lack in the description of the aspect sensitivity and the frequency dependence. Besides, the Booker theory describes no time variation of the scattering irregularities.

Some years ago Buneman [1963] and Farley [1963] pointed out independently that in an ionospheric current system "two stream plasma instabilities" can occur so that acoustic plasma waves are generated. The periodical density oscillation caused by these plasma waves are the field-aligned centers which give rise to the backscattering of VHF radio waves. This plasma instability appears when the relative drift velocity between the ions and electrons in the electrojet exceeds a certain critical value (threshold) which is close to the thermal velocity of the ions. Above this threshold acoustic plasma waves in shape of longitudinal density waves then are generated which propagate perpendicularly to the geomagnetic lines of force. Bowles, Balsley and Cohen [1963] and Cohen and Bowles [1963] have shown that the backscattering centers in the equatorial electrojet are caused by these plasma waves. These authors pointed out that the backscattering centers in the PEJ obviously are caused by the same mechanism. The purpose of the network shown in Figure 1 is among others to check whether this assumption is correct. First results from observations carried out with this network have been published by Czechowsky [1969] and Czechowsky and Lange-Hesse [1969].

Results of the backscatter observations using beacon transmitters

During the strong geomagnetic storm from October 31 to November 2, 1968 all receiving stations shown in Figure 1 recorded for the first time backscatter echoes of large amplitude. These results shall be represented and discussed in the following sections.

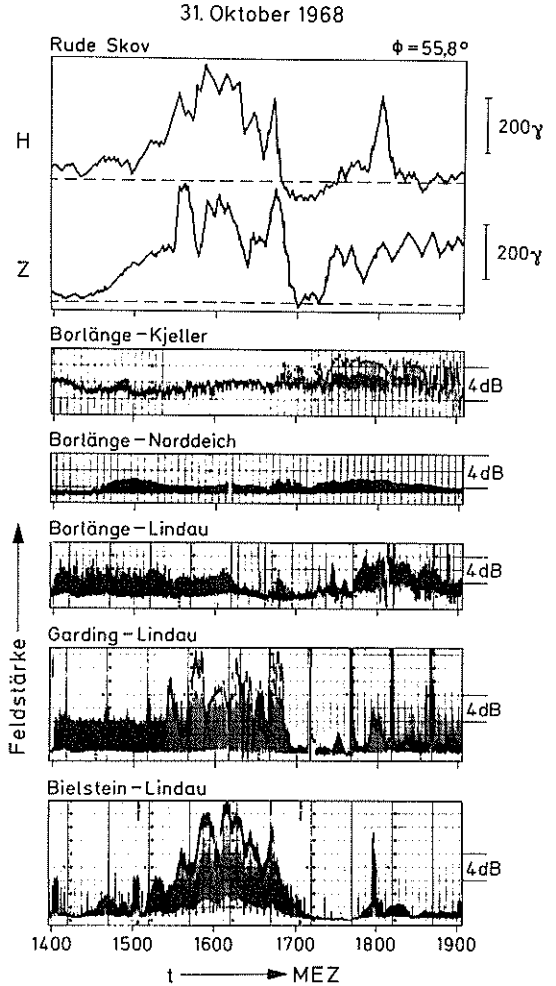

Fig. 2. Backscatter records on Oct. 31, 1968 of the mentioned pairs of stations from north (at the top) to south (at the bottom). Location of the stations see Figure 1.
Horizontal: Time in MEZ=MET=Middle European Time = Time 15°E.
Vertical: Field strength of the backscattered signal.

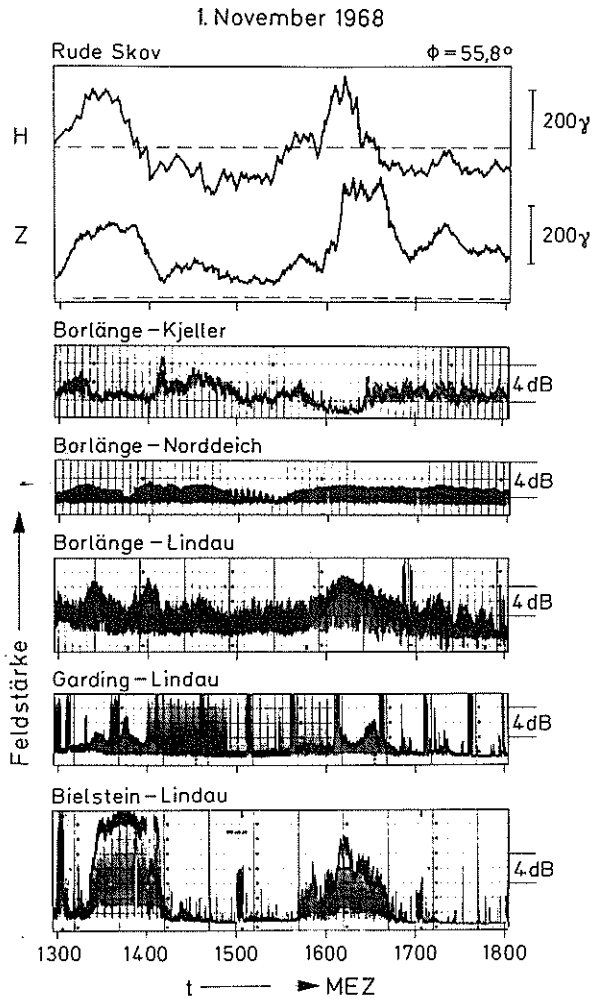

Fig. 3. Backscatter records on Nov. 1, 1968 of the mentioned pairs of stations from north (at the top) to south (at the bottom). Location of the stations see Figure 1. For explanation of horizontal and vertical see text Figure 2.

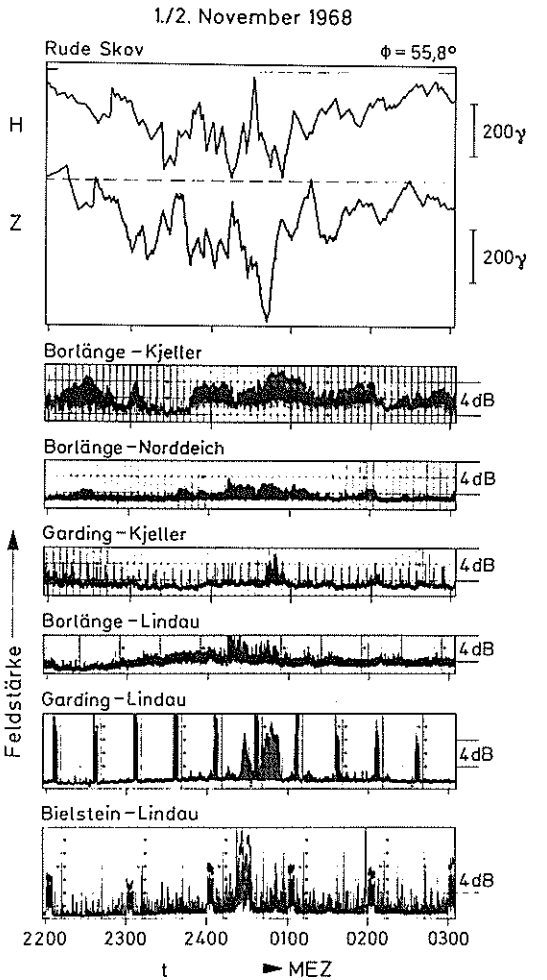

Fig. 4. Backscatter records on Nov. 1-2, 1968 of the mentioned pairs of stations from north (at the top) to south (at the bottom). Location of the stations see Figure 1. For explanation of horizontal and vertical see text Figure 2.

In Figures 2, 3 and 4 are shown the recordings of the pairs of stations mentioned in Figure 1 arranged from the north to the south. According to the plasma acoustic wave theory a correlation is supposed between the location and intensity of the polar electrojet (PEJ) and the appearance of backscatter echoes. Therefore, the H- and Z-magnetograms of the geomagnetic observatory Rude Skov are plotted above the backscatter recordings. Rude Skov is located approximately in the middle between the backscatter curves for Garding - Lindau and Bielstein - Lindau and, furthermore, close to the backscatter curve for the Lindau radar. In addition to this the H- and Z-components of the magnetograms from five geomagnetic observatories from the region of the backscatter curves are shown in the Figures 5 to 8. For the discussion of the results and the comparison with geomagnetic disturbances the authors use the PEJ-model after Akasofu, Chapman and Meng [1965].

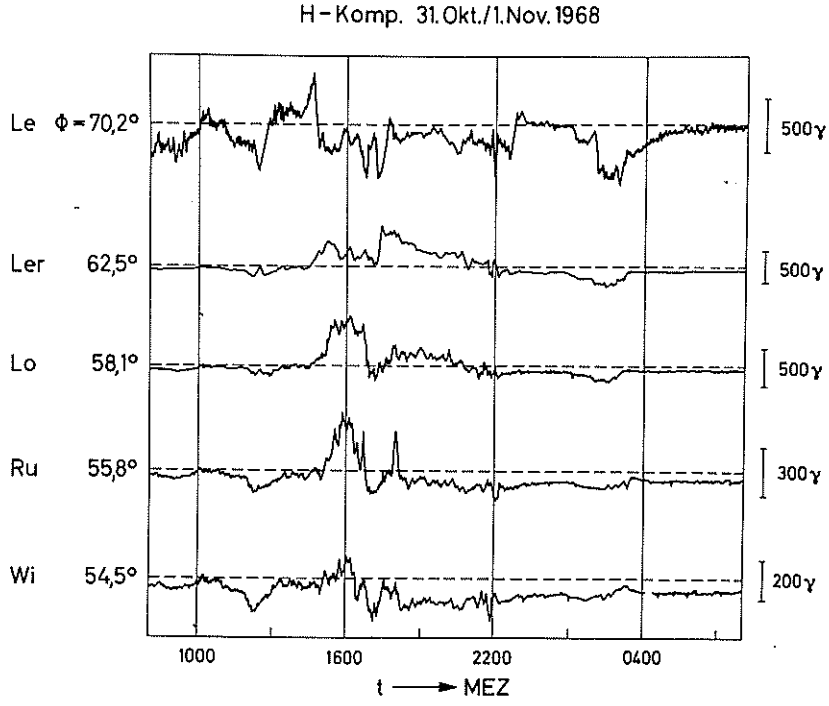

Fig. 5. Magnetograms of the H-component of the observatories Leirvogur (Le), Lerwick (Ler), Lovö (Lo), Rude Skov (Ru) and Wingst (Wi) on Oct. 31-Nov. 1, 1968 (see Fig. 10). For explanation of horizontal see text Figure 2.

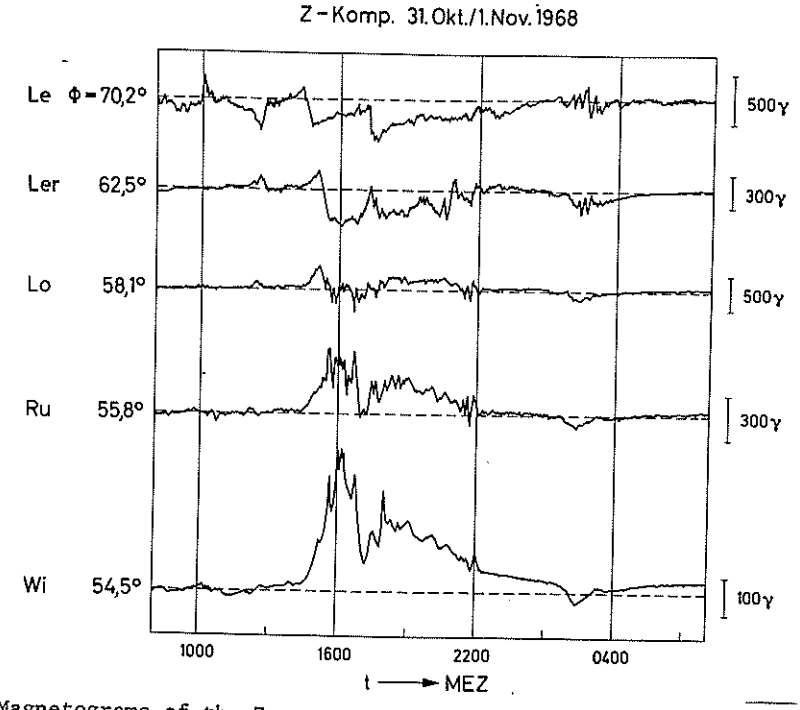

Fig. 6. Magnetograms of the Z-component of the observatories mentioned in Figure 5 on Oct. 31-Nov. 1, 1968.

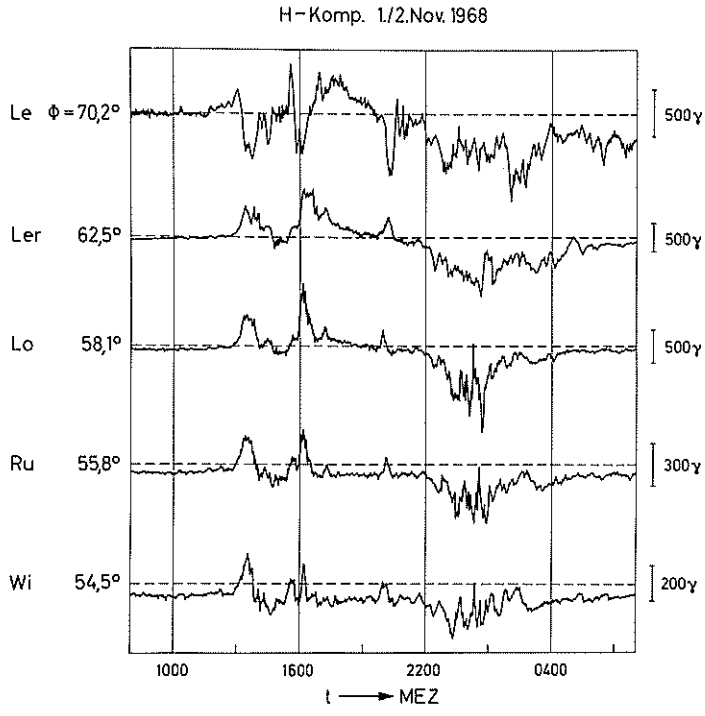

Fig. 7. Magnetograms of the H-component of the observatories mentioned in Figure 5 on November 1-2, 1968.

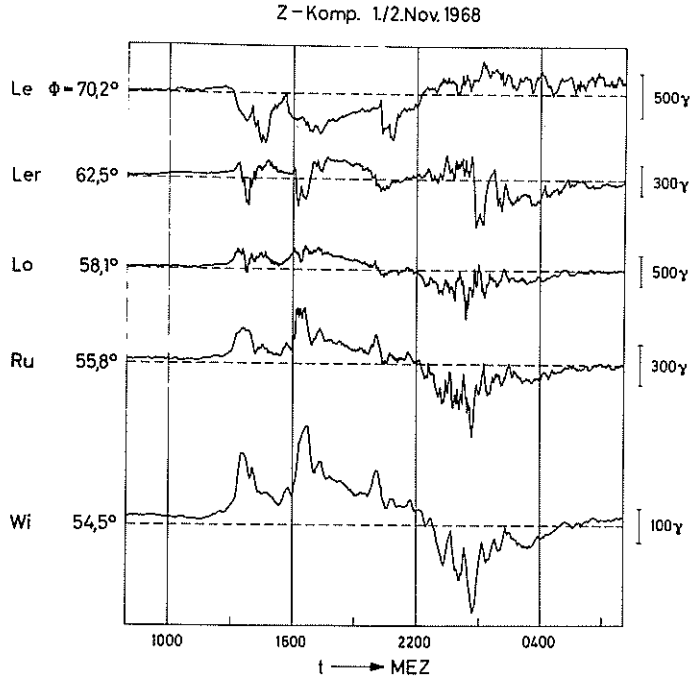

Fig. 8. Magnetograms of the Z-component of the observatories mentioned in Figure 5 on November 1-2, 1968.

A first examination of the recordings and the magnetograms shows the following result: With increasing geomagnetic activity a decrease of the echo amplitude occurs on the northern communication lines and an increase on the more southern ones. Well pronounced is this phenomenon on the two most southerly lines Garding - Lindau and Bielstein - Lindau on the frequencies 145.971 MHz and 29.0 MHz. During the peaks of the geomagnetic disturbance maximum echo amplitudes occur on these two lines, however, no frequency dependence of the backscattered signal can be recognized which should be the case according to the Booker theory.

In the following section the interrelation between the PEJ and the occurrence of backscatter echoes shall be discussed in detail. An equivalent ionospheric line current system can be computed according to a method given first by Birkeland [1901] and extended and improved by Chapman [1935] and Akasofu [1960] using the perturbation vectors ΔD, ΔH and ΔZ. For the following calculations of such line currents a height of 110 km for the PEJ is adopted. The influence of the induced currents in the earth is taken into account by using the factors 2/3 for ΔH and 3 for ΔZ. Line currents calculated according to the above mentioned method cause the same perturbation vector as observed, however, their location can deviate from the true current distribution around the geomagnetic observatory. Using the perturbation vectors from different observatories arranged in a north-south direction the center of the line current system can be calculated with sufficient accuracy (see e.g. Kochan [1967]).

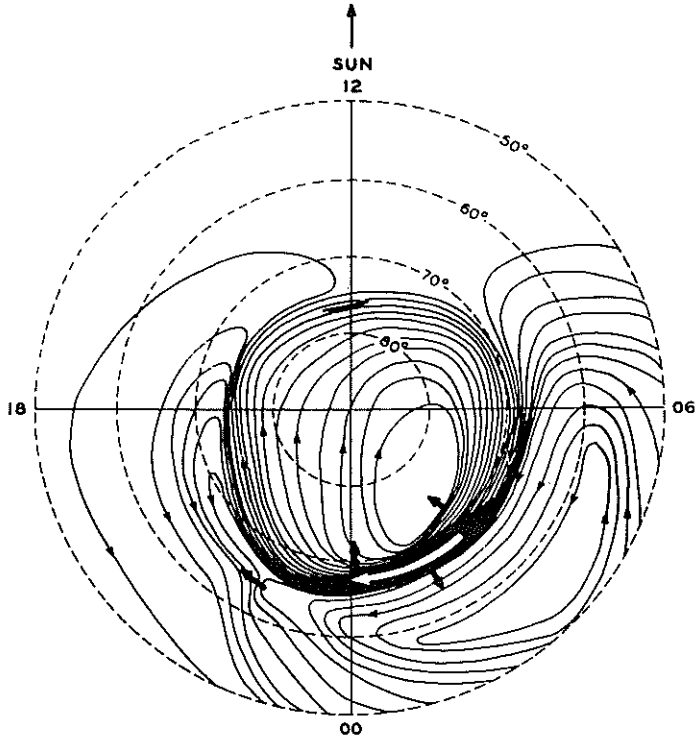

Proposed model current system for an intense polar magnetic substorm: view from above dp. north pole; the direction of the sun is indicated at the maximum epoch.

Fig. 9. Model of the polar electrojet (PEJ) after Akasofu et al. [1965].

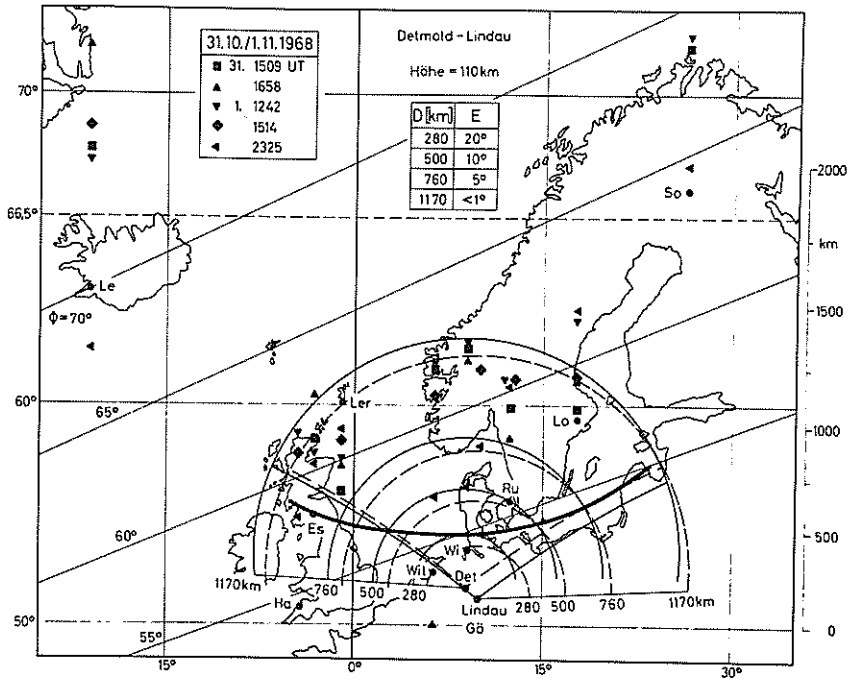

Fig. 10. Backscatter-curve Detmold (DLØAR) - Lindau (height 110 km) and position of the calculated equivalent line currents for the same height on Oct. 31 - Nov. 1, 1968. Geomagnetic observatories: Ha = Hartland, So = Sodankylä, Es = Eskdalemuir, Wit = Witteveen, Le = Leirvogur, Ler = Lerwick, Lo = Lovo, Ru = Rude Skov and Wi = Wingst.

According to the above mentioned method the location of the equivalent line currents was calculated for five special times from the period Oct. 31 to Nov. 2, 1968. At these special times backscatter echoes occurred on the two most southerly lines Bielstein - Lindau and Garding - Lindau. The different symbols explained in Figure 10 indicate the location of the line currents at different times. At four times on Oct. 31 at 1509 UT (1609 MET = Middle European Time = Time 15° East) and 1658 UT (1758 MET) and Nov. 1 at 1242 UT (1342 MET) and 1514 UT (1614 MET) the main part of the PEJ flows from east to west in the north from Leirvogur (Le) and Sodankylä (So). On Oct. 31 at 1658 UT and on Nov. 1 at 1514 UT the location of the current is outside the map at a geographic latitude $\phi = 74.88°$ and $\phi = 74.24°$. The eastward flowing back current during these four special times is located between the geomagnetic latitude from $\Phi = 58.0°$ to $62.5°$. These calculated positions of the equivalent current system coincide very well with the PEJ-model after Akasofu (Fig. 9). The backscatter curves for the pairs of stations Garding - Lindau and Bielstein - Lindau (Fig. 1) are spread in the region of the eastward flowing back current of the PEJ. The backscatter curves for Borlange - Lindau and Borlange - Norddeich are located at the northern border of this region, however, the curve for Borlange - Kjeller is outside of this region. The backscatter recordings on Oct. 31, therefore, show the following picture: From about 1500 MET to 1700 MET no signals occur on the line Borlange - Kjeller, weak signals on the lines Borlange - Norddeich and Borlange - Lindau but strong signals are recorded on the most southerly lines Garding - Lindau and Bielstein - Lindau. Simultaneous radar observations at 1526 MET (224.4 MHz) from Lindau show very similar results: Strong echoes from a distance of about 400 km and weak echoes from 700 km to 1100 km (Fig. 11). Just before 1700 MET the northern lines also show an increase of echo amplitude. The same behaviour can be seen on the radar record (Fig. 11) at the same time (1652 MET): Backscatter echoes of nearly the same amplitude from 400 - 1200 km distance. The observations indicate a coincidence between the location of the eastward flowing back current of the PEJ and the backscattering centers. According to the plasma acoustic wave theory the threshold mentioned before must have been exceeded in this case.

On Oct. 31 during the time from about 1700 - 1800 MET the amplitudes of the perturbation in the H- and Z-magnetograms show a strong decrease (Figs. 5 and 6) which can be explained in the following way: The whole PEJ current has shifted towards the equator so that the westward flowing main current can be observed down to Rude Skov ($\phi = 55.8°$). The backscatter curves of the northern lines are now intersected by this main current which causes an increase of the amplitude of the backscattered signal. The backscatter curves for the two most southerly lines are located about in the latitude of Rude Skov, that means at this special time (1700 - 1800 MET) at the southern border of the main current. In this region obviously the main current and the eastwards flowing back current influence each other in such a manner that the relative drift velocity between ions and electrons necessary for the generation of ion acoustic waves is not reached and no backscatter-

ing centers occur in this region. Therefore, the echo amplitude on these two most southerly lines disappears completely (Fig. 2). A confirmation of the above mentioned location of the PEJ system is given by the picture of the radar display from 1732 MET (Fig. 11). The echoes occur from northwestern directions at distances from 900 km to 1200 km. The location of the appertaining backscatter centers is at a geomagnetic latitude of about $\Phi \approx 60°$. In this latitude which is higher than those for Lovö (Fig. 1) the main current of the PEJ is located and has a strong influence.

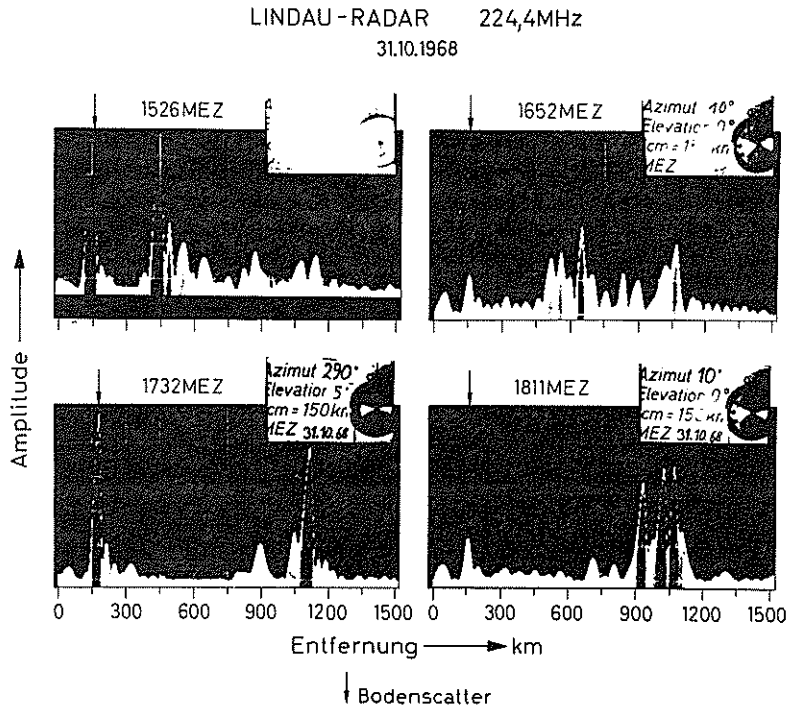

Fig. 11. Records of the Lindau radar station (224.4 MHz) on Oct. 31, 1968 at 1526 15° E-time and 1732 15° E-time (azimuth angle 290°, elevation angle 5° and 10°) and at 1652 15° E-time and 1811 15° E-time (azimuth angle 10°, elevation angle 0°). Horizontal: Distance in km; Bodenscatter = ground scatter.

At about 1800 MET the whole PEJ system seems to shift back to the north. The calculation of the equivalent line current at the time 1658 UT (1758 MET) (see Fig. 10) shows a westward flowing main current north of Leirvogur (Φ = 70.2°) and Sodankylä (Φ = 63.8°) and an eastward flowing back current between the geomagnetic latitudes Φ = 58° and 63°. The backscatter curves for all pairs of stations are located in the region of this back current, therefore all records show moderately strong echoes at about 1800 MET. Simultaneous radar observations (1811 MET, Fig. 11) confirm these results: Weak echoes from short and stronger echoes from larger distances.

During the afternoon of Nov. 1 it can be concluded from the H- and Z-magnetograms (Figs. 7 and 8) that the PEJ system has a similar location and direction and shows a similar shift as at the late afternoon and evening of Oct. 31 (Fig. 10). The backscatter records in Figure 3 therefore have nearly the same course as that shown in Figure 2: From 1300 MET to 1420 MET and from 1540 MET to 1700 MET strong echoes appear on the southern lines, however, no echoes are observed on the northern lines. During the time from about 1420 MET to 1540 MET the westward flowing main current shifts to the south (see Figs. 7 and 8) and gets similar influence as mentioned already above (see Fig. 2, 1700 - 1800 MET).

In the following section the closer relation between auroral backscatter echoes (line Bielstein - Lindau) and the geomagnetic disturbance (Rude Skov) is investigated in detail. The variation of the backscattered echo signals (in scale units) as a function of the horizontal perturbation vector H_d (in γ) is shown in Figure 12. The H_d vector is computed from the values ΔH, ΔD and the base-line value H_o. It can be seen from the diagram of this figure that a threshold value of the order of 110γ must be exceeded before the backscatter process starts at about 1315 MET (see Fig. 3, Bielstein - Lindau). A hysteresis like behavior can also be seen in this diagram, that means that a stronger PEJ current (higher H_d value) is necessary for the generation of the waves than for the maintenance of the plasma waves which give rise to the backscattering process. Hysteresis like behavior of the PEJ was observed e.g. by Czechowsky [1969] and Czechowsky and Lange-Hesse [1969]. Leadabrand [1965] found no pronounced hysteresis effect.

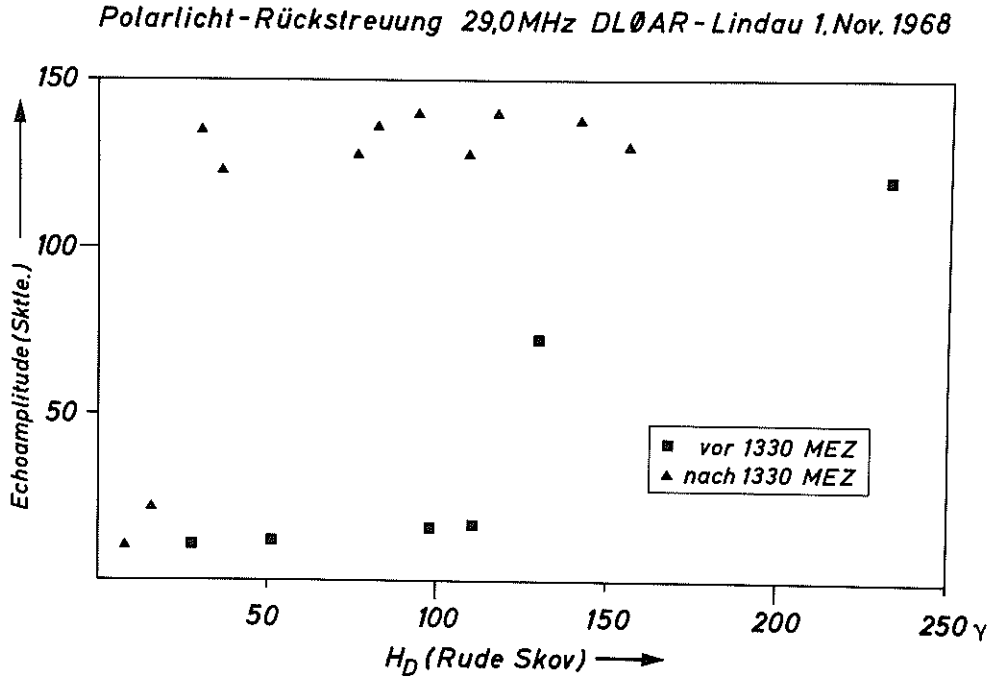

Fig. 12. Relation between the amplitude of aurora backscatter echoes (scale units) and the variation of the horizontal disturbance vector H_d (in γ).

During the hours around midnight of Nov. 1-2 the H- and Z-magnetograms (Figs. 7 and 8) indicate only the main current of the PEJ flowing in a broad band to the west with the center between Lerwick and Lovö before 0030 MET and between Lerwick and Leirvogur after that time. The maximum current strength occurs at about 0030 MET revealed by the strongest bay of the order of more than 1000γ in the H-magnetogram from Lovö. At this time the backscatter signals start on the southern lines (Fig. 4). On the two northern lines, however, backscatter signals occur nearly during the whole time of the flow of the main current. During the peak of the magnetic storm at about 0030 MET the backscattering centers have the most extended north-southerly distribution. The calculation of the equivalent line current for the time 0025 MET (2325 UT) on Nov. 2 (Fig. 10) shows a similar picture: An extended westward flowing main current is located between the geomagnetic latitudes $\Phi = 55.0°$ and 68.0°. This main current generates in an extended region backscattering centers in form of ion acoustic waves. These results agree well with the model of Akasofu et al. (Fig. 9).

Results from measurements with an oblique-incidence sounder

In addition to the cw-backscatter equipments an oblique-incidence sounder operating in Lindau delivers helpful results for the study of the northern ionosphere. The antenna system of this equipment consists of 20 horizontal rhombic antennas which are used for transmitting and receiving in 10 segments of the compass card. Each segment is 36° broad. The frequency is swept from 2.8 MHz to 45 MHz. The elevation angles are between 0 and 45 degrees and the peak power of the transmitter is 500 kW.

A similar sounder was installed in Sodankylä (northern Finland). The distance Lindau - Sodankylä is around 2000 km, the azimuth from Lindau to Sodankylä 21° (east=90°). The transmitters and the receivers of both of these stations are synchronized so that in addition to the mutual backscattered signals the signals of the other station can be received. The latter signals propagate via the ionosphere. Therefore, it is possible to determine the propagation path and the reflectivity of the ionosphere depending on the electron density distribution. For details see Möller [1963].

The results of the long-range propagation measurements between Sodankylä (transmitter) and Lindau (receiver) as well as the results of the backscatter measurements with variable frequency made in Lindau are shown in Figure 13.

First of all these results shall be discussed which are in accordance with the cw-radio aurora backscatter measurements. On Oct. 31, 1968 from 1500 to 1700 MET, on Nov. 1, 1968 from 1300 to 1400 MET and from 1540 to 1700 MET and on Nov. 2, 1968 between 0000 and 0100 MET, when the two most southerly lines Bielstein - Lindau and Garding - Lindau record maximum backscatter signals, the oblique-incidence sounder, too, receives strong echoes coming from the E-region. The echoes appear up to the highest sounding frequency of 45 MHz. The radar measurements (224.4 MHz) mentioned before

confirm these results. On Oct. 31, 1968 from 1500 to 1700 MET and on Nov. 1, 1968 from 1300 to 1400 MET the oblique-incidence sounder receives strong backscatter echoes, but no long-range propagation from Sodankylä to Lindau via an Es-layer is observed. Long-range transmissions in the upper HF- and the lower part of the VHF-band are only possible if the electron density of the F2-layer is high enough or if an intense Es-layer exists near the point of reflection between the transmitter and receiver. The fact that in the time interval of interest no long-range propagation is observed leads to the following conclusions: Firstly that the reflectivity of the F2-layer enables no reflection of the radio waves and secondly that no intense Es-layer exists.

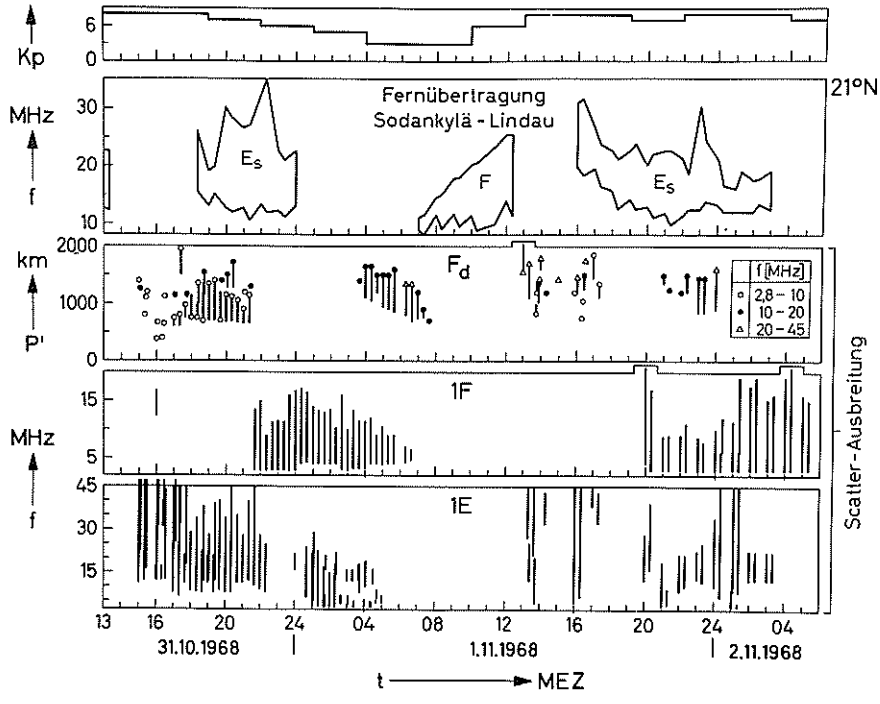

Fig. 13 a - e from above

a) variation of the geomagnetic Kp-index of October 31-November 2, 1968,

b - e) results of the impulse-backscatter soundings and the oblique-incidence soundings carried out at Lindau from October 31-November 2, 1968 (direction of the antenna for both measurements: 21° east by north),

b) upper and lower limit of the oblique-incidence sounding-frequency between Sodankylä and Lindau and statement of the individual propagation mechanism,

c) path-diagram of the diffuse backscatter-echoes from the F-region for three frequency intervals,

d) frequency diagram of 1xF-backscatter-echoes,

e) frequency diagram of 1xE-backscatter-echoes.

In the afternoon of October 31, 1968 and also of November 1, 1968 1xE- and diffuse F-region echoes are received together, but these observations show two differences. On October 31, the echoes are going up to 20 MHz and the cw-backscatter records of the lines Garding-Lindau (145.971 MHz) and Bielstein - Lindau (29.0 MHz) show nearly the same amplitude. On November 1, up to the highest sounding frequency of 45 MHz the diffuse F-region echoes are received and at the same time the backscatter record of the line Bielstein - Lindau shows a much greater amplitude than that of the line Garding - Lindau (see Figs. 2, 3 and 13c).

The backscatter curves of both pairs of stations are extended in almost the same region. The difference in echo strength can be explained with the assumption that in the afternoon of November 1 in Lindau the energy scattered back from the E- and the F-region was received simultaneously. The observations made with the oblique-incidence sounder already mentioned confirm this assumption. Also in the F-region of the ionosphere field-aligned irregularities exist and the scatter mechanism is quite the same as in the E-region, e.g. the maximum echoes are received when the direction cosines of the incoming and the scattered waves are equal with respect to the direction of the geomagnetic field. In the radar case (transmitter and receiver at the same site) the maximum height where this condition is fulfilled is around 220 km (Möller [1964], Kochan [1967]).

In the following section the authors want to discuss the behavior of the F2-layer during the period from October 30 to November 5, 1968. As mentioned before a F2-long-range propagation of HF radio waves is possible if the electron density of this layer is high enough. After a reflection on the F2-layer the radio waves are scattered from the earth surface in all directions. The backscattered part of the energy propagates, therefore, on a similar path to the receiver as the incident wave. This mechanism is called 2xF-ground-backscattering.

During geomagnetic quiet periods it is commonly possible to receive the signals from the beacon transmitter DLØAR (29.0 MHz) via this 2xF-ground-scatter propagation path between 0900 MET and 1700 MET. During geomagnetic disturbances the reflectivity of the F2-layer decreases especially in the auroral and subauroral zone. Therefore, no 2xF-ground-backscatter propagation is possible. Figure 14 shows the daily variation of this propagation mechanism for the line Bielstein - Lindau recorded from October 30 to November 5, 1968. The upper diagram shows a typical course of the field strength on undisturbed days. The decrease of the signal between 1345 MET and 1500 MET is a consequence of a short wave fade out (see Schwentek, contribution in this Report). On Oct. 31 at about 1000 MET the geomagnetic storm starts and on the following days the 2xF-ground-backscatter signals disappear completely.

Using the distance between the ionospheric observatory Uppsala and Lindau e.g. Bielstein of about 1000 km and a height of the F2-layer of about 300 km the calculation leads to an elevation angle of E of nearly 10°. This corresponds to the maximum lobe of the antenna of the Bielstein transmitter. Therefore, the foF2-values of Uppsala must be well correlated with the 2xF-ground-backscatter propagation from Bielstein to Lindau. On November 2 and 3 the maximum value of the critical frequency foF2 at Uppsala is only 6.4 MHz. However, on November 4 these values increase up to 10 MHz and from 1100 MET to 1400 MET weak 2xF-backscatter signals reappear. On November 5 these signals become stronger that means the normal state of the F2-layer is reestablished. For a comparison with the 29.0 MHz backscatter records the foF2-values of Uppsala are tabulated for the period from October 30 to November 5, 1968.

The recorded signals on October 31 from 1500 to 1700 MET and on November 1 from 1300 to 1400 MET and from 1540 to 1700 MET (Fig. 14) are the same backscatter echoes as shown in the Figures 2 and 3 in the lower diagram.

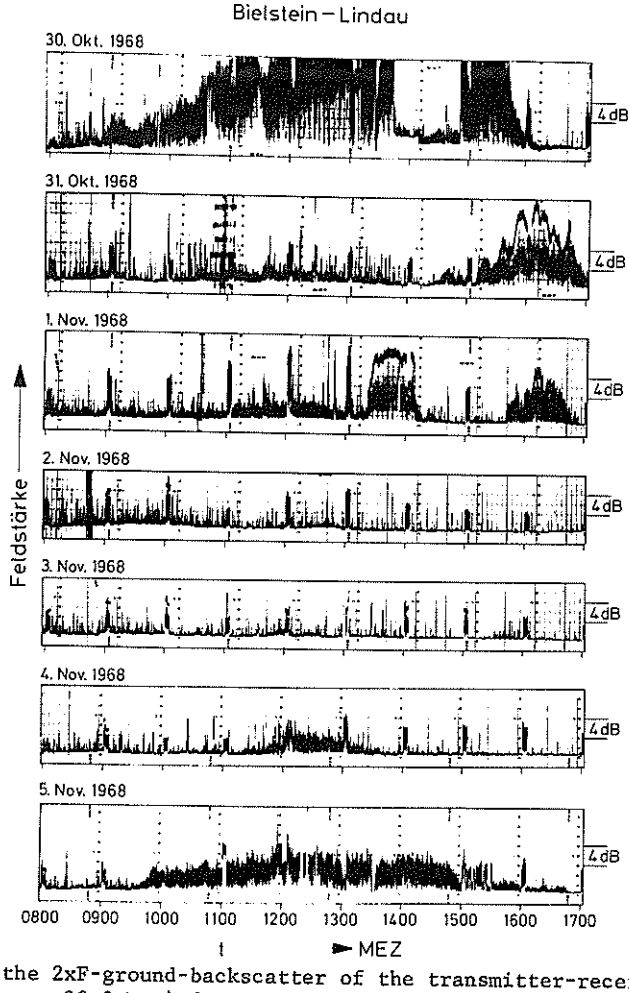

Fig. 14. Variation of the 2xF-ground-backscatter of the transmitter-receiver-line Bielstein - Lindau (frequency 29.0 MHz) from October 30 - November 5, 1968.

foF2 Uppsala Oct. 30 - Nov. 5, 1968 [MHz]

Date UT	0900	1000	1100	1200	1300	1400	1500	1600	1700
30	8.9 S	S	11.0	11.8	J 12.1 S	12.1 S	11.2 S	V	S
31	6.8 Z	8.0 Z	9.0	9.0 Z	9.1	9.3	B	B	B
1	6.0	7.1 Z	8.0 Z	8.9	8.1	B	F	B	B
2	F	4.9	B	5.7	5.2	6.4	5.0 V	F	F
3	5.2	5.5	5.7	6.1	6.4	6.4 Z	S	5.7	F
4	7.0 Z	8.0	9.0	10.2	9.5	8.4	J 8.0 S	F	F
5	8.2 S	9.0	J 10.1 R	J 10.2 R	10.8	10.0	9.0	J 7.9 S	7.1 S

B = Measurement influenced by, or impossible because of, absorption in the vicinity of fmin
F = Measurement influenced by, or impossible because of, the presence of spread echoes
J = Qualifying letter only: Ordinary component characteristic deduced from the extraordinary component
R = Measurement influenced by, or impossible because of, attenuation in the vicinity of a critical frequency
S = Measurement influenced by, or impossible because of, interference or atmospherics
V = Forked trace which may influence the measurement
Z = Measurement deduced from the third magnetoionic component

Optical observations

Optical observations of the night sky were carried out at Lindau (Fig. 1) (geomagnetic latitude $\phi \approx 51.5°$) with a scanning filter photometer using filters for the 6300 Å and 5577 Å emission and for the background emission. During the observation time at the night Oct. 31/Nov. 1 the intensity of the 6300 Å emission increased up to a peak of about seven times of the normal airglow intensity (Fig. 15). This luminous sheet was not homogeneous but had a wave-like structure moving from the south to the north. At about midnight this movement stopped and the wave structure disappeared.

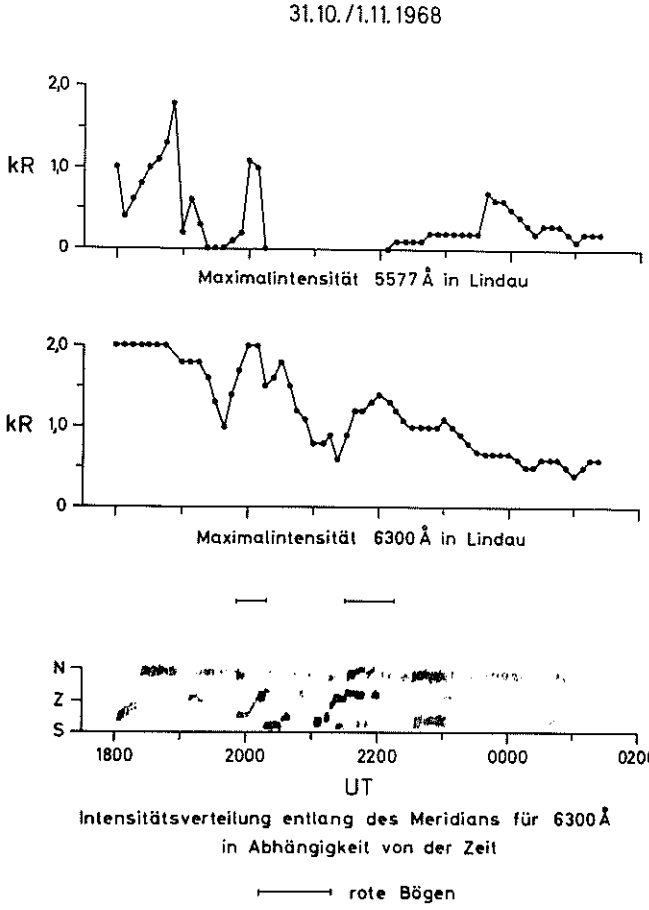

Fig. 15. Results of the photometer-observations of the green (5577 Å) and red (6300 Å) oxygen line at Lindau on Oct. 31-Nov. 1, 1968. The upper diagrams show the time variation of the intensities of the above mentioned green and red lines. The lower diagram indicates the position of spots emitting red light in the meridian plane from south to north. The graduation of white, gray and black indicates the intensity distribution. Rote Bögen=red arcs.

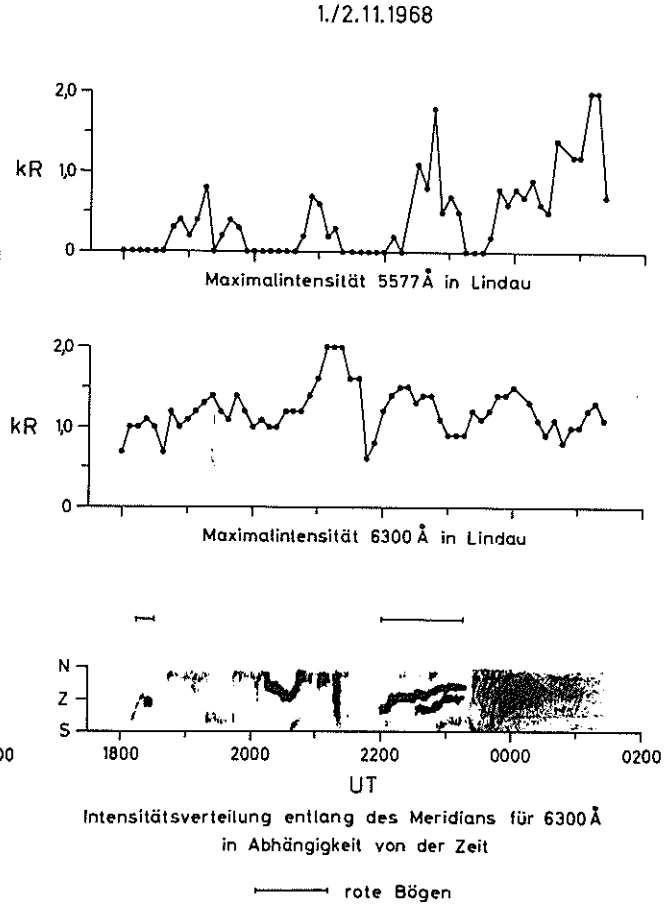

Fig. 16. Results of the photometer-observations at Lindau on Nov. 1-2, 1968. For explanations see Figure 15.

The emission of the green oxygen line 5577 Å mainly originates in the E region of the ionosphere, that means at a height region where also the backscattering centers and the PEJ are located. Therefore, the 5577 Å photometer observations shall be compared with the backscatter observations during the time around midnight Nov. 1-2 (Fig. 16).

At 2322 MET (2222 UT) a marked increase of the 5577 Å intensity up to about 0.8 kR (1 kR = 10^9 photons/cm^2 column sec) occurred at an elevation angle of about 30° to the north. At the same time the first weak echoes appeared on the most southerly line Bielstein - Lindau (Figs. 1 and 4). At about 0030 MET the 5577 Å intensity over the northern horizon increased very much and reached a maximum of 1.1 kR at about 0045 MET. On the most southerly line Bielstein - Lindau the strongest echoes are recorded at about 0030 MET, whereas at 0045 MET stronger echoes were recorded on the more northerly lines (Figs. 1 and 4) than on the most southerly line. The optical and backscatter activity showed a slow decrease until 0130 MET. At 0207 MET the green emission again increased up to more than 2 kR (such an intensity can already be seen by the naked eye). Weak backscatter echoes, however, occurred only on the three northern lines (Figs. 1 and 4) during this time.

During the peak of the magnetic storm on Nov. 2 at 0030 MET (peak of the strongest bay of the order of more than 1000γ in the H-magnetogram from Lovö, Fig. 8) a German merchant ship reported a red aurora in the North Atlantic Ocean at $\phi = 38.7°$ N, $\lambda = 61.8°$ W (at an elevation angle of 60° above the horizon). Another German ship reported from 2230 MET to 2400 MET a rayed arc of green colour at $\phi = 46.6°$ N, $\lambda = 54.0°$ W (about 57° geomagnetic latitude). The elevation angle of the lower border was first 15°, then increasing to 40°. Later red colour appeared in the west extending up to 80° elevation angle. From about 2400 MET the weather conditions allowed no more observations. No visual aurora was reported from Scandinavia at that time caused by cloudy sky.

Acknowledgement

The authors wish to express their thanks to the Norwegian Defence Research Establishment (Kjeller), to the Royal Swedish Telecommunication Board and the Swedish Radio Amateur Organization, SSA (SM4MPI) and to the German Federal Post (Garding, Norddeich) as well as to the TV station Teutoburger Wald of the West German Broadcasting Corporation, WDR (DLØAR) for the service work at the equipments. They further wish to thank several European geomagnetic observatories for the copies of the magnetograms, and the Marine Weather Office (Seewetteramt) Hamburg for the collection of auroral observations from German merchant ships, and the technical staff of the Max-Planck-Institute for Aeronomy for the assistance and cooperation. Finally, the authors wish to thank Prof. W. Dieminger, Head of the Max-Planck-Institute for Aeronomy, for the help and support to carry out these extended projects.

REFERENCES

AKASOFU, S.-I. 1960 Large-scale auroral motions and polar magnetic disturbances, I, J. Atmosph. Terr. Phys., 19, 10-25.

AKASOFU, S.-I., S. CHAPMAN and C. J. MENG 1965 The polar electrojet, J. Atmosph. Terr. Phys., 27, 1275-1303.

BIRKELAND, K. 1901 Expedition Norvégienne de 1899 - 1900 résultats magnétique, Vidensk. Skrifter, I. Mat. Naturv. Kl., 1-80.

BOOKER, H. G. 1956 A theory of scattering by nonisotropic irregularities with application to radar reflections from the aurora, J. Atmosph. Terr. Phys., 8, 204-221.

BOWLES, K. L., B. B. BALSLEY and R. COHEN 1963 Field-aligned E-region irregularities identified with acoustic plasma waves, J. Geophys. Res., 68, 2485-2501.

BUNEMAN, O. 1963 Excitation of field-aligned sound waves by electron streams, Phys. Rev. Letters, 10, 285-287.

CHAPMAN, S. 1935 The electric current systems of magnetic storms, Terr. Magn. Atmos. Elect., 40, 349-370.

CHAPMAN, S. 1952 The geometry of radio echoes from aurorae, J. Atmosph. Terr. Phys., 3, 1-29.

COHEN, R. and K. L. BOWLES 1963 The association of plane-wave electron density irregularities with the equatorial electrojet, J. Geophys. Res., 68, 2503-2525.

COOLINS, C. and P. A. FORSYTH 1959 A bistatic radio investigation of auroral ionization, J. Atmosph. Terr. Phys., 13, 315-345.

CZECHOWSKY, P. 1966 Analyse von Rückstreubeobachtungen ultrakurzer Wellen an Polarlichtern, Kleinheubacher Berichte Nr. 11, 165-171.

CZECHOWSKY, P. and G. LANGE-HESSE 1969 Substorm influences on VHF continuous wave auroral backscatter, Contribution to ESRO-Aurora I-Satellite-Symposium, Nordwijk, Netherlands.

CZECHOWSKY, P. 1969 Statistische Auswertung von Polarlicht-Rückstreubeobachtungen und Vergleich mit der Theorie der Plasma-Instabilität, Kleinheubacher Berichte Nr. 13.

FARLEY, D. T. 1963 A plasma instability resulting in field-aligned irregularities in the ionosphere, J. Geophys. Res., 68, 6083-6097.

KOCHAN, H. 1967 Rückstreubeobachtungen an Polarlichtern mit einer Meteor-Scatter-Anlage, Kleinheubacher Berichte Nr. 12, 23-33.

LEADABRAND, R. L. 1965 A comparison of radar auroral reflection data with acoustic wave theory, Radio Science, 69 D, No. 7, 959-964.

MILLMAN, G. H. 1959 The geometry of the earth's magnetic field at ionospheric heights, J. Geophys. Res., 64, 717-726.

MÖLLER, H. G. 1963 Impulsübertragungsversuche mit schräger Inzidenz und veränderlicher Frequenz über Entfernungen zwischen 1000 km und 2000 km, Forschungsberichte des Landes Nordrhein-Westfalen, Nr. 1149.

MÖLLER, H. G. 1964 Rückstreubeobachtungen mit variabler Frequenz in Lindau am Harz, Gerlands Beitrage zur Geophysik, 73, Heft 2, 81-92.

MOORCROFT, D. R. 1961 Models of auroral ionization, Part I + II, Can. J. Phys., 39, 677-715.

TAO, K. 1962 On the theoretical study of F-scatter, J. Geomagnet. and Geoelectr., 14, 71-85.

THOMAS, J. A., E. W. DEARDEN, E. M. MATTHEW, R. W. E. MC NICOL, B. A. MC INNES, D. G. SINGLETON, G. L. GOODWIN, G. J. E. LYNCH and J. CROUCHLEY 1962 Final report on observations of field-aligned irregularities and transequatorial propagation, Radio Research Section, Department of Physics, University of Queensland, Brisbane, Australia, Scientific Report No. 16.

ACKNOWLEDGEMENTS

This Report would not have been possible without the many contributions from the worldwide scientific community. However, special thanks should be given to Mrs. Lorraine Bower and Miss May Starr for the huge task of typing and correcting this manuscript.

ALPHABETICAL INDEX

INDEX BY DATE

USCOMM-ESSA-ASHEVILLE-3-5-70-1100

Upper Atmosphere Geophysics Report UAG-1
"IQSY Night Airglow Data" by L. L. Smith, F. E. Roach and J. M. McKennan of Aeronomy Laboratory, ESSA Research Laboratories, July 1968, single copy price $1.75.

Upper Atmosphere Geophysics Report UAG-2
"A Reevaluation of Solar Flares, 1964-1966" by Helen W. Dodson and E. Ruth Hedeman of McMath-Hulbert Observatory, The University of Michigan, August 1968, single copy price 30 cents.

Upper Atmosphere Geophysics Report UAG-3
"Observations of Jupiter's Sporadic Radio Emission in the Range 7.6-41MHz, 6 July 1966 through 8 September 1968" by James W. Warwick and George A. Dulk, Department of Astro-Geophysics, University of Colorado, October 1968, single copy price 30 cents.

Upper Atmosphere Geophysics Report UAG-4
"Abbreviated Calendar Record 1966-1967" by J. Virginia Lincoln, Hope I. Leighton and Dorothy K. Kropp of Aeronomy and Space Data Center, Space Disturbances Laboratory, ESSA Research Laboratories, January 1969, single copy price $1.25.

Upper Atmosphere Geophysics Report UAG-5
"Data on Solar Event of May 23, 1967 and its Geophysical Effects" compiled by J. Virginia Lincoln, World Data Center A, Upper Atmosphere Geophysics, ESSA, February 1969, single copy price 65 cents.

Upper Atmosphere Geophysics Report UAG-6
"International Geophysical Calendars 1957-1969" by A. H. Shapley and J. Virginia Lincoln, ESSA Research Laboratories, March 1969, single copy price 30 cents.

Upper Atmosphere Geophysics Report UAG-7
"Observations of the Solar Electron Corona: February 1964 - January 1968" by Richard T. Hansen, High Altitude Observatory, Boulder, Colorado and Kamuela, Hawaii, October 1969, single copy price 15 cents.